IN VITRO STUDIES ON GENOTOXICITY AND GENE EXPRESSION IN SPERMATOGENIC CELLS: MECHANISMS AND ASSAY DEVELOPMENT

K.S.A. HABAS

PhD

UNIVERSITY OF BRADFORD

2015

In vitro studies on genotoxicity and gene expression in spermatogenic cells: mechanisms and assay development

Khaled Said Ali Habas

Submitted for the degree of Doctor of Philosophy

Faculty of Life Sciences

University of Bradford

2015

Abstract

Khaled Said Ali Habas

In vitro studies on genotoxicity and gene expression in spermatogenic cells: mechanisms and assay development.

Keywords: Spermatogenesis; *in vitro*; Doxorubicin; hydrogen peroxide; rodent; Staput; TUNEL assay; Comet assay; cloning; gene expression.

Spermatogenesis is a complex process of male germ cell development from diploid spermatogonia to haploid fertile spermatozoa. Apoptosis plays a vital role in limiting cell numbers and eliminating defective germ cells. This requires novel gene products, and precise and well-coordinated programmes of gene expression. It is therefore possible that a disruption of transcription factor function would significantly impact germ cell development.

The present work was undertaken to use Staput separation followed by culture of purified germ cells of rodent testis since mammalian spermatogenesis cannot yet be recreated in vitro. Specificity of separation was assessed using immunocytochemistry to identify spermatogonia, spermatocytes and spermatids. The genotoxins H_2O_2, doxorubicin, N-ethyl-N-nitrosourea, N-methyl-N-nitrosourea, 6-mercaptopurine, 5-bromodeoxyuridine, methyl methanesulphonate and ethyl methanesulphonate were investigated.

Cells were cultured and treated with different concentrations for each agent. DNA damage and apoptosis were measured by Comet and TUNEL assays

respectively. Up-regulation of expression of the transcription factors Tbpl1, FHL5 and Gtf2a1l that are important post-meiotically, were examined using RT-PCR and qPCR. Protein production was evaluated using Western blotting.

Tbpl1, FHL5 and Gtf2a1l were cloned in-frame into the inducible expression vector pET/100-TOPO. The recombinant clones were induced and successful expression of the proteins in *E. coli* was confirmed by SDS-PAGE and Western blotting. The recombinant clones obtained were used to demonstrate genotoxin induced impairment of gene expression.

Thus, Staput-isolated rodent testicular germ cells seem to be a suitable model to study genotoxicity *in vitro* yielding result comparable to those reported *in vivo*. Furthermore, the work shows that genotoxins can impair gene expression.

Published papers

Habas, K., Anderson, D. and Brinkworth, M. H. (2014). Development of an in vitro test system for assessment of male, reproductive toxicity. Toxicology Letters. Vol. 25, No.1, pp. 86-91.

Conference Contributions

1. Khaled Habas, Anderson, D. and Brinkworth, M. H (2012). Development of an *in vitro* test system for assessment of male, reproductive toxicity. The 34th Annual Meeting of the British Andrology Society. School of Life Sciences, University of Bradford, Bradford. UK (Poster).

2. Khaled Habas, Anderson, D. and Brinkworth, M. H (2013). Development of an *in vitro* test system for assessment of male, reproductive toxicity. School of Life Sciences, University of Bradford, Bradford. UK (Poster).

3. Khaled Habas, Anderson, D. and Brinkworth, M. H (2014). Germ cell response to doxorubicin exposure *in vitro*. 18th European Testis workshop, International European workshop on the molecular and cellular endocrinology of the testis, Elsionre, Denmark (Poster).

4. Khaled Habas, Anderson, D. and Brinkworth, M. H (2014). Germ cell DNA damage by Comet assay in rat cells following *in vitro* genotoxin exposure. International European environmental mutagen society (EEMS). Lancaster University UK (Poster).

5. Khaled Habas, Anderson, D. and Brinkworth, M. H (2014). *In vitro* effects of hydrogen peroxide on ALF expression in male mouse germ cells. International Word Congress of reproductive biology, EICC, Edinburgh UK (Poster).

Acknowledgments

My first thank is to Allah the almighty for giving me the health and knowledge to see the completion of my thesis.

Secondly, I would like to convey my sincere thanks to my supervisor Dr. Martin Brinkworth for all the effort, personal attention, suggestions, endless encouragement and support he has provided me throughout my PhD study and without whom I would not have been able to produce this thesis. He has been my mentor and has always motivated and encouraged me. I also welcome and appreciate his suggestions on the development of this thesis as well as explaining the logic and purpose of each step during the experiments.

I am also grateful to my secondary supervisor, Professor Diana Anderson, Established Chair of Biomedical Science, who has always been very helpful and given me strong hopes at times when I have struggled. Her valuable experience and ways of managing a PhD has been very beneficial. She has helped me with her attention to details in aspects of my work.

I would like to express my thanks to all my family and friends especially to my brothers for supporting me by their thoughts and prayers. With the whole of my heart, I would like to thank my wife ASMA for her patience, support and for helping me in every possible way during my studies. My sincere appreciation also goes to my daughter, RAHF and my lovely son, AHMED. I wish them success in all their endeavours.

Glossary of abbreviations

Terms	Definitions
6-MP	6-Mercaptopurine
6-MeTIMP	6-methyl thioinosine monophosphate
ACT	Activator of CREM in testis
Alanine	Ala (A)
ALF	TFIIA alpha/beta-like factor
Amp	Ampicillin
Arg (R)	Arginine
Asn (N)	Asparagine
Asp (D)	Aspartic acid
BAS	Bovine serum albumin
bp	Base pairs
BrdU	5-Bromo-2′-deoxyuridine
cDNA	Complementary DNA
CREM	Camp response element modulator
Cys (C)	Cysteine
dH_2O	Distilled water
DMEM	Dulbecco's Modified Eagle Medium
DMSO	Dimethyl sulfoxide
DNA	Deoxyribonucleic acid
DNase	Deoxyribonuclease
dNTP	Deoxyribonucleotide
DOX	Doxorubicin

DREF	DNA replicating element related factor
DTT	Dithiothreitol
E.coli	Escherichia coli
ECL	Chemiluminescence
EDTA	Ethylenediamineterta acetic acid
EMS	Ethyl methanesulfonate
ENU	N-ethyl-N-nitrosourea
EtBr	Ethidium bromide
FADD	Fas-associated death domain
FASL	Fas receptor-Fas ligand
FBS	Fetal bovine serum
FHL5	Four and a half LIM domains protein 5
GAPDH	Glyceraldehyde-3-Phosphate Dehydrogenase
GDNFR	Glial cell line derived neurotrophic factor receptor
Gln (Q)	Glutamine
Glu (E)	Glutamic acid
Gly (G)	Glycine
Gtf2a1l	General transcription factor IIA, 1-like
H1	Histone 1
H2A	Histone 2A
H2B	Histone 2B
H3	Histone 3
H4	Histone 4
HCl	Hydrochloric acid
His (H)	Histidine

HRP	Horseradish peroxidase
IHC	Immunohistochemistry
Ile (I)	Isoleucine
IPTG	Isopropyl β-D-1-thiogalactopyranoside
kb	Kilobases
KCl	Potassium chloride
kDa	Kilo dalton
KH_2PO_4	Potassium dihydrogen phosphate
KIF17b	Kinesin protein 17b
LB	Luria bertain broth
Lys (K)	Lysine
$MgSO_4$	Magnesium sulphate
Met (M)	Methionine
$MgCl_2$	Magnesium chloride
miRNA	Micro RNA
MMS	Methyl methanesulfonate
MNU	N-methyl-N-nitrosourea
mRNA	Messenger RNA
MW	Molecular weight
NaCl	Sodium chloride
NaH_2PO_4	Sodium dihydrogen phosphate
NaOH	Sodium hydroxide
NF-1	Neurofibromin gene
NF-1	Neurofibromin protein 1
ORF	Open reading frame

OTM	Olive tail moment
PAGE	Polyacrylamide gel electrophoresis
PBS	Phosphate buffered saline
PBST	Phosphate-buffered Saline with Tween
PCR	Polymerase chain reaction
Phe (F)	Phenylalanine
PRM	Protamine protein
Pro (P)	Proline
QRT-PCR	Quantitative reverse transcription polymerase chain reaction
RNA	Ribonucleic acid
RNase	Ribonuclease
ROS	Reactive oxygen species
RT-PCR	Reverse transcription polymerase chain reaction
SCP3	Synaptonemal complex protein 3
Ser (S)	Serine
SSCs	Spermatogonial stem cells
STA-PUT	Velocity sedimentation separation
TAF	Transcription factor associated factor
TAF7	Transcription initiation factor TFIID subunit 7
TBP	TATA binding protein
TBP	TATA box-binding protein
Tbpl1	TATA box binding protein-like 1
TBS	Tris buffered saline
TEMED	N, N, N, N- Tetramethylethylenediamine
TFIIA	Transcription Factor II A

TFIIB	Transcription Factor II B
TFIID	Transcription Factor II D
TFIIE	Transcription Factor II E
TFIIF	Transcription Factor II F
TFIIH	Transcription Factor II H
Thr (T)	Threonine
TLF	TATA binding protein like factor gene
TLF	TATA binding protein like factor protein
TLF-BS	TLF-binding site
TLP	Synonym TLF
TP1	Transition protein 1
TRF2	Synonym TLF
TRP	Synonym TLF
Trp (W)	Tryptophan
TUNEL	Terminal uridine-deoxynucleotide end-labelling
Tyr (Y)	Tyrosine
UTR	Untranslated region
UV	Ultraviolet
v/v	Volume per volume
Val (V)	Valine
w/v	Weight per volume

Table of content

List of tables

List of figures

Chapter 1. Introduction

1.1 Background

During spermatogenesis the male germ cell undergoes complex morphological, biochemical and physiological changes, resulting in the formation of a mature spermatozoon (Dadoune, 2003). Major modifications in both cytoplasmic and nuclear structures continue during spermatogenesis as stringent chronological and stage-specific gene expression is a precondition for the correct differentiation of round spermatids into mature spermatozoa. As spermatogenesis progresses, there is an extensive reorganization of the haploid genome and subsequently widespread DNA condensation (Steger, 1999, Hecht, 1998, Xie et al., 2007). It is now known that the testis has specialised transcription complexes that organize the differentiation programme of spermatogenesis, which includes the up-regulation of expression of TATA-binding protein (TBP) family and its cofactors (Kimmins et al., 2004). The transcriptional and post-transcriptional regulation of gene expression during post-meiotic male germ cells is vital and many controlling proteins have been identified that are fundamental for these processes to occur correctly (Tanaka and Baba, 2005, O'Bryan and de Kretser, 2006). These proteins are transcription factors and it is their fundamental role as critical control elements of cell growth, differentiation, and programmed cell death (apoptosis) that has stimulated a rising interest in them as possible pharmaceutical targets for therapeutic intervention in various diseases, including cancer (Karamouzis et al., 2002). Post meiotic factors such as germ cell nuclear factor (GCNF) have been proposed as targets for pharmaceutical invention as male contraceptive (Ivell et al., 2004).

Reproductive and developmental disorders are increasingly important areas of toxicology. Identified causes of such disorders include maternal metabolic imbalances, as well as therapeutic, and environmental exposure of the developing germ cells or embryo/foetus to damaging chemicals and physical agents. Although considerable progress has been made in determining causes, the aetiology of the majority of birth defects is unknown or only poorly established (Achermann et al., 2002). It has yet to be understood how toxicological mechanisms leading to congenital defects operate and what is the role of the genetic and environmental factors in triggering such mechanisms (Hood, 2006). Thus, it is clear that both mechanistic studies of known developmental toxicants and the toxicological assessment of pharmaceutical agents, industrial chemicals and environmental pollutants, to which pregnant women may be exposed, will be of importance in the future. Gametogenesis is an extremely important biological process that is sensitive to toxic insult (Adler, 2000, Iona et al., 2002). It is well established from animal models that germ cells affected by chemicals during maturation can result infertility, cancer in the offspring, and negative effects on the development of offspring. Certain mutagens, for example, produce heritable gene mutations and heritable structural and numerical chromosomal aberrations in germ cells (Allen et al., 1986, Janes et al., 2001).The consequences of germ cell mutation for subsequent generations include the following: genetically determined phenotypic alterations without signs of illness; reduction in fertility; congenital malformations with varying degrees of severity; and genetic diseases with varying degrees of health impairment (Brinkworth, 2000).

However, many defence mechanisms exist in order to maintain the integrity of germ cells; for example, proper chromosome synapsis and correct repair of DNA double strand breaks. They are vital during meiotic cell division in order to maintain germ cell integrity (Xu et al., 2012). Another defence mechanism against the induction of genetic damage in germ cells is apoptosis itself. Programmed cell death is an active process that controls cell numbers in several tissues and is involved in morphogenesis during embryonic development and throughout adult life (Raff et al., 1993, Schwartzman and Cidlowski, 1993, Williams, 1991, Elmore, 2007). Apoptosis also occurs spontaneously at a variety of phases of germ cell development and has been shown to play a major role during spermatogenesis (Bartke, 1995, Shaha et al., 2010). Germ cells are highly specialized cells that are responsible for the propagation of DNA to direct the development of future generations. Therefore, to ensure the continuation of the species, it is essential for organisms to maintain the integrity of germ cell DNA. Previous studies have shown that spermatogenic cells have higher mutation frequency than somatic cells (Walter et al., 1998, Winn et al., 2000). As a result, any increase in this rate as a result of toxic exposure increases the risk of adverse outcomes even higher than somatic cells. Male germ cells may be vulnerable to damage via chemical toxicants in mitotic spermatogonial cells, meiotic germ cells spermatocytes, post meiotic spermatids and spermatozoa under maturation in the epididymis. This could affect the production and integrity of the mature sperm; in addition, both single stranded and double breaks might occur in the DNA (Delbes et al., 2010).

1.2 Spermatogenesis

Spermatogenesis is a complex process of proliferation and differentiation of male germ cells to create fertile spermatozoa. Spermatogenesis happens in the seminiferous epithelium and the process of spermatozoa formation is organised into three distinct phases; mitotic proliferation of spermatogonia, meiosis in which the diploid spermatocytes undergo two divisions to form four haploid spermatids, and spermiogenesis which involves a stepwise maturation of the spermatids to mature spermatozoa. The landmark changes occurring during spermiogenesis include condensation of chromatin, formation of the acrosome and the removal of the excess cytoplasm at the time of spermiation (Eddy, 2002). This process involves complex signaling mechanisms that regulate gene expression and post-transcriptional and post-translational modifications during spermatogenesis. These factors include both paracrine and autocrine (from Sertoli and germ cells) and endocrine (e.g. androgens, retinoic acids) factors (Hess R, 2005, White-Cooper and Davidson, 2011).

1.2.1 Developmental spermatogenic stages and cycle

Spermatogenesis in mammals has a synchronized, cyclic form where the cellular sequence of differentiating germ cells and their intimate, physical association with Sertoli cells are preserved in a continuous and repeated way (de Rooij and Russell, 2000). Utilizing this information, the seminiferous epithelium can be classified into different 'stages' based on the cellular complement present in a given segment of seminiferous tubule (Figure 1.1). Assessment of these cellular relations has identified 12 stages of the

seminiferous epithelium in mice and 14 stages in rats (Oakberg, 1956, Leblond and Clermont, 1952, Hermann et al., 2010). Figure 1.1 shows stages of spermatogenesis and the duration of the spermatogenic cycle.

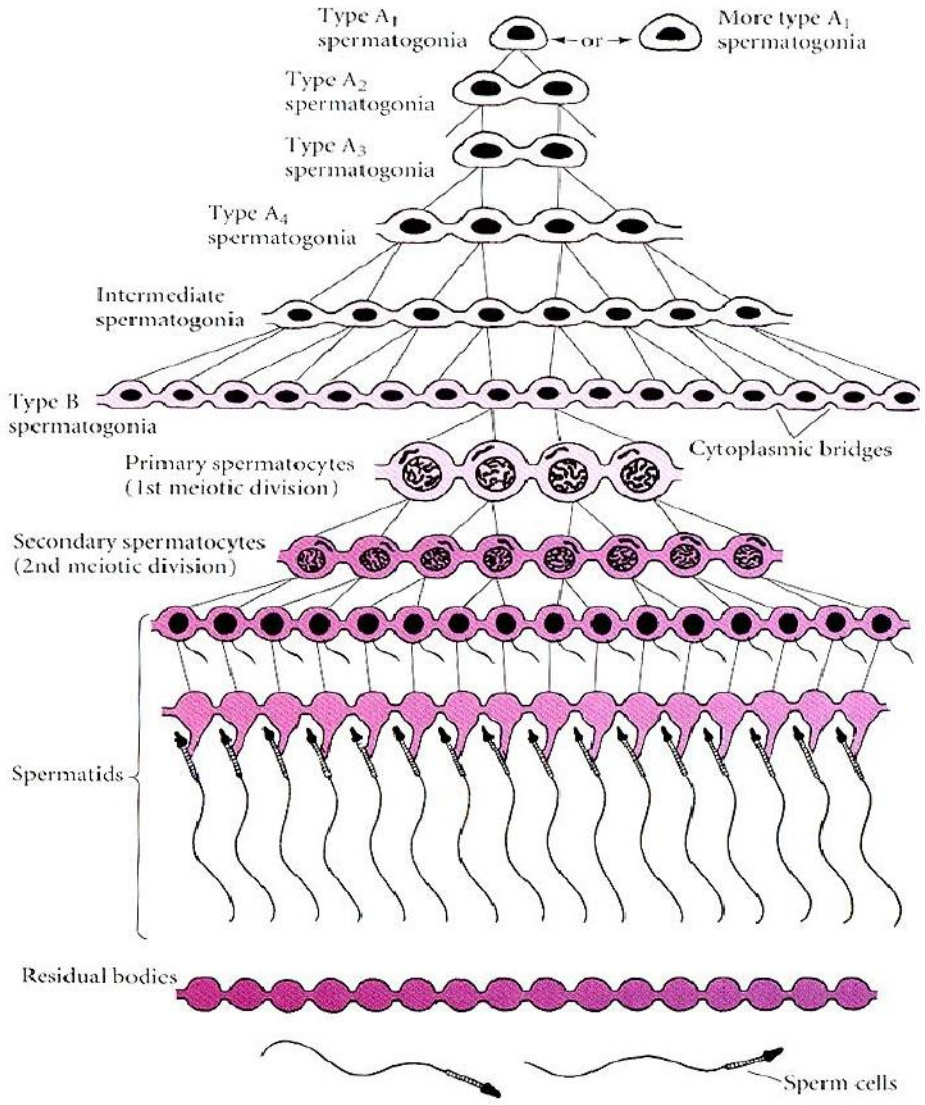

Figure 1.1: Diagram showing the cycle of the germ cells. Taken from Bloom and Fawcett (1975).

1.2.2 Sertoli cells

Sertoli cells (SCs) are the epithelial supporting cells of the seminiferous tubules. The SCs play a central role in testis development and

spermatogenesis (Johnson et al., 2008). They facilitate the progression of spermatogenesis to spermatozoa by direct contact and by regulating the microenvironment in the seminiferous tubules (Griswold, 1998, Johnson et al., 2008). Moreover, they deliver structural support and nutrition to developing spermatogenic cells, undertake phagocytosis of degenerating germ cells and residual bodies, allow release of (maturation phase) spermatids at spermiation and making of a host of proteins that help control spermatogenesis in response to pituitary hormones, in particular by stimulating the mitosis in spermatogonial cells (Bellve and Zheng, 1989, Buch et al., 1988, Johnson et al., 2008).

1.2.3 Spermatogonia

The spermatogonial stem cell is an undifferentiated germ cell that preserves the balance of self-renewal and differentiation in germ cells in order to ensure progressive creation of gametes in adult male (Hermann et al., 2010). Spermatogonia lie at the interface of the blood testes barrier and the extracellular milieu. Many cells, including Sertoli cells, myoid cells and Leydig cells contribute to the microenvironment necessary for the correct development of SSCs (Hermann et al., 2010, Cheng and Mruk, 2012). Spermatogonial stem cells (SSCs) undergo a number of mitotic divisions in giving rise to differentiating spermatogonia that are committed to meiosis and germ cell formation. In mice and rat three different types of SSCs have recognized depended on cell and nuclear morphology (Hermann et al., 2010, Monesi, 1962, Phillips et al., 2010). These are A $_{single}$ (A_s); A $_{paired}$ (Ap); A $_{aligned}$ (Tegelenbosch and Derooij, 1993, Oakberg, 1970). In non-primate mammals (mice), A-single (As) spermatogonia are the stem cells of

spermatogenesis. As spermatogonia are single cells that upon mitosis can divide into two new stem cells. A-paired (Apr) spermatogonia produce daughter cells that remain connected by an intercellular bridge. The Apr spermatogonia are predestined to develop further along the spermatogenic line and to divide into chains of four A-aligned spermatogonia (de Rooij, 2001).

There are some well characterized markers of stem progenitor spermatogonia and (A_{single}, A_{paired} and $A_{aligned}$ such as GFRα1 and cKIT. However, in the two primates different pools of cells have recognized these are A_{dark} (dark staining nucleus) and A_{pale} (pale staining of nucleus). It is believed that A_{dark} aids as the reserve pool which the true progenitors much alike the As; A paired , while in the mouse and rat as A_{pale} which aid as the one that gives rise to the differentiated for B1-spermatogonia (White-Cooper and Bausek, 2010, Grisanti et al., 2009, Waheeb and Hofmann, 2011).

1.2.4 Spermatocytes

Spermatocytes are the largest spermatogenic cells. They have a round shape with a large round nucleus that has a distinct chromatin network, thread-like appearance characteristic of entrance into cells division (Manochantr et al., 2003). After their formation, they enter the prophase of the first meiotic division. In this prophase, the cell passes through 5 sub-phases: preleptotene, leptotene, zygotene, pachytene and diplotene, taking about 22 days in mice. Primary spermatocytes replicate their DNA as preleptotene spermatocytes and therefore are 2N (46 [44+XY] chromosomes) but have 4C DNA content. This first meiotic division gives rise

to smaller cells called secondary spermatocytes. These have less dense nuclear chromatin with only 23 chromosomes and are therefore haploid despite having 2C DNA. They have a short life, enter the second meiotic division quickly, and are hence relatively rare in the seminiferous epithelium. Division of the secondary spermatocytes results in spermatids (Ogura et al., 1998, Ogura et al., 1997, Tanaka et al., 2003).

1.2.5 Spermatids

Initially, spermatids are small, round cells with a small round nucleus containing areas of condensed chromatin. They contain 23 chromosomes with 1C DNA content. Spermatid differentiation is a complex process called spermiogenesis, involving the formation of the acrosome, chromatin condensation, elongation of the nucleus, development of the flagellum, and loss of excess cytoplasm into structures called residual bodies. In mouse, the development of the acrosome of spermatids is divided into four phases which include the Golgi stage, cap stage, acrosomal stage and the maturation stage (Vernet et al., 2012). Throughout the Golgi stage, many pro-acrosomic granules are deposited in Golgi vesicles followed by clustering in the vesicle into a single acrosomic granule, which associates with the nuclear envelope. Within the subsequent cap and acrosomal stage, the acrosome increases in size as a result of fusion of extra Golgi-derived vesicles and spreads over the anterior nuclear pole. The acrosome covers two thirds of the nucleus at the end of the acrosomal stage and achieves its definitive hook shape during the maturation phase. During the maturation phase, virtually all the cytoplasm is shed as residual bodies and phagocytosed by Sertoli cells. The spermatids

are in effect immature spermatozoa by now and are released into the lumen of the tubule (Oakberg, 1956b, Vernet et al., 2012).

Most of the divisions of spermatogonial cells are unfinished regarding the cytoplasm and thus spermatogonia, spermatocytes and spermatids remain associated with cytoplasmic bridges until maturation into spermatozoa (Braun et al., 1989). The intercellular bridges deliver a link among the primary and secondary spermatocytes and spermatids derived from a single spermatogonium via passing the interchange of information from cell to cell, these bridges play a vital role in organizing the sequence of events in spermatogenesis (Braun et al., 1989, Dym, 1994).

1.3 Gene expression during spermatogenesis

Spermatogenesis is a unique process that occurs in the testis and involves different phases. First, it is part of an adult's development process which begins at puberty and progresses during the reproductive life of an adult male. Second, it is a cellular and physiological procedure which includes meiosis. The meiotic phase involves cell division which happens within gametogenesis which is vital for preserving the right chromosomal complement. Third, the final outcome of the process is a cell type (spermatozoa) that is functionally and morphologically different from other cell types in the body. The fourth and final stage of spermatogenesis includes cell to cell contact, cross-talk and elaborate signaling among them. For these phases of spermatogenesis to take place, there needs to be closely controlled regulation of gene expression. During male germ cells formation, regulation of gene expression occurs on three levels; intrinsic,

interactive and extrinsic control (Eddy, 2002, Kwon et al., 2014). The intrinsic process regulates which genes are used and when these genes are expressed. The unique character of this process is germ cell and stage specific gene expression. The interactive process provides vital support for germ cell proliferation and progression during the phases of development. Finally, extrinsic influences, including the steroid and peptide hormones regulate gene expression and signaling mechanism in somatic cells of seminiferous tubules which in turn modulates the activity of the germ cells (Eddy, 2002, Kwon et al., 2014).

Furthermore, during spermatogenesis gene expression is extremely arranged and accurately regulated at two main levels, transcriptional and translational. In order to complete the progression of spermatozoa, this process requires numbers of specific transcriptional regulators and the expression of testis-specific genes or isoforms and unique chromatin remodeling (Steger, 1999, Meikar et al., 2013, Kimmins et al., 2004). Regulation of gene expression during spermatogenesis is described in details in the following section.

1.3.1 Regulation of gene transcription during spermatogenesis

Transcription is controlled both by epigenetic chromatin modifications and by several transcription factors that bind to the specific side of DNA sequences in the promoter regions, thus permitting alterations in chromatin structure and modulating activity of the transcriptional machinery (Steger, 1999, Meikar et al., 2013). Some transcription factors are omnipresent and control numerous genes in a variety of tissues, while others are limited in distribution and

control tissue-specific gene expression (Eddy, 1998, Yu et al., 2003). High levels of transcription of some genes in testicular cells are associated with the up-regulation of general transcription factors such as TFIIB, TFIID, TBP and RNA Polymerase II and the presence of testis-specific transcription factors such as CREM (Eddy, 2002, Han et al., 2001). CREM is a c-AMP responsive element binding protein that binds to CRE (c-AMP response elements) on promoter of target genes of both transcriptional activators (CREMτ, τ1, and τ2) (Daniel et al., 2000, Kimmins et al., 2004). CREMτ is the main transcriptional activator isoform in the testis, with strong expression in spermatogenesis where it regulates expression of genes vital for spermatogenesis (Kimmins et al., 2004, Sassone-Corsi, 2000). Furthermore, some genes have been found that encode proteins with necessary roles in the specific function and structure of spermatogenic cells such as protamines and transition proteins. Transition proteins are families of extremely basic chromosomal structural proteins that consecutively substitute the histones within elongating and elongated spermatids, leading to conversion of chromatin from a nucleosomal organization to smooth fibrils (Zhao et al., 2004, Kleene, 2001). Some multi-subunit transcription factor complexes bind a varied range of regulatory elements in the promoter regions of many spermatogenesis-expressed genes instead of merely TATA box, CRE box or other specific DNA promoter sequences used in somatic cells.

DNA methylation is a process that requires conserved DNA sequences at cytosine bases to be converted to 5-methylcytosine by DNA methyl transferase (DNMT) enzymes (Suzuki and Bird, 2008). Methylation is thought to play a vital role in containing gene expression, probably by blocking the

promoters at which activating transcription factors would bind. Disturbance of proper DNA methylation shows that it is fundamental for cell differentiation and in modulating gene expression with increased methylation of promoters generally correlating with low or no transcription (Suzuki and Bird, 2008). Although methylation patterns can be influenced by exogenous signals, in spermatogenic cells, it is mainly determined by the intrinsic genetic programme of the cell (Estecio and Issa, 2011).

1.3.2 Regulation of translation during spermatogenesis

Regulation of translation is an essential feature of gene expression in meiotic and haploid spermatogenic cells in mammals (Kleene, 2003). Translational regulation of nucleoprotein transcripts has been shown to be important for control of the expression of transition proteins, protamines and other post-meiotically expressed factors (Kleene, 2003, Steger et al., 1998). The genes for protamines and transition proteins are transcribed in both round and elongating spermatids (Steger et al., 2000). The mRNAs transcripts of transition protein and protamines are stored for several days as ribonucleoprotein (MRNP) and are then translated in elongating and elongated spermatids (Kleene, 1996, Dadoune, 1995, Tseden et al., 2007). It has been shown that, in haploid spermatids, virtually every mRNA displays evidence of translational repression. This involves protein repressors which bind to the poly-A tail or specific RNA sequences located in the 3'-UTR (Steger, 1999, Steger et al., 2000). For example, Studies in transgenic mice have shown that a sequence in the last 62 nucleotides of the 3' untranslated region UTR regulates translation of protamine 1 mRNA in spermatids (Kleene, 2003, Braun et al., 1989).

1.3.3 TATA binding protein family

Differentiation of spermatids involves upregulated expression of the TATA-binding protein (TBP) family and its associated cofactors (TBP) family (Kimmins et al., 2004). TBP is a part of the general transcriptional machinery that is involved in transcription from three distinct nuclear RNA polymerases, each of which requires a unique set of general transcription factors (Hernandez, 1993, Lescure et al., 1994, Koster and Timmers, 2014). TBP was discovered as the key component of the transcription factor TFIID complex, mediating contact with the core promoter by interaction with the TATA-box (Kao et al., 1990, Blair et al., 2012). In addition, it was found to mediate DNA contact in the SL1 complex and the TFIIIB complex during transcription of rRNAs via RNA polymerase I (Hernandez, 1993, Knutson and Hahn, 2011). Additionally, other members of the TBP-family were identified, first termed the TBP related factors (TRFs), which are especially found in metazoa (Dantonel et al., 1999, Sepe et al., 2011). They function in some complexes involved in core promoter recognition and assembly of the pre-initiation complex. As a result of gene duplication, eukaryotes have expanded their repertoire of TATA-binding proteins, leading to a variable composition of the transcription machinery. In vertebrates, this repertoire consists of TBP, TBP-like factor (TLF) and TBP2. All three factors are essential, with TLF and TBP2 playing a significant role in development and differentiation, specifically gametogenesis and early embryonic development, while TBP dominates somatic cell transcription. TBP-related factors might compete for promoters when co-expressed, but also show preferential interactions with subsets of promoters. Initiation factor switching occurs as a

result of differential expression of these proteins in gametes, embryos and somatic cells. Paralogs of TFIIA and TAF subunits account for additional variation in the transcription initiation complex. This variation in core promoter recognition accommodates the expanded regulatory capacity and specificity required for germ cells and embryonic development in higher eukaryotes (Akhtar and Veenstra, 2011).

1.3.4 TATA box binding protein-like 1 (Tbpl 1)

Tbpl 1 is a protein usually thought to belong to the general transcription initiation complex (Martianov et al., 2002).The rule of transcription initiation by RNA polymerase II (Pol II) is vital to any developmental process. Nevertheless, there are different types of TATA-binding protein like factor (TLF) between metazoan species, from C.elegans to human (Dantonel et al., 1999, Koster and Timmers, 2014). These include: TLF (Kaltenbach et al., 2000, Akhtar and Veenstra, 2011), TBP related factor 2 (TRF2) (Rabenstein et al., 1999, Duttke et al., 2014), TRF and TBP related protein (TRP) (Li et al., 2014 , Moore et al., 1999, Maldonado, 1999); TLF is similar in sequence to TBP but has a unique distribution in spermatogenesis. Transcription reactions *in vitro* have clearly demonstrated that TLF is unable to substitute for TBP (Moore et al., 1999, Verma et al., 2013) due to variations in the DNA interaction region (Berk, 2000). TLF does interact however with the general transcription factors TFIIA and TFIIB, and has been demonstrated to bind the pes-10 promoter (Kaltenbach et al., 2000). Overexpression of TLF in human cells can lead to reciprocal regulation of the NF1 and c-fos genes. As the TATA-less NF1 gene is directly up-regulated; the TATA-dependent c-fos gene is repressed by the overexpression of TLF (Chong et al., 2005b). TLF

has been found to be part of a complex with DNA replication-related element binding factor (DREF). Certainly, the DREF/TLF complex is demonstrated to control the DRE-element involving an upstream promoter in the tandem promoter of the Drosophila PCNA gene (Hochheimer et al., 2002). An additional target is the histone H1 promoter, which is exclusively regulated by TLF, while the core histones (H2A, H2B, H3 and H4) in the tandemly arranged Drosophila histone gene cluster are regulated in a TBP-dependent manner. DREF is unable to co-localize with TLF at the histone cluster suggesting the existence of a distinct TLF-containing promoter recognition complex (Isogai et al., 2007). However, TLF shows redundancy in early embryogenesis in mouse as TLF knockout mice are viable. The males are infertile due to late arrest in spermiogenesis, which is concordant with the differential expression of TLF in humans and mice whereby high post-meiotic expression levels are seen (Martianov et al., 2001).

1.3.5 Four and a half LIM domains 5 (FHL5)

The transcriptional regulation of postmeiotic genes follows highly specific rules that seem to be unique to male germ cells (Sassone-Corsi, 2002, Gan et al., 2013). CREM has been described as a master switch for numerous postmeiotic genes, and its function involves some components of the general transcription machinery, such as transcription factor IIA (De Cesare et al., 2003, Wu et al., 2010) and a testis-specific co-activator, ACT (Fimia et al., 1999). ACT, activator of cAMP-responsive element modulator in testis is a LIM-only protein that interacts with transcription factor CREM in postmeiotic male germ cells and enhances CREM-dependent transcription. CREM regulates many crucial genes required for spermatid maturation, and

targeted mutation of the Crem gene in the mouse germ-line blocks spermatogenesis (Fimia et al., 1999, Wu et al., 2010). The CREM has been shown to bind Fhl5 which is specially expressed in meiotic spermatocytes and extremely persuaded into the post-meiotic round spermatids (Lardenois et al., 2009). Fhl5 is a protein having four and a half LIM domains which are protein-protein interaction motifs that form numerous factors needed for physiological processes such as transcription and signal transduction (Blendy et al., 1996, Kimmins et al., 2004). In yeast and mammals, transfection assay using heterologous promoter constructs has shown that FHL5 protein mediated strong reporter gene expression. Furthermore, FHL5 has been found to be dynamic with its pattern of nuclear and cytoplasmic localization throughout early and late phases of spermiogenesis, which is mediated by direct interaction with the Kif17b kinesin motor protein (Fimia et al., 1999, Macho et al., 2002).

During the postmeiotic phase of spermatogenesis, a testis specific protein is required: Activator of CREM in the Testis (ACT), which allows stage-specific activation of CREM and thus induction of gene expression (Cheng, 2008, Lardenois et al., 2009). Both ACT and the transcription factor CREM are essential for the temporal control of gene expression (Fimia et al., 2000). Transcriptional activation of those genes is principally regulated by the transcription factor CREM, activates phosphorylation, which in turn by its co-activator ACT (Fimia et al., 1999, Wu et al., 2010). It has been found that for normal spermatogenesis, the correct expression of ACT and the CREM-regulated gene expression pathway is crucial (Nantel et al., 1996, Liu et al., 2010). Sub-cellular localisation of ACT is regulated by a kinesin motor

protein (KIF17b), which interacts with ACT in haploid spermatids. This allows ACT to be transported from the nucleus to the cytoplasm at particular steps of spermatids development (Wong-Riley and Besharse, 2012, Kotaja et al., 2004). ACT is detected in both the nucleus and cytoplasm of the elongating spermatids (Macho et al., 2002, Wong-Riley and Besharse, 2012) and it plays a major role in the regulation of the expression of protamines and other key spermiogenesis proteins (Carrell et al., 2007).

Thus, there have been a number of transcription factors identified, which play a crucial role in the transcriptional activation of genes in haploid spermatids; unfortunately, due to the lack of any spermatid cell lines many questions concerning haploid gene expression are still unanswered (Bukowska et al., 2013, Bellefroid et al., 1998, Cunliffe et al., 1990, Lee et al., 1996). Many genes with essential functions in spermatogenesis contain the cAMP response element in their proximal promorter (Sassone-Corsi, 1998, Liu et al., 2010). This recognizes via the CREM modulator, a main regulator of gene expression in germ cells (Masquilier et al., 1993, Kimmins et al., 2004, VanGompel and Xu, 2010).

1.3.6 General transcription factor IIA, 1-like (Gtf2a1l)

ALF (TFIIA alpha/beta-like factor) is a germ cell-specific counterpart of the large (alpha/beta) subunit of the general transcription factor TFIIA. This factor is able to interact with the small TFIIA subunit (γ) to form a heterodimeric complex that stabilizes binding of TBP to promoter DNA (Upadhyaya et al., 2002, Akhtar and Veenstra, 2011). It binds specific DNA sequences to control the transcription of genetic information from DNA to

mRNA. This protein contributes to post-meiotic gene expression during spermatogenesis as a regulator of transcription. Transcription factors place RNA polymerase at the start of protein coding sequences. Subsequently the polymerase is released to transcribe the mRNA. ALF is generally expressed and transcriptionally up-regulated in male germ cells (Han et al., 2001, Upadhyaya et al., 2002). Previous work has demonstrated that the expression of ALF is restricted to male germ cells in the testis of mice and humans (Upadhyaya et al., 1999, Ozer et al., 2000), specifically in the pachytene stage of meiosis I along with a number of other transcription factors (Han et al., 2001). However, biochemical characterization of recombinant ALF-TFIIAγ and TFIIAα/β-TFIIAγ complexes did not reveal significant differences in vitro (Upadhyaya et al., 2002), and it remains unclear what specific role ALF might play during germ cell development (Huang et al., 2006).

Expression of ALF protein and investigation of its function in the testis of mouse make it valuable for the study of male infertility as many different defects in the protein can damage sperm production (Huang et al., 2006). ALF is an interesting model for the study of gene regulation in germ cells because its developmentally regulated expression through the pachytene stage of meiotic prophase in males parallels that of other germ cell-specific transcription factors (Schmidt and Schibler, 1995, Han et al., 2001, Catena et al., 2005).

1.3.7 Mechanism of transcription regulation factors during male germ cells

Transcription factors of the cAMP-response-element binding protein (CREB)-CREM family, target genes with cAMP response element containing the palindromic consensus sequence TGACGTCA (Sassone-Corsi et al., 1988). CREM is a key regulatory gene for spermatogenesis. *In vivo*, CREM is regulated by the secretion of follicle stimulating hormone (FSH) as demonstrated in rats and golden hamster (Foulkes et al., 1993). Activation of CREM results in downstream phosphorylation of protein kinase A or mitogen activated protein kinases (MAPKs). Phosphorylation of CREM at serine 117 results in interaction with co-activators which link CREM to the transcription machinery through TFIIB, which are core proteins of the preinitiation complex (Foulkes et al., 1993). The activity of CREM is enhanced through association with the LIM-only protein, activator of CREM in the testis (ACT). The CREM-ACT pair is regulated by a kinesin protein named KIF17b, which is similar to an isoform found in the brain, KIF17 (Macho et al., 2002). The cellular distribution of KIF17b and ACT are spermatogenic-stage-specific. They are both present in the nucleus in the round spermatid stage and are both in the cytoplasm at stage VIII in elongated spermatids. This suggests that KIF17b regulates the transcription of CREM by removing ACT from the nucleus. This assertion is supported by the inhibition of the expression of CREM target genes by KIF17b through sequestration of ACT in the cytosol (Macho et al., 2002). CREM is a key regulator of transcription in male germ cells in association with general transcription initiation complex. Transcription is initiated by basal transcription factors (TFIIA, B, D, E) and their associated

factors- TBP-associated factors (TAFs) through interaction with the promoter elements which includes a TATA-box. All proteins aggregating at the TATA box are referred to as TATA-box binding proteins (TBPs). TBP is important but not essential for RNA polymerase II interaction with the promoter and initiation of transcription (Wieczorek et al., 1998). While TFIIAα/β-like factor is expressed in the testis, TFIIB, TBP and RNA polymerase II are highly expressed in round spermatids (Kimmins et al., 2004). TBP-like factor (TLF) has sequence similarity with TBP but cannot substitute for TBP. TLF interacts with TFIIA and TFIIB at the pes-10 promoter. This has been linked to a possible role in gene transcription from a TATA-less promoter, a feature of CYP51, a post-meiotic CREM target gene (Kaltenbach et al., 2000). TFIID, a component of the TBP complex is essential for the transcription of protein coding genes. TAF7L, a testis specific paralogue of TAF7 associates with TFIID (Bhattacharya et al., 2014). TAF7 and TAF7L have mutually exclusive roles; while TAF7 is found in the nucleus in developing germ cell and in late-pachytene stage, TAF7L appears in the nucleus as TAF7 moves to the cytosol and remains in the nucleus until transition to elongating spermatids (Kimmins et al., 2004).

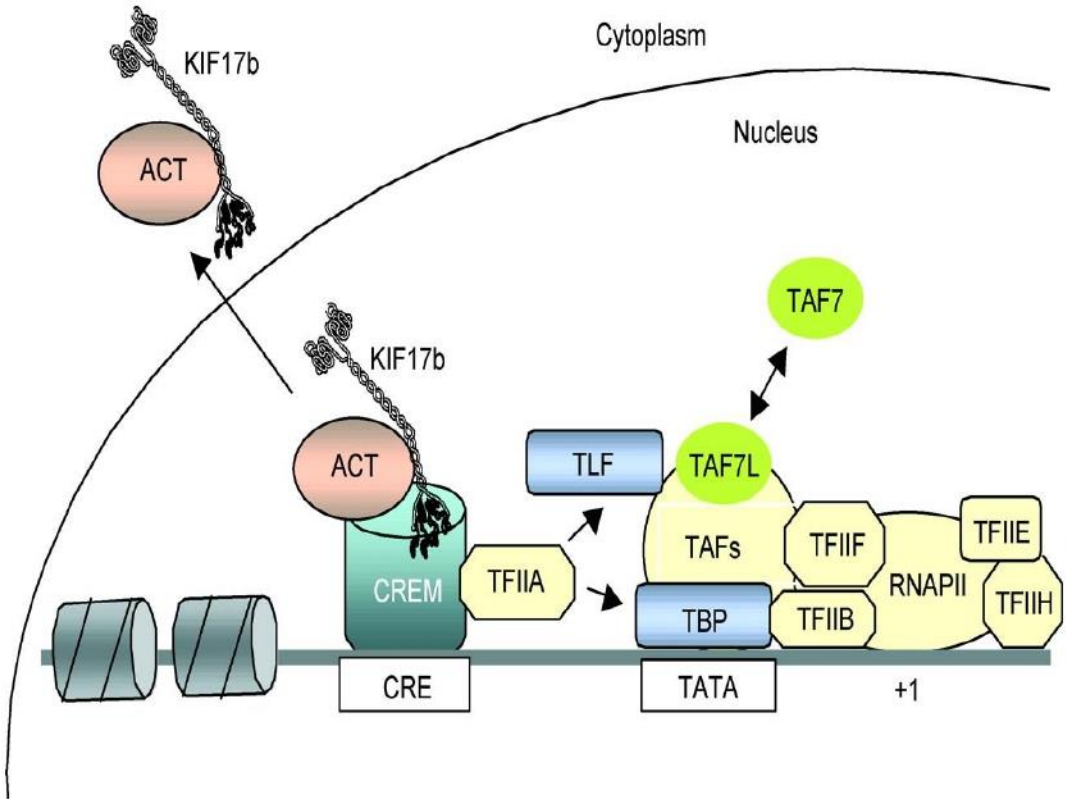

Figure 1.2: Transcription initiation complexes that organize spermiogenesis. Adapted from Kimmins et al., (2004).

1.4 Genotoxicity

Genotoxins are a large group of substances that induce changes to the structure and/or function of genes by chemical interaction with DNA and non-DNA targets (Maurici et al., 2005).

Male reproductive genotoxins are chemicals that can affect reproductive competence in the male via genetic damage, apoptosis or mutation in the gametes. They may cause fertility impairment and may also be risk factors for developmental defects and heritable diseases in the offspring. This latter process is known as male-mediated teratogenesis (Anderson et al., 2014, Anderson, 2005). There is rising concern over the possible heritable effects

of chemical mutagens used as anticancer drugs (Witt and Bishop, 1996, Vilarino-Guell et al., 2003).

1.4.1 DNA damage

DNA damage is broadly divided into two major classes, endogenous DNA damage and exogenously or environmentally-induced DNA damage. Endogenous DNA damage includes the DNA damage caused by free radicals or alkylating agents endogenously generated during cellular metabolism, hydrolytic damage and DNA replication errors and chemical mutagens. Environmentally-induced DNA damage refers to that caused by physical and chemical agents generated outside the cell (Tuteja et al., 2001, Rastogi et al., 2010). There are many different types of DNA damage and some examples are shown in Figure 1.3.

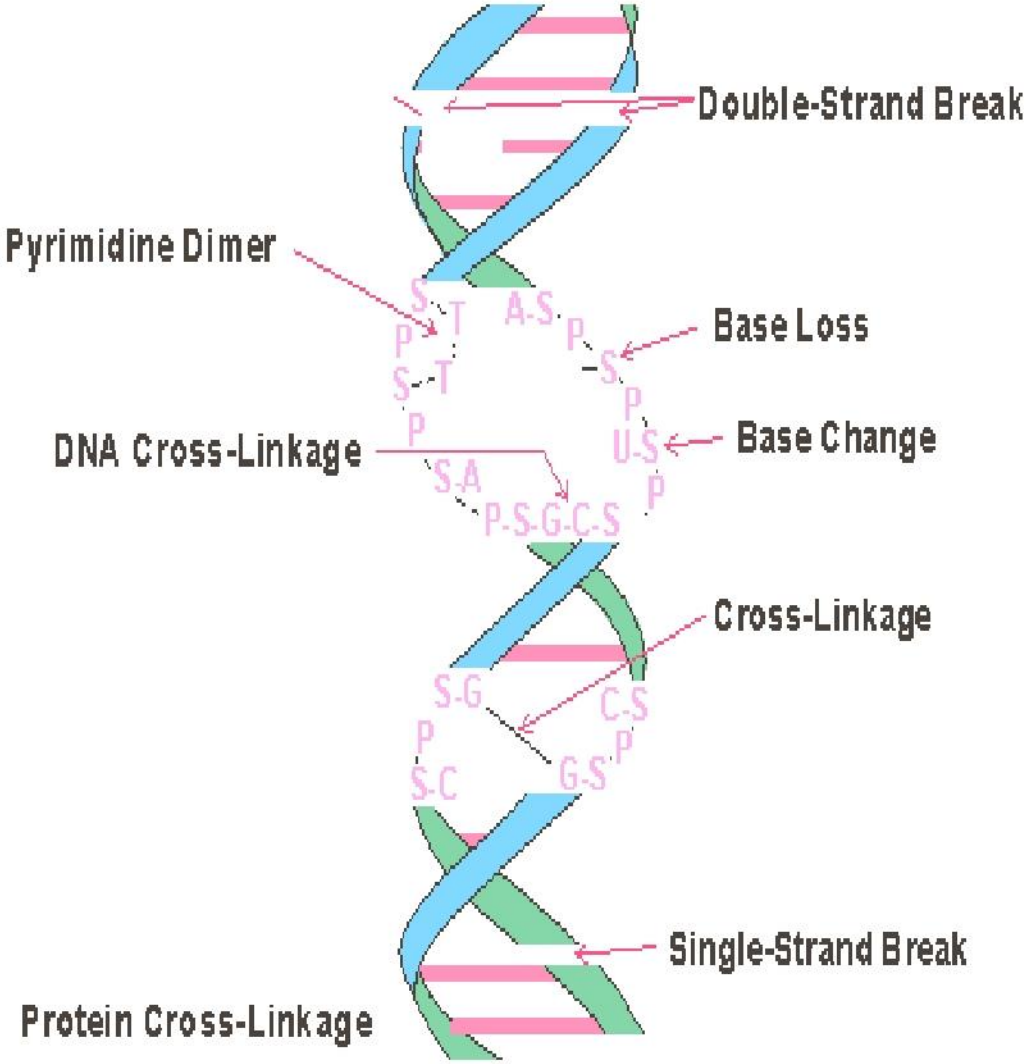

Figure 1.3: Different types of DNA damage that can occur after exposure to chemicals or radiation (From http://www.radiation-scott.org/radsource/3-0.htm, accessed on 23/01/2015).

1.4.1.1 Types of DNA damage

1.4.1.1.1 Oxidation

Oxidative DNA damage includes reactive oxygen species (ROS). ROS readily attack DNA and can produce many types of DNA lesions, such as oxidized DNA bases, basic sites, and both single-(SSB) and double-strand DNA breaks (DSB), which, if they eventually involve damage to DNA repair enzyme genes, can lead to genomic instability (Evans et al., 2004, Krokan et al., 1997). DNA oxidation by ROS that are generated during the cells via normal aerobic metabolism is one of the most common types of endogenous DNA damage (Wang et al., 2013). ROS react with nucleic acids and proteins, producing oxidative damage to these macromolecules (Chakravarti and Chakravarti, 2007, Karihtala and Soini, 2007). The most reactive ROS is the hydroxyl radical. This can cause the oxidation of DNA bases; the most common adduct formed is 7, 8-dihydro-8-oxo-deoxyguanosine (8-oxodG) (Dizdaroglu et al., 2002). It is an extremely mutagenic lesion that in consequence leads to G: C to T: A transversions (Grollman and Moriya, 1993, Wang et al., 2013). In addition, the hydroxyl radical can react with adenine in a similar way to guanine, however this lesion is far more uncommon in DNA damage than 8-oxodG. If unrepaired, the 8-oxodG base will no longer pair with cytosine but instead pairs with adenosine and is replaced with a thymine at the next round of DNA replication (Russo et al., 2004). Damage caused by ROS can be neutralized by raised antioxidant defenses, which include superoxide dismutase, glutathione peroxidase and catalase to scavenge ROS and convert it to nontoxic forms (Alexeyev, 2009). Many studies have reported that oxidative damage is common in sperm and

testicular DNA (Wellejus et al., 2000, Tremellen, 2008, Kushwaha and Jena, 2012). Furthermore, it has been found that the level of damage in terms of (8-oxodG) is closely associated with male infertility (Loft et al., 2003, Wellejus et al., 2004).

There are two step theories for the origins of DNA damage in the male germ. This theory suggests that an extensive diversity of clinical and environmental factors is susceptive, alone or in combination, of making oxidative stress in the testes (Aitken and Koppers, 2011). During step one, oxidative stress damages spermiogenesis resulting in the making of faulty spermatozoa having poorly protaminated chromatin (Aitken and Koppers, 2011). These faulty spermatozoa have a propensity to default to an apoptotic cascade that includes the generation of ROS via the sperm mitochondria (Aitken and Koppers, 2011). During the step two, these ROS attacks the poorly changed chromatin making oxidized DNA base adducts (8OHdG) that eventually results in DNA strand breakage and cell death (Aitken and Koppers, 2011, De Iuliis et al., 2009, Irvine et al., 2000) as shown in Figure1.4.

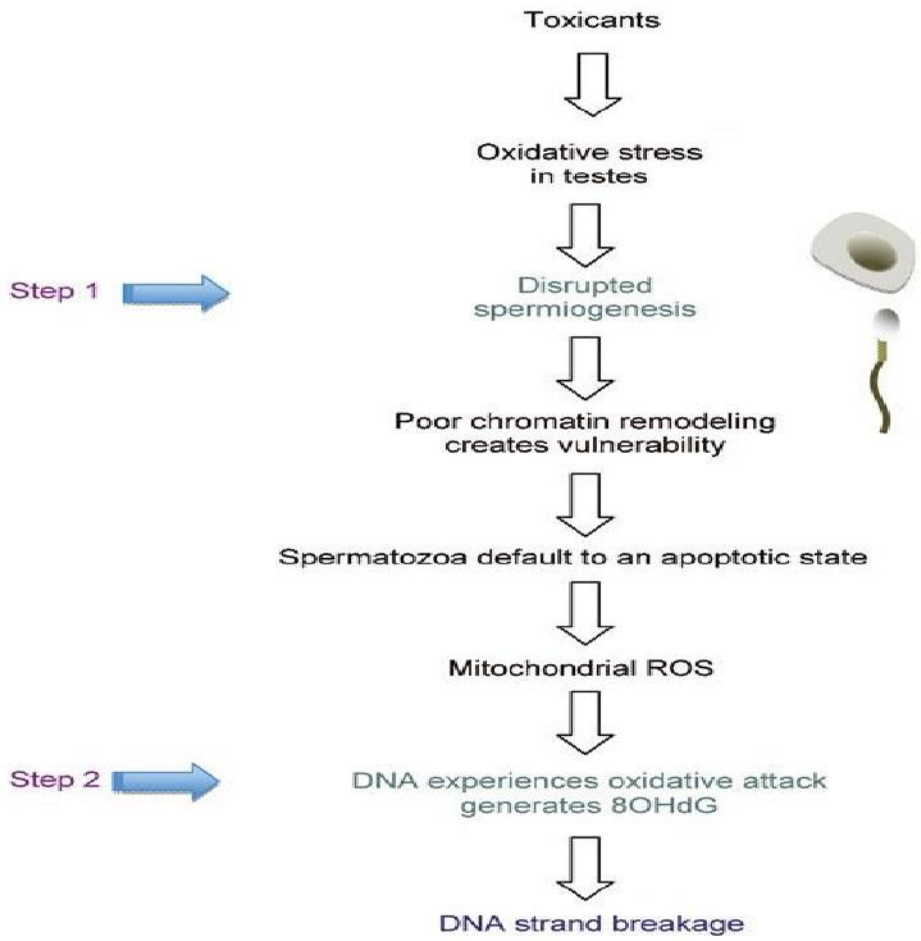

Figure 1.4: Two step theories for the origins of DNA damage into the male germ line. Adapted from Aitken and Koppers (2011).

1.4.1.1.2 Alkylation

Alkylation is the transfer of an alkyl group from one molecule to another, leading to a base alteration, with the simplest type of modification being methylation. Alkylation is accomplished by an alkyl electrophile, alkyl nucleophile or sometimes as alkyl radical (Gocke et al., 2009, Drablos et al., 2004a).

Absorption of ultraviolet radiation affects adjacent thymine residues causing a DNA strand to be joined via creation of the bond resulting in thymine dimer formation (Narayanan et al., 2010).

1.4.1.1.3 Alkylating agents

Many alkylating agents have roles as chemotherapeutic agents against a range of experimental and human cancers (Kondo et al., 2010, Sancar et al., 2004). These agents exhibit cellular cytotoxicity as they interact directly with cellular DNA, creating a huge range of genetic alterations such as base alkylation, double- and single-DNA strand breaks and cross-linking etc (Kondo et al., 2010, Sancar et al., 2004).

Alkylating agents represent one of the most important types of anticancer agents and play an important role in the treatment of numerous types of cancers (Kondo et al., 2010). Exposure to alkylating agents is principal cause of DNA and RNA damage, generating adducts that can compromise genomic integrity (Drablos et al., 2004b). Formed adducts can disrupt transcription and replication, and initiate apoptosis or be mutagenic if left unrepaired (Drablos et al., 2004b, Hecht, 1999, Bahadur et al., 2005). It has even been suggested that exposure to chemotherapy is one of the causes of the alleged significant decrease in the sperm counts for the past 50 years. Male germ cells were shown to be acutely influenced via different chemotherapeutic agent (Holm et al., 2009).

1.4.1.1.3.1 N-ethyl-N-nitrosourea (ENU) and N-methyl-N-nitrosourea (MNU) mutagenesis

N-ethyl-N-nitrosourea (ENU) and N-methyl-N-nitrosourea (MNU) (Figures 1.5 and 1.6) are well-known, potent, direct-acting, transplacental mutagens and carcinogens (Donovan and Smith, 2010). ENU and MNU are potent mutagens, and mainly affect spermatogonial stem cells. ENU and MNU have found be induced random point mutations in the spermatogonial stem cells at a frequency of ~150 × 10-5 per locus in mice (Russell et al., 1979).

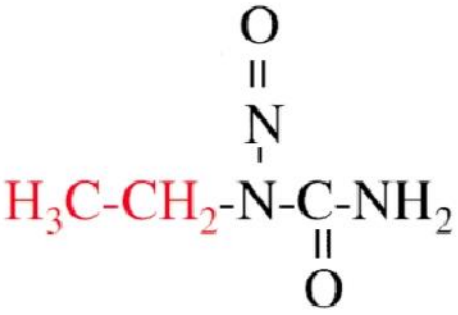

Figure 1.5: Structural formula of ENU

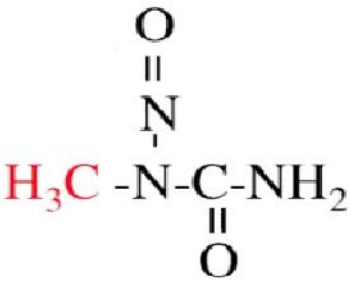

Figure 1.6: Structural formula of MNU

The molecular damage caused by alkylating agents is enormous. Both ENU and MNU cause DNA damage by transferring a methyl or ethyl group to the

oxygen or nitrogen atoms of nucleic acid bases (van Boxtel et al., 2010, Noveroske et al., 2000, Wyatt and Pittman, 2006). For example, ENU causes ethylation of the bases in DNA at the 7-N and the 6-O positions. When 7-ethylguanine is produced, it pairs with thymine to cause G: C to A: T transition mutation (Noveroske et al., 2000).

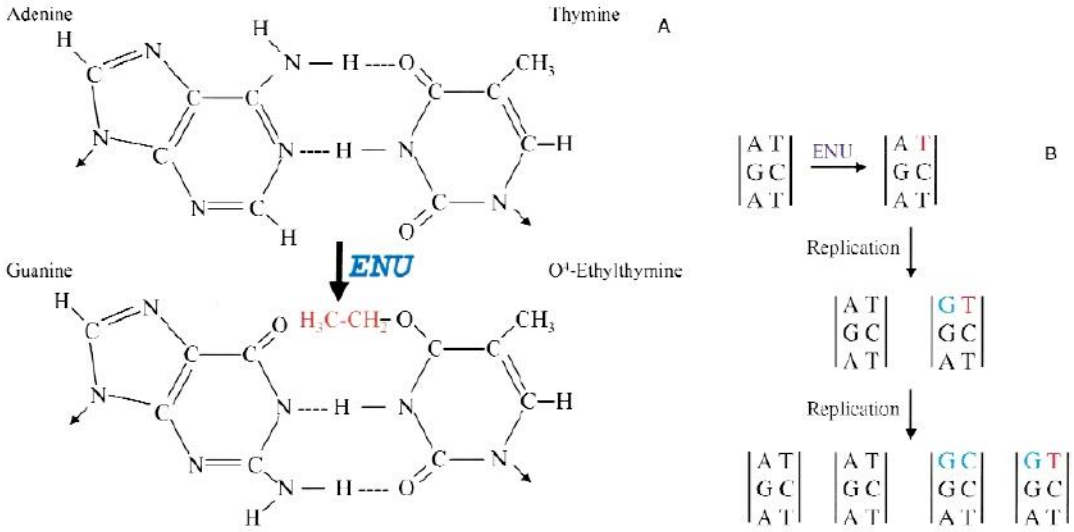

Figure 1.7: Mechanism of action of ENU. A) Alkylation of thymine results in the formation of O4-ethylthymine which is recognised as cytosine and mispairs with guanine. B) Mispairing leads to the corresponding base exchange during DNA replication. Taken from Noveroske et al., (2000).

1.4.1.2.1.2 Methyl methanesulfonate (MMS) and ethyl methanesulfonate (EMS) mutagenesis

Methyl methanesulfonate (MMS) and ethyl methanesulfonate (EMS) are monofunctional DNA methylation agents that chemically alter DNA and are known carcinogens (Greer and Rinehart, 2009, Beranek, 1990). Many possible reaction sites for MMS and EMS have been identified in the four bases of DNA although the different bases have different ranges of reactive sites: guanine, N1, N3, N7, N2; adenine, N1, N3, N7 and N6; and O6; cytosine, N3, N4 and O2; thymine, N3, O2 and O4 (Friedberg et al., 2006). Adducts of these chemicals can block DNA synthesis and may form mismatches leading to transition mutations (Lindahl et al., 1988). MMS and EMS mainly methylate DNA on N7-deoxyguanine and N3-deoxyadenine (Wang et al., 1992). MMS is a directly acting DNA-methylating agent effecting alkylation of base nitrogens such as 7-methylguanine, while the oxidizing agent peroxynitrite creates reactive oxygen species (ROS) and oxidized base damage such as 8-oxoguanine (Horton and Wilson, 2013). These N-alkylations have the ability to be repaired rapidly and have a minimal potential for mutagenicity. Thus, MMS mutagenicity can occur via abasic site by β-elimination of the N-glycosylic bond or by a DNA glycosylase repair enzyme (Glaab et al., 1998, Seidel et al., 2004).

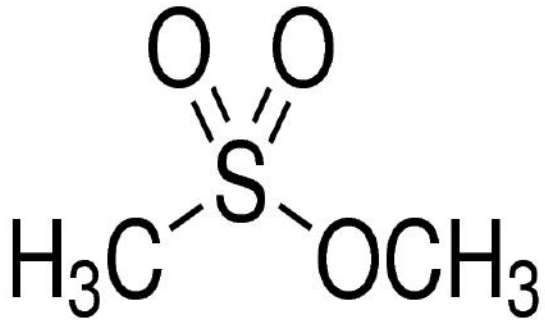

Figure 1.8: Structural formula of MMS

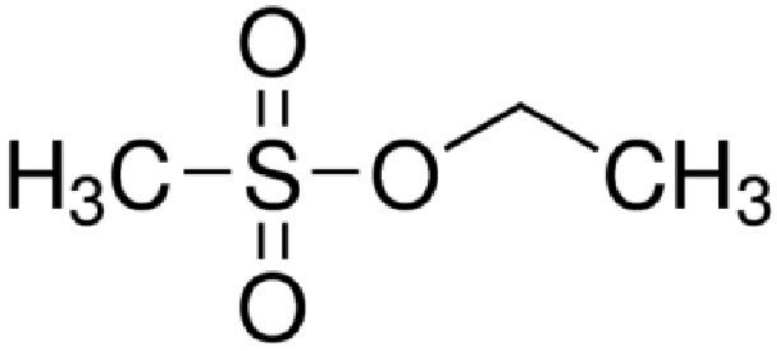

Figure 1.9: Structural formula of EMS

1.4.1.2.1.3 6 Mercaptopurine (6MP)

6-Mercaptopurine (6MP) is one of the most common chemotherapy agents used to treatment of childhood acute lymphoblastic leukemia (Rehman et al., 2014, Karran, 2006). It is also used in the treatment of inflammatory disorders, and as an immunosuppressant (Rehman et al., 2014). 6-MP is a member of the antimetabolite class of chemotherapy agents that leads to inhibition of *de novo* purine synthesis (Swann et al., 1996, Rehman et al., 2014). Different mechanisms of action of 6-MP have been described for thiopurines including: the blocking of replication via incorporation into DNA

and transcription via incorporation into RNA; blocking Rac-1-mediated signal transduction; and an antimetabolic effect during inhibition of GTP synthesis by 6-methyl thioinosine monophosphate (6-MeTIMP) (Cara et al., 2004, Prufer et al., 2014). 6-MP is also able to regulate the expression of genes, which it can either up- or down-regulate (Taki et al., 2013).

A gene expression study has also reported thiopurine-induced mutation during the expression of genes involved in protein- and ATP-biosynthesis (Zaza et al., 2005). Mice treated with 6-MP has showed that, significant mutation were showed in the expression of genes related to inflammatory responses, oxidative stress, and cell death (Kim HL et al.,2006).

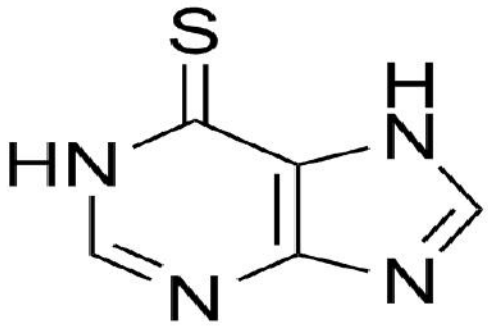

Figure 1.10: Structural formula of 6 Mercaptopurine

1.4.1.2.1.4 5-Bromo-2′-deoxyuridine (5-BrdU)

Bromodeoxyuridine (BrdU) is a synthetic thymidine analog that is commonly used in the detection of proliferating cells in living tissues and as a cell cycle marker (Webster et al., 2014). BrdU is incorporation into DNA results in many types of DNA damage, including mutations, sister chromatid

exchanges, chromatid breaks and micronucleation (Anisimov, 1994, Wojcik et al., 2003, Sato et al., 1993). Furthermore, it has been shown to induce polyploidization and hypermethylation of DNA (Call and Thilly, 1991, Hsu and Somers, 1962, Masterson and O'Dea, 2007). BrdU is incorporated into replicating DNA when the cell is preparing for division (during the S-phase of the cell), thus increasing the risk of transition mutations in dividing cells (Webster et al., 2014). Its effect on gene expression has not been investigated. However, an *in vitro* study by Endoh et al. (2007) showed that the expression of ectopic genes increased when cells were treated with BrdU close to the time of transfection (Endoh et al., 2007). In contrast, BrdU was found to decrease expression of endogenous genes (Meleady and Clynes, 2001, Lin et al., 1989, Webster et al., 2014). In many primary and transformed cell types, it has been shown that, BrdU administration results in the upregulation of some senescence-related mRNAs and proteins (Suzuki et al., 2001, Ross et al., 2008).

Work by Schmid et al., (2001) showed an effect of BrdU on the duration of meiosis in male mice. The development time from meiotic divisions in spermatocytes to epididymal sperm was evaluated by labeling cells with BrdU within the last S-phase preleptotene (Schmid et al., 2001).

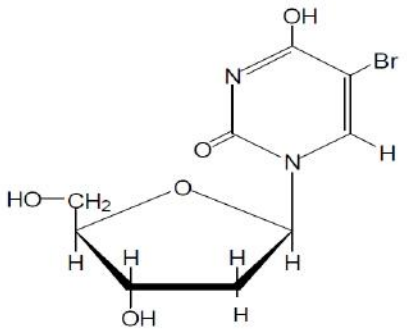

Figure 1.11: Structural formula of 5-Bromo-2′-deoxyuridine

The incorporation of BrdU into DNA has been found to be very valuable in many biological systems to study the fraction of S phase cells, the banding pattern of early and late replicating regions of chromosomes and their subnuclear localization, as well as the size and distribution of replicons on separate DNA fibers (Dolbeare, 1995, Lengronne et al., 2001).

1.4.1.2.1.5 Doxorubicin (Adriamycin)

Doxorubicin is one of the most common chemotherapeutic agents used in the treatment of a variety of cancers. Doxorubicin is an anthracycline antibiotic isolated from the bacterium Streptomyces peucetius var. caesius which was obtained from S. peucetius via mutagenic treatment (Li et al., 2008, Arcamone et al., 2000). It causes antitumour activity by producing DNA damage through three major mechanisms. The first is intercalation into DNA, which may disrupt replication and transcription of genomic DNA and lead to the death of cancer cells (Tewey et al., 1984, Lei et al., 2012). Secondly, it inhibits both cellular DNA and RNA synthesis, presumably by direct binding (Momparler et al., 1976, Li et al., 2008). The third mechanism is its action as an inhibitor of DNA topoisomerases I and II (Wassermann et

al., 1990). Doxorubicin can also interact with the cell membrane, by binding to negatively charged phospholipids; it changes the membrane dynamics and fluidity, this causes lipid peroxidation and interferes with membrane related enzyme activity (Speelmans et al., 1994, Parker et al., 2001). However, an indirect mechanism for doxorubicin action has been proposed. Metabolism of doxorubicin inside the cell creates free radicals by means of redox reactions. This reactive oxygen species can then harm DNA by oxidation of bases and effect lipid peroxidation in the cell membrane, causing indirect cytotoxicity of doxorubicin (Umlauf and Horky, 2002, Suominen et al., 2003).

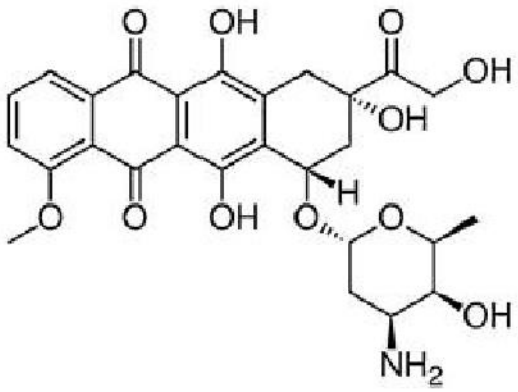

Figure 1.12: Structural formula of doxorubicin

Many studies have reported that doxorubicin can impair male fertility by the induction of DNA damage in spermatogenic cells (Baumgartner et al., 2004, Kang et al., 2002). Throughout spermatogenesis, the different germ cell types have different susceptibilities to genotoxic agents (Aguilar-Mahecha et al., 2005). Therefore, the nature and extent of genotoxicity caused by doxorubicin during spermatogenesis is cell-type dependent (Kang et al., 2002, Prahalathan et al., 2004). The genotoxicity of doxorubicin on spermatogonial cells and spermatocytes during meiosis and rapidly differentiation has been evident by a number of studies (Kang et al., 2002, Prahalathan et al., 2004).

1.4.2 Mismatches of DNA

The cell requires continual repair to maintain integrity of DNA replication, to preserve genome stability and to ensure the proliferation of species (Mukherjee et al., 2010). Mutation can occur through mismatches of DNA bases resulting in replication errors in which the wrong DNA bases are stitched into place in newly forming DNA strands. Other replication errors include the skipping over or incorrect insertion of DNA bases. Spontaneous or induced base modifications and recombination errors can also lead to mutation (Marti et al., 2002). Some genotoxic agents such as the alkylating agents described above can covalently bind to DNA and produce errors in DNA replication, thus increasing the number of mutations (Fox et al., 2012).

1.4.3 Cross linkages

DNA crosslinking damage happen when crosslinking agents covalently join two nucleotide residues from either the same DNA strand (intrastrand crosslink [ICLs]) or different strands (interstrand crosslink). Intrastrand crosslinks can be easily removed via the nucleotide excision repair (NER) mechanism (Y Huang et al., 2013, Odonovan et al., 1994). Bulky adducts produced by exposure to exogenous compounds, including some antibiotics such as mitomycin C, can react with reagents such as nitrite ion to form covalent linkages between bases in one strand (Hlavin et al., 2010, Balu et al., 2006). More focused studies have been reported on the chemistry of DNA crosslinking compounds used as chemotherapeutic agents (Brulikova et al., 2012, Rajski and Williams, 1998). DNA crosslinks can also occurred by ultra violet light, especially the formation of intrastrand dimers between two pyrimidines, known as cyclobutane pyrimidine dimers (CPDs) on the same strand (Nejedly et al., 2001, Cecchini et al., 2005, Ichihashi et al., 2003).

1.5 Apoptosis

Apoptosis (programmed cell death) is a well-defined physiological process that serves to eliminate damaged, diseased, or superfluous cells from various tissues of the body (Wyllie et al., 1980, Richburg, 2000, Thompson, 1995). Kerr, Wyllie and Currie were the first to use the term apoptosis or programmed cell death (Kerr et al., 1972, Wyllie et al., 1980). Apoptosis of germ cells plays a crucial role in regulating the number of spermatogenic cells supported by Sertoli cells through the first wave of spermatogenesis (Silva et al., 2011). Apoptosis during spermatogenesis has been widely

studied in mice and rat (Choi et al., 2004). The balance between levels of germ cell differentiation, proliferation and apoptosis is vital to the regulation of germ cell number during spermatogenesis. During the initiation of spermatogenesis, an apoptotic wave is required to remove irregular germ cells and to preserve the correct ratio between maturing germ cells and Sertoli cells (Koji, 2001, Giampietri et al., 2005). Many studies have shown that pathological conditions such as exposure to anticancer agents, exposure to ionizing radiation or toxic substances, hormonal depletion, heat stress, and loss of stem cell factor signalling can induce male germ cells apoptosis (Richburg, 2000, Choi et al., 2004, Gosden and Spears, 1997).

1.5.1 The process of apoptosis

Apoptosis is arbitrarily divided into initiation, signalling and execution stages by which cells speedily execute a death programme (Steller, 1995). There are two main pathways for apoptosis: The extrinsic or death receptor pathway and the intrinsic or mitochondrial pathway and molecules of one pathway can influence the other (Igney and Krammer, 2002, Zimmermann and Green, 2001). In addition, other pathways can be involved, such as the perforin/granzyme pathway that induces apoptosis by either granzyme A or granzyme B (Martinvalet et al., 2005).

Apoptosis is characterized by specific morphologic and biochemical properties. Morphologically, apoptosis is characterised by a series of structural changes such as membrane blebbing, chromatin condensation, cell volume shrinkage and cellular fragmentation into membrane apoptotic bodies (Steller, 1995, Majno and Joris, 1995, Wyllie et al., 1980).

Biochemically, apoptosis is characterised by events that include DNA laddering and DNA cleavage, phosphatidylserine exposure to the external leaflet of the plasma membrane and activation of caspase cascades (Fadok et al., 1992, Wyllie et al., 1980, Shaha et al., 2010).

1.5.2 Apoptosis in male germ cells

1.5.2.1 Apoptosis via the intrinsic pathway

The intrinsic pathway is activated in response to many forms of cellular stimuli, including DNA damage, oxidative stress and endoplasmic reticulum stress (Kroemer et al., 2007). These types of stimuli lead to mitochondrial dysfunction, involving changes in the inner mitochondrial membrane and opening of the mitochondrial penetrability transition pore (Kroemer et al., 2007). Subsequent activation of pro apoptotic, BH3-on of the members of the Bcl-2 family, down-regulate the anti-apoptotic proteins Bcl-2, Bcl-xL and Mcl-1, leading to disruption of mitochondrial membrane potential and release of Cytochrome c and S mac from the mitochondria into the cytosol, where Cytochrome c binds to apoptotic protease activating factor 1 (Apaf 1) and dATP. The subsequent activation of initiator caspase 9 and the following proteolytic activation of caspases 3, 6, and 7 ultimately results in the death of the cell (Taylor et al., 2008). See Figure 1.13 below for a summary of the process.

1.5.2.2 Apoptosis via the extrinsic pathway

The extrinsic pathway of apoptosis is activated by the binding of a death receptor, such as Fas, DR5 or tumour necrosis factor (TNF) receptor 1 to its

respective ligand (Peter and Krammer, 2003, Janssen et al., 2003). FASL binds to FAS, which induces the trimerization of FAS receptors and results in the binding of the adapter protein Fas-associated death domain-containing protein. The association of the adaptor FADD with Fas by the death domain leads to recruitment of pro-caspase 8 and results in the formation of the death inducing signalling complex (DISC), which leads to the auto-proteolytic processing of the caspases and initiates the process of apoptosis (Wajant, 2002). Similarly, binding of TNF ligand to TNF receptor results in the binding of the adapter protein TRADD. The extrinsic pathway via Fas is also illustrated in (Figure 1.13).

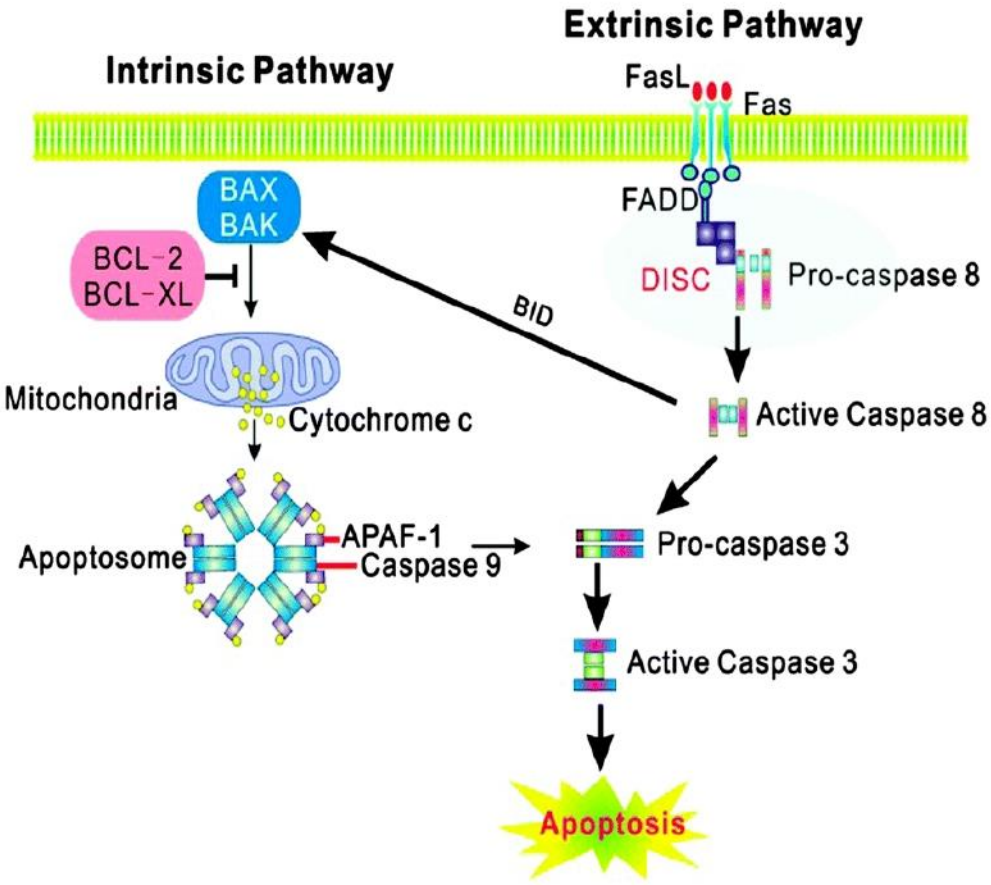

Figure 1.13: Schematic representation of the intrinsic and extrinsic pathways of apoptosis. Taken from Tan et al., (2014).

Many studies have shown that the intracellular balance of BclxL and Bax proteins plays a vital role during the early apoptotic wave (Russell et al., 2002, Yan et al., 2000, Adams and Cory, 2007, Vergara et al., 2011). A number of studies have also shown that the Fas/FasL system is the major inducer of germ cell apoptosis under particular pathological conditions such as exposure to chemotherapy drugs and hormone deprivation (Francavilla et al., 2000, Rockett et al., 2001, Aitken and Baker, 2013). In fact, some authors have reported that Fasl is only expressed in germ cells (Francavilla et al., 2000, Xu et al., 1999), while other authors claim that Fasl is present only in Sertoli cells (Woolveridge et al., 1999, Riccioli et al., 2000). The p53 is another common protein and has been defined as controller of both cell proliferation and apoptosis. Similar to Bcl-2 family members, p53 modulates the intracellular death-signaling pathway. A number of reports have showed the role of p53 in apoptosis during spermatogenesis. p53 plays a critical role in mediating both spontaneous and injury induced apoptosis in spermatogonial cells. Nevertheless, the majority of these reports showed that p53 is associated with regulation of apoptosis during mitotically active of spermatogonia. Another report showed that p53 might also control apoptosis in meiotic and postmeiotic germ cells (Figure 1.14) (Richburg, 2000, Beumer et al., 1998, Inoue et al., 2014).

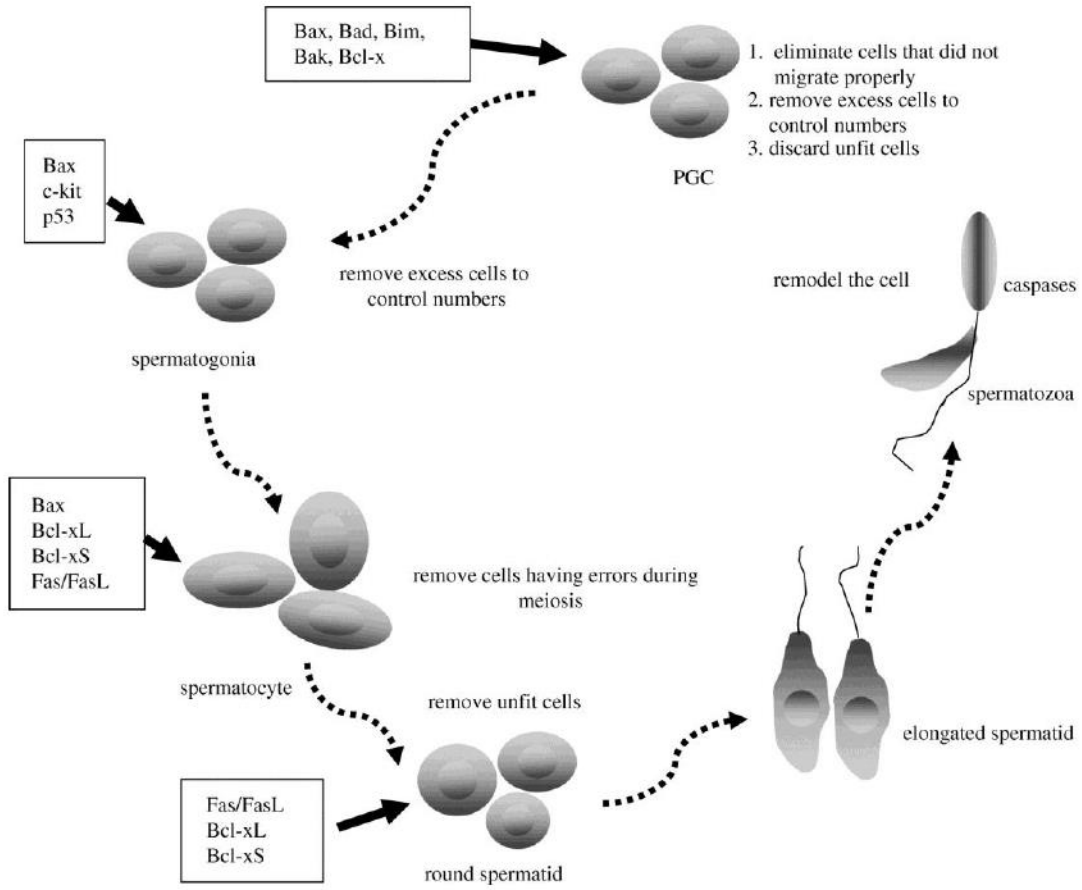

Figure 1.14: Diagram drawing illustrated points at which apoptosis happens within germ cells, the pro- and anti-apoptotic molecules involved and the functions of the apoptotic process associated with different phases of sperm differentiation and maturation. Taken from Shaha et al., (2010).

1.6 Methodologies to detect DNA damage, apoptosis and mutations in germ cells

Many methods have been used to investigate the induction of DNA damage and heritable effects of toxins in germ cells (Sutherland et al., 2000, Brendler-Schwaab et al., 2005).

The isolation of homogeneous populations of individual spermatogenic cell types is increasingly viewed as a model system for different types of studies of germ cell proliferation and differentiation (Chang et al., 2011b). There is no dependable cell culture system for spermatogenic differentiation in vitro, in addition most biological investigations on spermatogenic cells need tissue harvested from animal models such as mouse and rat (Bryant et al., 2013), The testis contains both non-spermatogenic cells (Leydig, Sertoli, myeloid, and epithelial cells) and spermatogenic cells (spermatogonia, spermatocytes, round spermatids, condensing spermatids and spermatozoa); hence, mechanistic studies in spermatogenesis need the isolation and enrichment of these different cell types (Bryant et al., 2013).

The possibility of obtaining homogeneous germ cells at defined stages of development is a prerequisite for the study of meiotic and post-meiotic germ cell function. Several methods have been proposed for separation of animal cells based on velocity sedimentation, equilibrium density fractionation, electrophoretic mobility and partition through aqueous, two-phase polymer systems (Bellve, 1993, Guo et al., 2004). The isolation and culture of homogeneous populations of the individual germ cells has permitted the analysis of gene expression in these cells in addition to studying their

mechanisms and growth requirements (De Miguel and Donovan, 2000, Dolci et al., 1991). Some important factors have been found in spermatogenic cells cultures in vitro; these factors are physiologically related to spermatogenic cells growth and development in vivo. Such factors include leukemia inhibitory factor (LIF) which was recognized as an important spermatogenic cells survival factor and mitogen in culture (De Miguel and Donovan, 2000, Dolci et al., 1991). Because of the complex process of spermatogenesis which depends on special hormones and different molecular conditions int the testes, a dependable *in vitro* culture system for the full procedure of germ cells have not yet been fully developed (Hess et al., 2006, Dores et al., 2012). Methods of cell culture have been established in order to create or to mimic cells, which are similar to primordial germ. However, to date these methods were unable to produce large numbers of these cells and also failed to generate later spermatogenic cell types in vitro (Hayashi et al., 2011, Easley et al., 2012). It is well known that the spermatogenic cell types are significantly different in size, this difference allows for a single cell suspension gained from whole testes to be separated with liquid gradient (Miller and Phillips, 1969, Bryant et al., 2013). The staput method is a unity-gravity cells sedimentation system that allows the purification of specific cell types based on size and density through a linear BSA gradient. The optimal conditions for rodent cells have been reported (Miller, 1984, Bryant et al., 2013). The successful application of this technique to male germ cell fractions has been described (Lam et al., 1970, Meistric.Ml et al., 1973, Bryant et al., 2013, Boucheron and Baxendale, 2012). The staput has numerous advantages compared with the two commonly used approaches

for isolating germ cells types; FACS and elutriation. The method needs only numerous pieces of specific glassware assembled in a cold room. Therefore, it is cheaper than using a cell sorter or an elutriator (Bastos et al., 2005). The sta-put method yields higher amounts of cells per cell type and the purity of each cell population is higher than those obtained with FACS (Getun et al., 2011). Currently, cell sorting using magnetic beads, magnetic activated cell sorting (MACS) has been used for enrichment of spermatogonial cells from a mixed germ cell population; however, it is not appropriate for isolation of spermatocytes and spermatids because of lack of information of suitable surface markers (Gassei et al., 2009). For study that needs large number of yields of germ cells types at ~90% purity, the sta-put is a perfect technique (Bryant et al., 2013).

In vitro experiments demonstrated that the unit-gravity sedimentation cell separation could be a valuable method to make appropriate assessment of DNA, mRNA and protein and investigate the biochemical and toxic effects of pharmacological agents on germ cells.

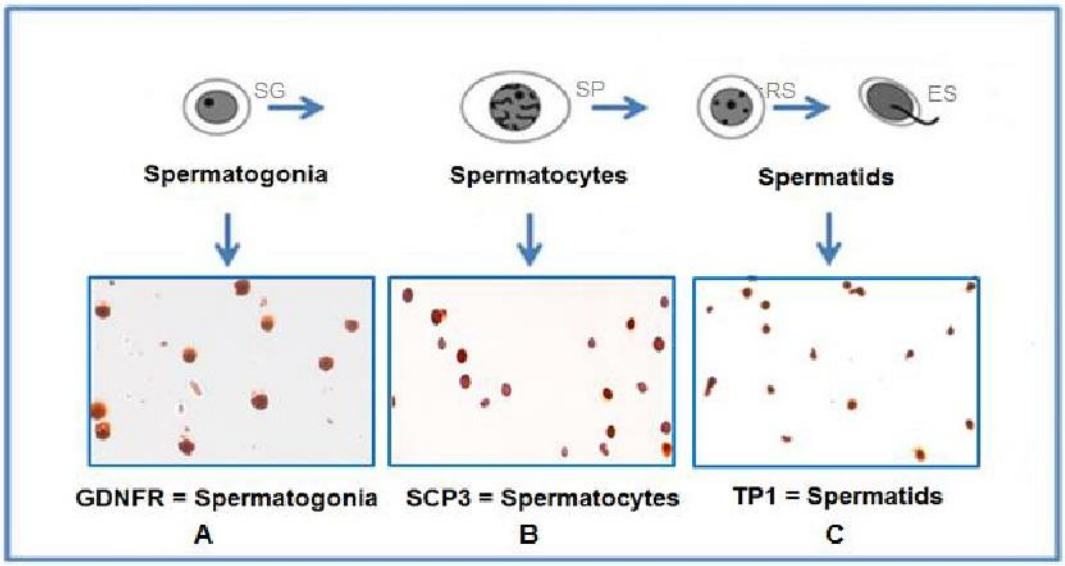

Figure 1.15: Diagram of staput purified of male cells that were stained with antibodies for specific proteins. Spermatogonia were detected with anti-GDNFR (Panel A); spermatocytes were detected anti-SCP3 (Panel B) and Spermatids were detected with anti-TP1 (Panel C). Viewing magnification ×400.

1.6.1 Terminal deoxynucleotidyl transferase dUTP nick end labelling assay

Recently, increasing numbers of tests have become available to assess DNA damage in germ cells. (TUNEL) assay is one of the most common tests to measure DNA damage in germ cells. The TUNEL assay measures both single and double strand DNA fragmentations, measures a definitive end point (presence of 3′-OH) (Sun et al., 1997, Zini and Sigman, 2009). The terminal deoxynucleotidyl transferase dUTP nick end labelling (TUNEL) assay was first reported by Gavrieli et al., in 1992, and since then, it has been widely used for detecting apoptotic cells in situ, and has been the most commonly used test to assess DNA damage in spermatozoa (Sharma et al.,

2010, Gavrieli et al., 1992). The assay is based on the ability of the enzyme terminal deoxynucleotidyl transferase (TdT) to catalyze the addition of dUTP to the 3′-OH end of the fragmented DNA. The enzyme can also add labeled nucleotides for example biotin-dUTP, DIG-dUTP or fluorescein-dUTP to the 3′ terminus of a DNA molecule (Figure 1.16) (Alipour et al., 2011, Kyrylkova et al., 2012).

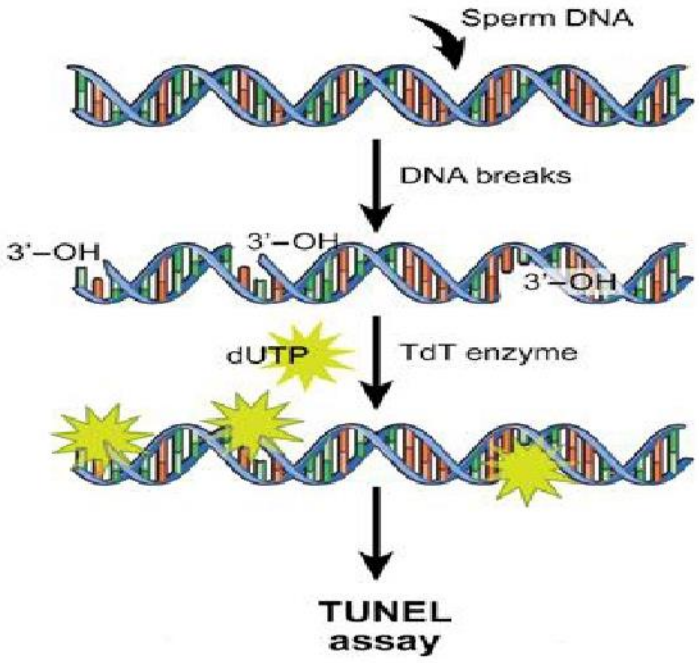

Figure 1.16: Schematics of TUNEL assay for measurement of DNA damage in sperm. Adapted from Malvezzi et al., (2014).

1.6.2 Comet assay single cell gel electrophoresis

The single cell gel electrophoresis (SCG or SCGE) assay (also called the Comet assay) is a sensitive, visual, rapid and quantitative technique that is used to detect and measure DNA damage, including double-strand and

single-strand breaks, in cells or nuclei isolated from multiple tissues of animals, usually rodents after a variety of genotoxic insults (Tice et al., 2000, Haines et al., 2002, Burlinson et al., 2007). The assay has been applied to both human and animal cells. It has also been reviewed and recommendations published by numerous expert groups (Kirkland and Speit, 2008, Rothfuss et al., 2010, Tice et al., 2000, Haines et al., 1998). The alkaline version of the Comet assay with a pH ≥13 has demonstrated its reliability in numerous testing conditions. It is an accepted assay for genotoxicological assessments and has been approved via the UK Committee on Mutagenicity of Chemicals in Food, Consumer Products and Environment and US Food and Drug Administration (Burlinson et al., 2007). Part of the reason for this approval has been the development of a standard protocol and acceptance criteria for the assay through the IWGT working parties and international Comet assay workshops (Tice et al., 2000, Collins, 2004, Hartmann et al., 2003).

DNA damage is assessed subsequently by denaturation of the DNA into single-stranded DNA. This procedure involves numerous steps. Firstly, cells are embedded in an agarose layer on slides between other layers of agarose. Next, cells are lysed with detergent and salt which acts to remove cellular protein content. Nucleoids are formed containing supercoiled loops of DNA. Then, either under alkaline or neutral pH conditions, the DNA is allowed to unwind before being subjected to electrophoresis.

The principle of the Comet assay is the migration of DNA in an agarose matrix under electrophoretic conditions. Ethidium bromide (EtBr) is then applied to stain the DNA prior to being observed under a fluorescence

microscope. Thus EtBr-based staining permits the analysis of an image that resembles a comet with a distinct head and tail. The cells have the appearance of a comet, in which the head contains undamaged/intact DNA, whilst the tail consists of fragmented and/or damaged DNA segments (Hartmann et al., 2003, Collins, 2004). Detection of changed DNA migration is reliant on many parameters for example the temperature, the duration of alkaline unwinding, pH, the concentration of agarose in the gel, voltage, amperage and duration of electrophoresis (Hartmann et al., 2003).

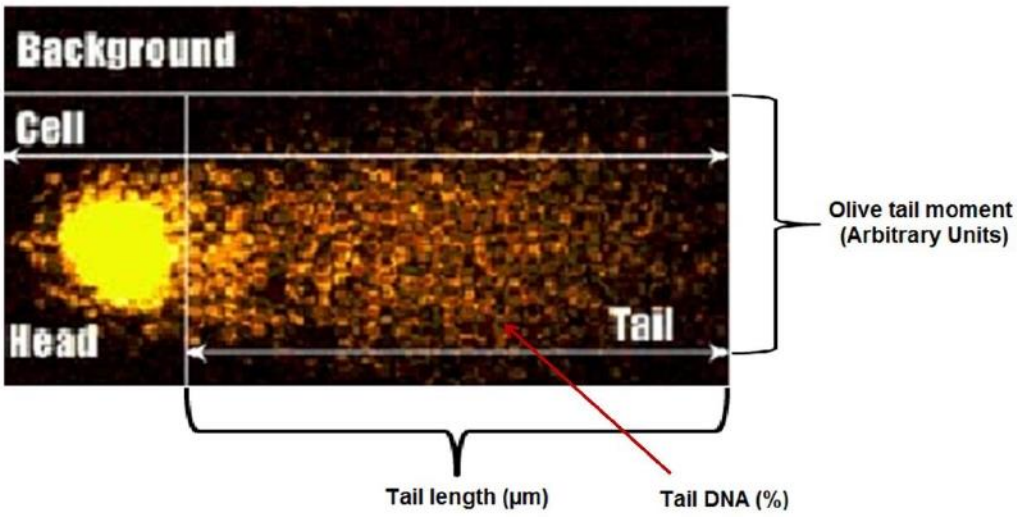

Figure 1.17: An image of cells marked with comet parameters, showing parts of head undamaged DNA and tail damaged DNA.

For *in vitro* toxicity of environmental chemicals, the Comet assay has been used on different cell types and has also been used *in vivo* toxicity in tissue samples harvested from animals. Furthermore, it is a valid method to assess whether antioxidants micronutrients are able to keep the integrity of the genetic material (Heaton et al., 2002, Anderson et al., 1997, Novotna et al., 2007). Many genotoxicity studies have used Comet assay to assess DNA

damage in early mixed male germ cells (Nixon et al., 2012, Nixon et al., 2014, Villani et al., 2013).

The Comet assay is an easy and rapid technique that is simple to perform. It needs only small amounts of test substance and can be performed on different types of cells. The Comet assay is therefore a key technique in the early development of drugs and other compounds for human use. It acts as a mechanistic tool and genotoxicity predictor (Apostolou et al., 2014).

1.7 Aims of project

It has been suggested that exposure to environmental toxicants causes DNA damage and/or apoptosis, potentially leading to male fertility problems or heritable DNA damage or mutation in human. Since current assays are heavily reliant on *in vivo* tests, the development of rapid, *in vitro* assays is urgently required.

The specific objectives of this project are as follows:

A. Separation of spermatogenic cell types using staput velocity sedimentation. Isolated cells will be characterized further by using specific markers to identify spermatogonia, spermatocytes and spermatids.

B. To investigate the effect of H_2O_2 and doxorubicin on isolated germ cell apoptosis.

C. To evaluate the cytotoxic and genotoxic potential of N-ethyl-N-nitrosourea (ENU) and N-methyl-N-nitrosourea (MNU), 6-mercaptopurine (6-MP) and 5-Bromo-2′-deoxyuridine (5-BrdU) and methyl methanesulfonate (MMS) and ethyl methanesulfonate (EMS) in isolated germ cells.

D. To clone and express Tbpl1, FHL5 and Gtf2a1l from mouse testis. This will enable the expression patterns of the Tbpl1, FHL5 and Gtf2a1l genes in spermatocytes and spermatids at both the mRNA and protein levels to be confirmed. The effect of ENU and MMS on Tbpl1, FHL5 and Gtf2a1l expression in spermatocytes and spermatids at both mRNA and protein levels which are expressed in *E. coli* will then be assessed.

Chapter 2. Material and methods

2.1 Materials

2.1.1 Chemicals and reagents

General Laboratory reagents and Dulbecco's Modified Eagle's Medium - high glucose were purchased from Fisher Scientific Co. (Itasca, IL) and Sigma Chemical Co. (Gillingham, UK). N-Nitroso-N-methylurea (MNU); N-Nitroso-N-ethylurea (ENU), 5-Bromo-2′-deoxyuridine (5-BrdU), ethyl methanesulfonate (EMS), methyl methanesulfonate, (MMS) was dissolved in Phosphate buffered saline (PBS; pH 7.3 ± 0.2) before treatment, and 6-mercaptopurine (6-MP) (Sigma) was dissolved in dimethyl sulfoxide (DMSO) before treatment, and the concentrations were adjusted to (0.05, 0.5 and 1.0 mM).

PCR reagents and endonuclease were purchased from Promega (Southampton Science, UK) and used according to the manufacturer's protocol. Cloning vector pET100/D TOPO was from Invitrogen (Carlsbad, USA). PCR primers were obtained from Sigma. All other reagents and chemicals were purchased from Sigma or Fisher Scientific (Loughborough, UK) unless otherwise specified. Ethidium Bromide was also purchased from Sigma (E-8751).

2.1.2 Buffers and solutions

The following solutions and buffers were used for this study: Tris-acetate-EDTA buffer (50 X) (TAE; 2 M Tris/HCl; 5.7 % (v/v) acetic acid; 50 mM EDTA; pH 8.0). Tris-Boric acid- EDTA buffer (5 X) (TBE; 440 mM Tris; 440 mM boric acid; 10 mM EDTA; pH 8.4). Sodium dodecyl sulfate loading buffer (1 X) (SDS; 250 mM Tris-HCl; 500 mM DTT; 10 % (w/v) SEMS; 0.5% (w/v)).

Sodium dodecyl sulfate-polyacrylamide gel electrophoresis buffer (10 X) (SDS-PAGE; 250 mM Tris-HCl; 2.5 M glycine; 1 % (w/v) SDS; pH 8.3). Coomassie bright blue staining buffer: 2.5 g Coomassie R250; 45.5 % (v/v) methanol; 9.2 % (v/v) acetic acid. Coomassie bright blue destaining buffer: 25 % (v/v) isopropanol; 10 % (v/v) acetic acid. Bouin Solution (75% (v/v) saturated picric acid, 5% (v/v) glacial acetic acid, and 9% (v/v) formaldehyde in water.

2.2 Cell culture

2.2.1 Staput isolation of germ cells fractions

2.2.1.1 Testis isolation

Sexually mature NMRI mice and rat (National Medical Research Institute) weighing 25-30 g mice and rats weighing 250-300 g (10-12 weeks old) were used in this study. Animals were sacrificed by cervical dislocation under CO_2 anaesthesia. Animals were obtained from the Institute of Cancer Therapeutics, University of Bradford, UK where they were maintained under standard conditions. All animal care procedures were carried out according to the National Research Council's Guide for the Care and Use of Laboratory Animals. The testes are removed and pooled in 50 mL of ice-cold DMEM, in a 50 mL Falcon tube, on ice. Once all testes are collected, each testicle in the pool is quickly decapsulated in a large culture plate containing fresh ice-cold DMEM, using two pairs of forceps. The seminiferous cords are transferred into a new 50 mL tube containing 20 mL of fresh DMEM, on ice.

After the decapsulated testis/seminiferous cords settle on the bottom of the tube, the supernatant is gently removed with a pipette.

2.2.1.2 Tissue digestion

The progressive digestion of testicular tissue is the key to an efficient isolation of individual cells. There are three basic steps. In the first step, the seminiferous tubules are treated with a mixture of collagenase, hyaluronidase, and DNase I, to remove the interstitial cells, namely, myoid and Leydig cells. The second step is digestion with trypsin which dissociates the seminiferous tubules and releases the Sertoli and germ cells. DNase I is added to this step to reduce viscosity thus, cellular aggregation. Finally, the cell suspension is further purified, by panning; this exploits the fact that sertoli cells will adhere to the surface of the plastic culture dish while germ cells remain in suspension. At this point, tissue digestion and the primary separation of adherent and nonadherent cells are complete; the sample is ready for additional purification through a BSA gradient.

Seminiferous tubule pellet was incubated in a solution of DMEM containing 2 mg/ml collagenase I, 0.5 mg/ml DNase I and 1 mg/ml hyaluronidase. Sample was then gently swirl by hand and placed in water bath at 37 °C for 30 minutes with shaking at 5 minutes interval. Sample was then removed from the water bath and the tubule tissue was allowed to settle to the bottom of the tube. Supernatant in the tube containing the interstitial cells was gently pipetted off with more care to avoided removing the partially digested tubules. A 3 ml of 0.25 % Trypsin-EDTA and 300 µl DNase I were added to the tubule tissue pellet, containing predominantly germ cells and Sertoli cells.

Sample was swirled by hand and placed in a water bath at 37 °C for 15 minutes with gentle shaking at 5 minutes interval during this period to allow the tissue to settle to the bottom of the tube again. Supernatant containing cells in suspension was transferred without disturbing the larger chunks, into a fresh falcon tube containing 20 ml of DMEM + 10 % FBS on ice to inhibit proteolytic activity. 3 ml of 0.25 % Trypsin-EDTA and 300 µl DNase I was added to the remaining cell pellet and swirled by hand then placed in a water bath for 15 minutes incubation at 37 °C. The tube was shaken by hand every 5 min during this period to assist in dissociating the germ cells and the Sertoli cells. The supernatant was removed gently and added to the previously prepared 50 ml Falcon tube containing 20 ml of DMEM + 10 % FBS and the first supernatant removed from the digestion. This pool should now contain predominantly germ and sertoli cells. The cell suspension was filtered through a sterile 0.80 µm nylon filter to remove any undigested fragments or cell clumps. The filtered cells were centrifuged at 800 x g for 10 minutes at room temperature. Remove the supernatant and resuspend the cell pellet in 10 ml DMEM.

2.2.1.3 BSA gradient

Good construction of the gradient is essential for effective cell separation. Extreme care should be taken to ensure that the gradient is both even and stable. After the cells have been grossly separated into Sertoli cell (adhering to the culture plates) and germ cell (in suspension in culture medium) fractions. As many of the supernatant, enriched with germ cells were removed and transferred to fresh 50 ml tubes. The supernatant was centrifuged for 10 minutes at 800 x g. The BSA gradient was prepared using

250 ml of 4 % and 250 mL of 2 % BSA in DMEM. Both BSA solutions were filtered before used with a 0.45-μm filter mounted.

2.2.1.4 Principles of staput

The BSA solutions were transferred into the gradient maker apparatus, which was assembled as shown in figure 2.1 and connected to a 250 ml cell buffer chamber. The gradient valve between the two chambers was opened to allow the two BSA solutions to mix, and then opened the release valve allowing the BSA to flow into the syringe to generate the gradient. While the BSA gradient is stabilizing, the supernatant was removed from the centrifuged of the cell suspension. Pool the pellets from several tubes together, and resuspend in DMEM media to a total volume of 3 ml. 10 μl was taken from the suspension to determine the cell number by using a haemocytometer under light microscopy. Gently overlay the top of the formed BSA gradient with the 3 mL cell suspension. The top of the syringe containing cells/gradient was covered with parafilm to minimize disturbance and changes in pH due to oxidation. After 2.5 h at room temperature, cells were collected in 12 ml fractions eluted drop wise into 45 test tubes (Figure 2.1). Fractions were placed on the ice immediately after collection (Bryant et al., 2013, Bellve et al., 1977).

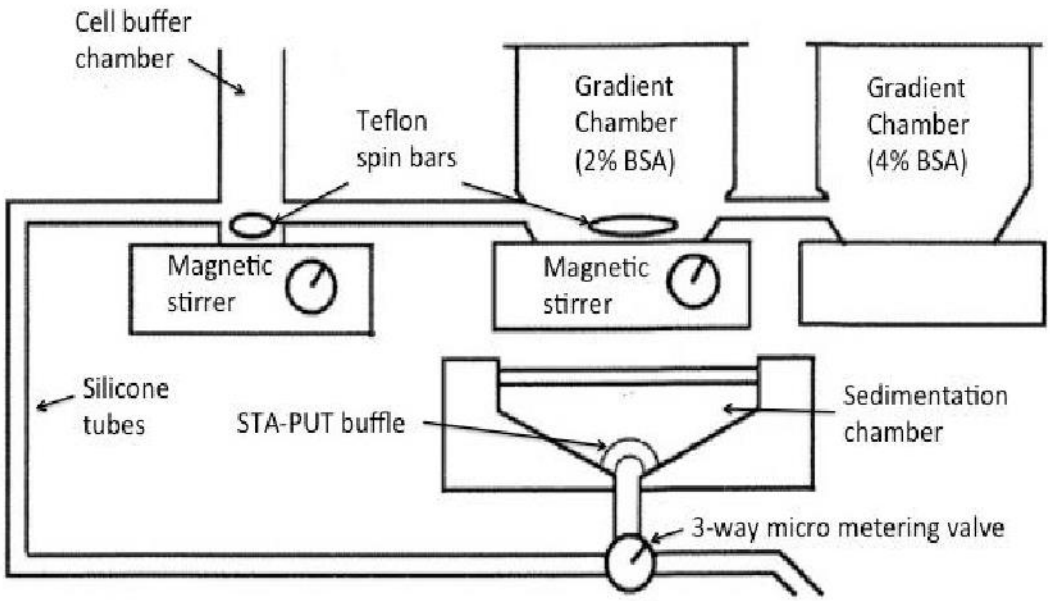

Figure 2.1: Diagram shows the staput apparatus involve of two graduated gradient chambers, a cell buffer chamber, two magnetic stirrers, two Teflon spin bars, a sedimentation chamber with a staput buffle and a 3 way micro metering valve. Silicone tubes connect the graduated gradient chambers, cell buffer chamber and the sedimentation chamber to each other.

2.2.1.5 Cell counting

In order for the cells to be counted, 100 µl of the original cell suspension was transferred to an Eppendorf tube. A dilution of 1:1 was conducted when the cell suspension was mixed with 100 µl of 0.4 % trypan blue solution. A neubauer haemocytometer slide with coverslip was prepared and 10 µl of this cell suspension was transferred to the chamber. The cells were counted in 4 grids per chamber under the microscope, using the 10 x focus. The average number of cells of 4 grids was calculated and this number was used to count the total number of cells by using the following calculations:-

Number of cells/ml = [average cell number] x [10^4] x [dilution factor]

Total number of cells = [Cells/ml] x [volume of original cell suspension (ml)]

2.2.1.6 Viabilities

Viability of the germ cells in the cell suspension obtained after enzymatic digestion and in each isolated fraction was determined using the Trypan blue exclusion test (10 µl of 0.05 % Trypan blue was added to 10 µl of cell suspension) (Talbot and Chacon, 1981).10 µl from each tube was transferred to a haemocytometer and observed under a microscope. Cells that stained blue were considered dead.

2.2.1.7 Cell identification

The percentage number of germ cells types was determined based on size and morphology and confirmed by using specific cell markers and evaluated by immunohistochemical staining.

2.3 Immunohistochemical

2.3.1 Collection and fixation

The tissues were fixed in Bouin's solution, after fixation, the tissue samples were prepared for processing and embedding. Shandon Citadel 2000 Tissue Processor was used for automated tissue processing (Table 2.1). Processed tissue samples were then embedded in paraffin.

Table 2.1: Shows the protocol for mouse section processing

Step	Substance	Duration
1	Formalin/mouse testis	-
2	70% EtOH	3h
3	80% EtOH	3h
4	90% EtOH	3h
5	Abs. EtOH	1h
6	Abs. EtOH	2h
7	Abs. EtOH	2h
8	Xylene	1h
9	Xylene	2h
10	Xylene	2h
11	Paraffin (58 °C)	2h
12	Paraffin (58 °C)	1.5-4 h

2.3.2 Tissue preparation

The tissue blocks were first placed on a 4°C cold plate for 15 minutes before sectioning. Leitz wetzlar 1512 microtome blades were utilized to cut 5 - 8 μm thick sections. The sections were placed in a water bath at room temperature, attached to Super Frost™ Plus micro-scope slides on glass slides coated with poly-l-lysine, and placed shortly in 52°C water bath to straighten the tissue section. The slides were left at room temperature in an

upwards position for 30 - 60 minutes to remove excess water. The slides were then placed in an oven at 45°C for either 2 hours or overnight. After the heat-treatment, the slides were ready for immunohistochemistry staining.

2.3.3 Immunohistochemical staining of mouse tissue sections

An immunostaining procedure was performed on paraffin-embedded mouse tissue sections. Paraffin embedding tissue samples were fixed with 4 % formaldehyde in PBS. 4-5 µm thick paraffin tissue sections were deparaffinised with Histoclear (Fisher Scientific) and graded ethanol, and antigen retrieval was performed by heating the sections in 10 mM sodium citrate buffer, pH 6.0, at 95° C for 30 minutes in a microwave. The blocking step prior to incubation with the primary antibody was performed with either 5-10% normal goat serum or 1 % BSA in PBS. Anti-GDNFR (1:100; Abcam, Cambridge, UK), anti-SCP3 rabbit polyclonal antibody (1:400; Abcam, Cambridge, UK), rabbit polyclonal anti-TP1 antibody (1:50; Abcam, Cambridge, UK), rabbit polyclonal were used as the primary antibodies. The sections were then incubated at 4°C overnight, followed by washing with PBS. For bright-field microscopy, bound primary antibodies were detected with secondary, biotinylated anti-rabbit-IgG antibody for 30 minutes at room temperature. Signals were developed with 3, 3-diaminobenzine (DAB) for 10 minutes and counterstained with haematoxylin and a coverslip was applied using histomount mounting medium (Fisher Scientific, Fair Lawn, NJ). Immunostained sections were examined on a Zeiss Axio Imager Z1 microscope. Microscopy images were captured using AxioCam digital microscope cameras and AxioVision image processing (Carl Zeiss Vision, Germany).

2.3.4 Immunohistochemical staining of isolated germ cells

The fractions of cells used were grown on coverslips in 6-well plastic culture plates with DMEM containing 10 % FBS, 100 Unit/ml penicillin, and 100 mg/ml streptomycin. The cells were serum starved in DMEM (with the antibiotics) for 16 h to allow the cells to attach to the coverslips, fixed with 4 % formaldehyde for 10 min and washed twice, each for 5 min, in PBS containing 0.5 % BSA. A 1 h block in PBS containing 0.1 % BSA, 0.05 % Triton X-100, and 1% goat serum was performed. Anti-SCP3 rabbit polyclonal antibody (1:400; Abcam, Cambridge, UK), rabbit polyclonal anti-TP1 antibody (1:50; Abcam, Cambridge, UK), rabbit polyclonal anti-GDNFR (1:100; Abcam, Cambridge, UK), were used as the primary antibodies, and were incubated at 4°C overnight, followed by washing with PBS. The slides were subsequently incubated with secondary, biotinylated anti-rabbit-IgG antibody for 30 min at room temperature. Signals were developed with 3,3'-Diaminobenzidine (DAB) for 10 min and counterstained with haematoxylin (Hsu et al., 1981, Khalfaoui et al., 2011), and a coverslip was applied using Histomount mounting medium (Fisher Scientific, Fair Lawn, NJ). Preparations of cells representing each fraction were scored for the presence of cells positive for each of the three markers and their total number per fraction calculated. Only fractions showing suitable purity of a specific cell type were used to set up the cultures.

2.4 Testicular germ cells culture prior to TUNEL assay

The isolated testicular germ cells were seeded onto coverslips in 6-well plastic culture plates with DMEM containing 10 % foetal bovine serum (FBS),

100 Unit/ml penicillin, and 100 mg/ml streptomycin (5×10^6 cells/ml; 1 ml per well) at 37°C then the medium was changed and they were serum starved in DMEM (with antibiotics) for 16 hours to allow the cells to attach to the coverslips. They were then incubated for 2 hours with or without treatment. Incubations with treatments were made at final concentrations of drugs in triplicate. A temperature of 37 °C would not be suitable for long-term cultures of spermatogenic cells, which thrive best at a temperature 1-2 °C below core body temperature in humans. Attempts to recreate spermatogenesis in vitro typically use a culture temperature of 35 °C, often maintained for several weeks (Reuter et al., 2012). Cells cultured for a single day at 37 °C are healthy in appearance and only minimal numbers fail to survive, so these conditions were deemed suitable for the short-term experiments reported here (Habas et al., 2014). Treated and untreated cells were fixed with 4 % formaldehyde for 10 minutes and washed twice, each for 5 minutes in PBS containing 0.5 % BSA and stored in 70 % (v/v) ethanol until further use.

2.5 TUNEL assay

TUNEL assay for apoptosis evaluation were performed on separate cell samples of the same cell populations as previously described (Gavrieli et al., 1992). Briefly, the slides were incubated with TUNEL reaction mixture (30 mM Tris pH 7.4; 140 mM sodium cacodylate; 1 mM cobalt chloride; 5 µM biotin-16-deoxyuridine triphosphate; 0.3 U/µl terminal deoxynucleotidyl transferase [Tdt];all from Sigma) for 60 minutes (humidity chamber, 37°C) and then washed twice in PBS. (H_2O_2-blocking of endogenous peroxidases was not performed as the testis is low in peroxidases so it is rarely necessary). After multiple washing steps, the cells were treated with 2 % v/v

extravidin peroxidase in TBS with 0.1 % w/v BSA for 30 min (humidity chamber, 37°C), rinsed with PBS, and visualised by adding 3, 3-diaminobenzine (DAB) for 10 minutes at room temperature. They were washed in PBS, counterstained using haematoxylin staining, and finally, mounted for light microscopic observation. For the negative controls, sections were incubated with the reaction mix without TdT instead of the full TUNEL reaction mixture.

2.6 Single cell gel electrophoresis (SGCE) Comet assay

2.6.1 Treatment cells

Freshly isolated germ approximately (1.5 - 2.5 x 10^5 cell/ml) suspensions were mixed with fresh RPMI medium (total volume 1000 µl). 100 µl of mixed germ cells were then added to each treatment tube (100 µl mixed germ cells, 890 µl RPMI medium, plus 10 µl of chemical or 900 µl for the negative control). Cells were treated with different concentrations of drugs for 1 hour at 37 °C, then the germ cells treated and untreated were immediately used in the Comet assay.

2.6.2 Embedding of cells in agarose

Fully frosted microscope slides were covered with a basic layer of 1 % normal melting point agarose (Invitrogen, Paisley, UK: 15517-022). The slides were dried in a 60 °C cabinet overnight and then stored at room temperature. Dry slides were stored until used. Purified germ cells (spermatogonia, spermatocytes and spermatids) were assayed for DNA damage using alkaline single-cell electrophoresis assay using the method

described by Anderson et al (1997) with slight modifications. Briefly, after treatment, isolated germ cells samples were centrifuged and the supernatant was discarded. Next, 100 μl of 1 % low melting agarose (LMP) (Invitrogen, Paisley, UK: 15517-022) was added to cell pellet to create a cell suspension. The cell suspension was transferred to slides pre-coated with 1 % normal melting point (NMP) agarose. The slides were placed on an ice block for 5 min, after which 100 μl of 0.5 % LMP was added on top and slides were placed on ice for 5 minutes. The slides then were submerged in cell lysis buffer (2.5 M NaCl, 100 mM EDTA), 10 mM Tris HCl pH 10.0 containing 1 % Triton X-100 and 40 mM dithiothreitol) for 1 hour at room temperature and protected from light. Following this initial lysis period, proteinase K was added to the lysis solution (final concentration 10 μg/ml) and additional lysis was performed at 37 °C for 2.5 hours (Hughes et al., 1997). Following lysis, slides were placed in the electrophoresis buffer (0.3 M NaOH, 1 mM EDTA) for 30 minutes and then subjected to electrophoresis at a setting of 20 V (approximately 300 mA) for 30 minutes at 4 °C. After electrophoresis, slides were neutralised 3 times for 5 minutes using Tris buffer. Cells were stained using EtBr (20 μl/ml) and slides were covered with cover slips and the DNA integrity of 50-100 cells per slide were scored at 200 X magnification with an Olympus fluorescent microscope (Leica, UK) equipped with a BP546/10 excitation filter and a 590 nm barrier filter. Slides were analyzed by a computerized image analysis system (Comet 6.0; Kinetic Imaging, UK) was used from each replicate slide. In the Comet assay, Olive tail moment and tail DNA were measured for isolated germ cells.

2.6.3 Scoring and analysis of Comet slides

Visual and computerized image analyses of DNA damage were carried out in accordance with the published protocols (Anderson and Plewa, 1998). Samples were run in triplicates, and 100 cells were randomly analyzed per slide at 200 x magnification with an Olympus fluorescent microscope (Andor Technology Ltd, Belfast, UK). Equipped with a BP546/10 excitation filter and a 590 nm barrier filter. Slides were analyzed by a computerized image analysis system using Comet 6 software; Kinetic Imaging (Andor Technology Ltd, Belfast, UK) was used. Comet tail length is the maximum distance the damaged DNA migrates from the centre of the cell nucleus, and the tail movement is a product of the tail length and the percentage of tail DNA, which gives a more integrated measurement of overall DNA damage in the isolated germ cells.

2.6.4 Scoring and analysis of TUNEL slides

For TUNEL staining, Spermatogonia, spermatocytes and spermatids were evaluated for morphology and staining, The following findings were considered to represent apoptosis: marked condensation of chromatin and cytoplasm clearly staining strongly brown or brown/black; The TUNEL-positive cells were scored in several fields on each coverslip to yield a total of at least 100 cells under a 40 × objective of an Olympus CKX31 microscope. Values represent percentages from at least 100 cells from each culture. SPSS statistical software was used to perform One-Way ANOVA (Bonferroni), Mann Whitney U and Kolmogorov-Smirnov Z tests for differences were considered as significant at $p < 0.05$.

2.7 Periodic acid-Schiff/Hematoxylin staining

The slides were placed 2 times for 5 minutes each in xylene, 100 % ethanol, 96 % ethanol, 80 % and 70 % ethanol. Finally the slides were washed with distilled water and placed in 0.5 % periodic acid for 5 minutes. After washing the slides in 3 changes of water, they were incubated in Schiff's reagent for 15 minutes. Slides were incubated 2 x with 0.55 % potassium metabisulfite for 1 minutes to remove excess reagent and washed in running tap water for 10 minutes to allow the colour to develop. After counterstaining with acidified hematoxylin for 90 seconds, slides were dehydrated using, 70 %, 80 %, 96 % Ethanol, 100 % ethanol and xylene for 5 minutes each and mounted with Histomount II.

2.8 Molecular biology: RT-PCR

2.8.1 RNA extraction from tissue

The total RNA and mRNA were extracted from the mouse testis using either a TRIzol reagent (Invitrogen) or ™ Mammalian Total RNA Miniprep Kit (Sigma, Aldrich). The testes were obtained from adult male mice (NMRI, 12-16 weeks old), which were sacrificed by cervical dislocation after anaesthetising with CO_2 and then were removed, and stored at -80 ºC until use.

2.8.2 RNA preparation

To avoid RNAse contamination, disposable plastic ware and RNAse-free water was used whenever possible.

2.8.3 Total RNA isolation from cells

The PureLink™ RNA Mini Kit (Invitrogen life technologies, UK) was used for total RNA preparation. In the case of RNA isolation from cultured cells, the dishes were placed on ice and the medium was removed; cell layers were collected by scraping in 1 ml RNA lysis buffer The lysate was passed through a 20 G needle 10 times, the samples were centrifuged at 11,000×g for 2 min and the supernatants were collected. The eluate was transferred into a filtration column and centrifuged for 2 min at 13000 x g, Then 70 % ethanol was added to the filtration column and mixed thoroughly. This combination of lysate filtrate and ethanol was transferred to a binding column and centrifuged for 15 seconds at 10000 x g, the flow through was discarded. The binding column was washed to remove contaminants. This was achieved by the addition of 500 µl of wash solution 1 to the column and centrifugation for 15 seconds at 10000 x g. Then 500 µl of wash solution 1 was added to the column and centrifuged at 10000 x g for 15 seconds. The filtrate column was transferred to a new collection tube; 750 µl of wash solution 2 was added and centrifuged for 2 minutes at 10000 x g. The filtrate column transferred to a new collection tube and 50 µl of elution solution was added and centrifuged for 1 minute at 10000 x g. The elution buffer releases the purified RNA from the column. The eluted RNA was stored at -80ºC for subsequent use.

2.8.4 mRNA isolation

mRNA was isolated from total RNA for use in oligo-dT primer reverse transcription using a Genelute™ Mammalian mRNA Miniprep Kit (Sigma,

Aldrich, UK). Approximately 30 mg of testis tissue was lysed and homogenized. The homogenate was transferred onto a filtration column and centrifuged for 2 min at 10000 x g. Then, 70% ethanol was added to the filtration column and mixed thoroughly. This combination of lysate filtrate and ethanol was transferred to a binding column and after centrifugation for 15 seconds at 10000 x g, the flow- through was discarded. The binding column was then washed to remove contaminants. This was achieved by the addition of 500 µl of wash solution 1 to the column and centrifugation for 15 seconds at 10000 x g. This step was repeated with DNase 1; 10 µl of DNase 1 was added to 70 µl of DNase digest buffer and mixed by inversion and 80 µl was transferred directly onto the filter in the binding column. The sample was incubated at room temperature for 15 minutes. Then 500 µl of wash solution 1 was added to the column and centrifuged at 10000 x g for 15 seconds. The filtrate column was transferred to a new collection tube; 500 µl of wash solution 2 was added and centrifuged for 2 min at 10000 x g. The filtrate column transferred to a new collection tube and 50 µl of elution solution was added and centrifuged for 1 minute at 10000 x g.

2.8.5 Measurement of quantity and purity of total RNA

The concentration of the RNA samples extracted was determined by electrophoresis through a 1 % (w/v) agarose gel, the quality of total RNA samples were estimated by visualising the sharply defined ribosomal units 28s and 18s, present at 4.7 Kb and 1.9 Kb respectively for mouse. The purity of the RNA yield was quantified spectrophotometrically by calculating the ratio of the samples optical density at 260 nm and 280 nm. RNA samples with an OD260/280 ratio between 1.9 and 2.1 were considered to be

sufficiently pure for further experiments. The concentration in μg/ml can be calculated from the absorbance value:

$$A_{260} \text{ x dilution factor x } 40 \text{ μg/ml}$$

2.8.6 DNase I treatment

Amplification grade DNase I was used to remove any contaminating genomic DNA from the isolated RNA. 2 μg of RNA, manufacturer supplied reaction buffer and DNase I were incubated at room temperature for 15 minutes. To inactivate the DNase I, EDTA was added to a final concentration of 2.3 mM and the reaction was heated to 65 °C for 10 minutes. The resulting DNA-free RNA was then used for cDNA synthesis.

2.8.7 Reverse Transcription

The isolated RNA was reverse transcribed using Reverse Transcription System kit (Promega). The complimentary DNA (cDNA) reactions were carried out on a PCR Sprint or Whatman-Biometra thermal Cycler. In preparation for first-strand synthesis, 2 μl of total RNA (1ug) and 1 μl of Oligo (dT) Primer (0.5 μg / μl) or Random Primers (0.5 μg/μl) was incubated at 70 °C for 10 minutes. The reaction mix for first strand synthesis consisted of 4 μl of $MgCl_2$, 25mM, 2 μl of reverse transcription 10 X buffer, 2 μl of dNTPs mixture, 10 mM, 0.5 μl of Recombinant RNasin Ribonuclease Inhibitor, 15 U of AMV reverse transcriptase (High Conc.). The first strand synthesis reaction incubated at 42 °C for 15 minutes, and then at 90 °C for 5 minutes to inactivate the reverse transcriptase.

2.8.8 Primer design

For each gene, a pair of primers was designed using Primer3Plus software (www.bioinformatics.nl). The primers were ordered from Sigma-Aldrich Company Ltd. (Gillingham, UK), and were resuspended to a final concentration of 100 ng/µl in nuclease free water.

Table 2.2 Detailed the primers sequences and the PCR product sizes for each gene tested. In addition, gene β-actin was used as a positive control.

Gene	Primer
B-actin	F: 5´-TATCCCGGGTAACCCTTCTC-3´ R: 5´-TGCTGGGAGTCTCAGGACAG-3´
Tbpl1	F: 5´-CACCATGGATGCAGACAGTGATGTT-3´ R: 5´-TAAAATCTCCTTCCTGCTTTCA-3´
FHL5	F: 5´- CACCATGACAAGTAGTCAATTTGATTGT-3´ R: 5´-CTAAGCGTCAGTGTCTGC-3´
Gtf2a1l	F: 5´-CACCATGGCCTTCATCAACCTG-3´ R: 5´- CCACTCAGCTTCACCAATG-3´
T7-pET-100	F: 5´-TAATACGACTCACTATAGGG-3´ R: 5´-TAGTTATTGCTCAGCGGTGG-3´

2.8.9 Polymerase chain Reaction (PCR)

2.8.9.1 Standard PCR conditions:

PCRs were performed using 1 µl to 5 µl of cDNA (or Plasmid) template, 17 µl of nuclease free water, 2.5 µl of 10 x PCR buffer, 1.5 µl of magnesium chloride (25 mM), 1 µl of dNTPs (10 mM), 100 ng of forward primer, 100 ng of reverse primer and 2.5 U of Taq DNA polymerase in a total volume of 25 µl. reactions were denatured for 30 seconds at 94 ºC (or 5 minutes at 98 ºC with KOD DNA polymerase), then subjected to 30 cycles of 95 ºC for 30 ºC seconds, 58-63 ºC for 20 seconds, and 72 ºC for 1-2 minutes. This was followed by a final 10 minutes extension step at 72 °C and a 4 ºC hold step. The reaction mixture was run in either a thermal cycler (UVI gene thermal cycle, PCR Sprint or Whatman-Biometra thermal cyclers).

Pfu DNA polymerase (Promega) was used for high fidelity cloning PCRs. DNA was amplified in a 20 µl reaction containing 1 µl of cDNA template, 5 x amplifications buffer, 1 mM magnesium sulfate, 100 ng of each forward and reverse primer. 0.3 mM dNTPs, 2.5 U Pfu DNA polymerase and nuclease free water. Reactions were performed with a 2 minutes 98 ºC denaturation step, followed by 30 cycles of 15 seconds denaturation at 98 ºC, 30 seconds primer annealing at 58-63 ºC (depending on primer composition) and 5 minutes of primers extension (based on at least 1 minute per kb of DNA to be amplified) at 70 ºC. The final extension step of 5 minute at 72 ºC was followed by a 4 ºC hold step. A negative control without (cDNA template) was also incubated in the same manner. The samples were subjected to electrophoresis through 0.75 -1.5 % (w/v) agarose gel.

2.8.9.2 Quantitative real-time PCR assay

QRT-PCR reactions were carried out using the StepOnePlus™ real-time PCR instrument (Applied Biosystems). Quantitative RT-PCR was used to quantify the mRNA expression of Tbpl1, FHL5 and Gtf2a1l in isolated male germ cells and DNA plasmid purified from the host cells BL2 (DE3). QPCR was prepared in triplicates of 20 μl reaction mixture in MicroAmp optical 96-well reaction plates and sealed with optical adhesive covers (Applied Biosystems). Each reaction well contains 2 μl of template DNA, 2 μl of 10 × SYBR® Green PCR Master Mix (Applied Biosystems), and 12.5 pmol each of forward and reverse primers. Real-time QPCR was conducted with the following cycling conditions: 50 °C for 2 min, 95 °C for 20 sec, followed by 50 cycles of 95 °C for 15 s and 60 °C for 30 s each. The data obtained from each reaction was analysed by StepOne™ Software v 2.2.2. Relative representing groups the change level in the gene expression from real-time QPCR between experimental groups was calculated by comparative C_T method. The data was analysed by calculating the relative quantification (RQ) using the equation: $RQ = 2^{-\Delta CT}$ x100, where $\Delta C_T = C_T$ of target gene- C_T of endogenous gene (Housekeeping gene). Evaluation of $2^{-\Delta CT}$ indicates the fold change in gene expression, normalized to the internal control (β-actin) which enable the comparison between differently treated cells. DNA plasmid from untreated bacteria was used as the control value (internal positive control) in order to calculate the fold change in gene expression. Concentrations of plasmid were measured by absorbance at 260 nm with a UV/Vis Spectrophotometer (Beckman Coulter, Fullerton, CA). The ratio of

absorbance at 260 and 280 nm, (OD260 / OD280), was routinely found to be between 1.8 and 2.0, indicating minimum protein contamination.

2.9 Molecular biology: Methods for DNA

2.9.1 Agarose gel electrophoresis

RNA or DNA fragments were size-separated in the horizontal electrical field being embedded into the agarose-matrix. Depending on the expected sizes of RNA/DNA fragments, 0.75 to 2 % (w/v) agarose gels in 1X TBE buffer were prepared. Gels always contained 0.5 μg/ml ethidium bromine to visualize nucleic acids later on. Before loading into gel slots, nucleic acids were mixed 1/1 (v/v) with the DNA loading dye. The electrophoresis was run in the standard TBE-running buffer at 100-121 V in a horizontal electrophoresis tank (geneflow, UK). After the run, DNA/RNA bands were photographed under transillumination and recorded using a digital gel documentation system (UVItec, Cambridge, UK). Sizes of experimental bands were determined according to the standard DNA ladder run in parallel in (high, middle or low range) (Fermentas, UK).

2.9.2 Purifying gel DNA bands

DNA bands were weighed. Following the Qiagen MinElute Handbook for purifying the DNA, 3 times the volume of solubilizing Buffer QG (Qiagen) was added to 1 times the volume of gel and incubated for 10 minutes at 70 °C. The fluid was transferred to a Qiagen MinElute column and centrifuged for 1 minute at 10000 x g to bind the DNA to the column. The flow-through was discarded and the column washed with 500 □l of Buffer QG. This was re-

centrifuged and the flow-through discarded. 750 µl of washing Buffer PE (Qiagen) was added to the column, left to stand for 10 minutes and centrifuged at 10000 x g for 1 minute. The flow-through was discarded and the column re-spun for another minute. The column was placed in a sterile Eppendorf tube. 10 µl of eluting Buffer EB (Qiagen) was added to the column and left for 1 minute for optimal elution. This was centrifuged at 13000 x g for 1 minute. The DNA was then stored at -20 ^{o}C. The DNA was analysed by electrophoresis on a 1.5 % agarose gel.

2.9.3 Plasmid DNA isolation

Plasmid isolation was performed by the alkaline lysis procedure using the QIAprep Miniprep TM kit and protocol from Qiagen Inc (Valencia, CA, USA). Briefly, 3 ml of an overnight culture was centrifuged at 10,000 x g and the pellet was resuspended in buffer P1, 250 µl of 50 mM Tris.Cl (pH 8) buffer containing 10 mM EDTA and 0.1 mg/ml of RNase A. Following a sequential addition of buffer P2, 250 µl of 200 mM NaOH containing 1 % SDS solution and 350 µl of 3 M potassium acetate, the sample was mixed gently and centrifuged for 10 minutes at highest speed. The supernatant was carefully applied to the QIAprep column (Qiagen) and centrifuged briefly. The column was washed with buffer PB, 0.5 ml of guanidine HCl and isopropanol solution (pH 4.5), followed by buffer PE, 0.75 ml of 80 % ethanol. Finally, the plasmid DNA was eluted by the addition of buffer EB, 50 µl of 10 mM Tris.Cl, 1 mM EDTA (pH 8.5), and centrifuged for 1 minute at maximum speed in a micro centrifuge.

2.9.4 Restriction endonuclease digestion of plasmid DNA

Restriction enzymes digestion was carried out in a volume of 10 µl containing 1X buffer (10 mM Tris-HCl (pH 7.4), 300 mM NaCl, 1 mM DTT, 0.1 mM EDTA, 50% glycerol, 0.5 mg/ml BSA.), 1-10 µg of DNA plasmid or PCR product and 5 to 10 units of restriction enzymes and the volume made up to 20 µl with nuclease free water. The mixture was typically incubated at 37 ºC for one hour followed by heat inactivation at 65 ºC for 20 minutes. The restriction enzymes commonly used in this study were Hind III, EcoRI, EcoRV and PstI.

2.9.5 DNA quantification

The concentration of DNA was measured using measured in a Smart Spec Plus spectrophotometer (Bio-Rad, Richmond, CA). The purity of the DNA after purification was confirmed by analysis of absorbance ratio at 260/280. The 260/280 ratio was used for determination of DNA purity against protein contamination; the standard ratio for plasmid purity is 1.8 - 2.0.

2.10 Molecular Biology: cloning

2.10.1 Bacterial growth media

2.10.1.1 SOC medium

SOC medium was made by dissolving 2 % w/v bacto-tryptone, 0.5 % w/v yeast in a total volume of 1 litre of dH_2O containing 10 mM NaCl, 2.5 mM KCl, 10 mM $MaCl_2$ and 10 mM $MgSO_4$. The pH of the solutions was adjusted to pH 7.5 and autoclaved for sterilisation and 0.4 % v/v glucose solution added.

2.10.1.2 Luria-Bertani (LB) bacterial growth medium

LB medium was prepared with dH_2O containing 1 % (w/v) bacto-tryptone, 0.5 % (w/v) yeast, 1 % (w/v) NaCl in a total volume of 1 litre of dH_2O. The pH was adjusted to 7.0 and autoclaved for sterilization (121 ºC for 15 minutes). LB agar was made as described above, but supplemented with 2 % (w/v) per litre of bacto-agar added before adjusting the pH and sterilization.

2.10.1.3 Antibiotic stock solution

A. Ampicillin stocks were made (100 mg/ml): 1 g ampicillin was added to 10 ml dH_2O, sterilized by filtering the solution through syringe filter (0.2 mM), 1.0 mL aliquots in individual eppendorf tubes was prepared and stored at -20 ºC.

B. Kanamycin (100 mg/ml): 1 g kanamycin was added to 10 ml dH_2O; solution was sterile-filtered through syringe filter (0.2 mM), 1 mL aliquots in eppendorf tubes were stored at -20ºC.

2.10.1.4 Bacterial strains used for expression

Bacterial strains and plasmids used in this work were strains of *E.coli*. The pET100/D-TOPO^R vector from Invitrogen (Carlsbad, USA) containing the insert was used to transform BL21Star™ (DE3) from Invitrogen (Carlsbad, USA) competent cells (genotype: F-ompThSEMSB (rB-, mB-) gal dcm rne131 (DE3)) according to the manufacturer's instructions. Briefly, 10 ng of plasmid DNA was used to transform 50 µL of BL21 Star™ (DE3) One Shot^R cells, which were heat shocked at 42 ºC for 30 seconds and incubated in 250

μl SOC medium for 1 hour. The entire transformation reaction was added to 10 ml of LB containing 100 μg/ml ampicillin.

The recombinant of pET100/D-TOPO^{R} vector was used to transform DH5α competent cells (Genotype: F- Φ80lacZΔM15 Δ (lacZYA-argF) U169 recA1 endA1 hSEMR17 (rK-, mK+) phoAsupE44 λ- thi-1gyrA96 relA1). Barfly, 10 ng of vector was used to transform a 100 μl cell aliquot. Cells were then heat shocked at 42 ºC for 45 seconds and incubated in 200 μl SOC medium for 1 hour 50 minutes and 100 μl of each transformation was plated on selective LB plate containing100 μg/ ml ampicillin.

2.10.1.5 Cloning of the PCR product into PET100/D

The Tbpl1, FHL5 and Gtf2a1l fragments obtained by PCR amplification were cloned into the PET 100/D vector. Briefly, 2 μl of fresh PCR products were mixed with 1 μl of TOPO vector, 1 μl of salt solution and 3 μl of sterile distilled water. 3 μl of the above cloning reaction were used to transform 50 μl of *E. coli* Top 10 cells from Invitrogen (Carlsbad, USA), using the heat shock method. The cells were mixed with the insert, incubated at room temperature for 5 minutes, and then incubated on ice for 30 minutes. The reaction was heat-shocked for 30 seconds at 42 ºC. Then, 250 μl of SOC medium (Invitrogen) was added to the tube and incubated at 37 ºC with shaking for an additional 1 hour. Finally, 100 μl and 200 μl of the transformed cells were spread on pre-warmed LB-amp agar plates with 100 μg/ml ampicillin. Recombinant plasmid was isolated and analyzed by PCR amplification using T7 forward promoter primer (Invitrogen) and reverse

Tbpl1, FHL5 and Gtf2a1l primers (Schulte et al.), and restriction digestion by HindIII and EcoRV. Results were analyzed by agarose gel electrophoresis.

2.10.2 Protein expression

2.10.2.1 Expression of recombinant protein in *E. coli*

Recombinant plasmid (10 ng in a 5 μl volume) was used to transform 250 μl of competent *E. coli* BL21 Star (DE3) Star by the heat shock method. After 30 minutes of incubation at 37 ºC, the transformation reaction was added to 10 ml of LB-amp medium and grown for 16 hours at 37 ºC with shaking. 500 μl of the overnight culture was added to 10 ml of LB-amp medium and grown for another 2 hours or until OD_{600} reached 0.6 to 0.8. The culture was then divided into 2 tubes, one of which was induced by the addition of 1 mM isopropyl β-D thiogalactoside (IPTG), while the other was used as a non-induced control. Competent cells transformed with empty vector were used as a negative control. From each culture 500 μl were removed every hour for 4 to 6 hours and analyzed by SDS PAGE.

2.10.2.2 Purification of recombinant protein from *E. coli* lysates

Recombinant plasmid DNA was cloned into the pET vector in order to obtain a fusion protein with 6XHis-tag at the N- terminal in order to facilitate its purification by affinity column chromatography under native or denaturing condition using Sigma-HIS-Select® Spin Columns.

2.10.2.2.1 Purification under native condition

Purification was performed under native condition as described by the manufacturer. The pellet from an overnight 10 ml culture was harvested and

resuspended in 1 ml Lysis buffer containing 50 mM NaH_2PO_4; 300 mM NaCl; 10 mM imidazole (pH 8). The solution was sonicated on ice using six 10-second bursts at high intensity with a10-second cooling period between each burst. After 15 minute centrifugation at 3000 X g the supernatant was removed and purified under native conditions. In order to recover the insoluble proteins the pellet was purified under denaturing conditions. The supernatant was used for column purification. Columns were prepared according to the respective sample (soluble or insoluble). Initially, the resin was washed with native binding buffer 50 mM NaH_2PO_4, 300 mM NaCl, 20 mM imidazole, pH 8. The supernatant was aspirated and the resin was washed three times with native binding buffer and used to pack a column. The soluble protein was collected in 1ml fractions after the addition of 100 µl of native elution buffer. The sample containing insoluble proteins was added to the column and allowed to bind for 30 minutes. The resin was resuspended three times in native wash buffer and used to pack a column. Elution and collection of the protein was as above. Purified lysate of *E. coli* BL21 transformed with an empty vector served as the negative control. The samples obtained were analyzed by SDS-PAGE.

2.10.2.2.2 Purification under denaturing condition

For purification under denaturing conditions, a 10 ml form overnight culture of induced cells was harvested by centrifugation for 10 minute at 3000 X g and the supernatant discarded. The cells were resuspended in 1 ml of denaturing lysis buffer containing 7 M urea; 0.1 M NaH_2PO_4; 0.01 M Tris.Cl, pH 8.0 and gently vortexed for 30 seconds. The cells were then incubated with agitation for 15 min at room temperature. The lysate was the centrifuged at 12,000 x g

for 15 - 30 min at room temperature to remove the pellet the cellular debris and the supernatant containing the protein transferred to a fresh tube. Column was prepared according to the respective sample (soluble or insoluble). Initially, the resin was washed with denaturing binding buffer 7 M urea; 0.1 M NaH_2PO_4; 0.01 M Tris.Cl, pH 8.0 then centrifuged for 2 min at 890 x g. The resin was then pelleted by centrifugation at 10000 x g for 1 minute and the supernatant (saving 10 µl for SDS-PAGE analysis). The pellet was washed three times with denaturing binding buffer 8 M urea; 0.1 M NaH_2PO_4; 0.01 M Tris.Cl; pH 6.3 and the mixture centrifuged at 10000 x g for 1 minute and the supernatant saved. (saving 10 µl for SDS-PAGE analysis). The protein was eluted twice with 100 µl of elution buffer 8 M urea; 0.1 M NaH_2PO_4; 0.01 M Tris.Cl; pH 4.5. The fractions obtained were analyzed by SDS-PAGE.

2.11 Protein quantification

The amount of protein in cell lysates was quantified to ensure equal loading in western blot gels. The concentration of proteins purified by HIS-Select® Spin Columns and cell lysates was quantified using Bradford protein assay (Bio-rad 500-0120) according to the manufacturer's instructions, with the detergent compatible with use of bovine serum albumin as the standard (200, 400, 600, 800, and 1000 mg/ml). Initially, dilutions of the protein standard were prepared at above concentrations and 5 µl of the standard or the cell lysate were added to individual wells of a 96 well-plate in triplicate. 25 µl of reagent A* (2 % v/v reagent S in reagent A) was added to each well and 200 µl of reagent B then were added onto each well. Both samples and BSA controls were mixed by inversion and left at room temperature for 15

minutes. Prepared standard BSA concentration samples were read at absorbance 750 nm, each sample producing a triplicate reading to allow the average of these triplicates to be calculated and a standard curve was drawn (Figure 2.2). 30-40 µg of total protein was used for electrophoresis.

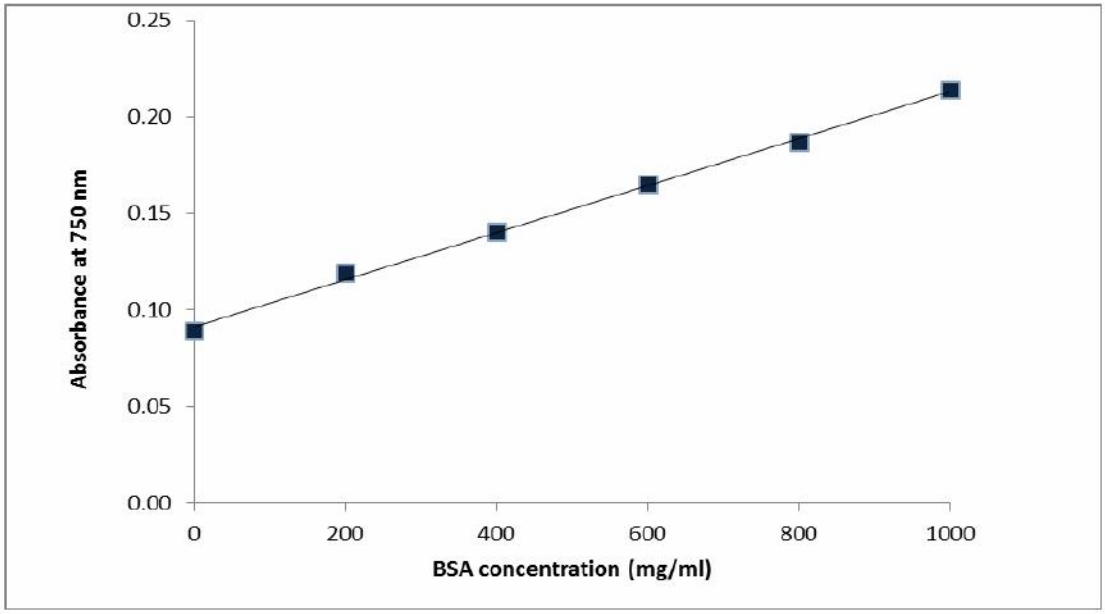

Figure 2.2 Shows standard curve of bovine serum albumin and protein concentrations. This curve was used to calculate the protein concentration of the protein extracts.

2.12 Western blot analysis

2.12.1 Total protein extraction

Total cellular protein was extracted from both untreated and treated cells (spermatocytes and spermatids). Cells were first washed with PBS and scrapped off into 300 µl of lysis buffer (60 mM Tris, 2 % SDS, 100 mM DTT). Detached cells were placed on ice for 5 minutes and then vortexed for 30 seconds. The cells were placed on ice for 30 minutes with occasional

vortexing. The samples were centrifuged at 12 000 x g at room temperature for 5 minutes. The proteins were then transferred to a new 1.5 ml centrifuge tubes. The protein concentrations were determined using Bradford assay as described in section 2.11. The samples were mixed with 2X sample buffer containing 10 mM DTT and stored at -80 ºC for further use.

2.12.2 SDS-polyacrylamide-gel-electrophoresis

Samples to be analyzed (recombinant *E. coli* cells, cell extract) were separated on 12 % SDS-PAGE gel. Separation was performed at 100 V for 2 hour and the gel was stained with Coomassie brilliant blue (R-250) for 1 hour. The denatured polypeptides bind SDS to get a uniform negative charge and therefore migrate through a polyacrylamide-gel according to their sizes. Before loading on the SDS-polyacrylamide gel, these samples were thawed and boiled for 5 minutes, 40 μg of protein were loaded onto a 12 % SDS PAGE.

2.12.3 Preparation of SDS PAGE

A Bio-Rad mini protein gel electrophoresis kit (500-0120) was used to run the gels. Tris buffers were prepared for both resolving gel and stacking gel. The resolving gel was prepared as follows, 10 % (w/v) of (bis/acrylamide 40 % - 37:5:1, 1.5 M Tris base and 0.4 % (w/v) SDS, pH 8.4). 0.03 % (w/v) of freshly prepared ammonium persulphate (APS) and 0.03 % (v/v) of TEMED were then added to solidify the gel. The resolving gel was immediately pipetted between glass plates and spacers (1.0 mm thick) to a level 1 cm below the bottom of the comb when inserted and overlaid with 0.1% (w/v) SDS solution and polymerisation allowed to occur for 1 hour. The overlaid SDS was

removed and a 3 % of stacking gel (bis/acrylamide 40 % -37:5:1, 0.5M Tris base and 0.4 % w/v SDS, 0.01 % (w/v) ammonium persulphate and 0.1 % (v/v) TEMED, pH 6.8) was poured on the top and a 1 mm comb was inserted. Following gel polymerization, they were assembled and placed in a prespex tank containing electrophoresis running buffer (25 mM Tris base, 192 mM glycine and 0.1% (w/v) SDS). Appropriate volume from each sample containing 30-40 µg protein was loaded per well as well as 5 µl prestained protein ladders (Thermo Fisher Scientific, UK) and biotinylated standards (New England Biolabs, UK). Samples were electrophoresed at a constant voltage of 100 V for 2 hours.

2.12.4 Commassie brilliant blue staining

The polyacrylamide gel was stained with Coomassie Blue to detect proteins. The gel was put into staining solution consisting of: 0.25 % (w/v) Coomassie Blue, 40 % (v/v) methanol, 7 % (v/v) acetic acid and placed on a shaker at 50 rmp for 1 hour. Enough stain was used to allow the gel to float freely in a Petri dish. The stain was replaced by 3 volumes of Destain I (4 % (v/v) methanol, 7 % (v/v) acetic acid) and shaken for 40 minutes. Destain II (5 % (v/v) methanol, 7 % (v/v) acetic acid) replaced Destain I. This was shaken overnight at room temperature and then inspected for bands.

2.12.5 Western blot analyses of Tbpl1, FHL5 and Gtf2a1l in isolated germ cells and purified recombinant protein.

Spermatocytes and spermatids were seeded onto 6-well plastic culture plates with DMEM containing 10 % foetal bovine serum (FBS), 100 Unit/ml penicillin, and 100 mg/ml streptomycin (5×10^6 cells/ml; 1 ml per well) at 37

°C The medium was changed and they were serum starved in DMEM (with antibiotics) for 16 hours. They were then incubated for 1 hour with or without drugs. Total cellular protein was extracted from both untreated and treated cells (spermatocytes and spermatids). Cells were lysed in SDS lysis buffer (60 mM Tris, 2 % SDS, 100 mM DTT) and protein concentrations were determined with a commercial kit (Bradford Protein Assay, Biorad, UK). 40 μg of total protein was mixed with an equal volume of 2 X SDS loading buffer, resolved by SDS PAGE (10 % SDS polyacrylamide gel) and transferred to nitrocellulose membranes. Blots were blocked for 1 hour with blocking buffer (PBS, 0.5 % skim milk powder, and 0.1 % Tween-20), and incubated with primary antibodies against Tbpl1, FHL5 and Gtf2a1l. Anti-Tbpl1 rabbit polyclonal antibody (1:5000; Sigma-Aldrich, UK), rabbit polyclonal anti-FHL5 antibody (1:2000; Sigma-Aldrich, UK), rabbit polyclonal anti- Gtf2a1l (1:3000; Sigma-Aldrich, UK), and mouse monoclonal anti-GAPDH (1:1,000; Abcam, Cambridge, UK), were incubated with blots in 1% BSA in TBS-T overnight at 4 °C. On the next day, blots were washed in PBST (PBS, 0.1 % Tween-20) and incubated with HRP-conjugated secondary antibody (1:5,000) for 1 hour at room temperature. Blots were then washed in PBST; the bands were visualized by Novex® ECL Chemiluminescent Substrate Reagent Kit according to the manufacturer's instructions. Digital images were captured and density measurements were made using commercial software (Quanity One, Biorad). In addition, Western blotting was performed on cells lysate samples containing Tbpl1, FHL5 and Gtf2a1l on the purified recombinant protein obtained under native conditions

or denaturing conditions. Membranes were exposed to Tbpl1, FHL5 and Gtf2a1l antibodies in 1 % BSA in TBS-T overnight at 4°C.

2.12.6 Western blot analyses of histidine tag in purified recombinant protein.

The anti-His antibody was used to detect His Tagged recombinant proteins by recognising five consecutive Histidine residues. The membrane was incubated over night with mouse anti-his HRP (AbD Serotec, UK) diluted 1: 5,000 in blocking buffer and washed three times with PBST at 4 °C. On the next day, blots were washed in PBST (PBS, 0.1% Tween-20) and incubated for 1 hour with sheep anti-mouse IgG diluted 1:30,000 for 1 h at RT. Blots were then washed in PBST; the bands were visualized by Novex® ECL Chemiluminescent Substrate Reagent Kit according to the manufacturer's instructions. Digital images were captured and density measurements were made using commercial software (Quanity One, Biorad).

2.13 Statistical analysis

Statistical analysis was performed with SPSS 16.0. The normality of the data was determined using the Kolmogorov-Smirnov test. The normality of the data was determined using the paired Student *t*-test. One-way-ANOVA analyses were performed to compare differences between control groups and treated groups. A 'P' value of (< 0.05) was considered statistically significant. The same statistical analyses were carried out in all chapters unless otherwise specified.

Chapter 3. Effect of hydrogen peroxide (H_2O_2) on germ cells in mice

3.1 Introduction

Testing germline-genotoxicity in the male is generally undertaken *in vivo*, partly because of the difficulty of achieving full spermatogenesis in vitro and partly because mating studies are currently the only reliable way of testing heritable effects. The associated expense and ethical issues mean there is a constant need for the development of novel *in vitro* assays (as demonstrated by the European REACH regulation [EU, 2007], for example). This will require an *in vitro* test system that allows examination of individual germ cell types. It should also have high sensitivity and be suitable for the rapid screening of large numbers of chemicals. We propose that the use of Staput to separate highly enriched populations of spermatogonia, spermatocytes and spermatids, and their subsequent culture in the presence of putative genotoxins or reproductive toxins, coupled with the measurement of appropriate end-points of damage, has the potential to meet this need. These three germ cell categories contain the three major events occurring in spermatogenesis: mitotic proliferation (spermatogonia); meiosis (spermatocytes); and spermiogenic differentiation (spermatids). Therefore, even though each type contains a number of different sub-types, they make suitable groupings for toxicity analysis as all the parts of each process are covered within each cell population used.

The ability to study specific germ cell types will also be useful in more fundamental studies of reproductive biology. During spermatogenesis, the male germ cell undergoes complex morphological, biochemical, and physiological changes, resulting in the formation of a mature spermatozoon. This dynamic procedure depends upon Sertoli cells that provide supply

nutrients, hormones and structural support to the germ cells and temporal regulation of their development, and on Leydig cells that synthesise the steroid hormones necessary for germ cell differentiation (Cheng and Mruk, 2010, O'Shaughnessy et al., 2009, Meistrich and Hess, 2013). Even after decades of research in the field of male fertility, critical spermatogenic events, including Sertoli cell-germ cell interaction and mechanisms of androgen action, remain to be completely understood. A more in-depth understanding of these spermatogenic events will require, for example, the ability to study specific molecular signatures of individual testicular cells. That in turn will require the isolation of purified populations of spermatogenic cells as one of the crucial steps to address these important issues. Over the years, a range of approaches have been used to successfully isolate testicular cells (Chang et al., 2011), including elutriation and fluorescence activated cell sorter (FACS) (Bastos et al., 2005, Meistrich and Trostle, 1975). Velocity sedimentation separation using Staput chambers is another of the approaches used to isolate spermatogenic cells (Han et al., 2001, Bellve et al., 1977) and has been more widely used, presumably because of the high purity of fractions that is possible and relatively low unit-cost of the experiments. Germ cell apoptosis is very common during the various stages of mammalian testicular development up to a point midway through spermatid development, when nuclear condensation has advanced too far to permit the de novo gene expression on which post-meiotic DNA repair and presumably apoptosis depends (Leduc et al., 2008). However, understanding of the mechanisms underlying male germ cell apoptosis is still limited (Koji and Hishikawa, 2003); although its role in removing genetically damaged

cells from the germ line is well accepted. Testicular cells are prone to oxidation by H_2O_2 and other reactive oxygen species (ROS) (Peltola et al., 1994, Maheshwari et al., 2009) which represent probably the commonest form of exposure to genotoxins that most cells encounter. ROS are chemically reactive molecules containing oxygen. They are generated as a natural by-product of the metabolism of oxygen and have a central role in sperm maturation as well as the acrosome reaction when expressed at low levels (Schulte et al., 2010). One of the main ROS formed during germ cells development is hydrogen peroxide (H_2O_2) (Moustafa et al., 2004). H_2O_2 constitutes the major ROS form in sperm but its effective role as an endogenous inducer of germ cell apoptosis is mostly uncertain (Aitken et al., 1998, Maheshwari et al., 2009). H_2O_2 is also known to modulate a variety of cell functions. It is a potent ROS, but its lower biological activity compared with many other ROS, combined with its capacity to cross membranes and diffuse away from the site of generation, makes it an ideal molecule in signal transduction, and it is involved in inducing the acrosome reaction in sperm (Hampton and Orrenius, 1997, Tremellen, 2008). The plasma membrane of testicular cells is rich in polyunsaturated fatty acids, thus making it prone to oxidation by H_2O_2 and other ROSs as it is well known that oxidative stress causes DNA damage (Tremellen, 2008). Previous studies have shown that male germ cells displayed a much higher sensitivity to H_2O_2 in comparison to other cells (Maheshwari et al., 2009).

Enriched populations of germ cells in the mouse thus seem suitable for analysis of the effects of genotoxins using the TUNEL assay. Since similar mechanisms could operate in the generation of pathological states in the

testis, the approach may also be important in studies of infertility in the future.

3.2 Materials and Methods

All information relevant to the experiments reported in this study is presented in section 2.1. Cell culture and the staput isolation of germ cell fractions are described in section 2.2 and 2.2.1 respectively. Cell counting in section 2.2.1.5. Viabilities of the cells in section 2.2.1.6. Cell identification in section 2.2.1.7. Immunohistochemistry, collection, and fixation and tissue preparation are described in sections 2.3, 2.3.1 and 2.3.2 respectively. Immunohistochemical staining of mouse tissue sections and isolation of germ cells are described in sections 2.3.3 and 2.3.4. TUNEL assay in section 2.4 and 2.5. Statistical analysis was performed in SPSS 16.0.

3.3 Results

3.3.1 Purification of germ cells

Microscopic examination of each of 12 ml fractions collected from the Staput chamber indicated that spermatids were concentrated in fractions 18-20, spermatocytes in the fractions 25-29, and spermatogonia in fractions 29-33, as shown in Figurer .3.1. This confirmed that different types of germ cells could be separated from each other on the basis of their density and size using staput.

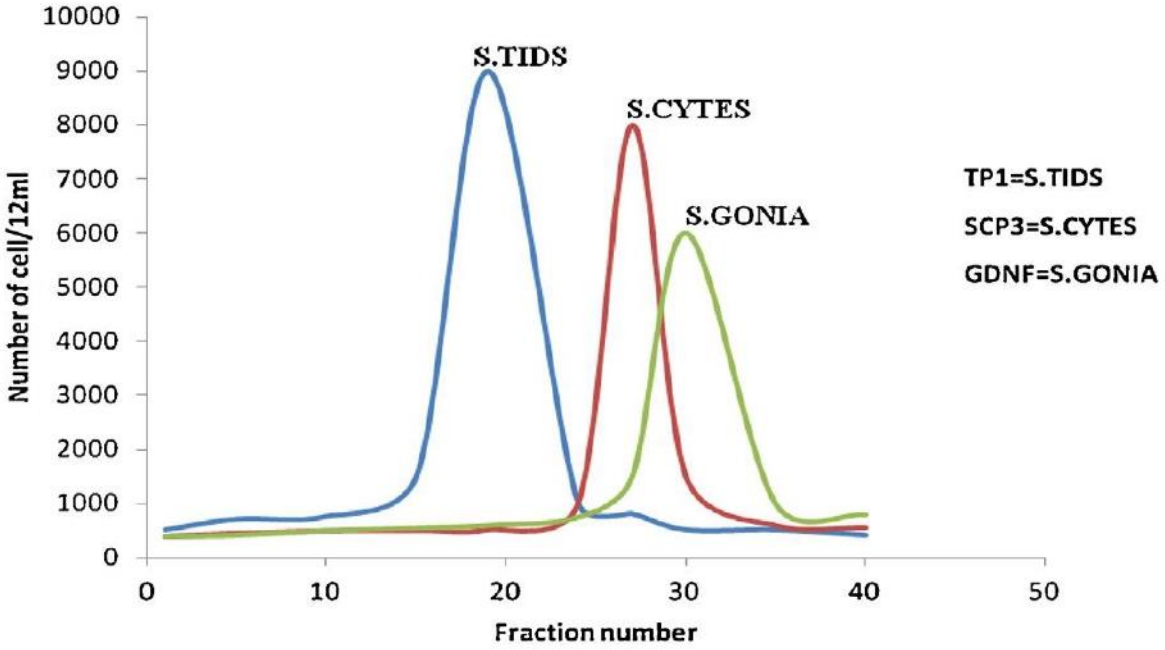

Figure 3.1: Velocity sedimentation separation of germ cells of the mouse Spermatids, characterised by Tp1 antibody staining, sediment first, followed by spermatocytes (Scp3 antibody staining), then spermatogonia (GDNFR antibody staining). Microscopic examination of each fraction isolated by Staput showed that the maximum concentration of spermatids was in the fractions (18-20), followed by spermatocytes in the fractions (25-29), spermatogina in the fractions (29-33).

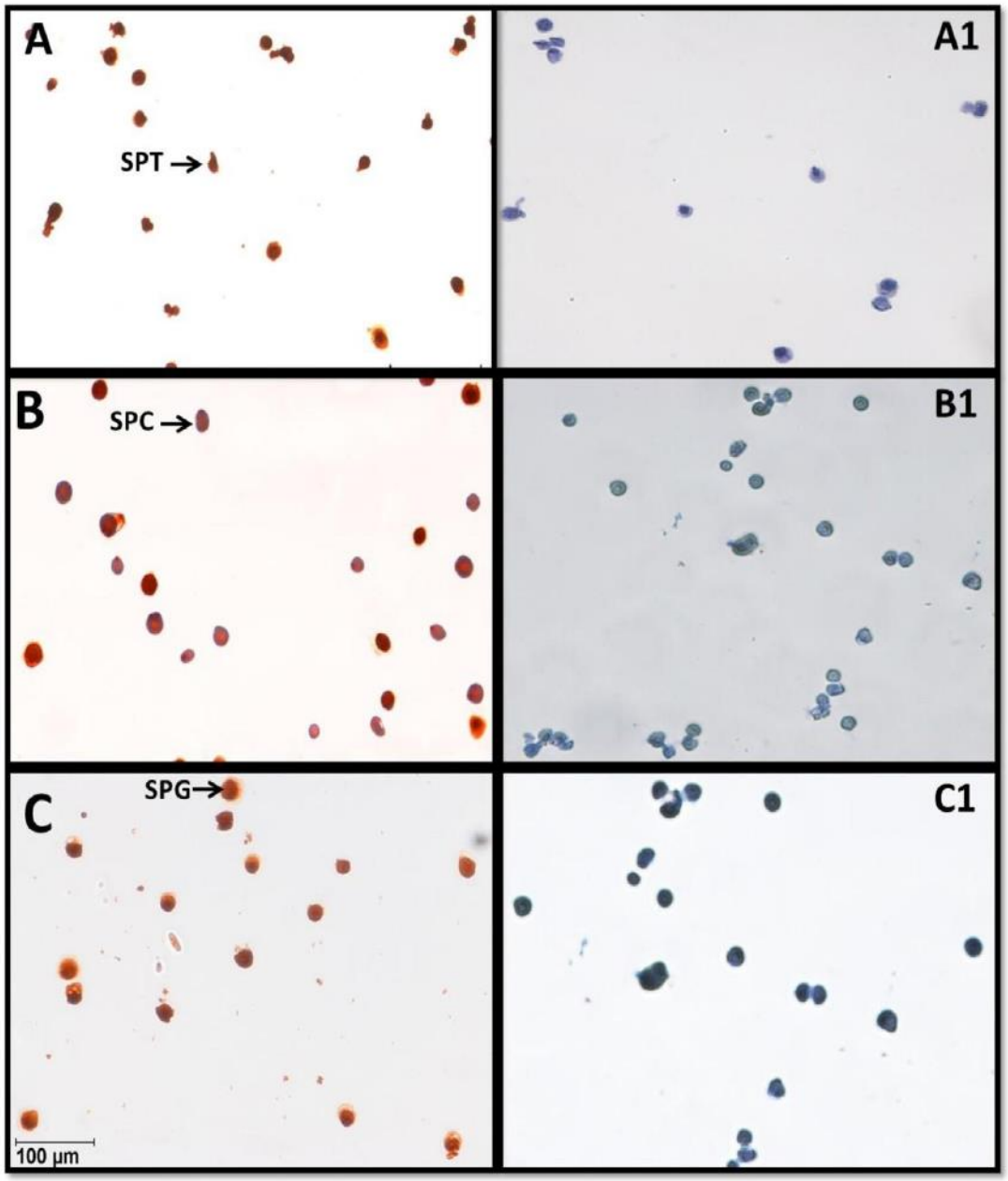

Figure 3.2: Immunohistochemical staining of Staput purified mouse testicular cells**.** Mouse testicular cells were stained with antibodies for specific proteins. Spermatids were detected with anti-TP1 (Panel A); spermatocytes were detected anti-SCP3 (Panel B) and spermatogonia were detected with anti-GDNFR (Panel C). Viewing magnification ×400.

3.3.2 Immunohistochemical staining of mouse tissue sections

An immunostaining procedure was performed on paraffin-embedded mouse tissue sections. Paraffin embedding tissue samples was processed as described in sections 2.3.3.

Figure 3.3: Immunohistochemical staining of paraffin embedded sections of mouse testis. Tissue sections from mouse testicles were paraffin-embedded and stained with anti-GDNFR in order to detect spermatogonia. Hematoxylin was used for counterstaining.

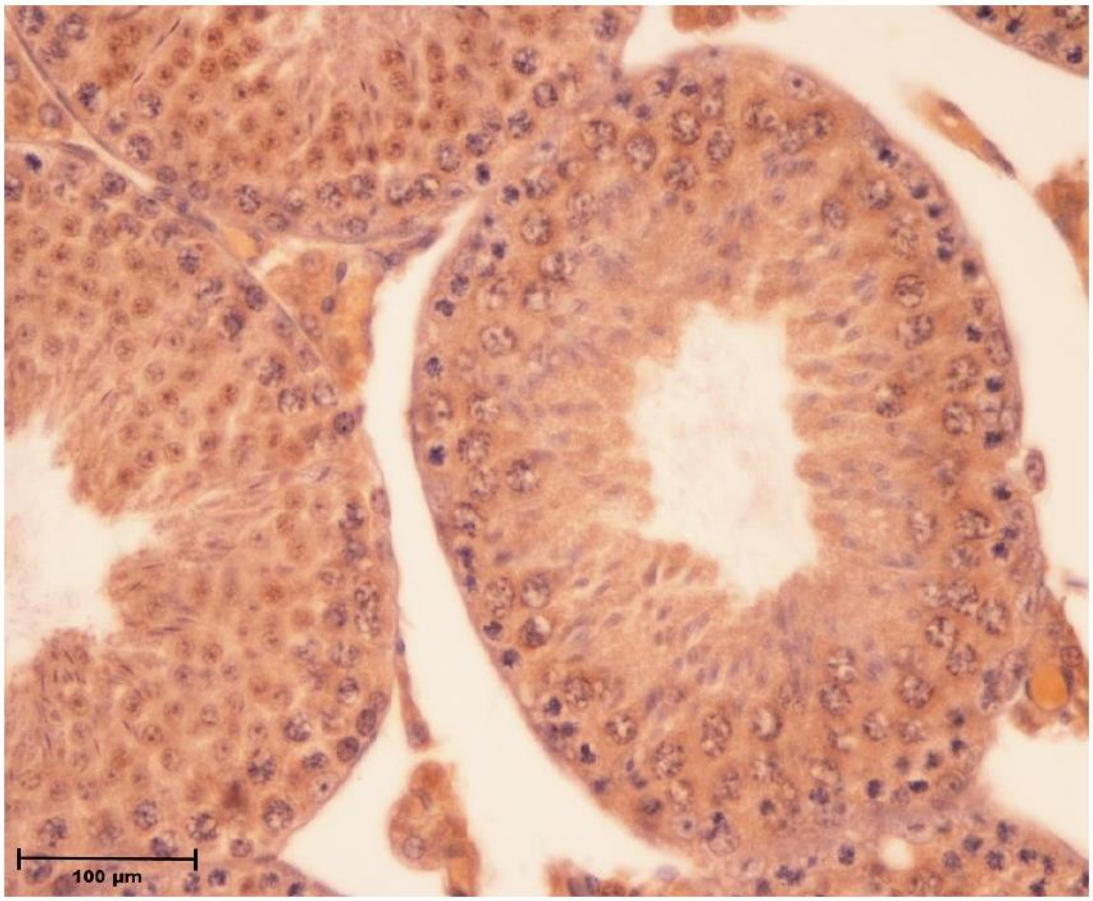

Figure 3.4: Spermatocytes staining using immunohistochemistry**.** Immunohistochemistry staining was performed on paraffin embedded sections of mouse testis. Hematoxylin was used for counterstaining. Spermatocytes were detected with anti-SCP3.

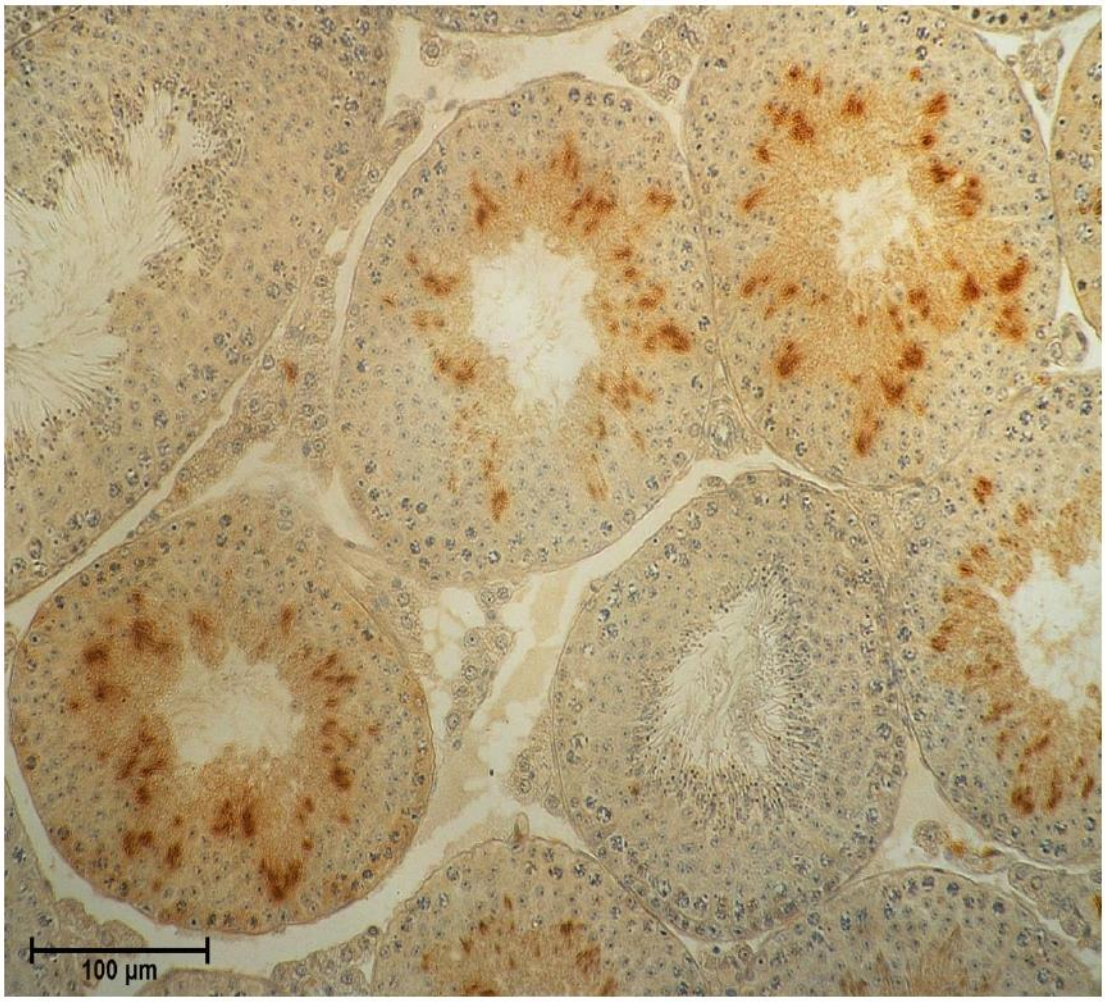

Figure 3.5: Immunohistochemical staining of spermatids. Immunohistochemical staining was performed on paraffin embedded sections of mouse testis. Hematoxylin was used for counterstaining. Spermatids were detected with anti-TP1.

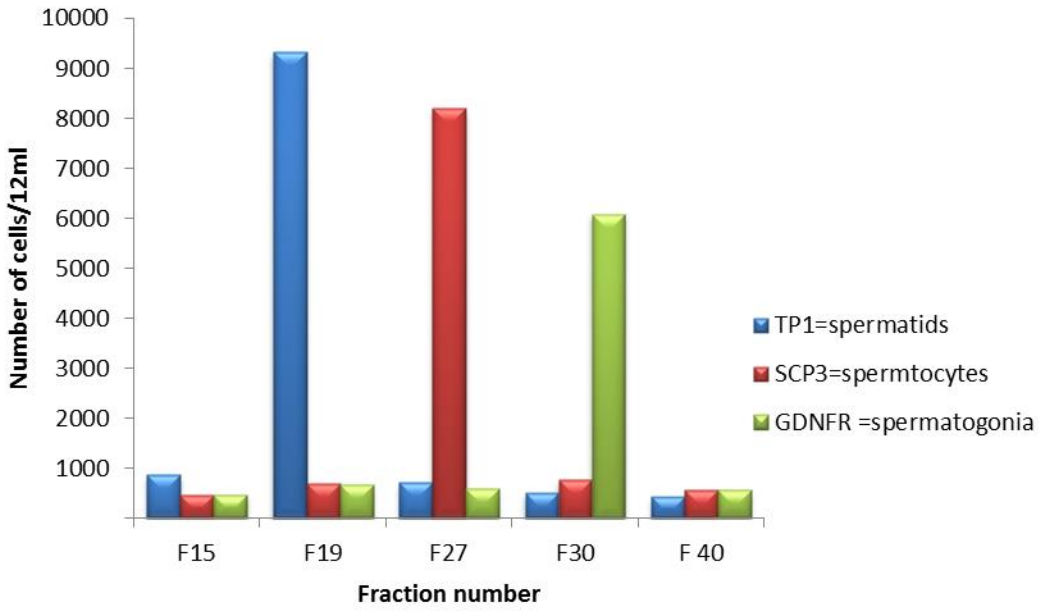

Figure 3.6: Assessment of the purity of the fractions**.** Cultured cells from all fractions were stained for each of the three antibodies and scored to determine their relative proportion in each fraction. The results for the three fractions showing the highest purity for each cell type are shown. The numbers are for total numbers of each cell type per fraction. It was found that specific fractions contained high purities of the individual cell types: spermatids in fraction F19; spermatocytes in F27; spermatogonia in F30; (Figure 3.3) so only these fractions were used for cell culture.

3.3.3 Purification of germ cells by western blot

Extractions of whole cell were made from each cell population and western blot analysis was performed to show protein expression differences for each population. Spermatids were detected with anti-TP1; spermatocytes were detected anti-SCP3 and spermatogonia were detected with anti-GDNFR.

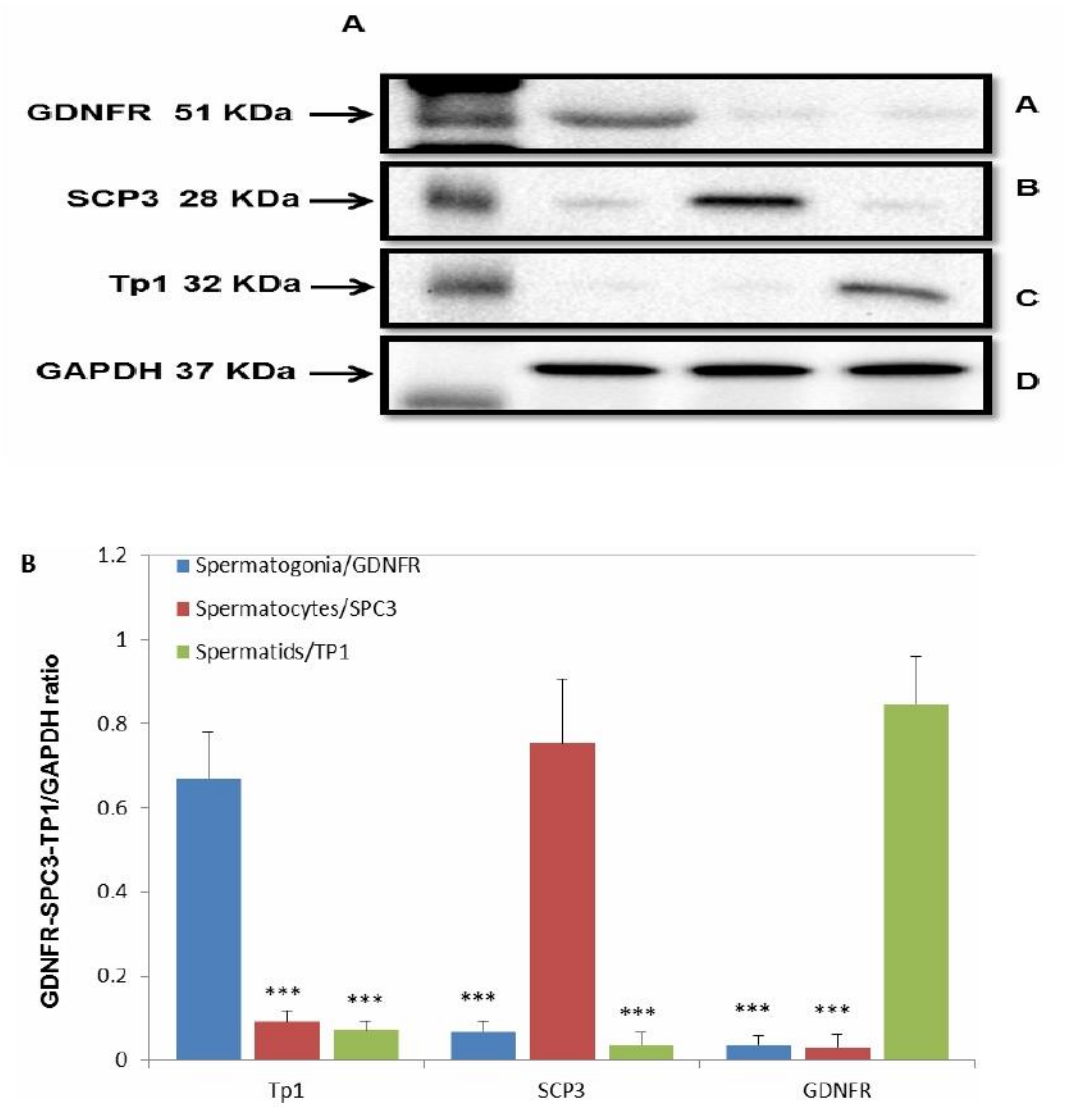

Figure 3.7: A Western blot analysis on Staput-purified mouse testicular cells Specific protein was detected in each isolated cell fraction by specific antibody. The anti-GDNF antibody was used to indicate the Spermatogonia (panel A), anti SCP-3 antibody was used to indicate the spermatocytes (panel B), anti-TP1antibody (panel C), and the protein loading control GAPDH were shown (panel D).

The relative expression level of GDNF, SPC3 and TP1 was measured by GDNF, SPC3 and TP1/ GAPDH ratio. Results are the mean ± SEM. from four independent experiments ***$p < 0.001$. B Comparison of GDFNR, SCP3 and TP1 respectively expression in isolated testicular germ cells, spermatogonia, spermatocytes, and spermatids were examined by western blot analysis and quantitative densitometry of GDNFR, SCP3 and Tp1 and GAPDH immunoblot bands was determined. The density of each band was quantified by the use of Image 1.45 software. The relative expression level of GDFNR, SCP3 and TP1 was measured by GDFNR, SCP3 and TP1 / GAPDH ratio. Results are the mean ± SEM. from three independent experiments (***$p < 0.001$) versus 24 day-old mouse testis.

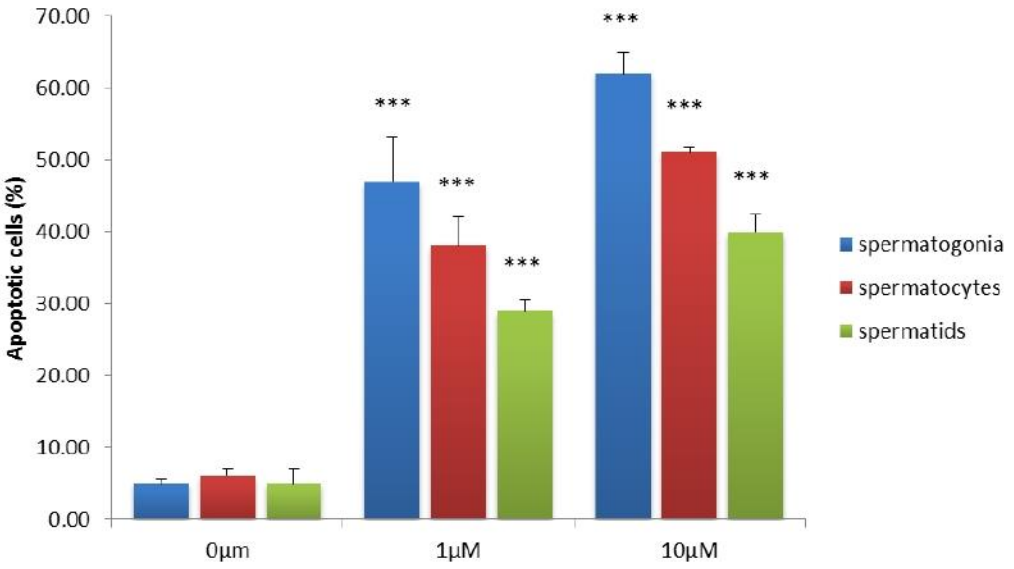

Figure 3.8: Effect of H_2O_2 treatment on germ cells evaluated in the TUNEL assay. Columns represent the mean percentages ± SEM of apoptotic cells for each of the three concentrations of hydrogen peroxide used (0, 1.0 and 10 µM). Data were obtained from three independent experiments. Each dose level within a cell type has been compared with the respective 0 µM group (***$p < 0.001$).

Immunocytochemistry analysis was used successfully in this study to identify the principal classes of male germ cells following separation via Staput: examples of cells labelled with the different antibodies are shown in Figure .3.2. It was critical to determine the purity of the fractions so that cells from each of the fractions could be scored after binding to different antibodies. It was found that specific fractions contained high purities of the individual cell types: spermatids in fraction F19; spermatocytes in F27; spermatogonia in F30; (Figure 3.6). Therefore, only these fractions were used for cell culture. It also provides valuable information about the presence and the cellular

localization of proteins within the cells on paraffin embedded sections of mouse testis (Figures 3.3, 3.4 and 3.5).

3.3.4 TUNEL assay

The outcome of H_2O_2 treatment on mouse testis was evaluated by the TUNEL assay and results expressed as percentages of apoptotic cells, are shown in Figurer 3.8. The TUNEL assay revealed that all cells types had undergone significant levels of apoptosis compared with the controls ($p \leq 0.001$). Representative apoptotic cells from treated and non-treated samples are illustrated in Figure 3.9 .The results of the induction of apoptosis by H_2O_2 treatment of different germ cell types are shown in Figure. 3.8. After treatment with H_2O_2 (1 and 10 µM) for 2 hours, a significant increase ($p \leq 0.001$) in spermatogonial apoptosis to 47% was observed when cells were treated with 1 µM H_2O_2. Moreover, the apoptosis of spermatogonial cells treated with 10 µM H_2O_2 showed a further significant increase to 62 % when compared with control ($p \leq 0.001$). Following treatment with 1 µM H_2O_2, spermatocytes showed an increase in cell apoptosis to 38%, which was statistically significant when compared with the corresponding controls ($p \leq 0.001$). A further increase to 51 % in cell apoptosis was observed when cells were treated with 10 µM H_2O_2. This increase was significant compared with controls ($p \leq 0.001$). Cell apoptosis was significantly increased to 29 % when cells were treated with 1 µM H_2O_2 ($p \leq 0.001$). The apoptosis of spermatids treated with 10 µM H_2O_2 was significantly increased to 40 % compared to the corresponding controls ($p \leq 0.001$). Figure 3.8 additionally shows that while the levels of spontaneous apoptosis are similar for all three germ cell types in the control group, the response of spermatids to both 1 and 10 µM H_2O_2 was

markedly lower than that of spermatogonia, with spermatocytes intermediate between them in both cases. The difference was statistically significant ($p \leq 0.001$) between the cell types.

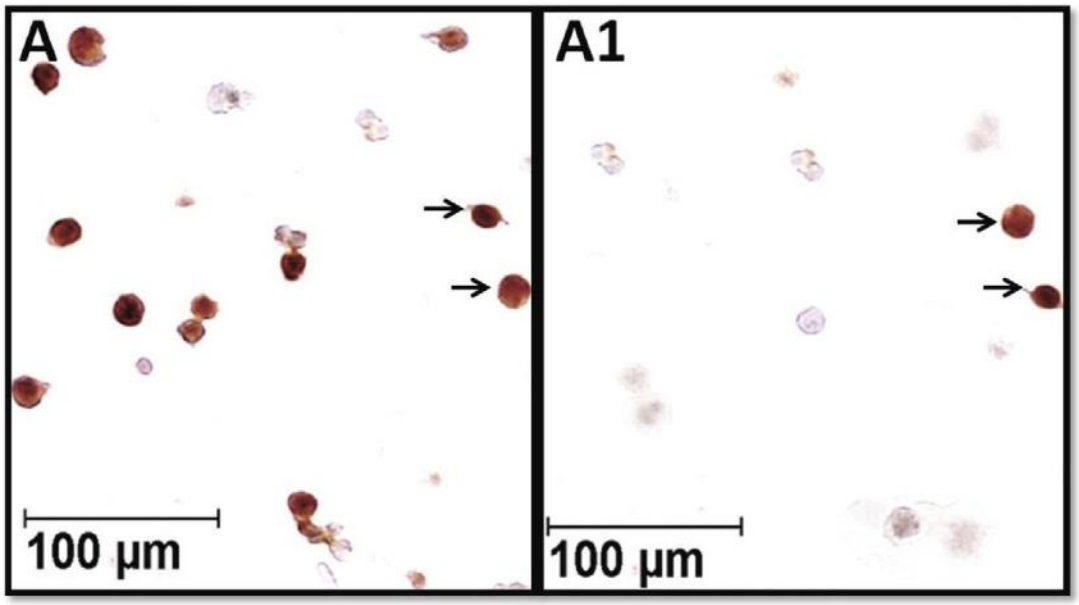

Figure 3.9: Effect of H_2O_2 treatment on germ cells of the mouse evaluated by the TUNEL assay**.** Cells treated with 10 µM H_2O_2 (A) were compared with untreated cells (A1). Arrows indicate representative TUNEL-positive (apoptotic) cells in each case. Viewing magnification × 400.

3.4 Discussion

Despite recent advances in the study of male germ line cells in terms of genetics and development, our understanding of the effect of toxins on specific cell types has been largely limited to what can be achieved by, often cumbersome, *in vivo* studies to make such distinctions. The results presented here demonstrate that a suspension of mouse germ cells can be obtained from testicular tissue and fractionated into large homogenous populations of spermatogonia, spermatocytes, spermatids and spermatozoa using staput.

Validation of the system involved using Western blot and immunohistochemistry to determine the purity of the cell populations isolated by staput (Bellve et al., 1977, Simon et al., 2010, Bryant et al., 2013), using antibodies against: TP1 to detect spermatids; SCP3 to detect spermatocytes; and GDNFR to detect spermatogonia. TP1 is an important nuclear protein in spermatids as histones are replaced by protamines during spermatogenesis. Its specificity to the haploid phase of spermatogenesis makes it a useful marker for spermatids as previously discussed (Meistrich et al., 1994, Yu et al., 2000). Spermatocytes can be located by the presence of Scp3. Synaptonemal complexes are structures formed between homologous chromosomes during meiotic prophase, thought to be involved in chromosome pairing and recombination (Brockway et al., 2014) . They comprise lateral and central elements and the two components have been identified in rodents, one of which is the SCP3 (Dobson et al., 1994, Lammers et al., 1995). Spermatogonia can be labelled by GDNFR (Savitt et al., 2012). Sertoli cells secrete a ligand to GDNFR called GFRα-1 (Viglietto et

al., 2000). The binding of this substrate-ligand complex activates the Ret receptor tyrosine kinase (Tadokoro et al., 2002).This mediates an intracellular response that is linked to the proliferation of an undifferentiated type A spermatogonia and is therefore considered a good marker for these types of spermatogonia (Meng et al., 2000). Hydrogen peroxide (H_2O_2) has been found to induce apoptosis in a various cell types and although the sensitivity of germ line cells to H_2O_2 is not fully understood, DNA strand breakage by the production of free radicals is the trigger for the programmed cell death. The results of the present study show that H_2O_2, even at a low concentration of H_2O_2 of 1 µM, has the ability to induce apoptosis in testicular germ cells *in vitro*. This is in line with what has been reported previously (Maheshwari et al., 2009) demonstrating concordance between our approach to preparing testicular germ cells and previous methodologies. In the present work, following 2 hours of treatment with 10 µm H_2O_2, a 10-fold increase in the proportion of apoptotic cells was found. There was a statistically significant induction of apoptosis in germ line cells ($p < 0.001$). The spermatogonia were significantly more affected by H_2O_2 than the spermatocytes, which were significantly more affected than spermatids. This correlates with the proportion of dividing cells expected to be present in these populations. Thus, if dividing cells are more susceptible to genetic damage than non-dividing cells, this could account for the lowest amount of apoptosis occurring in the latter population. Indeed, there are a number of different types of cells within spermatogonia, spermatocytes and spermatids, each of which could have different susceptibilities to genetic damage. Therefore, one challenge for the future will be to examine chemicals that

react primarily with each germ cell type, and to refine the Staput separation so as to isolate more specific and well defined populations. Furthermore, such a clear difference in sensitivity may be highly important in the toxicity assessment of other chemicals but would be very difficult to demonstrate with *in vivo* studies. Therefore, we believe that our approach holds significant advantages for the development of sensitive and specific in vitro reproductive and genetic toxicology assays.

Staput separation of specific germ cell types, coupled with short term in vitro culture shows potential for the rapid assessment of toxins in multiple germ cell types with high sensitivity. Notably, it allows the examination of high numbers of cells such as spermatogonia, which are normally present in relatively low amounts *in vivo*, compared with spermatocytes and spermatids. Overall, the present work shows that this *in vitro* system has potential to be a sensitive, rapid screen for reproductive toxins.

Chapter 4. Effect of doxorubicin on germ cells in mice

4.1 Introduction

Anthracyclines such as doxorubicin, widely used to treat various types of tumours, may result in induced testicular toxicity and oxidative stress (Badkoobeh et al., 2013). One of the frequently used chemotherapeutic drugs is the extremely effective anthracycline doxorubicin (Badkoobeh et al., 2013). Doxorubicin is the antineoplastic drug of choice in the treatment of various types of tumours, such as childhood leukemia and testicular cancer, though one of its adverse effects is male infertility (Shamberger et al., 1981, Imahie et al., 1995, Prahalathan et al., 2005, Vendramini et al., 2010). Doxorubicin has become the interest of several researchers since the mechanism by which it induces toxicity is known; however, novel strategies are being developed to prevent the harmful effects of this drug (Finn et al., 2011). A number of studies have reported the toxicity of doxorubicin in organs, such as liver and kidney as well as in testes, in which testicular dysfunction and male infertility has been reported (Hou et al., 2005, Yagmurca et al., 2007). Because of the importance of doxorubicin in treating many types of haematological and solid tumours, various pharmacological and non-pharmacological plans have recently been suggested to counteract its toxicity, specifically antioxidant supplements and physical exercise (Alshabanah et al., 2010). Increasing investigational evidence suggests that doxorubicin treatment induces testes dysfunction mostly due to excessive production of ROS and increased susceptibility to apoptosis, especially those under rapid and constant proliferation, such as the male germ cells (Hou et al., 2005, Shinoda et al., 1999, Yeh et al., 2007).

Doxorubicin has also been reported to be a somatic cell mutagen in humans and animals (Smith, 2003, Pulte et al., 2008). The number of male germ cells that undergo apoptosis has been increasing due to response to numerous chemotherapeutic agents involving anthracyclines (Sjoblom et al., 1998, Zanetti et al., 2007). The cells most sensitive to doxorubicin are the early spermatogenic cells, spermatogonia and meiotically dividing spermatocytes (Sjoblom et al., 1998, Shinoda et al., 1999, Zanetti et al., 2007). In 1979, (Lu and Meistrich, 1979) reported that even a low dose of doxorubicin was able to target male germ cells in mice, mainly spermatogonia, and lead eventually to seminiferous epithelium depletion. Moreover, it was harmless to primary spermatocytes (Lu and Meistrich, 1979). Doxorubicin caused testicular toxicity and it mainly exerts its effect on premeiotic spermatogonial cell, because of its high division rate and slow cell cycle (Lu and Meistrich, 1979, Bechter et al., 1987, Jahnukainen et al., 2000). Doxorubicin uses potent anticancer activity during a mechanism that includes intercalation with DNA and an inhibition of topoisomerase II activity that results in replication-dependent, site-selective double-strand breaks in DNA (Myers CE, 1990, Quiles et al., 2002). Doxorubicin also has been shown to interfere with a vital molecule included in transcription and stability of chromosome, the DNA methyl transferase 1 - DNMT1 inducing apoptosis (Yokochi and Robertson, 2004). Therefore, it can target the immature germ cell line, leading to long or short term male infertility (Dacunha et al., 1983, Meistrich, 2013). This genotoxic effect leads to up-regulation of cancer suppressor gene, p53, a substantial mediator of cell cycle arrest designed to prevent DNA replication in the presence of DNA damage and this leads to apoptosis (Bunz et al.,

1998). Recent studies have also shown that doxorubicin is capable of reducing the viability of cancer cells through RNA damage (Fimognari et al., 2008).

The chemical structure of doxorubicin favours the generation of free radicals and the compound can bind to iron and form complexes with DNA, resulting in DNA damage (Eliot et al., 1984, Ravi and Das, 2004). Moreover, it promotes the generation of free radicals and the initiation of oxidative stress, leading to cellular injury (Injac and Strukelj, 2008). This free radical generation from doxorubicin might contribute as genotoxicity in normal cells (Quiles et al., 2002). It has been reported that doxorubicin induces ROS generation in different cancer cells (Gouaze et al., 2001). However, the main mechanism of action of doxorubicin induced ROS in tumour cell is still not completely known. Many studies have shown that inhibition of overexpression of antioxidant enzymes that induced oxidative stress by doxorubicin prevents apoptosis in tumour cells (Gouaze et al., 2001, Suresh et al., 2003). Blocking the activity of endogenous antioxidants, such as glutathione produced by tumour cells, made them more vulnerable to doxorubicin (Mallery et al., 1999, Poirson-Bichat et al., 2000).

Many studies have showed that exposure to doxorubicin caused significant increase in chromosomal aberrations in spermatocyte (Attia et al., 2010, Meistrich et al., 1990, Abraham and Franz, 1983). It also increases the incidence of meiotic micronuclei in male rats resulting in reduced fertility (Baumgartner et al., 2004). Furthermore, increased total number of cells with structural chromosomal aberrations, and severe inhibition in the mitotic activity of spermatogonia was found following doxorubicin treatment in male

mice (Tohamy et al., 2003). The negative effect of doxorubicin on the premeiotic S-phase of mouse spermatocytes has been reported (Russo and Levis, 1992). In the rat testis, doxorubicin was shown to inhibit DNA synthesis and to induce apoptosis (Jahnukainen et al., 2000), in addition to induction of spermatid micronuclei (Lahdetie et al., 1994). Furthermore, incident of morphological changes and degeneration of male germ cells have showed that sperm cells were undergoing apoptosis as revealed by in situ terminal deoxynucleotidyl transferase mediated dUTP nick end labeling (TUNEL assay) (Shinoda et al., 1999, Yeh et al., 2009). Moreover, histological analysis and flow cytometry have showed an increase in apoptotic cells of both aneuploid and diploid spermatids of mouse male germ cells (Katoh et al., 1990).

The present investigation was designed to determine whether exposure of mice germ cells to doxorubicin induces DNA damage in the form of strand breaks and apoptosis in male germ cells. If so, what is the relative sensitivity of specific cell types to doxorubicin. Additionally, the usefulness of *in vitro* cultures of mice spermatogonia, spermatocytes and spermatids, in conjunction with the Comet assay TUNEL Assay is reported.

4.2 Materials and Methods

All information relevant to the experiments reported in this study is presented in section 2.1. Cell culture and the staput isolation of germ cell fractions are described in section 2.2 and 2.2.1 respectively. Cell counting in section 2.2.1.5. Viabilities of the cells in section 2.2.1.6. Cell identification in section 2.2.1.7. Immunohistochemistry, collection, and fixation and tissue

preparation were described in sections 2.3, 2.3.1 and 2.3.2 respectively. Immunohistochemical staining of mouse tissue sections and isolation of germ cells were described in sections 2.3.3 and 2.3.4. TUNEL assay in section 2.4 and Comet assay in section 2.5. Statistical analysis was performed in SPSS 16.0.

4.3 Results

4.3.1 Treatment of cells with doxorubicin

Cells were cultured and treated with different concentrations (0, 0.05, 0.5, and 1 mM) of doxorubicin for 1 hour at 37 °C. Germ cells (treated and untreated) were immediately used in the Comet assay as described previously in section 2.7. For TUNEL assay, doxorubicin was added to the isolated germ cells in 6-well plastic culture plates with DMEM media at 37 °C to yield final concentrations of 0.05, 0.5, and 1 mM, respectively. In both cases, treated and untreated cells were fixed with 4 % formaldehyde for 10 minutes and washed twice, each for 5 minutes in PBS containing 0.5 % BSA and stored at in 70 % (v/v) ethanol and TUNEL assay was performed as described in sections 2.5 and 2.6.

4.3.2 Effect of doxorubicin on isolated testicular germ cells

To verify the level of sensitivity of male germ cells to doxorubicin, purification of male germ cells from adult mice were used as cellular material, and doxorubicin was used as a source of genotoxicity. DNA damage in isolated germ cell spermatogonia, spermatocytes and spermatids was evaluated using the Comet assay. In addition the presence of apoptosis was

determined by terminal deoxynucleotidyl transferase-mediated dUTP nick end-labeling (TUNEL) detection in situ and by an increase in apoptotic cells.

4.3.2.1 Comet assay

The results of the single cell gel electrophoresis analysis are shown in Figure 4.1, 4.2 and 4.3. Comet image of isolated germ cells before (untreated cells) and after treatment with different concentration of doxorubicin. Control cells show an intact head, while the damaged cells show a reduced head and a comet tail; the bigger the damage, the greater the tail (Figure 4.1).

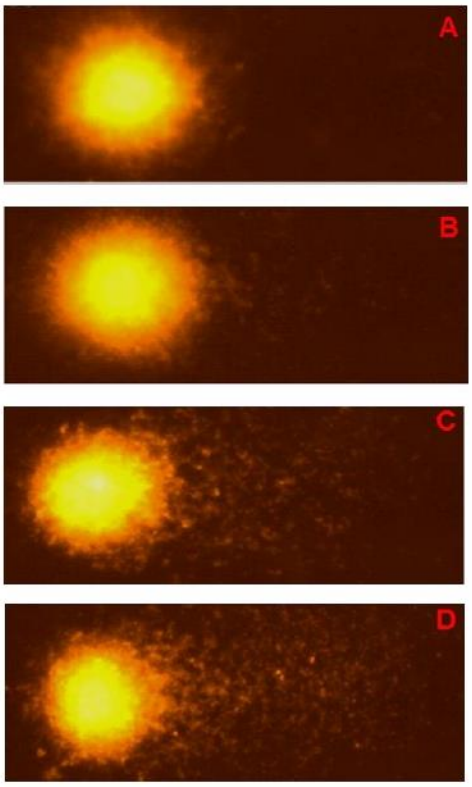

Figure 4.1: Comparison of control, comet, and apoptotic cells based on fluorescence microscopy germ cells treated with different concentration of DOX showing DNA damage (magnification X 400) (A) Control cells in standard alkaline Comet assay; (B) 0.05 mM DOX treated cells; (C) 0.5 mM DOX treated cells; (D) 1 mM DOX treated cells.

The responses of purified germ cells to DOX in the Comet assay (OTM and tail DNA) are shown in Figure 4.2 and 4.3. A significant increase in the OTM and tail DNA of spermatogina from 2.5 (OTM) and 37.17 % (tail DNA), respectively, was observed when treated with 0.05 mM DOX. Furthermore, at 0.5 mM, OTM and tail DNA damage showed a further significant increase to 4.9 and 46 % respectively in spermatogonial cells compared with control ($p \leq 0.001$). Additionally, on treatment of spermatogonial cells with 1 mM the DNA damage increased further to 7.4 for OTM and 59.35 % for tail DNA. In contrast, spermatocytes showed significant increase in the OTM and tail DNA at 0.5 mM DOX 3.8 for OTM and 40.97 % for tail DNA, which was statistically significant compared with the corresponding controls ($p \leq 0.01$). Additionally, when spermatocytes cells treated with 1 mM the DNA damage increased further to 5.7 for OTM and 43.61 % for tail DNA while, spermatids showed only significant increase in the olive tail moments but not in tail DNA at 0.5 mM DOX 2.1 for OTM, when compared with the corresponding controls ($p \leq 0.05$). Moreover, Cells when treated with 1 mM the DNA damage increased further to 4.25 for OTM and 42.21 % for tail DNA.

Results of the Comet assay with purified germ cells showed increase in olive moment, tail moments and increase in the tail DNA as indicators of DNA damage induced by doxorubicin exposure of germ cells *in vitro*. For the treatment with 0.05 mM DOX, hardly was any DNA damage found on the spermatocytes and spermatids, suggesting that there was very little or no cytotoxic on these cells; however, spermatogonia was found more sensitive to 0.05 mM which might be due to cytotoxic effects of DOX.

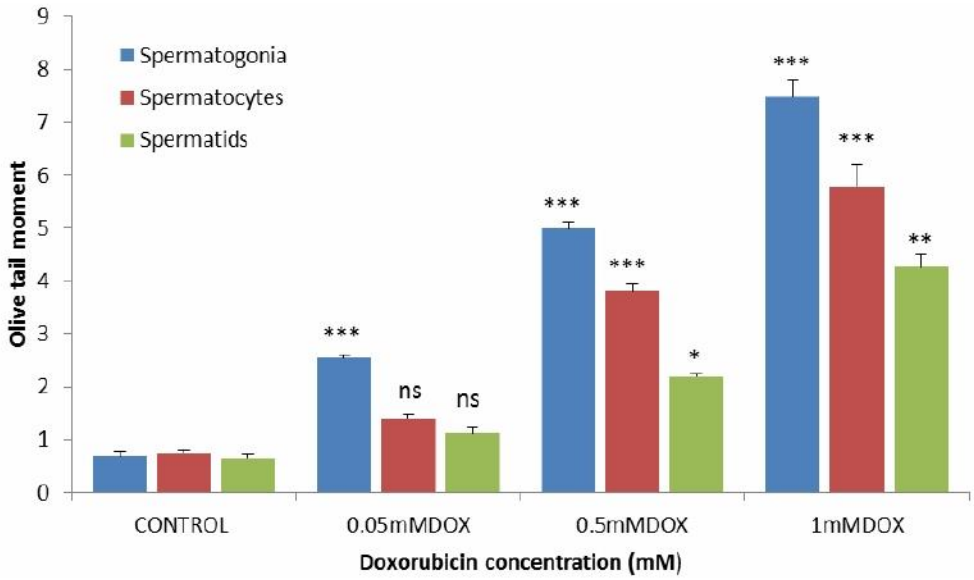

Figure 4.2: DNA damage induced in mice germ cells by doxorubicin treatment. The distribution of mouse spermatogonia, spermatocytes and spermatids with different extent of DNA damage (0 ± 3) was determined by the Olive tail moment after treatment with 0.05, 0.5 and 1 mM doxorubicin. The results are shown as mean ± SEM of 3 independent experiments, (*** $p<0.001$, ** $p<0.01$, * $p<0.05$ when compared with the respective control group).

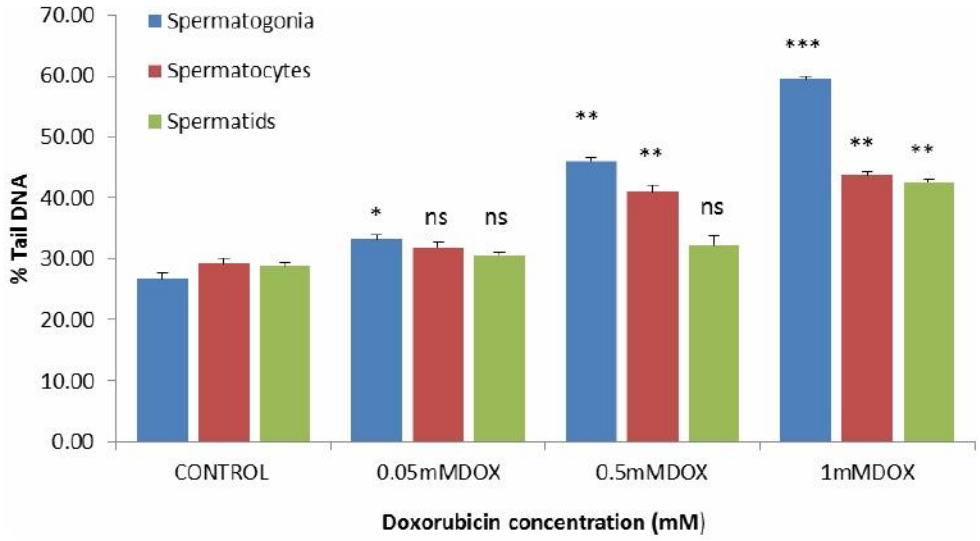

Figure 4.3: Comet assay results obtained from exposure of 0.05, 0.5, and 1 mM concentrations of doxorubicin to germ cells. Comet parameters, % tail DNA were taken into account to measure DNA damage. The results are shown as mean ± SEM of 3 independent experiments, (*** p<0.001, **p<0.01, *p<0.05 when compared with the respective control group).

4.3.3 TUNEL assay

TUNEL assays for apoptosis evaluation were performed on separate cell samples of the same cell populations as described in detail in sections 2.5 and 2.6. The result of doxorubicin treatment on isolated germ cells of mouse testis was expressed as mean percentages ± SEM of apoptotic cells. The TUNEL assay revealed that all cells types had undergone significant levels of apoptosis compared with the controls ($p \leq 0.001$). The results of the induction of apoptosis by DOX treatment of different germ cell types are shown in Figure 4.4. After treatment with DOX (0, 0.05, 0.5 and 1 mM) for 1 hour, a significant increase ($p \leq 0.01$) in spermatogonial apoptosis to 11 %

was observed when cells were treated with 0.05 mM DOX. Moreover, the apoptosis of spermatogonial cells treated with 0.5 mM dox showed a further significant increase to 23 % when compared with control ($p \leq 0.001$). Further increase was observed when the cells were treated with 1 mM DOX. Following treatment with 0.5 mM DOX, spermatocytes cells showed an increase in cell apoptosis to 15 %, which was statistically significant when compared with the corresponding controls ($p \leq 0.01$). A further increase to 34 % in cell apoptosis was observed when cells were treated with 1 mM DOX. This increase was significant compared with controls ($p \leq 0.001$). The apoptosis of spermatids treated with 0.5 mM dox was significantly increased to 13 % compared to the corresponding controls ($p \leq 0.05$). A further increase to 24 % in cell apoptosis was observed when cells were treated with 1 mM DOX. This increase was significant compared with controls ($p \leq 0.01$).

Furthermore, Figure 4.4 shows that though the levels of spontaneous apoptosis are different between all three germ cell types in the control group, the response of spermatids to 0.05, 0.5 and 1 mM DOX was clearly lower than that of spermatogonia, with spermatocytes intermediate among them in both cases. The difference was statistically significant ($p \leq 0.001$) between the cell types.

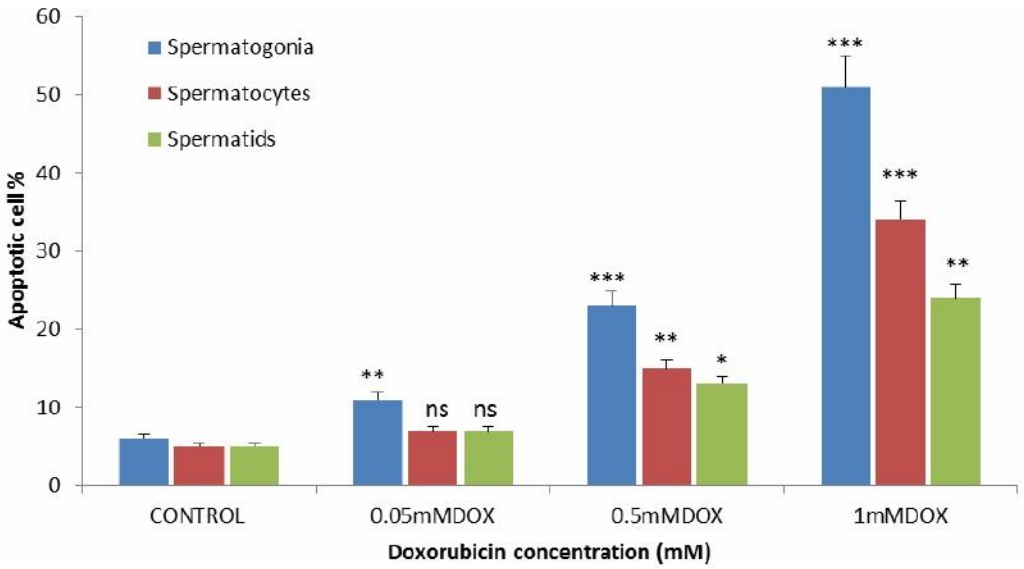

Figure 4.4: Effect of DOX treatment on germ cells evaluated in the TUNEL assay**.** Columns represent the mean percentages ± SEM of apoptotic cells for each of the three concentrations of DOX used (0, 0.05, 0.5 and 1 mM). Data were obtained from three independent experiments. Each dose level within a cell type has been compared with its respective control group (*P <0.05 = **P <0.01 = *** P <0.001).

4.4 Discussion

Male germ cells are known to be one of the tissues vulnerable to toxicity of chemotherapeutic drugs such as doxorubicin (Hou et al., 2005). The pervious study showed that the side effect of doxorubicin induces oxidative stress and precipitates cell apoptosis in testicular tissues (Yeh et al., 2009). In comparison to normal tissue, tumours are characterized by uncontrolled division. The process of cell division- normal or cancerous cell- is through the cell cycle. The cell cycle goes from the resting phase, through active growing phases and then to mitosis (division). The ability of chemotherapy to kill cancer cells depends on its ability to halt cell division. Therefore, chemotherapy is most effective at killing cells that are rapidly dividing. Unfortunately, chemotherapeutic agents can not differentiate between the cancerous and the normal cells. It has been shown that apoptosis is one of the mechanisms in cell destruction following chemotherapy (Hou et al., 2005). A wide range of conditions are known to increase the rate of germ cell apoptosis in testis such as testicular ischemia and toxic substances (Sakallioglu et al., 2007, Mendez Palacios et al., 2014, Mohammadnejad et al., 2012). The potential infertility causing complication renders protection of testicular tissue a critical issue whenever doxorubicin is employed for anti-neoplastic chemotherapy. A previous study has shown that doxorubicin impaired mouse testicular structure through inflicting oxidative stress and inducing cell apoptosis (Yeh et al., 2007). The present study clearly validates that the magnitude of DNA damage is related to both the dose administered and germ cell types exposed to doxorubicin. The goal of the current study was to investigate the usefulness of *in vitro* germ cell culture, in combination

with the Comet assay, to determine DNA damage induced via genotoxic agents in male germ cells in mice. As the genotoxic effect of doxorubicin on male germ cells is well recognized, this genotoxic agent was used in the present study. We report here the application of the Comet assay to the analysis of DNA strand-break evolution in cultured germ cells in mice (spermatogonia, spermatocytes and spermatids). Isolated germ cells were treated with doxorubicin for 1 hour at 37°C *in vitro* and DNA damage was assessed using the Comet assay. DNA damage showed a significant increase in Olive tail moment and tail DNA percentage after being exposed to doses of 0.05 and 0.5 mM doxorubicin (Figure 4.2 and 4.3). Our results indicate that spermatogonia reach the significance threshold with low concentrations of doxorubicin. This may be due to the fact that toxicity of this drug is mediated by its interaction with topoisomerase II, an enzyme that is abundant in cells undergoing rapid and constant proliferation (Brilhante et al., 2012). Thus, in the testis, spermatogonial cells are the main target of doxorubicin, because of their intense and continuous proliferative activity (Brilhante et al., 2012). The Comet assay is a very useful tool in genotoxicity studies (Tice et al., 2000, Gaivao and Sierra, 2014) and a method for sensitive and rapid detection of DNA strand breaks in individual cells (Fairbairn et al., 1995, Liao et al., 2009). The Comet assay also produces reliable result for induced DNA damage in a short time. Our results show that the Comet assay is useable for the investigation of DNA damage induction and provide a useful system for genotoxicity evaluation of chemicals and the investigation of DNA damage induction in isolated germ cells.

It is well recognized that doxorubicin induces apoptosis in early spermatogonia, which results in a decrease in the size of the pool of germ line stem cell (Holm et al., 2009, Hou et al., 2005). In addition, other studies have shown increased apoptosis in spermatogonia and spermatocytes following doxorubicin treatment (Baumgartner et al., 2004, Brilhante et al., 2012).

Based on the evidence provided in these studies; it could be asserted that the spermatogenic cells are prone to the effect of doxorubicin, especially those undergoing rapid proliferation, such as spermatogonia. The results derived from this study suggest that the initiation phase of spermatogenesis is highly sensitive to doxorubicin-induced apoptosis. The observations confirm the genotoxic capacity of doxorubicin as previously demonstrated by other authors using rats (Hou et al., 2005, Brilhante et al., 2012).

The results presented in this study provides firm evidence that doxorubicin can unfavourably damage the male germ cells and significantly increase DNA damage and apoptosis. Furthermore, the difference in DNA fragmentation between the treated and the control suggests reduced germ cells proliferation and increased apoptotic cells on the extremely proliferative germ cells, namely spermatogonia and spermatocytes.

Chapter 5. The development of an *in vitro* rat germ cell system to detect well-known *in vivo* germ cell mutagens

5.1 Introduction

The single-cell gel electrophoresis assay has been widely used to measure DNA damage in male germ cells in a variety of physiological and pathological conditions (Haines et al., 2002, Baumgartner et al., 2009). This chapter examined the same methodology in chapter 4 to investigate six well known *in vivo* germ cells mutagenesis. N-ethyl-N-nitrosourea (ENU), N-methyl-N-nitrosourea (MNU), 6-mercaptopurine (6MP), 5-bromo-2'-deoxyuridine (5-BrdU), methyl methanesulfonate (MMS) and ethyl methanesulfonate (EMS) are potent male rodent germ cell mutagens and have been widely used historically to characterise the susceptibility of different types of germ cells to the induction of genetic damage. Numerous strategies for the assessment of genotoxicity of chemical compounds or chemotherapeutic agents have been proposed. In the present study, the effect of genotoxicants that are known to affect germ cells *in vivo* were tested in isolated germ cells *in vitro* using methods for isolation and culture of adult male rat cell.

Genotoxicity testing is part of the legislative requirements for safety testing that have to be performed before a new compound can be released for human contact and/or the environment (Parasuraman, 2011). Many different experimental methods are in use for investigation of genotoxicity of chemicals in animals (Parasuraman, 2011). *In vivo* tests of genotoxicity can involve the use of large numbers of animals (Van der Jagt et al., 2004), take several weeks to perform, and often provide only a general indication of genotoxic hazards without information about the mechanisms of action of the tested compounds. *In vitro* test systems have been proposed as alternatives to whole animal testing for genotoxic toxicity (Makris et al., 2011). Therefore,

in vitro toxicity tests need to be recognized in order to decrease the number of test animals and expense, without compromising the safety of consumers. Furthermore, such *in vitro* approaches should be better suited to test a larger number of chemicals than those employed *in vivo* tests (Toppari et al., 1996, Genschow et al., 2002, Spielmann et al., 1997). The male reproductive system is particularly sensitive to the damage induced by anticancer agents targeting rapidly dividing cells (Clermont, 1972, Aguilar-Mahecha et al., 2002). Animal models have been extensively used to study spermatogenesis and have revealed various molecular mechanisms that are critical during this process (Jan et al., 2012). Faults in germ cell progress can result in infertility or DNA damage, and genetic alterations passed via germ cells might cause many disorders in the offspring (Li et al., 2014). Additionally, spermatogenic failure happens at different levels, involving defective migration of primordial germ cells, arrest during spermatogenesis, loss of spermatogonial stem cells and insufficient spermiogenesis or a disrupted micro-environment (Jan et al., 2012). All these complications can result to some common conditions such as azoospermia, severe oligozoospermia and asthenozoospermia. Moreover, a number of studies have established the role of specific genes in the regulation of proliferation and differentiation in vitro (Jan et al., 2012).

It is well known that ENU and MNU, which are direct acting alkylating agents (Seeley and Faustman, 1995, Beckwith et al., 2000), primarily affect spermatogonia in vivo (Hitotsumachi et al., 1985). These alkylating agents have been found to induce mutagenesis by transferring its ethyl/methyl groups to nucleophilic oxygen or nitrogen sites on deoxyribonucleotides, leading to base mismatch within DNA replication (van Boxtel et al., 2010,

Imai et al., 2000). Russell et al., (1979) reported that treating male mice with ENU causes mutations that affect the spermatogonial stem cells and they also found that the spermatogonia had the highest rate of mutation in all cell types examined. A high frequency of mutations was also found in spermatogonial cells after treatment with ENU (Katoh et al., 1994, Provost and Short, 1994, Russell et al., 2007). Previous studies showed that, most of the mutations were intragenic after treatment with ENU (Marker et al., 1997, Miltenberger et al., 2002). In addition, mutations induced by ENU in spermatogonia, were found to be single base pair changes (Miltenberger et al., 2002). MNU has been found to be highly mutagenic in differentiating spermatogonia (Russell and Hunsicker, 1983, Russell et al., 2007). 6-MP and 5-BrdU are considered as the major analog drugs for therapy of acute lymphoblastic leukemia and autoimmune diseases, and have been used for four decades. 6-MP is metabolized by enzyme activity of thiopurine methyltransferase (TPMT), and therefore is anabolized by several enzymes to form 6-thioguanine nucleotides, leading to the induction of cytotoxicity as a result of its incorporation into DNA (Kanemitsu et al., 2009). 6-MP has also been shown to cause chromosomal damage and aberrations in the spermatocytes of male mice (Mosesso and Palitti, 1993). Furthermore, it has been shown that germ cells treated with 6-MP have the greatest response in early meiotic spermatocytes (Generoso et al., 1975). The thymidine analog (5-BrdU) is a genotoxic compound that is incorporated into DNA, causing specific-locus mutations and inhibition of cell proliferation (Morris, 1991). 5-BrdU is a nucleoside nucleic acid base modified via halogen substitution, and its derivatives are widely used in antitumour agent studies (Kagawa et al.,

2008). Histological examination of cultured rat spermatocytes after injection with 5-BrdU has demonstrated that 5-BrdU mostly labelled spermatocytes (Hue et al., 1998).

EMS and MMS are alkylating agents that represent one of the most important classes of anticancer agents and play a major role in the treatment of several types of cancers (Kondo et al., 2010, Chaney and Sancar, 1996). MMS and EMS have been studied in mature spermatozoa to examine mutagenesis in different phases of spermatogenesis in male mice (van Delft et al., 1997). It has been found that EMS and MMS induce a high incidence of dominant lethal mutations in spermatids (Ehling, 1971). They have also been found to be mutagenic in the last phase of spermatogenesis, i.e. late spermatids and spermatozoa (van Delft et al., 1997). There are two ways to carry out a dominant lethal assay in males treated once. The first method in which male animals are mated for eight weeks (mice) or ten weeks (rats) to virgin female mice over the spermatogenic cycle and mated once a week (Anderson et al., 1981), or every few days (Ehling et al., 1978) to determine at which stage of the spermatogenic cycle the chemical is at its most active. There is a second method where animals are mated after 2 doses, one non-toxic. The animals are mated for 8-10 weeks and sampled twice (Topham, 1980) a similar approach has been used *in vivo* Comet assay (Hartmann et al., 2003b). The toxic dose will ensure that animal received the compound when a negative response is seen (Hartmann et al., 2003). The present study mimics the method of Anderson et al (1981). The three different types of isolated germ cells (spermatogonia, spermatocytes and spermatids) are examined but all cells are only exposed to single dose *in vitro* Comet assay.

5.2 Materials and Methods

All information relevant to the experiments reported in this study are presented in section 2.1. Germ cells isolation and preparation was described in section 2.2.1 and cell counting in section 2.2.1.5. The treatment time of isolated germ cells is reported in section 2.3.1.5.1 and evaluated using Comet assay parameters as reported in section 2.6 and 2.6.1. TUNEL assay in section 2.5 and 2.5.1 Data are expressed as mean ± SEM of at least three independent experiments with three replicates per experimental group. Statistical analyses were made by one-way ANOVA; for all experiments, a *P* value of < 0.05 was considered significant.

The alkaline version of the single cell gel electrophoresis assay was conducted on separate cultures of spermatogonia, spermatocytes and spermatids of male rats treated with 0.05 mM, 0.5 mM, 1 mM, of all six compounds. Hundreds of cells were scored for each cell type examined per slide, and two measures of DNA damage were made for each sample: % Tail DNA and OTM. The mean values from all cell types per treatment group are presented in the Comet and TUNEL assays data tables along with the results of the statistical analyses.

5.3 Results

5.3.1 Effect of ENU and MNU treatment

MNU and ENU displayed a dose-response curve in both assays used for this investigation. The lowest doses that induced a statistically significant increase in genetic damage were 0.05 mM ENU or 0.05 mM MNU for DNA

damage and 0.05 mM ENU or 0.05 mM MNU for apoptosis. In spermatogonia, both nitrosoureas ENU and MNU showed highly increased OTM, percentage tail DNA and the percentage of apoptotic cells. They were thus clearly much more potent as spermatogonial mutagens than 6-MP and 5-BrdU or the methanesulfonates (Figure 5.1, 5.2, 5.3, 5.4, 5.5 and 5.6). The response to ENU and MNU treatment was also different in the three types of cells analyzed: spermatogonia, showed the highest levels of DNA damage and apoptosis in response to ENU and MNU treatment in comparison to the other types of cells. Spermatogonial cells showed a clear dose-dependent, statistically significant increase in comet parameters and apoptosis from the concentration of 0.05 mM (Figures 5.3 and 5.6) upwards whereas the other compounds showed lower means at each dose with generally lower levels of significance and only significant at all from 0.5 mM upwards. The values of various comet measurements as quantified with Comet 6.0 software generated from ENU and MNU studies are given in Table 5.1.The results showed that OTM and %Tail DNA gave good correlations with the concentration/dose of ENU and MNU agents used.

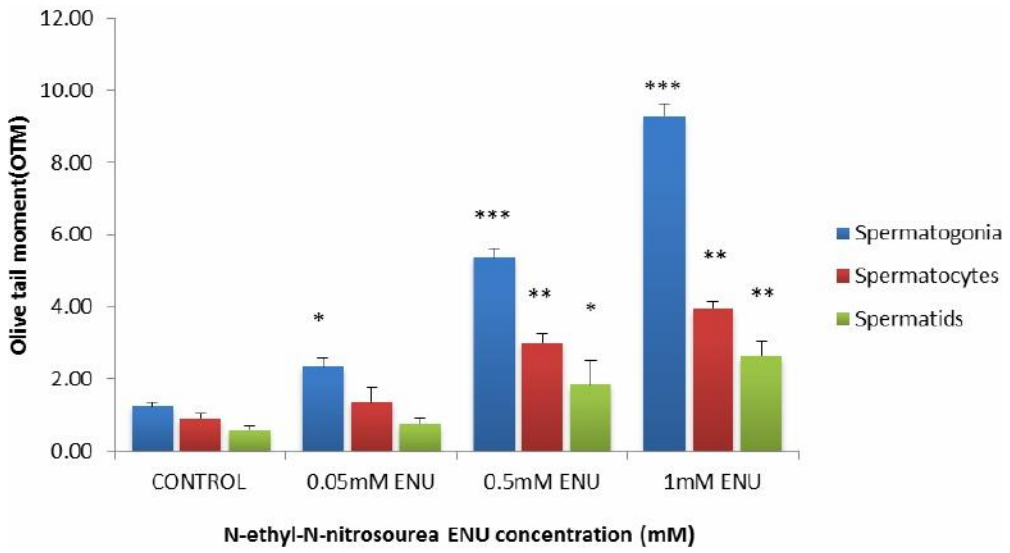

Figure 5.1: The dose response of isolated germ cells with the Comet assay (OTM) after 1h treatment, at 37 ºC with ENU at different concentrations: 0.05 mM, 0.5 mM and 1 mM. The bars indicate the mean ± SEM for three independent experiments by comparison with untreated control value. Asterisks denote values that are significantly different from that of the respective control group (**P* <0.05, ***P* <0.01 and *** *p* <0.001).

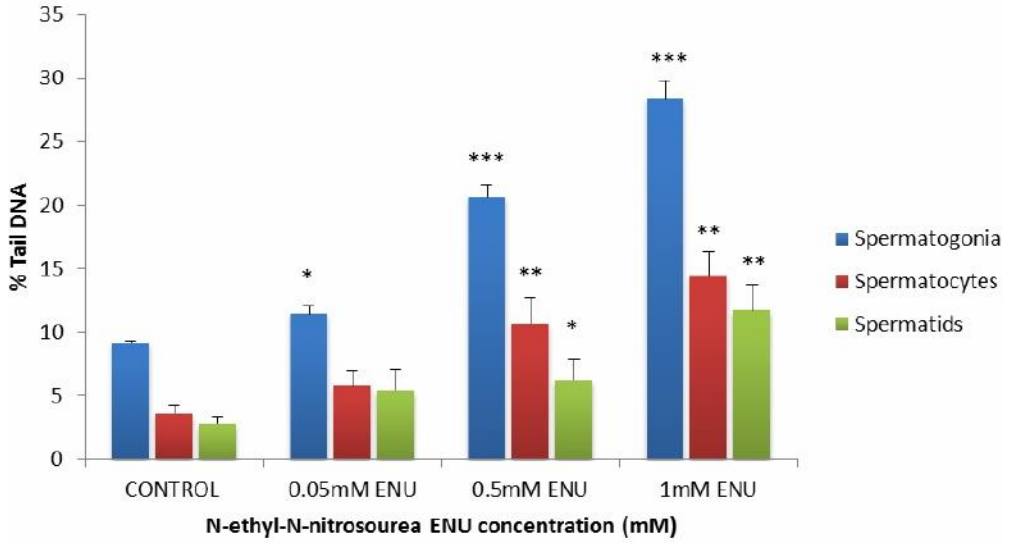

Figure 5.2: The dose response effects of ENU on testicular DNA damage assessed by the Comet assay (% tail DNA), after 1h treatment at 37 ºC with ENU at different concentrations: 0.05 mM, 0.5 mM and 1 mM. Data shown represent means ± SEM. Asterisks denote values that are significantly different from that of the respective control group (**P* <0.05, ***P* <0.01 and *** *P* <0.001).

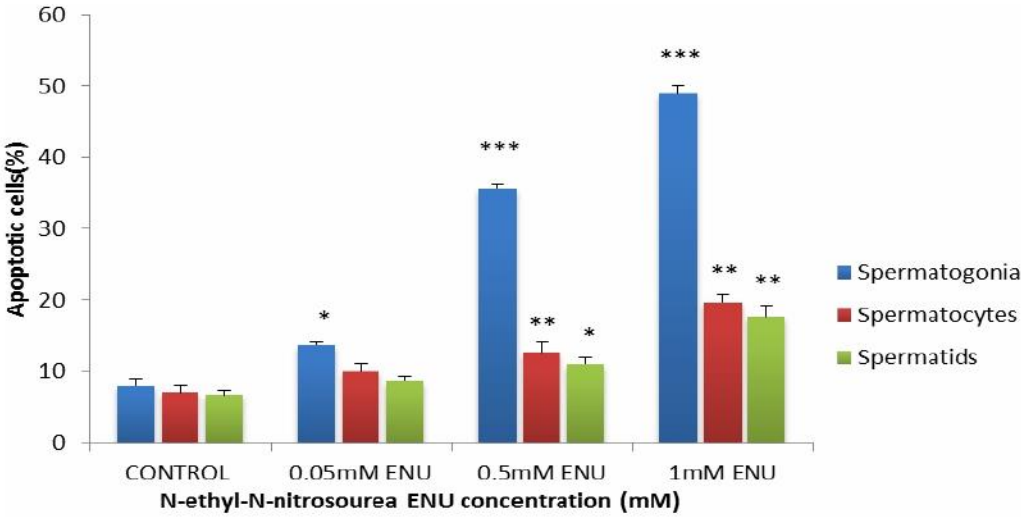

Figure 5.3: The dose response of isolated germ cells treated with ENU at different concentrations (0.05 mM, 0.5 mM and 1 mM), after 1h treatment at 37 ºC, evaluated in the TUNEL assay. Columns represent the mean percentages ± SEM of apoptotic cells. Data were obtained from three independent experiments. Asterisks denote values that are significantly different from that of the respective control group (**P* <0.05; ***P* <0.01; ****P* <0.001).

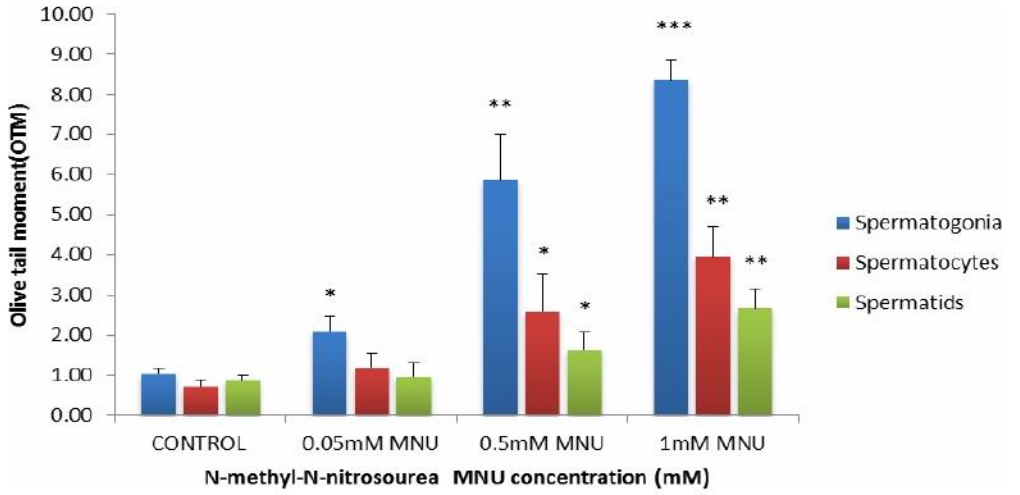

Figure 5.4: The dose response of isolated germ cells with the Comet assay (OTM), after 1h treatment, at 37 ºC with MNU at different concentrations: 0.05 mM, 0.5 mM and 1 mM. The bars represent the mean ± SEM for three independent experiments by comparison with untreated control value. Asterisks denote values that are significantly different from that of the respective control group (**P* <0.05, ***P* <0.01 and *** *P* <0.001).

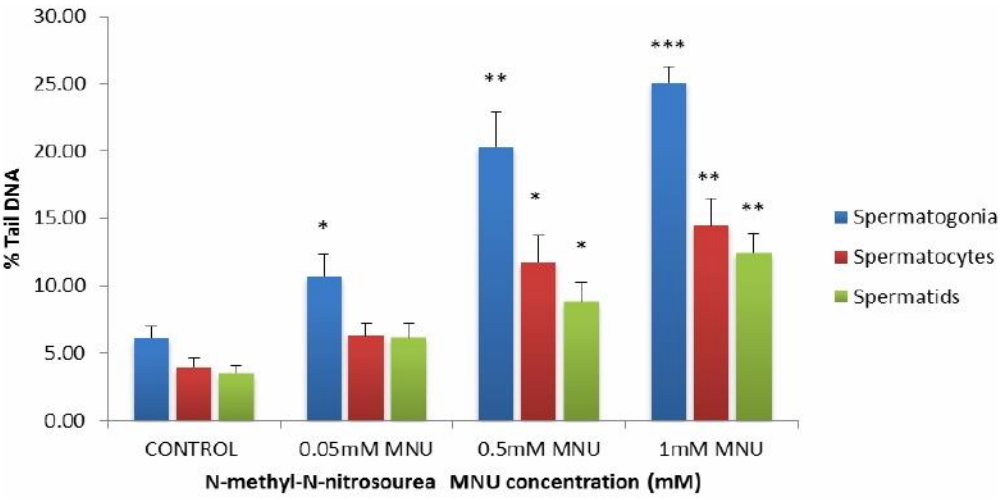

Figure 5.5: The dose response effects of MNU on testicular DNA damage assessed by the Comet assay (% tail DNA), after 1h treatment at 37 ºC with ENU at different concentrations: 0.05 mM, 0.5 mM and 1 mM. Data shown represent means ± SEM. Asterisks denote values that are significantly different from that of the respective control group (*P <0.05, **P <0.01 and *** P <0.001).

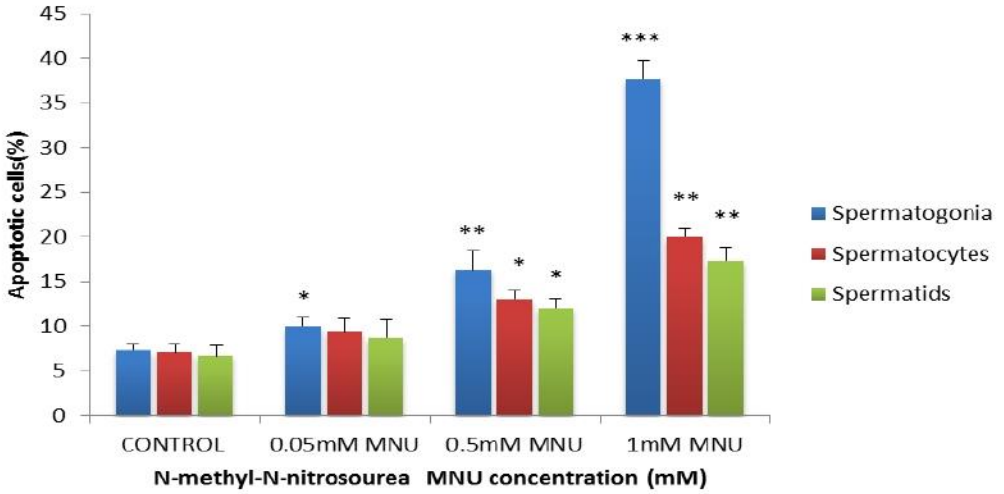

Figure 5.6: The dose response of isolated germ cells treated with MNU at different concentrations (0.05 mM, 0.5 mM and 1 mM), after 1h treatment at 37ºC, evaluated in the TUNEL assay. Columns represent the mean percentages ± SEM of apoptotic cells. Data were obtained from three independent experiments. Asterisks denote values that are significantly different from that of the respective control group (*P <0.05; **P <0.01; ***P <0.001).

Table 5.1: Summary table presenting the individual data for the effects of ENU and MNU on isolated germ cells' Comet measurements: Olive tail moment, and % tail DNA; and percentage of apoptotic cells. Data shown represent group values are (mean ± SEM) of three experiments (n=3) (100 cells per experimental). (ns) = not significant, *p <0.05, **p <0.01 and *** p <0.001 versus control.

Germ cells	Olive tail moment	(%)Tail DNA	Apoptotic cells (%)
Spermatogonia			
Control	1.23 ± 0.06	9.19 ± 0.06	8.00 ± 0.58
0.05mM ENU	2.33 ± 0.13**	11.45± 0.37**	13.67±0.33**
0.5mM ENU	6.21± 0.49 ***	20.64 ± 0.52***	35.67±0.33***
1mM ENU	9.29 ± 0.20***	28.38 ± 0.81***	49.00±0.58***
Control	1.03 ± 0.08	6.23 ± 0.33	7.33 ± 0.33
0.05mM MNU	2.09 ±0.21*	6.86 ± 0.42*	10.00 ± 0.58*
0.5mM MNU	5.87 ± 0.65**	20.29±1.51**	16.33 ± 1.20**
1mM MNU	8.34 ± 0.28***	25.10± 0.67**	37.67 ± 1.20***
Spermatocytes			
Control	0.91 ± 0.08	3.58 ± 0.36	7.00 ± 0.58
0.05mM ENU	1.35 ± 0.23 ns	5.74 ± 0.69 ns	10.00 ± 0.58 ns
0.5mM ENU	3.01 ± 0.15 *	10.71± 1.13 *	12.67 ± 0.88 *
1mM ENU	3.78 ± 0.21**	14.40 ± 1.12**	19.67 ± 0.67**
Control	0.72 ± 0.09	3.97 ± 0.37	7.00 ± 0.58
0.05mM MNU	1.19 ± 0.20 ns	6.28 ± 0.55 ns	9.33 ± 0.88 ns
0.5mM MNU	2.59 ± 0.53 *	11.73 ±1.16*	13.00 ± 0.58 *
1mM MNU	3.94 ± 0.43**	14.45 ±1.18*	20.00 ± 0.58 **
Spermatids			
Control	0.59 ± 0.05	2.77 ± 0.31	6.67 ± 0.33
0.05mM ENU	0.75 ± 0.09 ns	5.46 ± 0.95 ns	8.67 ± 0.33 ns
0.5mM ENU	1.87 ± 0.37 *	6.24 ± 0.92 *	12.00 ± 0.58*
1mM ENU	2.66 ± 0.28**	11.71± 1.20 **	17.67 ± 0.88**
Control	0.79 ± 0.08	3.50 ± 0.35	6.67 ± 0.67
0.05mM MNU	1.64 ± 0.20 ns	6.15 ± 0.61ns	8.67 ± 1.20 ns
0.5mM MNU	2.11± 0.24 *	8.82 ± 0.83 *	12.00 ± 0.58 *
1mM MNU	3.02 ± 0.28**	12.46 ±0.84**	17.33 ±0.88**

5.3.2 Effect of 6-MP and 5-BrdU treatment

6-MP and 5-BrdU showed a dose-response curve in both assays used for this study. The lowest doses that induced a statistically significant increase in genetic damage were 0.05 mM ENU or 0.05 mM MNU for DNA damage and 0.05 mM ENU or 0.05 mM MNU for apoptosis. In spermatocytes, both 6-MP and 5-Br-dU showed highly increased OTM, percentage tail DNA and the percentage of apoptotic cells. They were therefore clearly much more potent spermatocytes mutagens than MNU and ENU or the methanesulfonates (Figure 5.7, 5.8, 5.9, 5.10, 5.11 and 5.12). The response to 6-MP and 5-Br-dU treatment was also different for the three types of cells analyzed: spermatocytes, which showed the highest levels of DNA damage and apoptosis in response to 6-MP and 5-BrdU treatment than the other types of cells. Spermatocytes showed a clear dose-dependent, statistically significant increase in comet parameters and apoptosis from the concentration of 0.05 mM (Figure 5.9 and 5.12) upwards whereas the other compounds showed lower means at each dose with generally lower levels of significance and only significant from 0.5 mM upwards. Data for different Comet measurements/parameters are presented in Table 5.2. The results showed that OTM and %Tail DNA gave good correlations with the concentration/dose of 6-MP and 5-BrdU agents used.

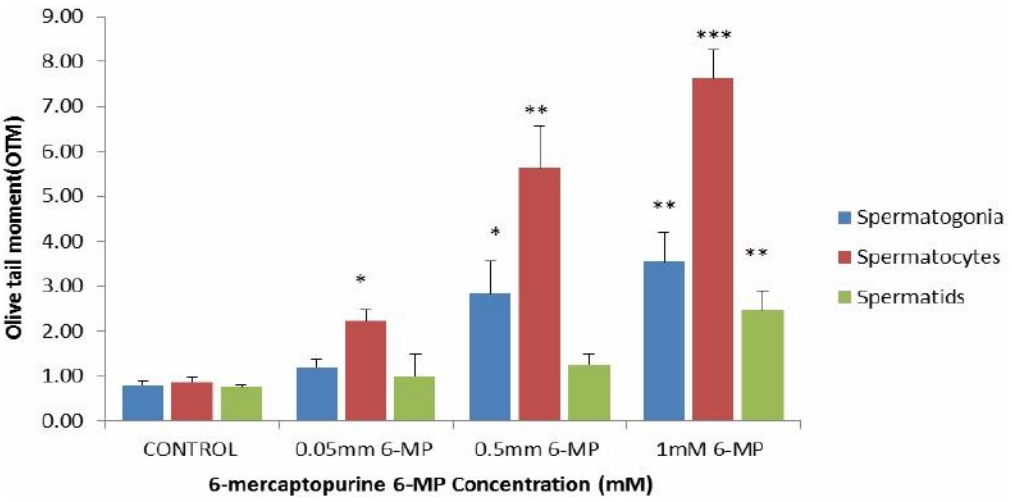

Figure 5.7: The dose response of isolated germ cells with the Comet assay (OTM), after 1h treatment, at 37 ºC with 6-MP at different concentrations: 0.05 mM, 0.5 mM and 1 mM. The bars indicate the mean ± SEM for three independent experiments by comparison with untreated control value. Asterisks denote values that are significantly different from that of the respective control group (*P <0.05, **P <0.01 and *** P <0.001).

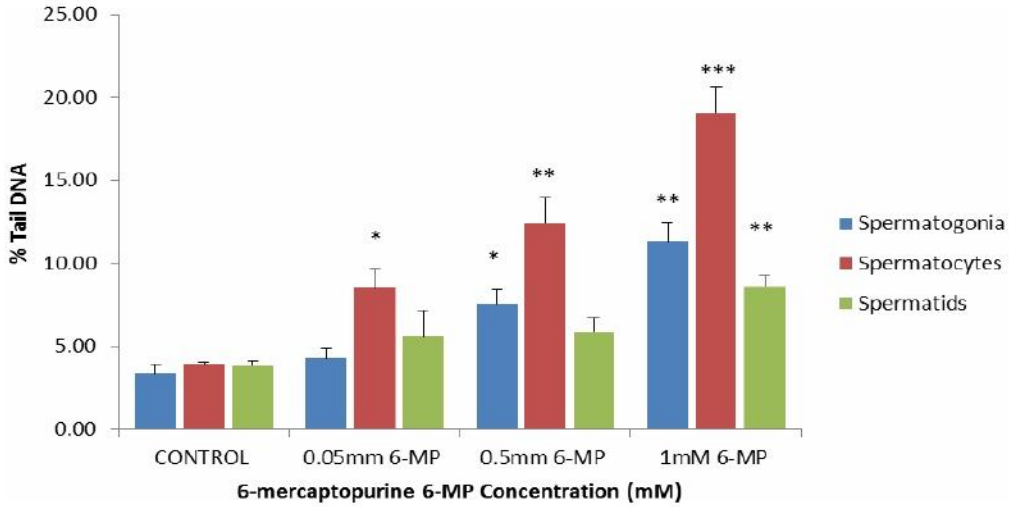

Figure 5.8: The dose response effects of 6-MP on testicular DNA damage assessed by the Comet assay (% tail DNA), after 1h treatment at 37 ºC with 6-MP at different concentrations: 0.05 mM, 0.5 mM and 1 mM. Data shown represent means ± SEM. Asterisks denote values that are significantly different from that of the respective control group (*P <0.05, **P <0.01 and *** P <0.001).

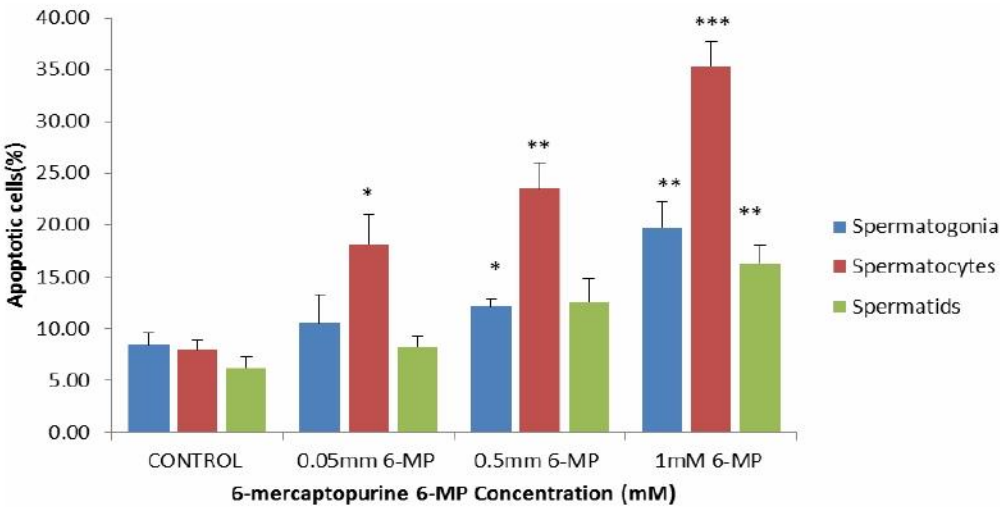

Figure 5.9: The dose response of isolated germ cells treated with 6-MP at different concentrations (0.05 mM, 0.5 mM and 1 mM), after 1hr treatment at 37ºC, evaluated in the TUNEL assay. Columns represent the mean percentages ± SEM of apoptotic cells. Data were obtained from three independent experiments. Asterisks denote values that are significantly different from that of the respective control group (*P <0.05; **P <0.01; ***P <0.001).

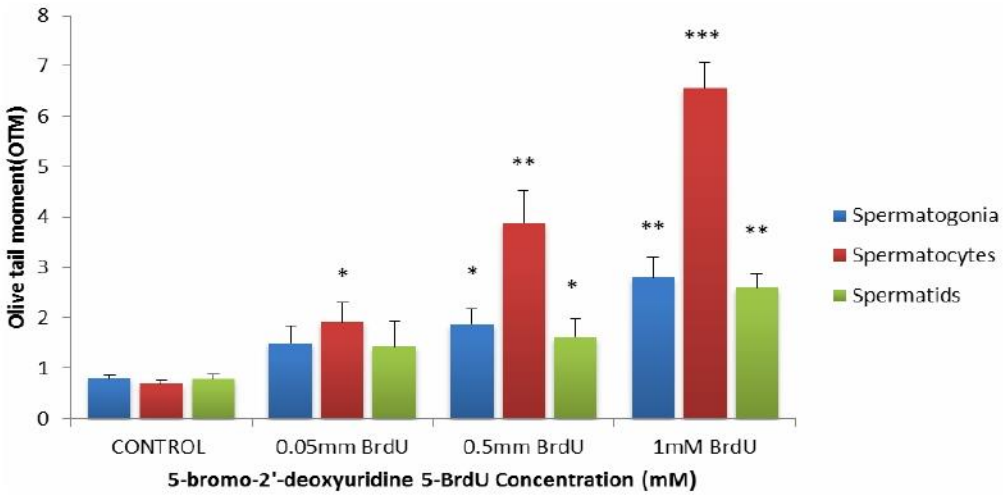

Figure 5.10: The dose response of isolated germ cells with the Comet assay (OTM), after 1hr treatment, at 37ºC with 5-BrdU at different concentrations: 0.05 mM, 0.5 mM and 1 mM. The bars indicate the standard error for three independent experiments by comparison with untreated control value. Asterisks denote values that are significantly different from that of the respective control group (*P <0.05, **P <0.01 and *** P <0.001).

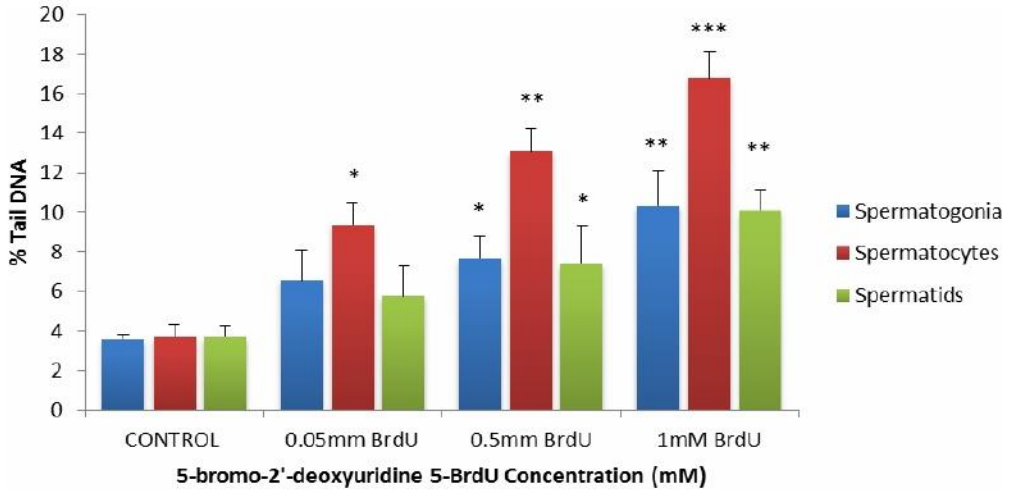

Figure 5.11: The dose response effects of 5-BrdU on testicular DNA damage assessed by the Comet assay (% tail DNA), after 1hr treatment at 37 ºC with 5-BrdU at different concentrations: 0.05 mM, 0.5 mM and 1 mM. Data shown represent means ± SEM. Asterisks denote values that are significantly different from that of the respective control group (**P* <0.05, ***P* <0.01 and *** *P* <0.001).

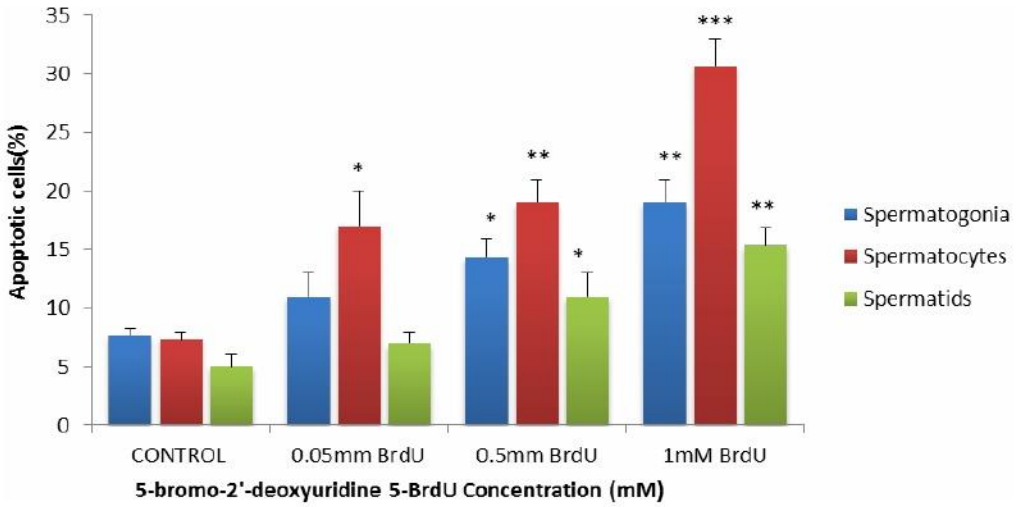

Figure 5.12: The dose response of isolated germ cells treated with 5-BrdU at different concentrations (0.05 mM, 0.5 mM and 1 mM), after 1h treatment at 37 ºC, evaluated in the TUNEL assay. Columns represent the mean percentages ± SEM of apoptotic cells. Data were obtained from three independent experiments. Asterisks denote values that are significantly different from that of the respective control group (**P* <0.05; ***P* <0.01; ****P* <0.001).

Table 5.2: Summary table presenting the individual data for the effects of 6-MP and 5-BrdU on isolated germ cells' Comet measurements: Olive tail moment and % tail DNA; and percentage of apoptotic cells. Data shown represent group (means ± SEM) of three experiments (100 cells per experimental). Ns not significant, *p <0.05, **p <0.01 and *** p <0.001 versus control.

Germ cells	Olive tail moment	(%)Tail DNA	Apoptotic cells (%)
Spermatogonia			
Control	0.80 ± 0.06	3.35 ± 0.33	8.38 ± 0.72
0.05mM 6-MP	1.20 ± 0.10ns	4.31± 0.30 ns	10.52 ± 1.56 ns
0.5mM 6-MP	2.63 ± 0.48ns	7.20 ± 0.70 ns	11.14 ± 0.50ns
1mM 6-MP	3.53 ± 0.38**	11.31± 0.64**	19.73 ±1.43**
Control	0.80 ± 0.04	3.59 ± 0.13	7.67 ± 0.33
0.05mM 5-BrdU	1.50 ±0.20ns	6.56 ± 0.89ns	11.00 ± 1.15ns
0.5mM 5-BrdU	1.88 ± 0.16*	7.66 ± 0.65*	14.33 ± 0.88*
1mM 5-BrdU	2.80 ± 0.23**	10.34 ± 1.01**	19.00 ± 1.15**
Spermatocytes			
Control	0.87 ±0.06	3.91± 0.08	7.97 ± 0.50
0.05mM 6-MP	2.22 ±0.15*	8.50 ±0.67 *	18.11 ± 1.69 *
0.5mM 6-MP	5.63 ±0.55 **	12.41 ±0.88 **	23.47 ± 1.44**
1mM 6-MP	7.63 ±0.36 ***	19.04 ±0.93 ***	35.33 ± 1.38***
Control	0.69 ± 0.04	3.71± 0.35	7.33 ± 0.33
0.05mM 5-BrdU	1.91± 0.22*	9.36 ± 0.63*	17.00± 1.73*
0.5mM 5-BrdU	3.88 ± 0.36**	13.09 ± 0.66**	19.00 ± 1.15**
1mM 5-BrdU	6.55 ± 0.29***	16.77± 0.79***	30.66± 1.37***
Spermatids			
Control	0.75 ± 0.03	3.81 ± 0.17	6.19 ± 0.58
0.05mM 6-MP	0.98 ± 0.28ns	5.58 ± 0.90ns	8.21 ± 0.62 ns
0.5mM 6-MP	1.24 ± 0.13ns	5.87 ± 0.48ns	12.52 ± 1.28 ns
1mM 6-MP	2.45 ±0.26**	8.60 ± 0.38**	16.27 ± 1.01**
Control	0.78 ± 0.06	3.69 ± 0.34	5.00 ± 0.58
0.05mM 5-BrdU	1.43 ± 0.29ns	5.77 ± 0.88 ns	7.00 ± 0.58 ns
0.5mM 5-BrdU	1.62 ± 0.21*	7.43 ± 1.11*	11.00 ±1.15*
1mM 5-BrdU	2.60 ± 0.16**	10.09 ± 0.61**	15.33 ± 0.88**

5.3.3 Effect of EMS and MMS treatment

MMS and EMS showed a dose-response curve in both assays used for this study. The lowest doses that induced a statistically significant increase in genetic damage were 0.05 mM MMS or 0.05 mM EMS for DNA damage and 0.05 mM MMS or 0.05 mM EMS for apoptosis. In spermatids, both methanesulfonates MMS and EMS showed highly increased OTM, percentage tail DNA and the percentage of apoptotic cells. They were therefore clearly much more potent spermatids mutagens than MNU and ENU or 6-MP and 5-Br-dU (Figure 5.13, 5.14, 5.15, 5.16, 5.17 and 5.18). The response to MMS and EMS treatment was also different for the three types of cells analyzed: Spermatids, which showed the highest levels of DNA damage and apoptosis in response to MMS and EMS treatment than the other types of cells. Spermatocytes showed a clear dose-dependent, statistically significant increase in comet parameters and apoptosis from the concentration of 0.05 mM (Figure 5.15 and 5.18) upwards whereas the other compounds showed lower means at each dose with generally lower levels of significance and only significant at all from 0.5 mM upwards. The values of various Comet measurements as quantified with Comet 6.0 software generated from MMS and EMS studies are presented in Table 5.3. The results showed that OTM and %Tail DNA gave good correlations with the concentration/dose of MMS and EMS agents used.

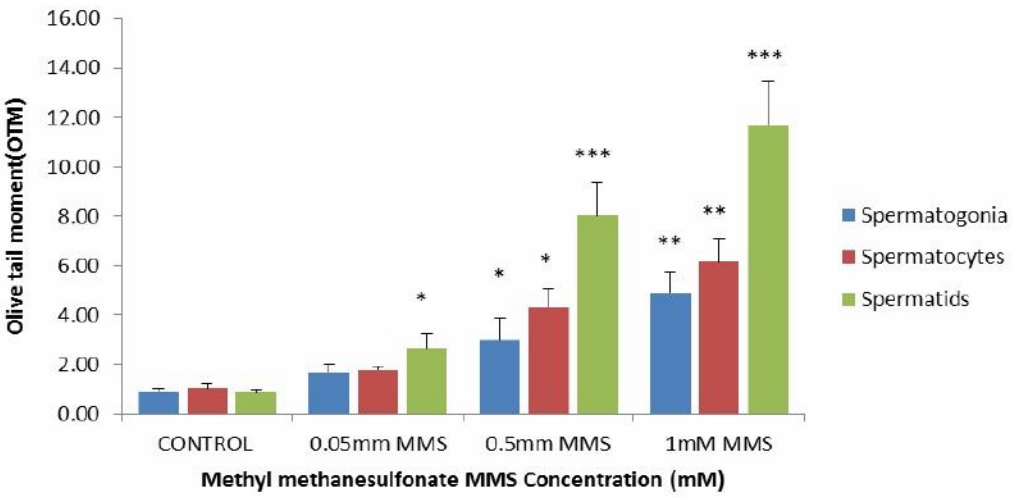

Figure 5.13: The dose response of isolated germ cells with MMS the Comet assay (OTM) after 1h treatment, at 37 ºC with MMS at different concentrations: 0.05 mM, 0.5 mM and 1 mM. The bars indicate the (mean ± SEM) for three independent experiments by comparison with untreated control value. Asterisks denote values that are significantly different from that of the respective control group (*P <0.05, **P <0.01 and *** P <0.001).

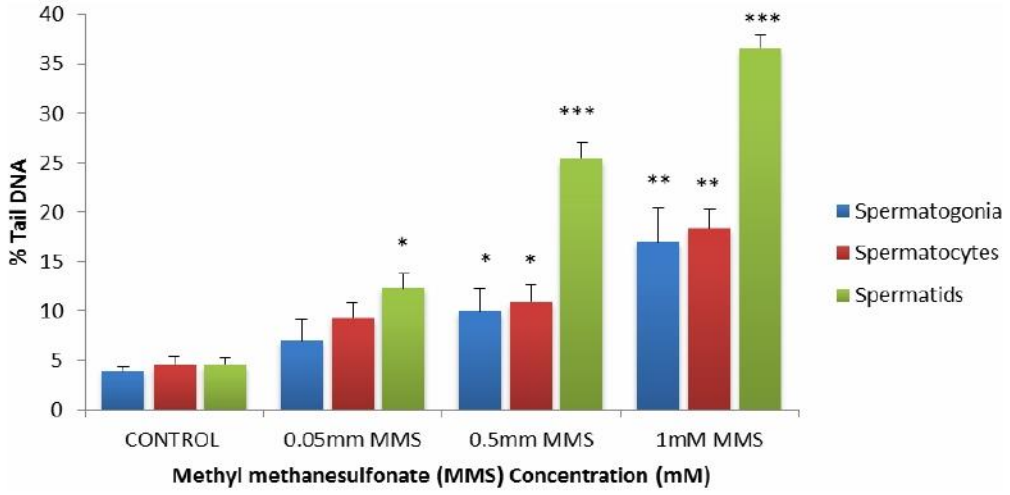

Figure 5.14: The dose response effects of MMS on testicular DNA damage, assessed by the Comet assay (% tail DNA) after 1hr treatment at 37ºC with MMS at different concentrations: 0.05 mM, 0.5 mM and 1 mM. Data shown represent means ± SEM. Asterisks denote values that are significantly different from that of the respective control group (*P <0.05, **P <0.01 and *** P <0.001).

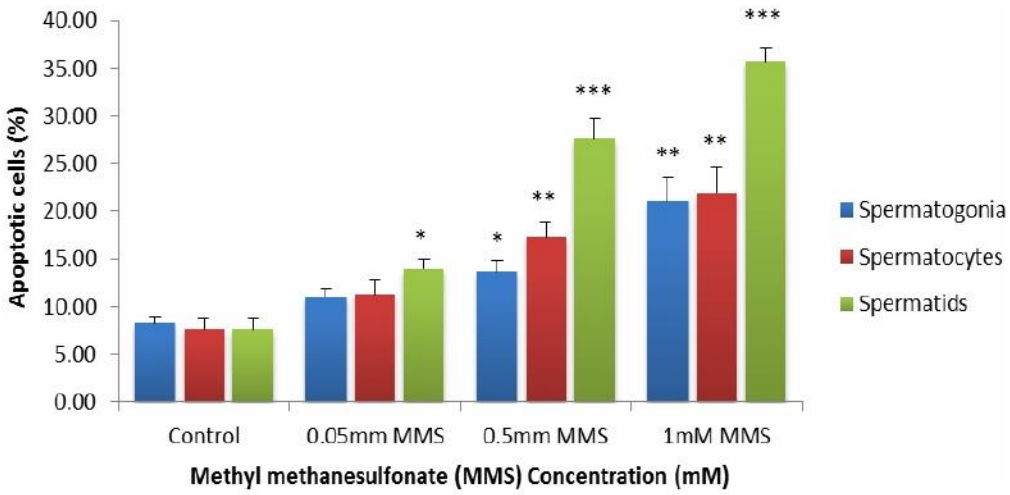

Figure 5.15: The dose response curve of isolated germ cells was treated with MMS at different concentrations 0.05 mM, 0.5 mM and 1 mM, after 1h treatment, at 37ºC, evaluated in the TUNEL assay. Columns represent the mean percentages ± SEM of apoptotic cells for each of the three concentrations of MMS used (0, 0.05, 0.5 and 1 mM). Data were obtained from three independent experiments. Each dose level within a cell type has been compared with its respective control group (**p* <0.05 ***p* <0.01 ****p* <0.001).

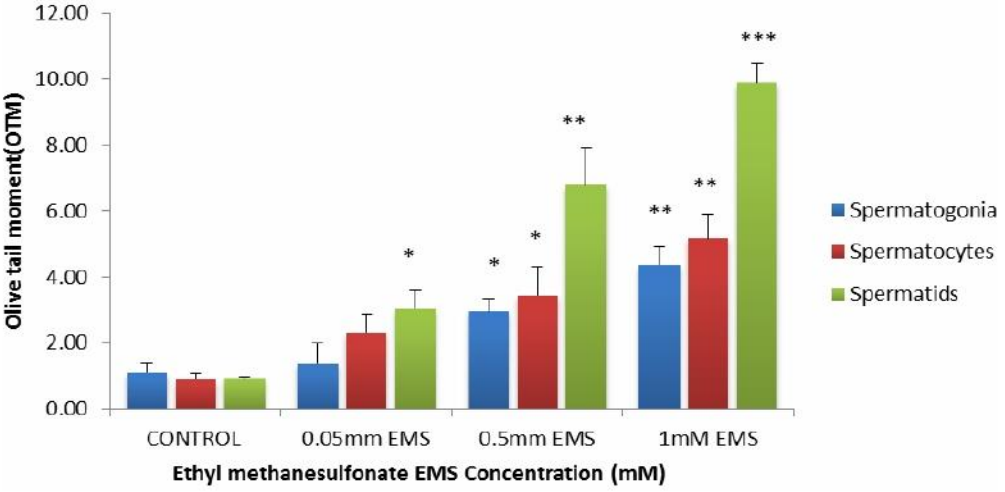

Figure 5.16: The dose response of isolated germ cells with the Comet assay (OTM) after 1hr treatment, at 37ºC with EMS at different concentrations: 0.05 mM, 0.5 mM and 1 mM. The bars indicate the means ± SEM for three independent experiments by comparison with untreated control value. Asterisks denote values that are significantly different from that of the respective control group (**P* <0.05, ***P* <0.01 and *** *P* <0.001).

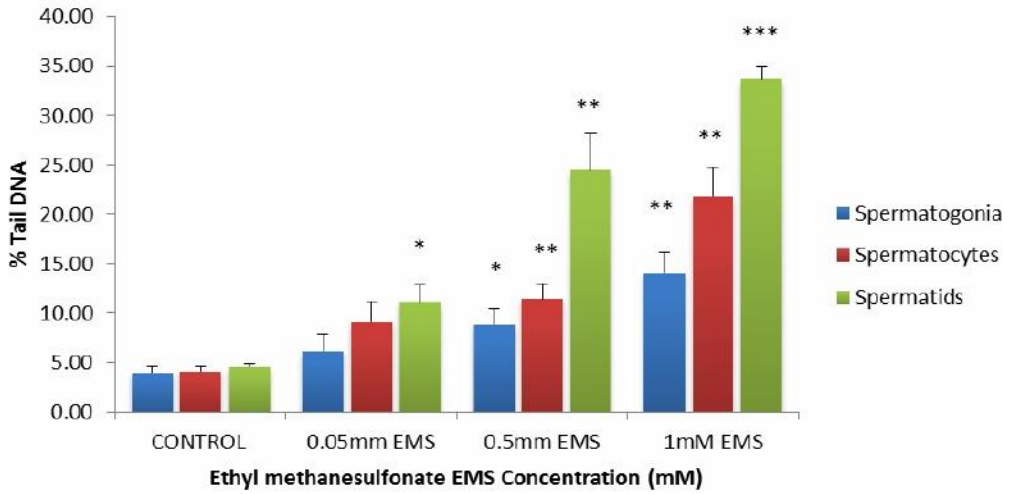

Figure 5.17: The dose response effects of EMS on testicular DNA damage assessed by the Comet assay (% tail DNA), after 1h treatment at 37ºC with EMS at different concentrations: 0.05 mM, 0.5 mM and 1 mM. Data shown represent means ± SEM. Asterisks denote values that are significantly different from that of the respective control group (*P <0.05, **P <0.01 and *** P <0.001).

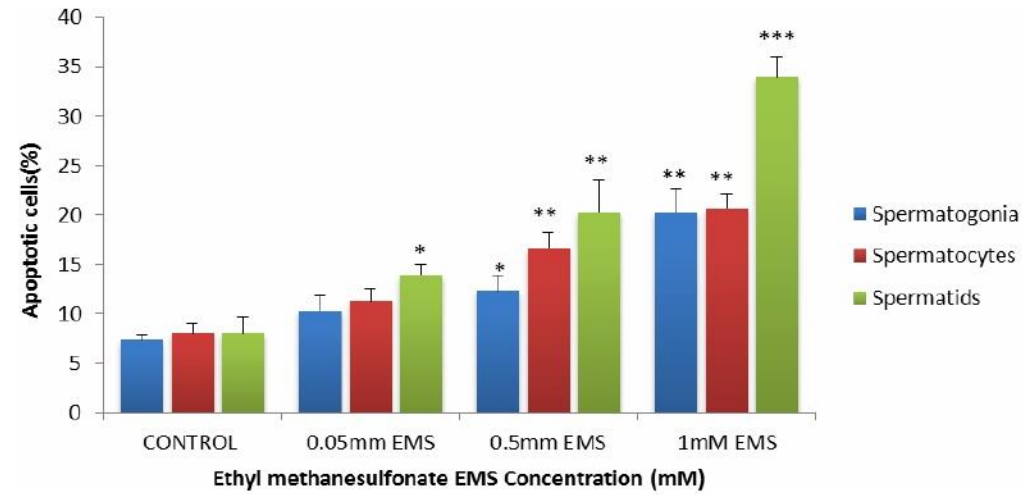

Figure 5.18: The dose response of isolated germ cells treated with EMS at different concentrations (0.05 mM, 0.5 mM and 1 mM), after 1h treatment at 37 ºC, evaluated in the TUNEL assay. Columns represent the mean percentages ± SEM of apoptotic cells. Data were obtained from three independent experiments. Asterisks denote values that are significantly different from that of the respective control group (*P <0.05; **P <0.01; ***P <0.001).

Table 5.3 : Summary table presenting the individual data for the effects of MMS and EMS on isolated germ cells' Comet measurements: Olive tail moment and % tail DNA; and percentage of apoptotic cells. Data shown represent group (means ± SEM) of three experiments (100 cells per experimental). Ns not significant, *p <0.05, **p <0.01 and *** p <0.001 versus control.

Germ cells	Olive tail moment	(%)Tail DNA	Apoptotic cells (%)
Spermatogonia			
Control	0.92 ± 0.06	3.96 ± 0.24	8.33 ± 0.33
0.05mM MMS	1.69 ± 0.19ns	6.98 ± 1.26ns	11.00 ± 0.58ns
0.5mM MMS	2.98 ± 0.53*	9.95 ± 1.37*	13.67 ± 0.6*
1mM MMS	4.91 ± 0.48**	16.96 ± 2.04**	21.00 ±1.53**
Control	1.11 ± 0.16	3.99 ± 0.38	7.33 ± 0.33
0.05mM EMS	1.37 ± 0.35 ns	6.15 ± 0.99ns	10.33 ± 0.88ns
0.5mM EMS	2.95 ± 0.21*	8.87 ± 0.92*	12.33 ± 0.88*
1mM EMS	4.36 ± 0.31**	14.09 ± 1.17**	20.33 ±1.33**
Spermatocytes			
Control	1.03 ± 0.13	4.59 ± 0.46	7.67 ± 0.67
0.05mM MMS	1.77 ± 0.09ns	9.35 ± 0.88 ns	11.33 ± 0.88 ns
0.5mM MMS	4.32 ± 0.41*	10.93 ± 0.97*	17.33 ± 0.88*
1mM MMS	6.15 ± 0.54**	18.36 ± 1.15**	22.00 ± 1.53**
Control	0.90 ± 0.09	4.12 ± 0.25	8.00 ± 0.58
0.05mM EMS	2.32 ± 0.31ns	9.12 ± 1.18ns	11.33 ± 0.67ns
0.5mM EMS	3.44 ± 0.49*	11.41 ± 0.91*	16.67 ± 0.88*
1mM EMS	5.17 ± 0.42**	21.81 ± 1.73**	20.67± 0.88**
Spermatids			
Control	0.89 ± 0.06	4.58± 0.37	7.67 ± 0.67
0.05mM MMS	2.65 ± 0.35*	12.34± 0.86*	14.00 ± 0.58*
0.5mM MMS	8.02 ± 0.76**	25.44± 0.94**	27.67 ± 1.20**
1mM MMS	11.66 ± 1.04***	36.63 ±0.75***	35.67 ± 0.88***
Control	0.92± 0.03	4.58 ± 0.22	8.00 ± 1.00
0.05mM EMS	3.04 ±0.32*	11.06 ± 1.04*	14.00 ± 0.58 *
0.5mM EMS	6.80 ±0.85**	24.49 ± 2.10**	20.33 ± 1.86**
1mM EMS	9.89 ±0.36***	33.64 ± 0.76***	34.00± 1.15***

5.4 Discussion

Genotoxicity assessment after exposure to N-ethyl-N-nitrosourea, N-methyl-N-nitrosourea, 6-mercaptopurine, 5-bromo-2'-deoxyuridine and , ethyl methanesulfonate or methyl methanesulfonate was conducted on three types of rat germ cells (spermatogonia, spermatocytes and spermatids). The alkali version of the Comet assay was used to detect DNA strand breaks. Spermatogonia were the most sensitive to ENU and MNU; spermatocytes were most sensitive to 6-MP and 5-BrdU while spermatids were found to be the most sensitive cell type to MMS and EMS. Parallel results were found using the TUNEL assay, which also showed highly significant, dose-dependent effects of these 6 genotoxins on spermatogonia, spermatocytes and spermatids in the same way as for DNA damage. Crucially, the specificity of effects on different germ cell types matches those found in vivo.

The results for ENU and MNU are similar to findings by (Russell et al., 2007) who also found genetic damage in spermatogonia when treated with ENU and MNU. In the present study, comparing the chemicals for the endpoints studied (i.e., Comet assay and TUNEL assay) revealed that ENU and MNU are much more effective on spermatogonia than spermatocytes and spermatids. These results suggest that both chemicals are highly mutagenic in differentiating spermatogonia (Russell et al., 2007, Russell and Hunsicker, 1983, Guenet, 2004, Siepka and Takahashi, 2005). In addition, increased spontaneous frequency of gene mutations and chromosome damage has been reported (O'Brien et al., 2013).

A similar trend was observed on spermatocytes when 6-MP and 5-BrdU induced Comet parameters were compared with those of ENU, MNU, MMS and EMS at 0.05, 0.5 and 1.0 mM. Spermatocytes showed a highly significant increase in DNA damage and apoptosis to 6-MP, 5-BrdU. This increase was dramatically greater in spermatids and spermatogonia. Thus, spermatocytes are the most sensitive to 6-MP and 5-BrdU in agreement with the findings *in vivo* that showed 6-MP to be a potent chemical for inducing DNA damage in spermatocytes (Mosesso and Palitti, 1993) along with 5-BrdU (Perrard et al., 2003).

Spermatids were found to be the most sensitive to MMS and EMS in the induction of genetic damage and apoptosis in agreement with in vivo studies that showed decrease in the number of spermatids and high frequency of chromosome aberrations induced by methanesulfonates in spermatids (Kuriyama et al., 2005, Matsuda et al., 1989).

This experiment using these chemicals also suggested that OTM and %Tail DNA give good correlations with the dose of genotoxic agents used. Statistically, our results did not find much difference between OTM and %DNA in the tail. Although Olive Tail moment appeared to be the most statistically significant measurement, it provides an estimate of DNA damage in arbitrary units. Moreover, the level of DNA damage is dependent on both the toxicant dose and the type of germ cell, and occurs at doses known to be relevant to testicular and reproductive toxicity. Furthermore, these results indicate that Staput-isolated rat testicular germ cells provide suitable model in vitro to study DNA damage in different phases of spermatogenesis.

Chapter 6. Effect of ENU and MMS on Tbpl1, FHL5 and Gtf2a1l expression in male mouse germ cells

6.1 Introduction

Loss of germ cells is common during mammalian spermatogenic development although different cell types have different capacities for apoptosis and different susceptibilities to apoptosis after toxin exposure. As a result, understanding of the mechanisms underlying germ cell death is still limited. This due to a number of factors: lack of availability of in vitro techniques to successfully achieve fully functional mammalian spermatogenesis outside the body; presence of numerous spermatogenesis-specific genes or isoforms; the difficulty of using microarrays in studies of pathological states because of cell ratio distortion; etc. Very often, the study of the function of genes involved in sperm production needs expensive animal models (Kennedy et al., 2005). All this makes the specific diagnosis and treatment of infertility in males difficult and highlights the importance of identifying and characterization of new genes and proteins involved in the production of functional male germ cells (Kennedy et al., 2005).

Because the similarities and differences between the mouse and human genomes are so well understood (relative to other animal species), the mouse has historically been the main model system to identify the genetic basis and mechanisms of the pathogenesis of many human diseases. Although the current mouse mutant databases are composed of a massive number of different knockout animals, which are a valuable source of models, only a minor amount of the probable total number of mammalian genes is covered.

The establishment of novel mutagenesis programmes using potent mammalian mutagens and carcinogens such as N-ethyl-N-nitrosourea (ENU) and methyl methanesulfonate (MMS) has started to fill this gap but is a rather laborious and very animal intensive process (Kennedy and O'Bryan, 2006, Cordes, 2005). N-ethyl-N-nitrosourea (ENU) is a potent monofunctional ethylating agent which has been found to be mutagenic and carcinogen in a wide variety of organisms from viruses to mammalian germ cells (Justice et al., 2000, Chen et al., 2002). ENU is a synthetic compound that causes random, single base pair mutations, acting directly on nucleic acids without any metabolic processing needed for its activation (Noveroske et al., 2000, Singer and Dosanjh, 1990). In the mouse testis, the most commonly studied mutations are AT-to-TA transversions or AT-to-GC transitions (Noveroske et al., 2000). The single base pair alterations induced by ENU can be invaluable for dissecting the fine structure of a protein (Justice, 2000).

Male germ cell development consists of a variety of unique processes, including genetic recombination and haploid gene expression. This processes are intricate, highly ordered, and require novel gene products and a precise and well-coordinated programme of gene expression to occur (Eddy, 2002). Other factors essential for postmeiotic stages of spermatogenesis include transcription factors (Eddy, 2002). Moreover, the most uncomplicated strategy to clarify differentiation mechanisms of male germ cell is to identify and characterize differentiation-specific molecules and their associated genes in germ cells. Yet, only a few genes specifically involved in spermatogenesis have been studied (Guo et al., 2004).

TATA box binding protein-like 1 (Tbpl1), also called TLF (Chong et al., 2005) is a protein commonly thought to belong to the general transcription initiation complex and it has been considered as a substitution factor for TATA-binding protein (TBP) in the basal transcriptional machinery of RNA polymerase II (Zhang et al., 2001, Ohbayashi et al., 1999). It also has a specialised function in spermatogenesis, as revealed by targeted mutation of the gene in both somatic and germ cells. The Tbpl1 mutation obtained leads to a complete arrest of late spermiogenesis and increased haploid cell apoptosis (Martianov et al., 2001). Four and a half LIM domains protein 5 (FHL5) is a LIM domain protein that interacts with transcription factor CREM in postmeiotic male germ cells and enhances CREM-dependent transcription (Lardenois et al., 2009). CREM regulates many crucial genes required for spermatid maturation, and targeted mutation of the Crem gene in the mouse germ-line blocks spermatogenesis (Fimia et al., 1999, Kotaja et al., 2004). General transcription factor IIA, 1-like (Gtf2a1l) is a germ cell-specific counterpart of the large (α/β) subunit of general transcription factor TFIIA. This factor is able to interact with the small TFIIA subunit (γ) to form a heterodimeric complex that stabilizes binding of TBP to promoter DNA (Upadhyaya et al., 2002). The selected genes (Tbpl1, FHL5 and Gtf2a1l) are known to be highly expressed in spermatocytes and spermatids as well as being thought to play a role in germ cells (Martianov et al., 2002, Han et al., 2001, Lardenois et al., 2009).

The previous chapter was able to determine DNA damage on spermatogonia, spermatocytes and spermatids using the Comet assay. In the present study, two different types of spermatogenic cells (spermatocytes

and spermatids) were isolated from mice testes using Staput. The expression of Tbpl1, FHL5 and Gtf2a1l genes were detected in two different stages of spermatogenic cells, suggesting that Tbpl1, FHL5 and Gtf2a1l genes were differentially expressed. The Tbpl1, FHL5 and Gtf2a1l differentially expressed genes were further analysed by reverse transcription polymerase chain reaction (RT-PCR) for stage and tissue specific expression characteristics. Based on the results of RT-PCR, Tbpl1, FHL5 and Gtf2a1l genes were highly expressed in both spermatocytes and spermatids. This was further clarified using Tbpl1, FHL5 and Gtf2a1l genes to quantify mRNA level expression in each cell types (spermatocytes and spermatids). Finally, spermatocytes, spermatids and most utilized mutagens (ENU and MMS) where analysed for protein levels of Tbpl1, FHL5 and Gtf2a1l using their specific antibodies.

6.2 Materials and Methods

All relevant information is shown in section (2.1). RNA extraction and preparation was described in section 2.8.1 and 2.8.2. Measurement of quantity and purity of total RNA is described in section 2.8.5. DNase I treatment is described in section 2.8.6, cDNA synthesis in section 2.8.7. Polymerase chain reaction (PCR) is described in section was described in section 2.8.9 and quantitative real-time PCR assay shown in section 2.8.9.2 Western Blot analysis is described in section 2.12.

6.3 Results

6.3.1 Quality of RNA Extraction

Total RNA was isolated from germ cell fractions (spermatocytes and spermatids) using Trizol Reagent, followed by incubation with RNase-free DNase I, for 1 h at 37°C, to avoid contamination by genomic DNA. The RNA quality was assessed by gel electrophoresis and spectrophotometric reading: see Figure 6.1

RT-PCR was performed on first strand cDNA for detection of the β-actin; a housekeeping gene constitutively expressed in mouse testis. This gene is regularly amplified to ensure synthesis of the first strand of cDNA had been successful and validation of PCR conditions. Gene expression studies require that the expression profiles of the various genes being studied should be normalized against a suitable internal control: see Figure 6.2

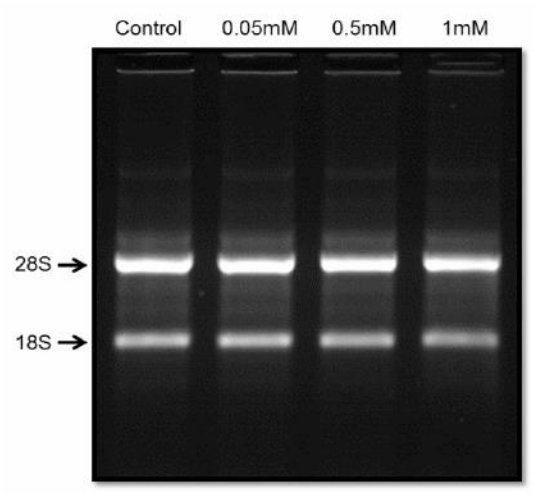

Figure 6.1: Two bands which represented the two ribosomal RNA components 28S and 18S. The intensity of 28S was higher than 18S with a ratio that confirmed the satisfactory purity of the RNA.

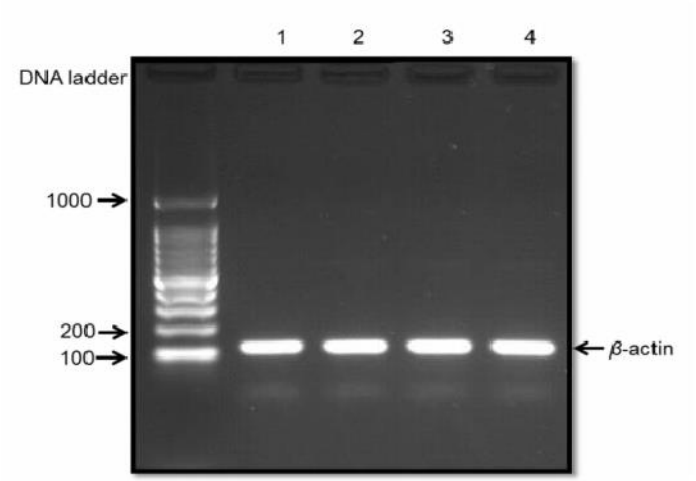

Figure 6.2: PCR detection of β-actin (149 bp). The samples were subjected to electrophoresis through a 1.5 % w/v agarose gel in 1 X TBE with 1 □g/ml ethidium bromide. The PCR conditions were 95°C (30sec), 60°C (30sec), 72 °C (30sec) for 30 cycles. Lane 1 shows the negative control with β-actin DNA. Lanes 2, 3 and 4 show an amplified fragment of β-actin from DNA of cells (spermatocytes and spermatids) treated with different concentration 0.05, 0.5 and 1 mM of ENU or MMS.

6.3.2 Effect of N-ethyl-N-nitrosourea (ENU) treatment on spermatocytes and spermatids.

6.3.2.1 Tbpl1

QPCR was chosen as the technique to provide confirmation of the changes in Tbpl1 gene expression that was seen after cells were treated with different concentrations of ENU. The samples were taken at 1 h following ENU treatment for both treated and untreated control cultures, and the expression levels of Tbpl1 were normalised with those of β-actin and statistically compared against the control level.

There was no statistically significant difference in the levels of Tbpl1 mRNA in spermatocytes after 1h of treatment with ENU (0.05 mM, 0.5 mM) compared with β-actin but there was with 1mM (*p<0.05) (Figures 6.3). A. Statistical analysis showed a significant decrease in the level of expression of Tbpl1 when spermatids were treated with 0.5 mM ENU (*p<0.05) and a further decrease was found with ENU 1 mM (**p<0.01). These results are shown in Figures 6.3. B.

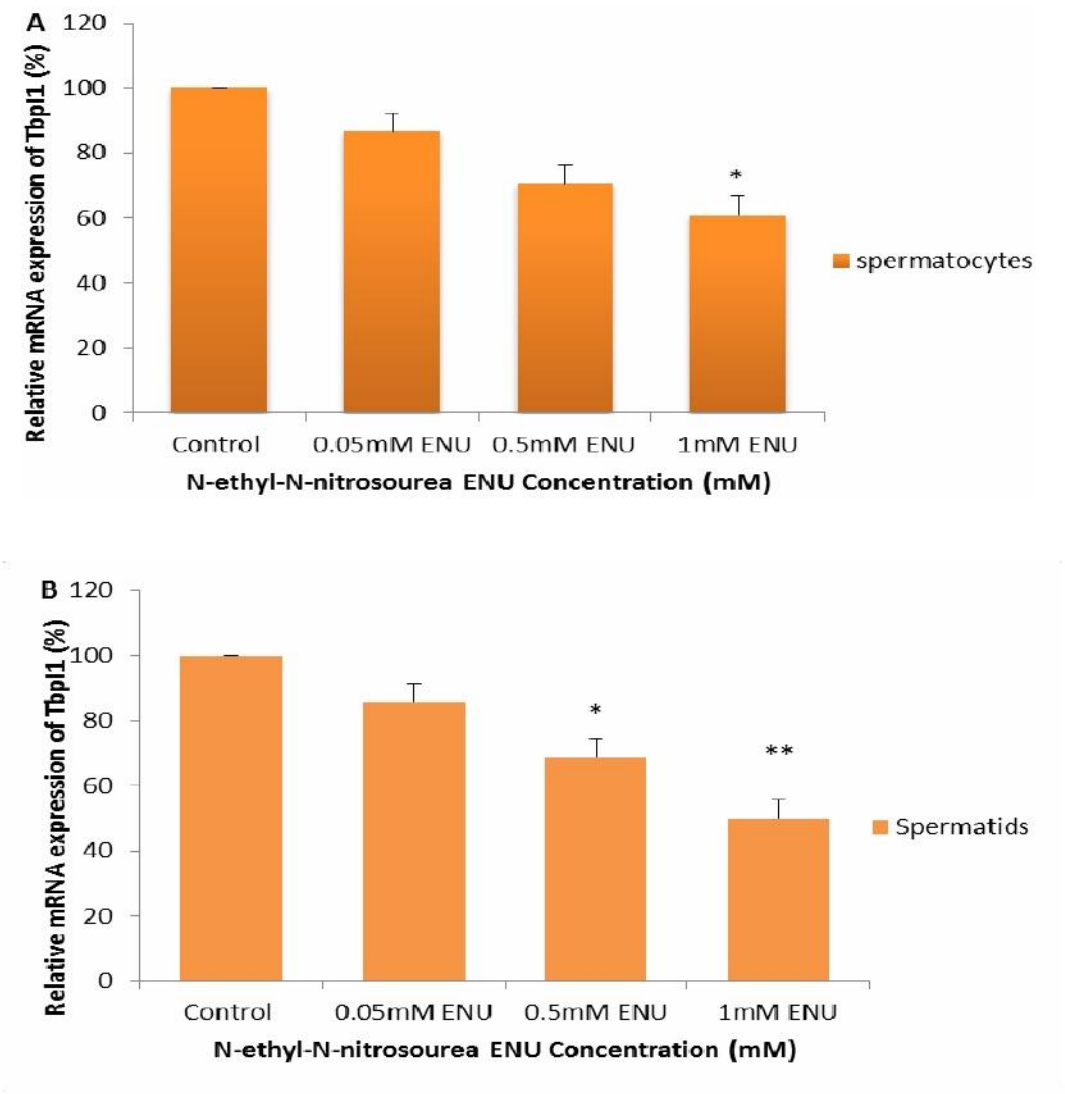

Figure 6.3: Effect of ENU on the Tbpl1 mRNA expression in spermatocytes and spermatids by qPCR. A. spermatocytes and B. spermatids after 1 h treatment, at 37 ºC with ENU at different concentrations: 0.05 mM, 0.5 mM and 1 mM. Non-treated cells' values were defined as 100% and other values were adjusted accordingly. Data are expressed as the mean ± SEM n=3 different biological replicates performed on three different occasions and analysed by one-way ANOVA followed by Data were analysed by One-way-ANOVA followed by Bonferroni's post-hoc comparisons tests, comparing each exposure level against the control level: (*p<0.05, **p<0.01).

The relative level of Tbpl1 expression in protein extracted from isolated germ cells of both spermatocytes and spermatids was determined by semi-quantitative western blotting. The samples were taken at 1 h following ENU treatment for both treated and untreated control cultures, and the expression levels of Tbpl1 were normalised to those of GAPDH before being compared with the control level.

There was no statistically significant difference in the levels of Tbpl1 protein at 0.05 mM and 0.5 mM ENU in spermatocytes. In contrast, spermatids showed a significant decrease (*p<0.05) at 0.5 mM. A further decrease was shown when the spermatocytes were treated with ENU 1 mM (*p<0.05) and spermatids treated with ENU 1 mM (**p<0.01). These results are shown in Figure 6.4 A and B.

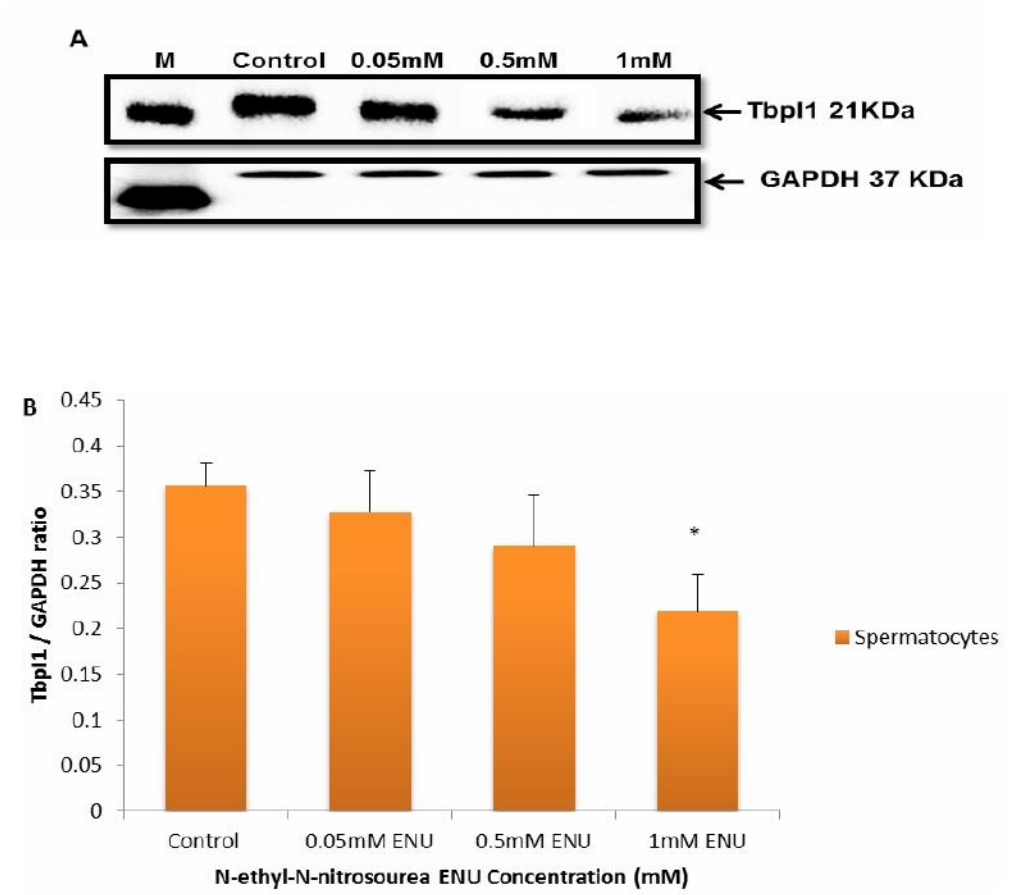

Figure 6.4: Spermatocytes were treated with ENU and the level of TbpI1 protein was examined 1 h after treatment. Sample Western blots of TbpI1 and GAPDH proteins are shown in (A) and quantified summary data are shown in (B). ENU treatment appeared to decrease the TbpI1 protein level at all doses but the decrease was only significant at 1 mM. The density of each band was quantified by the use of Image 1.45 software. The relative expression level of TbpI1 was measured by TbpI1/GAPDH ratio. Results are the mean ± SEM. From three independent experiments and statistical comparisons were made using one-way ANOVA followed by Bonferroni's post-hoc comparisons tests, comparing each dose against the control ($*P < 0.05$).

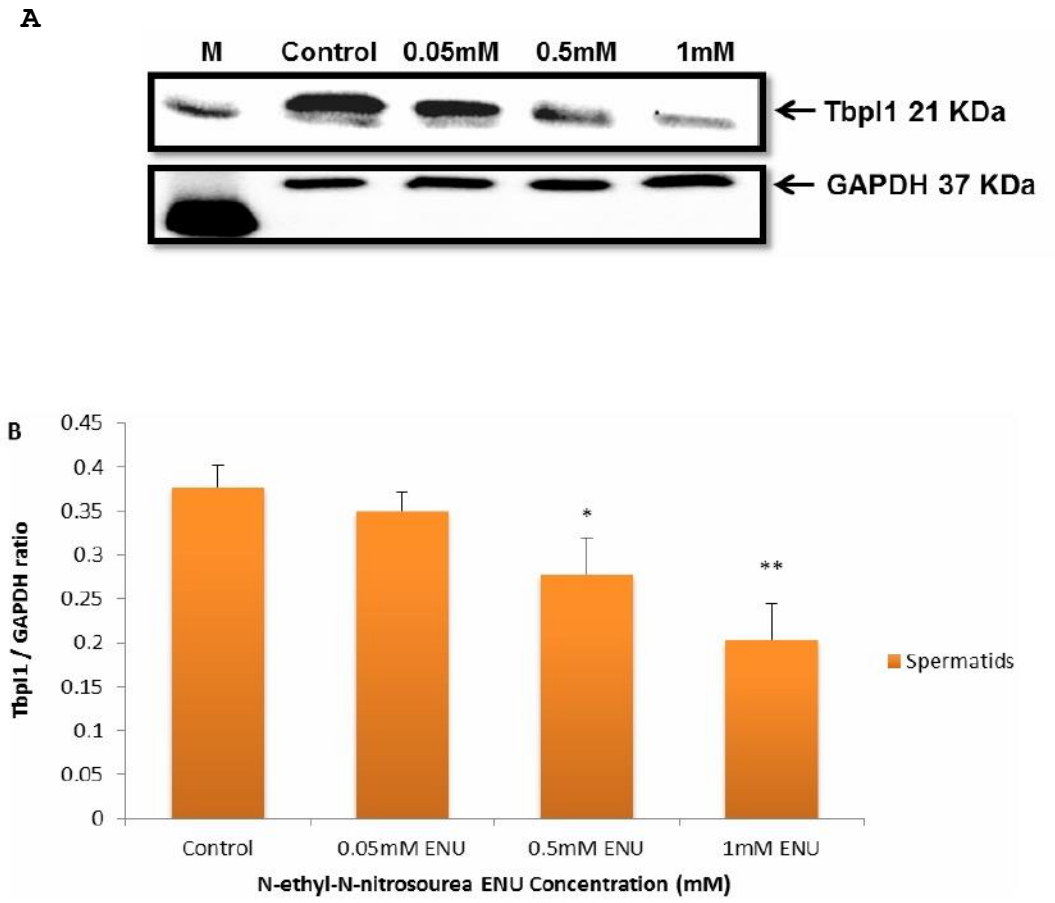

Figure 6.5: Spermatids were treated with ENU and the level of mature TbpI1 protein was examined 1 h after treatment. Sample Western blots of TbpI1 and GAPDH proteins are shown in (A) and quantified summary data are shown in (B). ENU treatment appeared to decrease the TbpI1 protein level at all doses and the decrease was significant at 0.5 and 1 mM. The density of each band was quantified by the use of Image 1.45 software. The relative expression level of TbpI1 was measured by TbpI1 / GAPDH ratio. Results are the mean ± SEM. From three independent experiments and statistical comparisons were made using one-way ANOVA followed by Bonferroni's post-hoc comparisons tests, comparing each dose against the control (*P <0.05; **P <0.01).

6.3.2.2 FHL5

QPCR was conducted on mRNA isolated from untreated and treated (0.05 mM, 0.5 mM and 1 mM ENU) spermatocytes and spermatids. Statistical analysis showed no significant effect on level expression of FHL5 gene when spermatocytes were treated with 0.05 and 0.5 mM ENU. However, a significant decrease was shown when spermatocytes treated with 1 mM (*p<0.05) as shown in Figure 6.6 A. In contrast, spermatids showed significant decrease when treated with 0.5 mM (*p<0.05) and 1mM ENU (**p<0.01) respectively as shown in Figure 6.6 B.

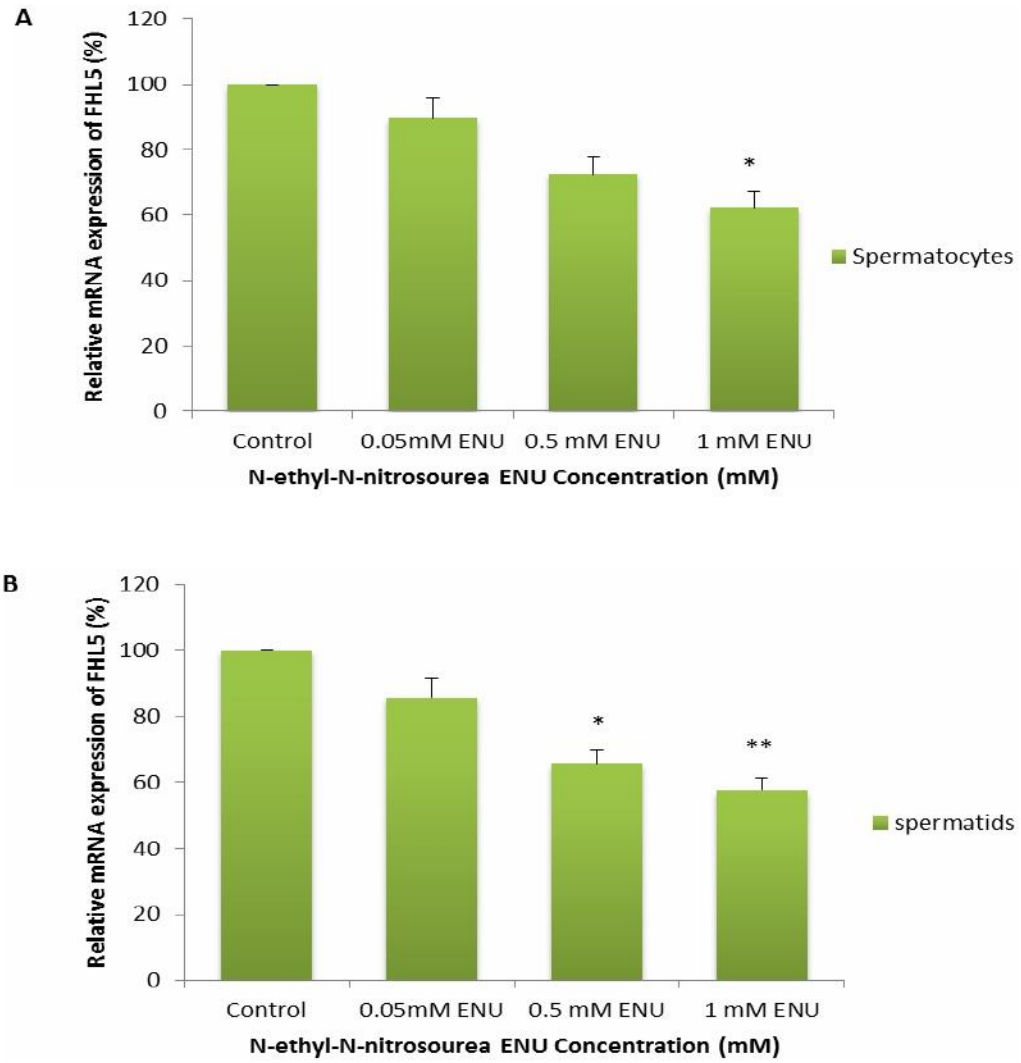

Figure 6.6: Effect of ENU on the FHL5 mRNA expression in spermatocytes and spermatids by qPCR A. Spermatocytes and B. Spermatids after 1 h treatment, at 37 ºC with ENU at different concentrations: 0.05 mM, 0.5 mM and 1 mM. Data are expressed as the mean ± SEM. n=3 different biological replicates performed on three different occasions and analysed by one-way ANOVA followed by Bonferroni's post-hoc, comparisons tests, comparing each exposure level against the control level (*p<0.05, **p<0.01).

Protein extracted from isolated germ cells of both spermatocytes and spermatids was determined by Western blotting to measure FHL5 protein expression. The samples were taken at 1 h following ENU treatment for both treated and untreated control cultures, and the expression levels of FHL5 normalised against those of GAPDH and compared with the normalised control value. FHL5 protein was differentially expressed between spermatocytes and spermatids when treated with ENU and was found to be down-regulated by ENU treatment.

There was no statistically significant difference in the levels of Fhl5 protein, at 0.5 mM concentrations of ENU on spermatocytes while spermatids showed significant decrease (*p<0.05). Moreover, further decrease was shown when spermatocytes treated with 1 mM (*p<0.05) as shown in Figure 6.7 A and B. In contrast, spermatids showed significant decrease when treated with 0.5 mM and 1mM ENU (*p<0.05) and (**p<0.01) respectively as shown in Figure 6.8 A and B.

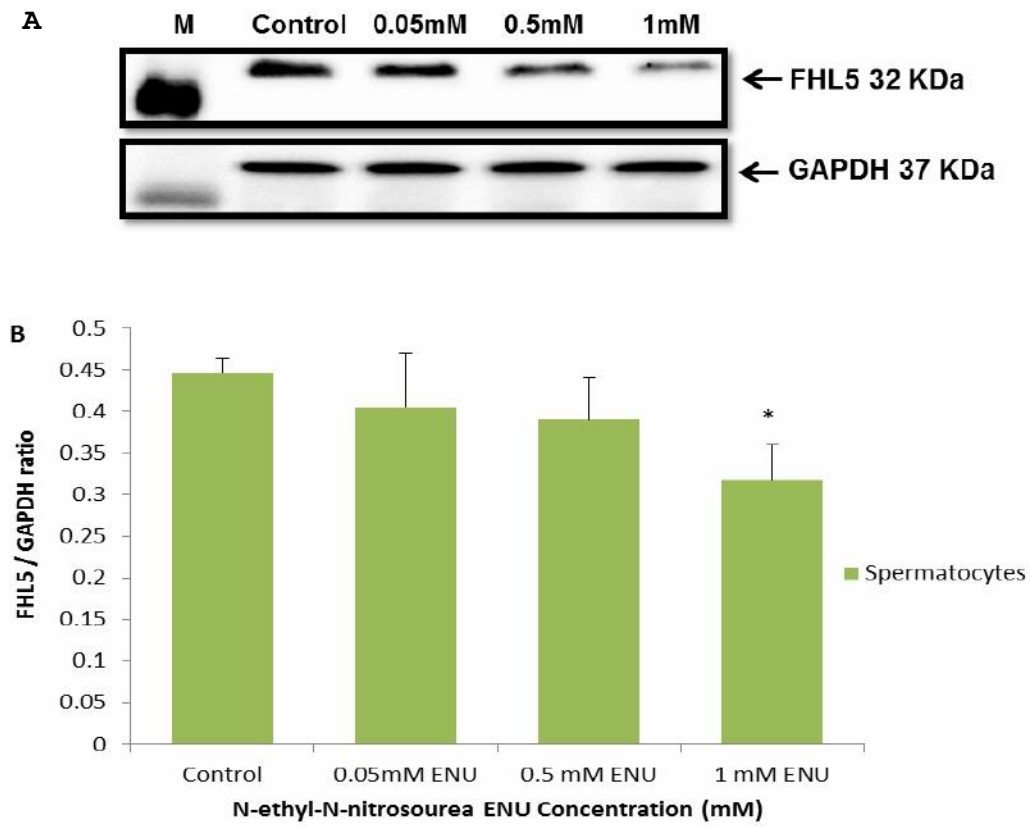

Figure 6.7: Spermatocytes were treated with ENU and the level of mature FHL5 protein was examined 1 h after treatment. Sample Western blots of FHL5 and GAPDH proteins are shown in (A) and quantified summary data are shown in (B). ENU treatment appeared to decrease the FHL5 protein level at all doses but the decrease was only significant at 1 mM. The density of each band was quantified by the use of Image 1.45 software. The relative expression level of FHL5 was measured by FHL5 / GAPDH ratio. Results are the mean ± SEM. From three independent experiments and statistical comparisons were made using one-way ANOVA followed by One-way-ANOVA followed by Bonferroni's post-hoc, comparing each dose against the control (*P <0.05).

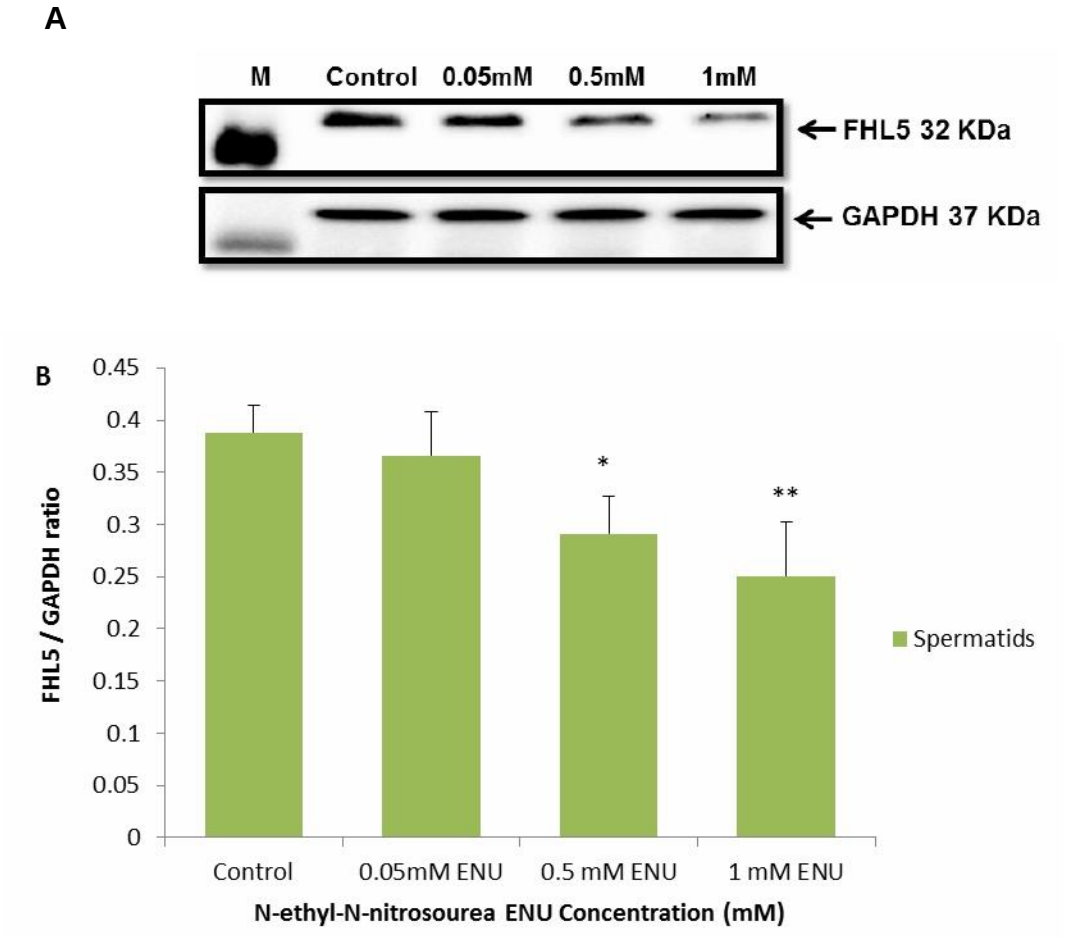

Figure 6.8: Spermatids were treated with ENU and the level of FHL5 protein was examined 1 h after treatment. Sample Western blots of FHL5 and GAPDH proteins are shown in (A) and quantified summary data are shown in (B). ENU treatment appeared to decrease the FHL5 protein level at all doses and the decrease was significant at 0.5 and 1mM. The density of each band was quantified by the use of Image 1.45 software. The relative expression level of FHL5 was measured by TbpI1 / GAPDH ratio. Results are the mean ± SEM From three independent experiments and statistical comparisons were made using one-way ANOVA followed by Bonferroni's post-hoc comparisons tests, comparing each dose against the control (*P <0.05; **P <0.01).

Different levels of expression of Gtf2a1I mRNA between spermatocytes and spermatids were seen after treatment with different concentrations of ENU. The samples were taken at 1 h following ENU treatment for both treated and untreated control cultures, and the expression levels of Gtf2a1I were normalised against those of □-actin and compared with the equivalent control value.

There was no statistically significant difference on the levels of Gtf2a1I after 1 h of treatment with 0.05 mM ENU in either spermatids or spermatocytes. However, a significant decrease in the level of expression of Gtf2a1I in spermatocytes treated with 0.5 mM and 1 mM ENU (*p<0.05) and (**p<0.01) respectively as shown in Figure 6.9 A and B. In contrast, spermatids treated with 0.5 mM and 1 mM ENU (*p<0.01) and (**p<0.001) respectively as shown in Figure 6.9 A and B.

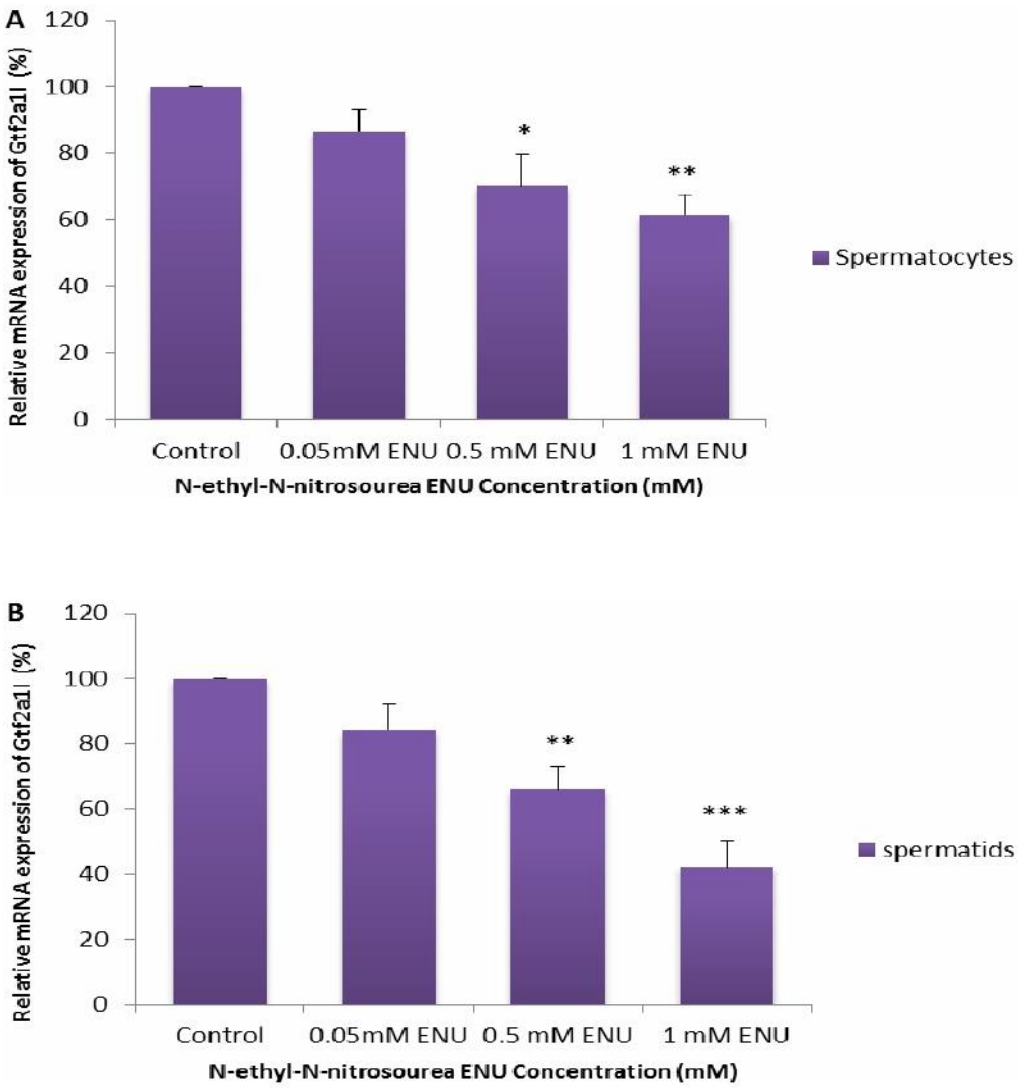

Figure 6.9: Effect of ENU on the Gtf2a1l mRNA expression in spermatocytes and spermatids by qPCR. A. spermatocytes and spermatids by qPCR Spermatocytes and B. spermatids after 1 h treatment, at 37 ºC with ENU at different concentrations: 0.05mM, 0.5mM and 1mM. Non-treated cells' values were defined as 100 % and other values were adjusted accordingly. Data are expressed as the mean ± SEM. n=3 different biological replicates performed on three different occasions and analysed by one-way ANOVA followed by Bonferroni's post-hoc comparisons tests, comparing each exposure level against the control level (*p<0.05, **p<0.01, **p<0.01).

The relative expression level of Gtf2a1I was measured by quantitative western blotting. The samples were taken at 1 h following ENU treatment for both treated and untreated control cultures, and the expression levels of Fhl5 were compared to GAPDH. A Gtf2a1I protein was differentially expressed between spermatocytes and spermatids when treated with ENU compared with the controls (ENU untreated cells) was considered to be expressively down-regulated by ENU treatment.

The relative expression level of Gtf2a1I protein was measured by semi-quantitative Western blotting. Again, the protein was differentially expressed between spermatocytes and spermatids when treated with ENU compared with the controls.

There was no statistically significant difference in the levels of Gtf2a1I protein, at 0.5 mM ENU on spermatocytes while in contrast, spermatids showed a significant decrease (*p<0.05). A further decrease was shown when the spermatocytes (*p<0.05) and spermatids (**p<0.01) were treated with 1 mM ENU. These results are shown in Figure 6.10 A and B and 6.11 A andB.

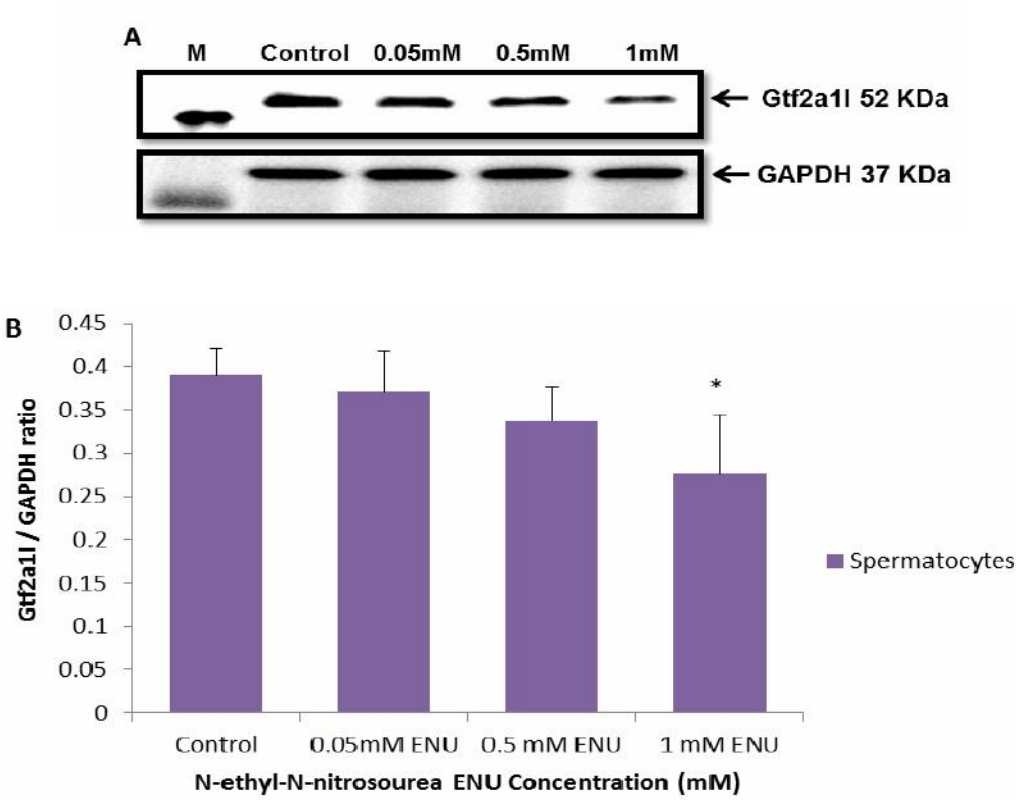

Figure 6.10: Spermatocytes were treated with ENU and the level of Gtf2a1l protein was examined 1 h after treatment. Sample Western blots of Gtf2a1l and GAPDH proteins are shown in (A) and quantified summary data are shown in (B). ENU treatment appeared to decrease the Gtf2a1l protein level at all doses but the decrease was only significant at 1 mM. The density of each band was quantified by the use of Image 1.45 software. The relative expression level of Gtf2a1l was measured by Gtf2a1l / GAPDH ratio. Results are the mean ± SEM From three independent experiments and statistical comparisons were made using one-way ANOVA followed by Bonferroni's post-hoc comparisons tests, comparing each dose against the control ($*P < 0.05$).

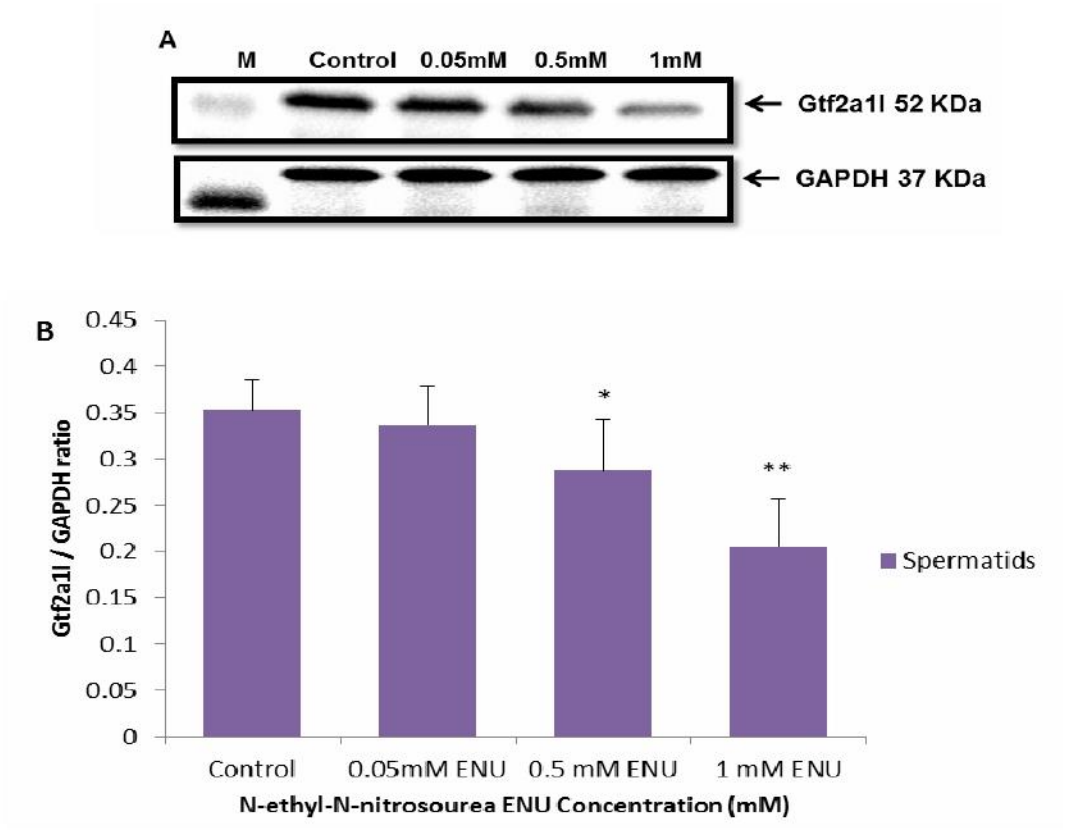

Figure 6.11: Spermatids were treated with ENU and the level of Gtf2a1l protein was examined 1 h after treatment. Sample Western blots of Gtf2a1l and GAPDH proteins are shown in (A) and quantified summary data are shown in (B). ENU treatment appeared to decrease the Gtf2a1l protein level at all doses and the decrease was significant at 0.5 and 1 mM. The density of each band was quantified by the use of Image 1.45 software. The relative expression level of Gtf2a1l was measured by Gtf2a1l / GAPDH ratio. Results are the mean ± SEM From three independent experiments and statistical comparisons were made using one-way ANOVA followed by Bonferroni's post-hoc comparisons tests, comparing each dose against the control ($*P$ <0.05; $**P$ <0.01).

6.3.3 Effect of methyl methanesulfonate (MMS) treatment on spermatocytes and spermatids.

6.3.3.1 Tbpl1

Spermatocytes and spermatids were treated with MMS at different concentrations: 0.05 mM, 0.5 mM and 1 mM. The samples were taken at 1 h following MMS treatment for both treated and untreated control cultures, the expression levels of Tbpl1 were normalised against □-actin and compared with the untreated control.

All treatments yielded progressive decreases in the levels of Tbpl1 mRNA after 1h of treatment with MMS but they were only significant at 0.5 and 1 mM. (Spermatocytes: **P* <0.05 at 0.5 mM and ***P* <0.01 at 1mM; spermatids: ***P* <0.01 at 0.5 mM and ****P* <0.001 at 1 mM). These results are shown in Figure 6.12 A and B.

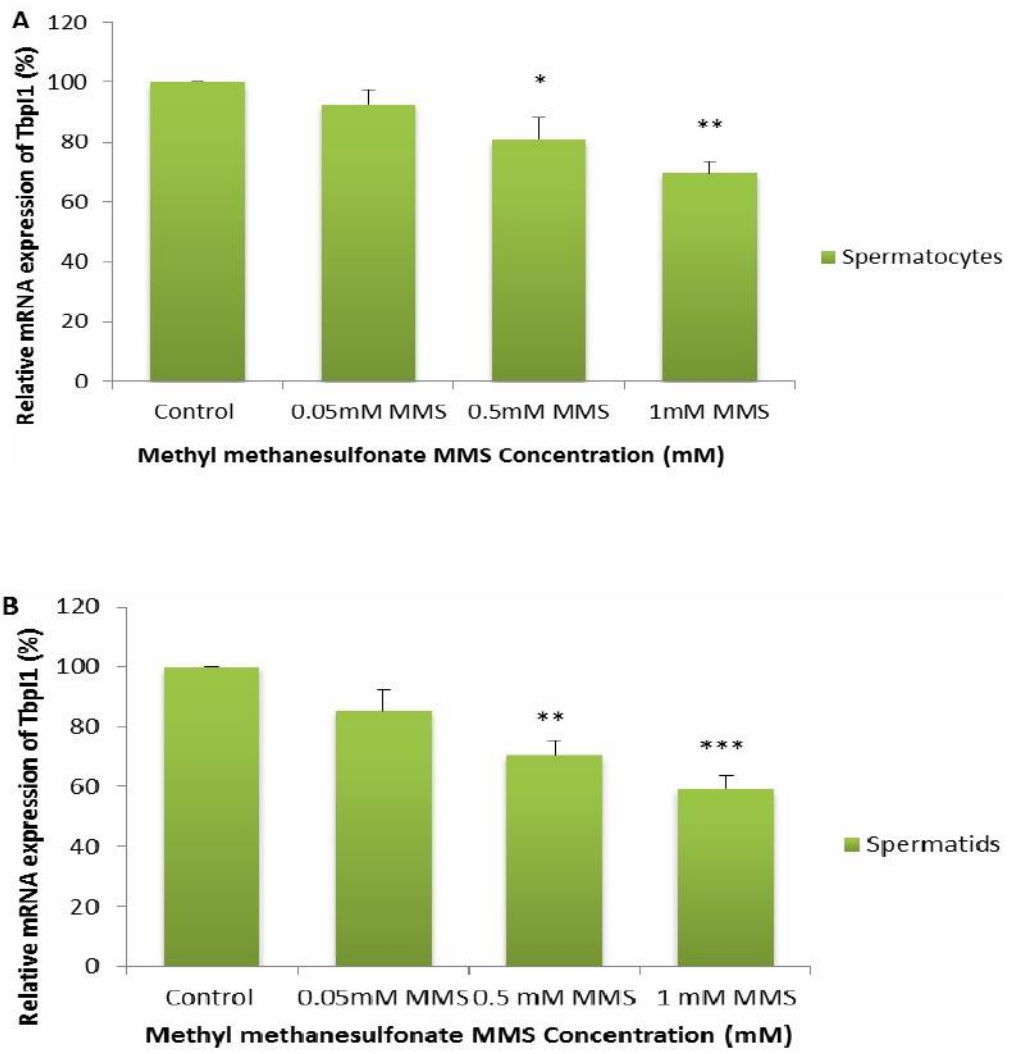

Figure 6.12: Effect of MMS on the Tbpl1 mRNA expression in spermatocytes and spermatids by qPCR. A. spermatocytes and B. spermatids after 1 h treatment, at 37 ºC with MMS at different concentrations: 0.05mM, 0.5mM and 1mM. Non-treated cells' values were defined as 100% and other values were adjusted accordingly. Data are expressed as the mean ± SEM n=3 different biological replicates performed on three different occasions and analysed by one-way ANOVA followed by Bonferroni's post-hoc comparisons tests, comparing each exposure level against the control level (*p<0.05, **p<0.01, ***p<0.01).

The relative protein expression level of TbpI1 was measured by quantitative western blotting. The samples were taken at 1 h following MMS treatment for both treated and -untreated control cultures, and the expression levels of TbpI1 were normalised against GAPDH and compared with the value for the untreated control. TbpI1 protein was differentially expressed between spermatocytes and spermatids but was down-regulated by MMS treatment in both cases.

Statistically significance was shown in the decreased levels of TbpI1 protein with 0.5 mM MMS (spermatocytes $*P < 0.05$, spermatids $**P < 0.01$). A further decrease was shown at 1 mM (spermatocytes $**P < 0.01$, spermatids $***P < 0.001$). These results are shown in Figure 6.13 A and B and 6.14 A and B.

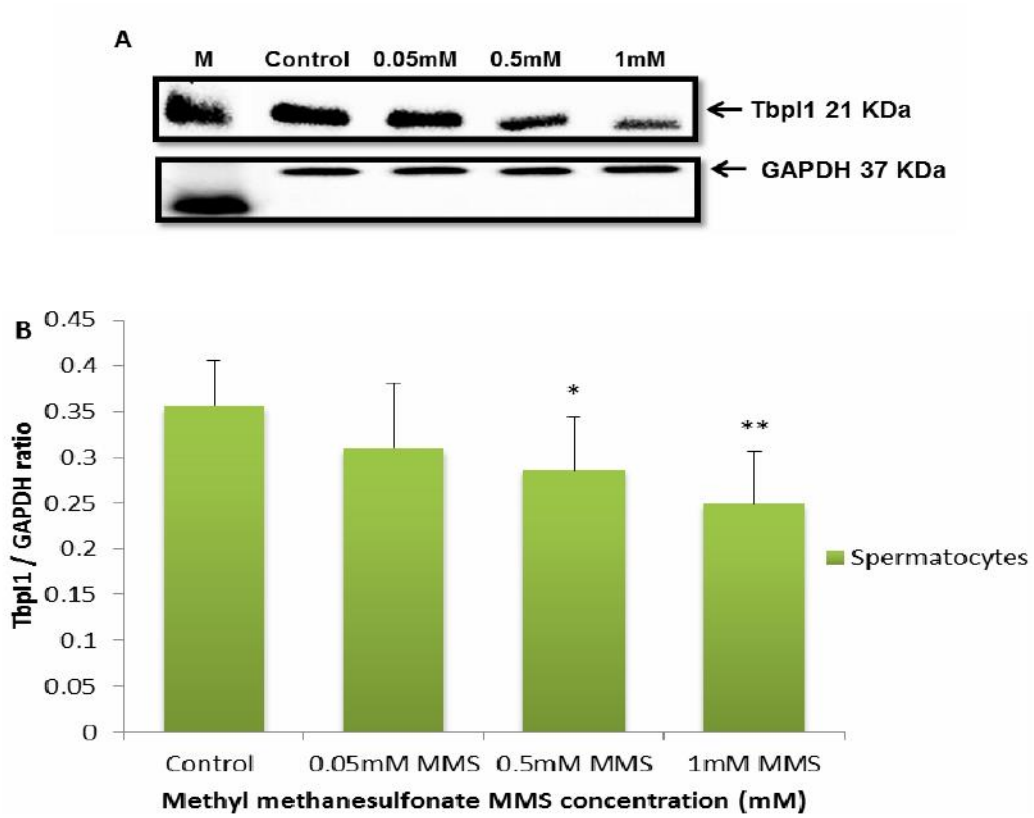

Figure 6.13: Spermatocytes were treated with MMS and the level of TbpI1 protein was examined 1 h after treatment. Sample Western blots of TbpI1 and GAPDH proteins are shown in (A) and quantified summary data are shown in (B). MMS treatment appeared to decrease the TbpI1 protein level at all doses and the decrease was significant at 0.5 and 1mM. The density of each band was quantified by the use of Image 1.45 software. The relative expression level of TbpI1 was measured by TbpI1 / GAPDH ratio. Results are the mean ± SEM. From three independent experiments and statistical comparisons were made using one-way ANOVA followed Bonferroni's post-hoc comparisons tests, comparing each dose against the control (*P <0.05; **P <0.01).

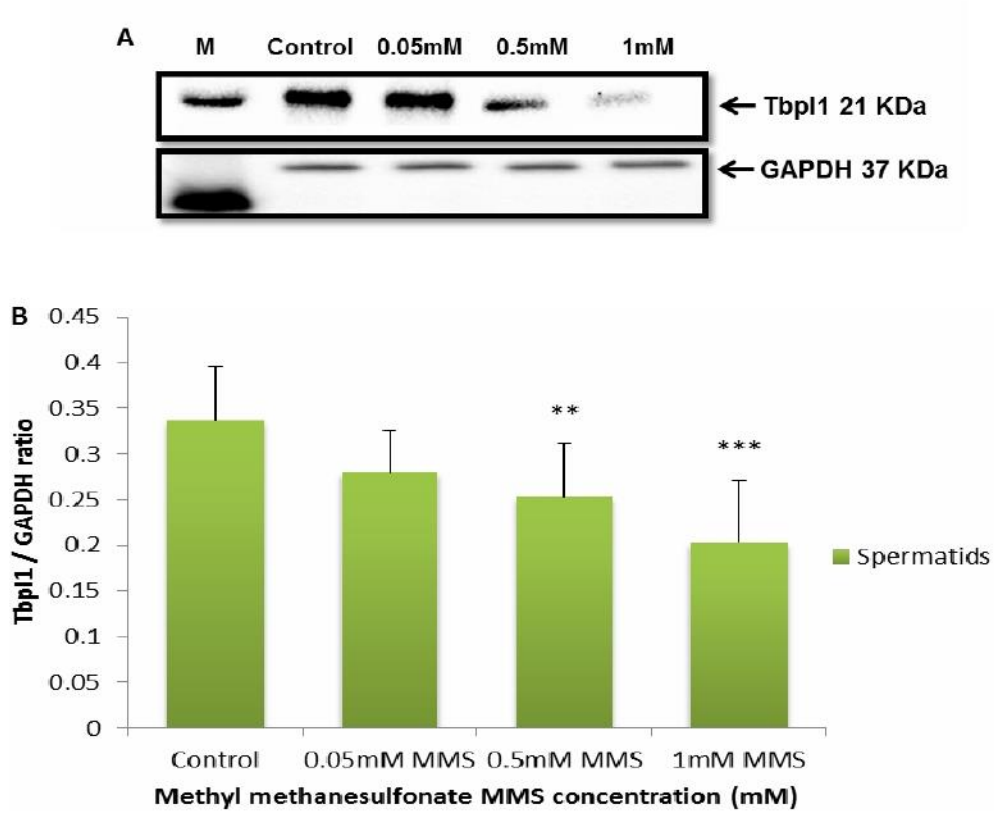

Figure 6.14: Spermatids were treated with MMS and the level of TbpI1 protein was examined 1 h after the treatment. Sample Western blots of TbpI1 and GAPDH proteins are shown in (A) and quantified summary data are shown in (B). MMS treatment decreased TbpI1 protein level. The density of each band was quantified by the use of Image 1.45 software. The relative expression level of TbpI1 was measured by TbpI1 / GAPDH ratio. Results are the mean ± SEM. from three independent experiments ($^{**}P < 0.01$ and $^{***}P < 0.001$).

6.3.3.2 FHL5

mRNA levels of the FHL5 gene also showed different mRNA expression in spermatocytes and spermatids after being treated with different concentrations of MMS (as above). The samples were taken at 1 h following MMS treatment for both treated and untreated control cultures, and the expression levels of FHL5 were normalised against those of β-actin and compared with the control values.

There was no statistically significant difference on the levels of FHL5 after 1 h of treatment with 0.05 mM MMS in either spermatids or spermatocytes. However, a significant decrease in the level of expression of FHL5 in spermatocytes treated with 0.5 mM and 1 mM MMS (*p<0.05) and (**p<0.01) respectively as shown in Figure 6.15 A and B. In contrast, spermatids treated with 0.5 mM and 1 mM MMS (**p<0.01) and (***p<0.001) respectively as shown in Figure 6.15 A and B.

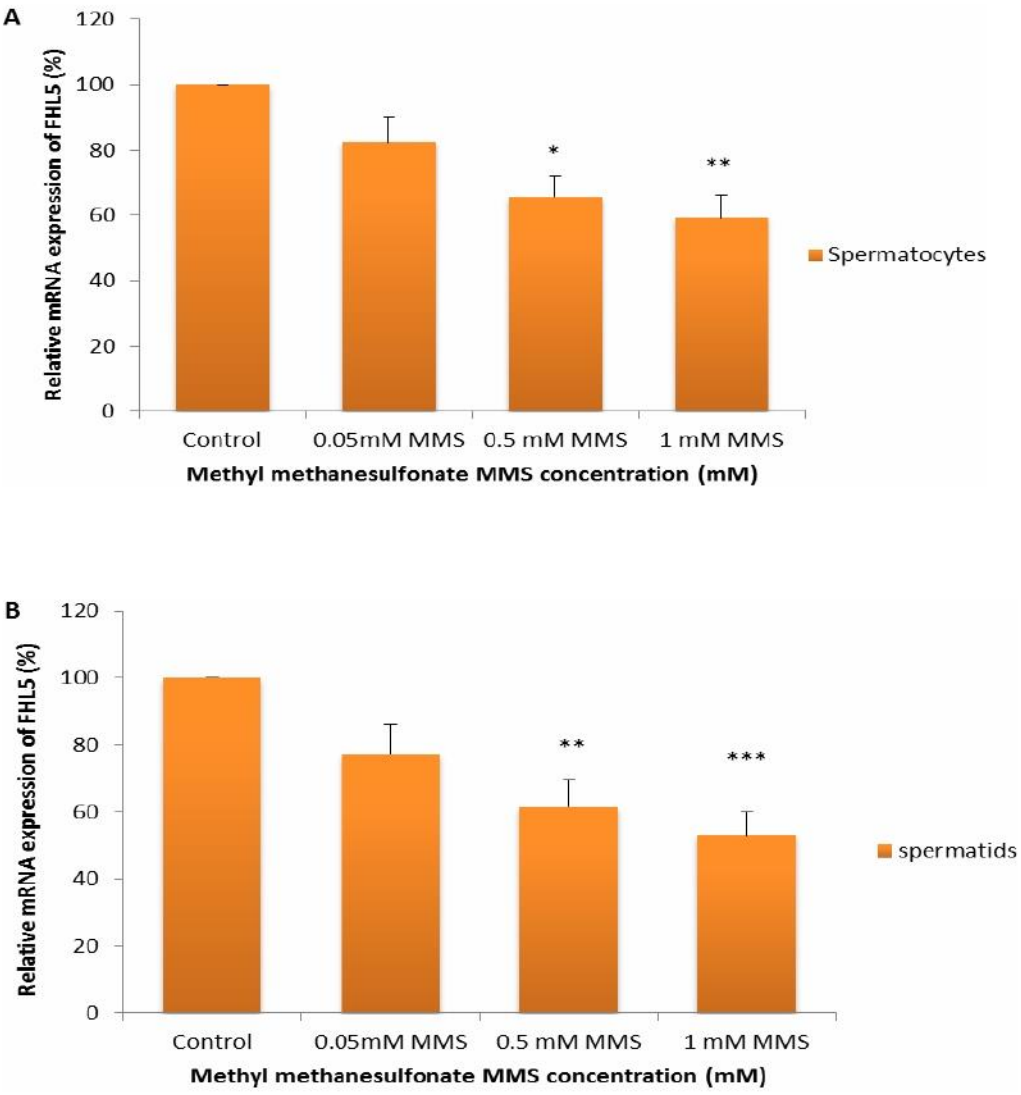

Figure 6.15: Effect of MMS on the Fhl5 mRNA expression in spermatocytes and spermatids by qPCR. A. spermatocytes and B. spermatids after 1 h treatment, at 37º C with MMS at different concentrations: 0.05 mM, 0.5 mM and 1 mM. Non-treated cells' values were defined as 100% and other values were adjusted accordingly. Data are expressed as the mean ± SEM. n=3 different biological replicates performed on three different occasions and analysed by one-way ANOVA followed by Bonferroni's post-hoc comparisons tests, comparing each exposure level against the control level (*P <0.05, **P <0.01, ***P <0.001).

The relative expression level of FHL5 was measured by quantitative Western blotting. The samples were taken at 1 h following MMS treatment for both treated and untreated control cultures, and the expression levels of FHL5 were normalised against GAPDH and compared with the control values. The same pattern of results was obtained with protein expression as with mRNA with statistically significant effects shown on the levels of FHL5 protein when spermatocytes treated with 0.5 mM and 1 mM MMS (*p<0.05) and (**p<0.01) respectively as shown in Figure 6.16 A and B. In contrast, spermatids treated with 0.5 mM and 1 mM MMS (**p<0.01) and (***p<0.001) respectively as shown in Figure 6.17 A and B.

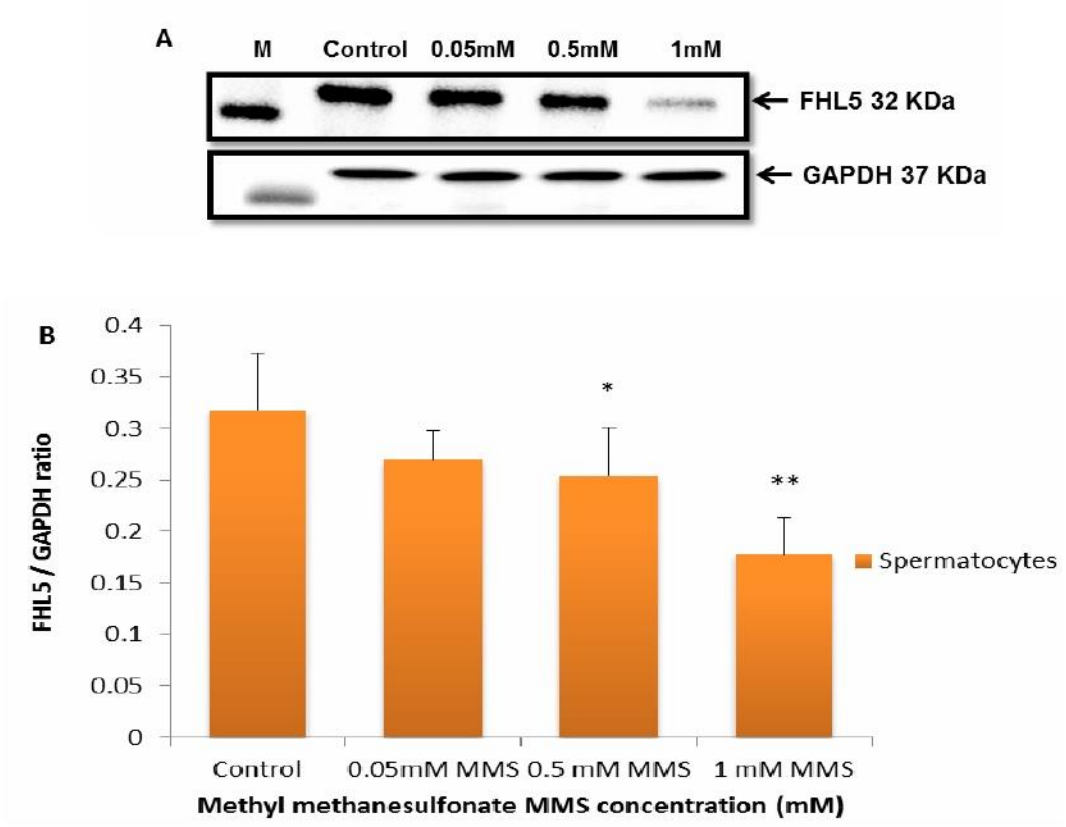

Figure 6.16: Spermatocytes were treated with MMS and the level of FHL5 protein was examined 1 h after treatment. Sample Western blots of FHL5 and GAPDH proteins are shown in (A) and quantified summary data are shown in (B). MMS treatment appeared to decrease the FHL5 protein level at all doses and the decrease was significant at 0.5 and 1 mM. The density of each band was quantified by the use of Image 1.45 software. The relative expression level of FHL5 was measured by FHL5 / GAPDH ratio. Results are the mean ± SEM From three independent experiments and statistical comparisons were made using one-way ANOVA followed by Bonferroni's post-hoc comparisons tests, comparing each dose against the control (*P <0.05; **P <0.01).

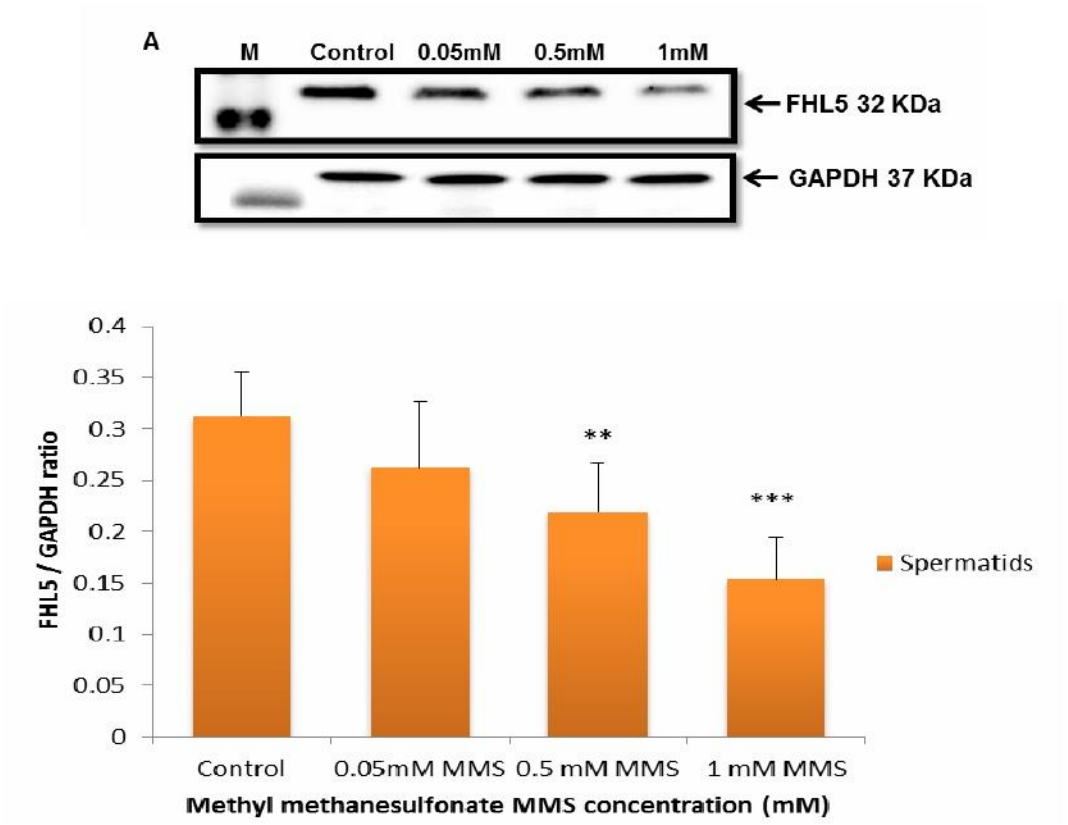

Figure 6.17: Spermatids were treated with MMS and the level of FHL5 protein was examined 1 h after treatment. Sample Western blots of FHL5 and GAPDH proteins are shown in (A) and quantified summary data are shown in (B). MMS treatment appeared to decrease the FHL5 protein level at all doses and the decrease was significant at 0.5 and 1mM. The density of each band was quantified by the use of Image 1.45 software. The relative expression level of FHL5 was measured by FHL5 / GAPDH ratio. Results are the mean ± SEM. from three independent experiments and statistical comparisons were made using one-way ANOVA followed by Bonferroni's post-hoc comparisons tests, comparing each dose against the control (***P* <0.01; ****P* <0.001).

6.3.3.3 Gtf2a1l

As with the other two transcription factors studied, the expression of the Gtf2a1I gene showed a different pattern of expression of mRNA between spermatocytes and spermatids after treatment with different concentrations of MMS. The samples were taken at 1 h following MMS treatment for both treated and untreated control cultures, and the expression levels of Gtf2a1I were normalised against □-actin and compared with the corresponding control value.

There was no statistically significant difference on the levels of Gtf2a1I after 1 h of treatment with 0.05 mM MMS in both spermatocytes and spermatids. However, a significant decrease in the level of expression of Gtf2a1I in spermatocytes treated with 0.5 mM and 1 mM MMS (*p<0.05) and (**p<0.01) respectively. In contrast, spermatids treated with 0.5 mM and 1 mM MMS (**p<0.01) and (***p<0.001) respectively. These results are shown in Figure 6.18 A and B.

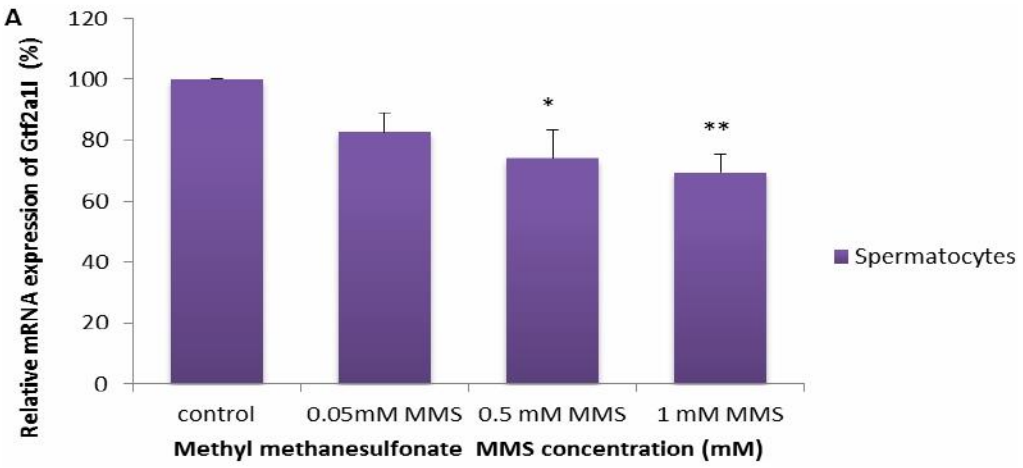

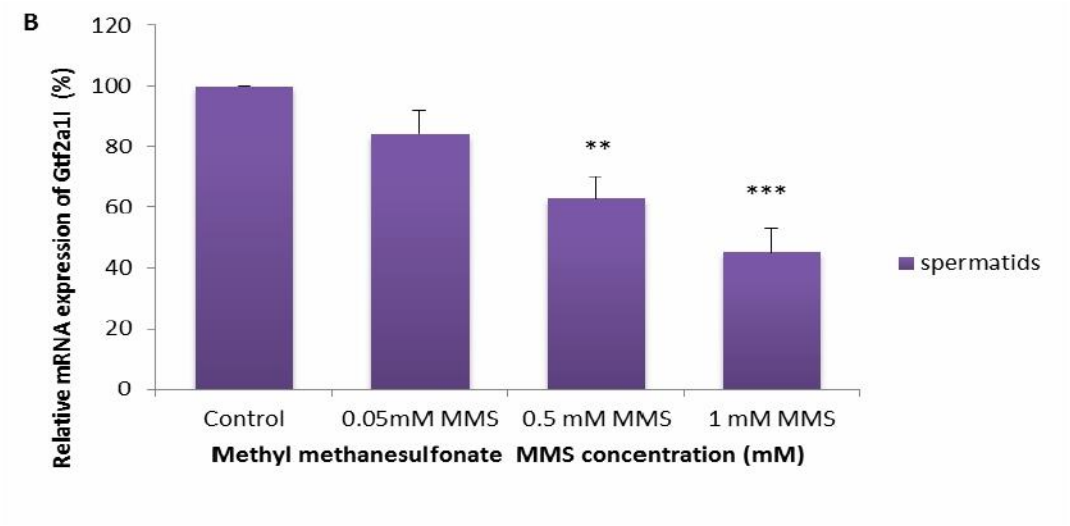

Figure 6.18: Effect of MMS on the Gtf2a1l mRNA expression in spermatocytes and spermatids by qPCR. A. spermatocytes and B. spermatids after 1 h treatment, at 37º C with MMS at different concentrations: 0.05 mM, 0.5 mM and 1 mM. Non-treated cells' values were defined as 100% and other values were adjusted accordingly. Data are expressed as the mean ± SEM. n=3 different biological replicates performed on three different occasions and analysed by one-way ANOVA followed by Bonferroni's post-hoc comparisons tests, comparing each exposure level against the control level (*p<0.05, **p<0.01, ***p<0.001).

The relative expression level of Gtf2a1I protein was measured by quantitative western blotting. The samples were taken at 1 h following MMS treatment for both treated and -untreated control cultures, and the expression levels of Gtf2a1I were normalised against those of GAPDH and compared with the appropriate control.

A statistically significant decrease was shown in the levels of Gtf2a1I protein when protein when spermatocytes treated with 0.5 mM and 1 mM MMS (*p<0.05) and (**p<0.01) respectively as shown in Figure 6.19 A and B. In contrast, spermatids treated with 0.5 mM and 1 mM MMS (**p<0.01) and (***p<0.001) respectively as shown in Figure 6.20 A and B.

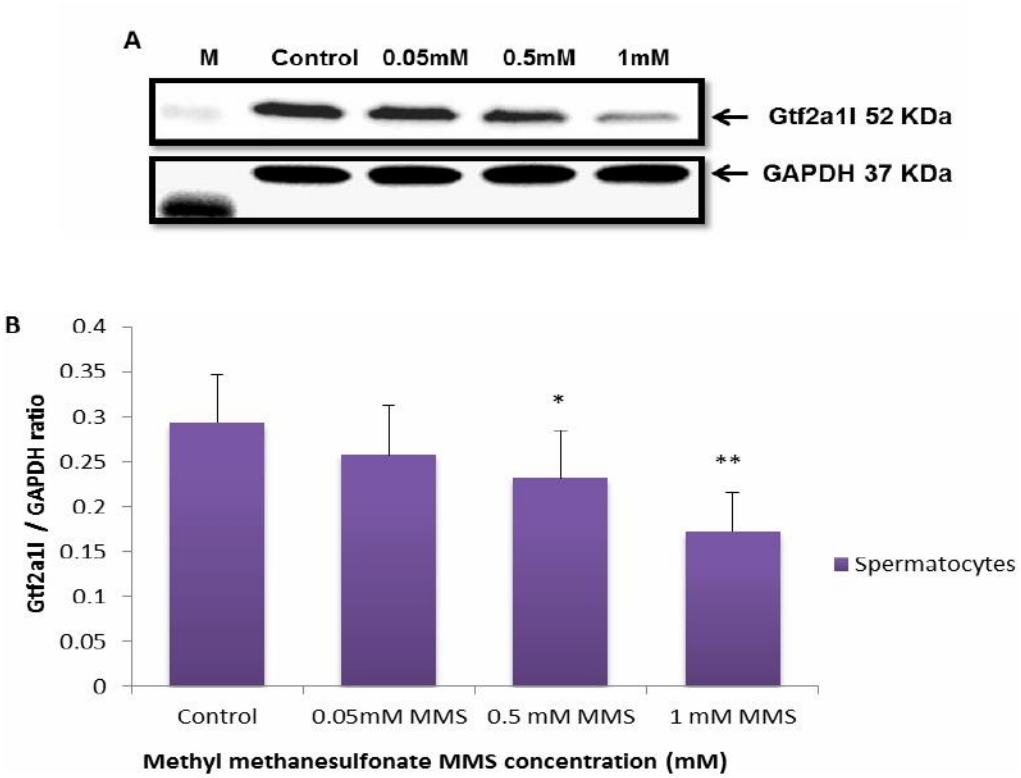

Figure 6.19: Spermatocytes were treated with MMS and the level of Gtf2a1l protein was examined 1 h after treatment. Sample Western blots of Gtf2a1l and GAPDH proteins are shown in (A) and quantified summary data are shown in (B). MMS treatment appeared to decrease the Gtf2a1l protein level at all doses and the decrease was significant at 0.5 and 1mM. The density of each band was quantified by the use of Image 1.45 software. The relative expression level of Gtf2a1l was measured by Gtf2a1l / GAPDH ratio. Results are the mean ± SEM From three independent experiments and statistical comparisons were made using one-way ANOVA followed by Bonferroni's post-hoc comparisons tests, comparing each dose against the control ($*P < 0.05$; $**P < 0.01$).

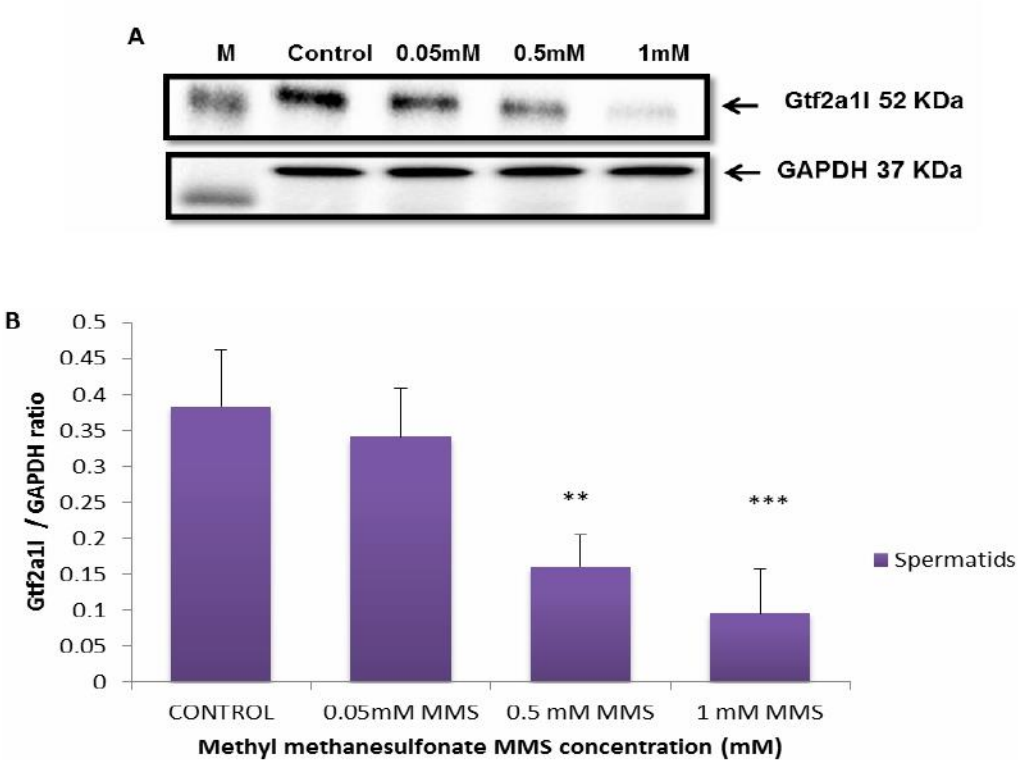

Figure 6.20: Spermatids were treated with MMS and the level of Gtf2a1l protein was examined 1 h after treatment. Sample Western blots of Gtf2a1l and GAPDH proteins are shown in (A) and quantified summary data are shown in (B). MMS treatment appeared to decrease the Gtf2a1l protein level at all doses and the decrease was significant at 0.5 and 1mM. The density of each band was quantified by the use of Image 1.45 software. The relative expression level of Gtf2a1l was measured by Gtf2a1l / GAPDH ratio. Results are the mean ± SEM From three independent experiments and statistical comparisons were made using one-way ANOVA followed by Bonferroni's post-hoc comparisons tests, comparing each dose against the control (***P* <0.01; ****P* <0.001).

6.4 Discussion

To investigate the ENU and MMS induced damage on mRNA, the expression level of TbpI1, Fhl5 and Gtf2a1l selected mRNA transcription factors in spermatocytes and spermatids were compared under control and treatment conditions. The selected genes are known to be highly expressed in spermatocytes and spermatids. Expression was measured by qPCR analysis. The PCR exponential phase was obtained and the optimal number of PCR cycles, which was 30 cycles, was determined. QPCR analysis showed that TbpI1 is present in spermatocytes and spermatids in male adult mouse and observed by a product band at 136 bp. The Fhl5 gene was represented by a product band at 102 bp and Gtf2a1l by a product band at 109 bp.

Mammalian spermatogenesis seems to be controlled via the organized stage and cell specific gene expression in both the germ cells and the supporting somatic cells. The molecular mechanisms of this process are believed to include the selective modulation of defined sets of genes that facilitate spermatogenic cell differentiation (Guo et al., 2004). The dynamic pattern of TLF expression is essential for the development and differentiation of male germ cells (Martianov et al., 2001, Akhtar and Veenstra, 2011). The expression of the FHL5 gene is highly specific to spermatocytes and spermatids (Steger et al., 2004, De Cesare et al., 2003). FHL5 is regulated via interaction with CREM, a main factor for the regulation of many postmeiotic genes in spermatid maturation (De Cesare et al., 2003). FHL5 expression is limited to late male germ cells (Fimia et al., 1999). A homozygous deletion of the FHL5 gene results in severe oligozoospermia,

though germ cells progress in FHL5-deficient mice seems normal. This result suggests that FHL5 is included in regulating genes for physical mechanisms involved in post-testicular sperm development (Kotaja et al., 2004). In agreement with the observations of Han et al. and Huang et al., (2001 and 2006) who showed that Gtf2a1I mRNA is present in spermatocytes and spermatids (Han et al., 2001, Huang et al., 2006), this gene was also found to be expressed in these cell types in the present study. Gtf2a1I is encoded by a germ cell-specific gene whose expression is up-regulated with other general transcription factors during male germ cell development in the mouse (Han et al., 2001, De Cesare et al., 2003). Recently, an endogenous homolog of Gtf2a1I has been found as a 52 kDa protein in human testis extracts (Ozer et al., 2000, Huang et al., 2006). It is therefore possible that the function of Gtf2a1I is the morphological development of the sperm. If so, a lack of Gtf2a1I protein could result in abnormal sperm formation (Huang et al., 2006).

The results presented in this chapter show that treating spermatocytes and spermatids isolated by Staput with ENU or MMS had a very marked effect on the mRNA and protein levels of these genes. Furthermore, it was found that the mRNA and protein levels were more affected in spermatids than in spermatocytes. This might be due to the mutational susceptibility of the different germ cell stages as a function of the chemical agent used. It is well known that the postmeiotic phase of mouse male germ cells is extremely sensitive to the induction of heritable genomic damage (Marchetti and Wyrobek, 2008). The high sensitivity of the postmeiotic period to mutagenic exposure has been associated with the reduced DNA repair capacity,

recombination and the types of chromosome-associated proteins and the extent of chromosomal condensation of late spermatids and sperm as compared other spermatogenic cell types (Singer et al., 2006, Sega, 1974, Olsen et al., 2005). All main DNA repair pathways appear to be less functional in late spermatids and sperm (Olsen et al., 2005, Hamer et al., 2003, Xu et al., 2005). This incapability of sperm to repair DNA lesions as they happen might make them mainly vulnerable to repeated exposures that take place because of environmental mutagens and occupational or life style reasons (Marchetti and Wyrobek, 2008). These clarifications suggest that genomic damage induced in late spermatids and sperm might accumulate in the fertilizing sperm and be transmitted to the embryo (Marchetti and Wyrobek, 2008). The qRT-PCR and Western blot analyses illustrated that the levels of TbpI1, FHL5 and Gtf2a1l expression in cells treated with ENU and MMS were highly down-regulated. This could suggest that these genes are essential for the progression of meiosis during germ cells development and in spermiogenesis.

This study briefly outlines the current hypotheses regarding possible mechanisms during the haploid phase of spermatogenesis that may lead to such decreased level mRNA and proteins expression, which could be including enzyme induced breaks, apoptosis-like processes or oxidative stress of DNA. A better understanding of the origin of these mechanisms will lead to further investigations on the genetic instability of TbpI1, FHL5 and Gtf2a1l and mutagenic potential induced by the mutagenesis of ENU and MMS.

Chapter 7. Cloning and characterisation of the post-meiotically expressed genes Tbpl1, FHL5 and Gtf2a1l for assessment of effects of ENU and MMS

7.1 Introduction

A number of stresses such as DNA damage can lead not only to mutation but also to alterations in gene expression patterns caused via a universal shutdown and reprogramming of protein synthesis (Spriggs et al., 2010). A selective recruitment of ribosomes to mRNA which contain protein products that are needed for stress responding, can occur as a result of DNA damage. This recruitment can be regulated via elements in the 5′ and 3′ untranslated regions of mRNAs, involving interior ribosome entry segments, upstream open-reading frames, and microRNA target sites (Spriggs et al., 2010). Exogenous DNA damage can occur from physical or chemical sources. Among the most potent of these are radiotherapy and chemical agents used in cancer therapy, which can cause a diversity of DNA lesions, alkylating agents such as MMS and ENU, which attach alkyl groups to DNA bases (Ciccia and Elledge, 2010). Bases modified by alkylation can be misrepaired leading to misincorporation and hence mutation (Lindahl and Barnes, 2000).

Spontaneous DNA mutation also occurs and can be due to dNTP misincorporation during DNA replication or interconversion among DNA bases produced by deamination. Alternatively, it can be due to loss of DNA bases resulting from DNA depurination (Lindahl and Barnes, 2000). In order to detect mutations caused in these ways, there is a range of genetic toxicology tests available for their detection. However, it is important to continue to develop new in vitro tests, especially those that can be used for high throughput testing.

The purpose of this study was to clone cDNA derived from testicular mRNA of the meiosis/spermiogenesis-specific transcription factors Tbpl1, FHL5 and Gtf2a1l respectively, given their apparent importance as targets described in Chapter 6. This will then enable the assessment of the toxicity of various doses of ENU and MMS on purified DNA plasmid by qPCR to evaluate the level expression of these genes in the in vitro model system of *E.coli*. The recombinant Tbpl1, FHL5 and Gtf2a1l proteins will be expressed, isolated using his-select spin columns and detected by Western blotting using a histidine Tag and Tbpl1-, FHL5- and Gtf2a1l-specific primary antibodies.

7.2 Materials and Methods

All relevant information is shown in section 2.1 RNA extraction and preparation is described in section 2.8.1. Measurement of quantity and purity of total RNA is described in section 2.8.5. DNase-I treatment is described in section 2.8.6 and cDNA synthesis in section 2.8.9 Plasmid DNA isolation is described in section 2.9.3. Restriction endonuclease digestion of plasmid DNA is described in section 2.9.4. Web-based genome databases (www.ensembl.org, www.bioinformatics.nl and www.ncbi.nlm.nih.gov) were used to analyse the genomic sequences and protein of the target genes to facilitate the design primers for qPCR. Full details of primer design are described in section 2.8.8. Polymerase chain reaction (PCR) is described in section 2.8.9. Cloning of the PCR Product into PET100/D is described in section 2.10.15. Protein expression is described in section 2.10.2 and Western Blot analysis was performed as described in section 2.12.

7.3 Results

7.3.1 RNA isolation

Total RNA was extracted from mouse testis using the GenElute™ Mammalian Total RNA Miniprep Kit (Sigma Aldrich) according to the manufacturer's instructions. The quality of RNA was analysed by using gel electrophoresis (1 % agarose gel in 1x TBE) and ethidium bromide staining.

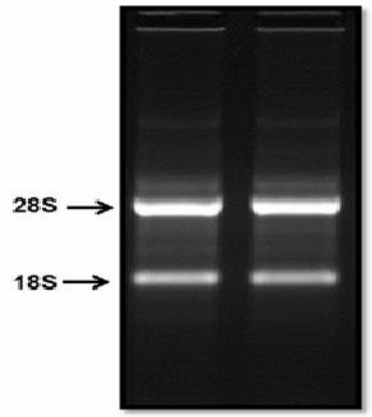

Figure 7.1: Optimised RNA extraction from mouse testis. Total RNA was extracted from 30mg testis tissue removed from 12 week old male NMRI mice. The samples were subjected to electrophoresis through a 1% w/v agarose gel in 1 X TBE with 1µg/ml ethidium bromide staining. Two sharp bands appeared on the gel which represents 28S and 18S ribosomal RNA bands with an approximate ratio of 2:1 indicating good quality RNA. In addition, there is a streak of mRNA from 200-2000 bp whose evenness in turn also reflects its quality.

7.3.2 β-Actin PCR

RT-PCR was performed on first strand cDNA for detection of β-actin; a housekeeping gene constitutively expressed in mouse testis. This gene is regularly amplified to ensure synthesis of the first strand of cDNA had been successful and to validate the PCR conditions. Gene expression studies require that the expression profiles of the various genes being studied should be normalized against a suitable internal control.

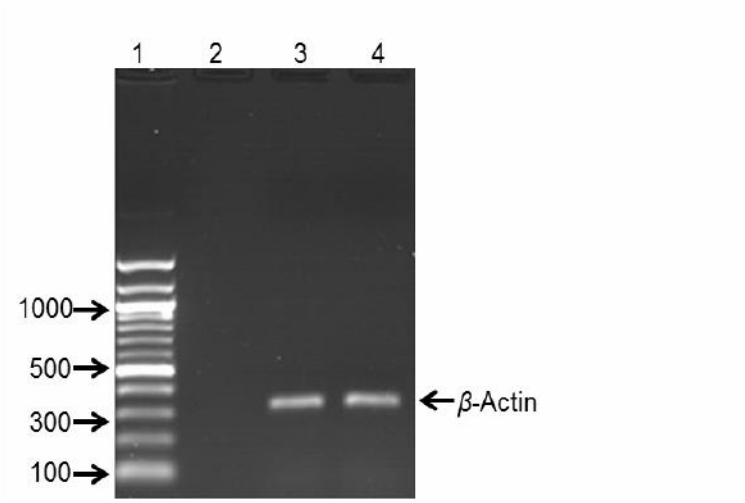

Figure 7.2: PCR amplification of β-actin product (327bp). The samples were subjected to electrophoresis through a 1.5% w/v agarose gel in 1X TBE with 1µg/ml ethidium bromide staining. The PCR conditions were 95°C (30sec), 59°C (30sec), 72 °C (30sec) for 30 cycles. The primers were forward 5-TATCCCGGGTAACCCTTCTC-3 and reverse 5-TGCTGGGAGTCTCAGGACAG-3. Lanes 1 shows DNA ladder. Lane 2 is a negative control containing no cDNA and lanes 3 and 4 show positive amplification of β-actin (327bp) product template.

Normalization ensures that the results have been corrected for discrepancies in concentration measurements, reaction inhibition and other extraneous errors. In these studies, the expression of the housekeeping gene actin was used as the RT-qPCR internal control standard. Figure 7.2 shows a clear single band of β-actin against the marker ladder and a control run without cDNA. The detection of β-actin (327bp) gave the expected size product, indicated it to be correct and, especially important, with no signs of contamination.

7.3.3 TATA box binding protein-like 1 (Tbpl1)

The full genomic sequence of the TATA box binding protein-like 1 is located on chromosome 10 at location 22,703,879-22,731,938, spanning over 27.57 kb. Tbpl1 has 7 exons with a transcribed length 2,873 bps, which encodes a peptide 186 amino acids in size. The Tbpl1 protein is a 20,886.52 g/mol (21 KDa).

```
  1 GAGAACCGGAAGTGAGTGGCTAGCCGGGATCCCCGGAGCTCCTGGGTCCGGCGGCGCTCT

 61 AGCCGCCTCGTGCCGCCTCTATGCCCCCGTGCGTCTAGTCTATTTATTGTCGCGGGGGAA

121 GCGGCGGCCGCCCTGTACCCGGAACAACAAAGCGAGAAACCGAGCTCGAGCCTTGGGGGG

181 CTCCTAGCAACGGGCCTGGGCGGGAGTTCCATGGAGACTGGGGAGCGGACCCGTTTTATC

241 TTCATCCTTGTCCTCCAGCTTCTTCTCCGCGTCCGACGCAACCAGCAGCAGCGCTGCCGC

301 CGTGTCCTTTACGACCGCCCCGTCTTCCCACGGATGTGATCTTCGTGGTGGGAACCAAGT

361 TTCTAAACTACCCCAATGGATGCAGACAGTGATGTTGCATTGGACATTTTAATTACAAAT
    ..............ATGGATGCAGACAGTGATGTTGCATTGGACATTTTAATTACAAAT
    ..............-M--D--A--D--S--D--V--A--L--D--I--L--I--T--N-

421 GTAGTCTGTGTTTTTAGAACAAGATGCCATTTGAACTTAAGGAAGATTGCTTTGGAGGGA
 46 GTAGTCTGTGTTTTTAGAACAAGATGCCATTTGAACTTAAGGAAGATTGCTTTGGAGGGA
 16 -V--V--C--V--F--R--T--R--C--H--L--N--L--R--K--I--A--L--E--G-

481 GCAAATGTAATTTATAAGCGTGATGTTGGGAAAGTATTAATGAAGCTTAGAAAACCTAGA
106 GCAAATGTAATTTATAAGCGTGATGTTGGGAAAGTATTAATGAAGCTTAGAAAACCTAGA
36 -A--N--V--I--Y--K--R--D--V--G--K--V--L--M--K--L--R--K--P--R-
541 ATTACAGCTACAATTTGGTCCTCAGGAAAAATTATTTGCACTGGAGCAACAAGTGAAGAA 166
ATTACAGCTACAATTTGGTCCTCAGGAAAAATTATTTGCACTGGAGCAACAAGTGAAGAA
```

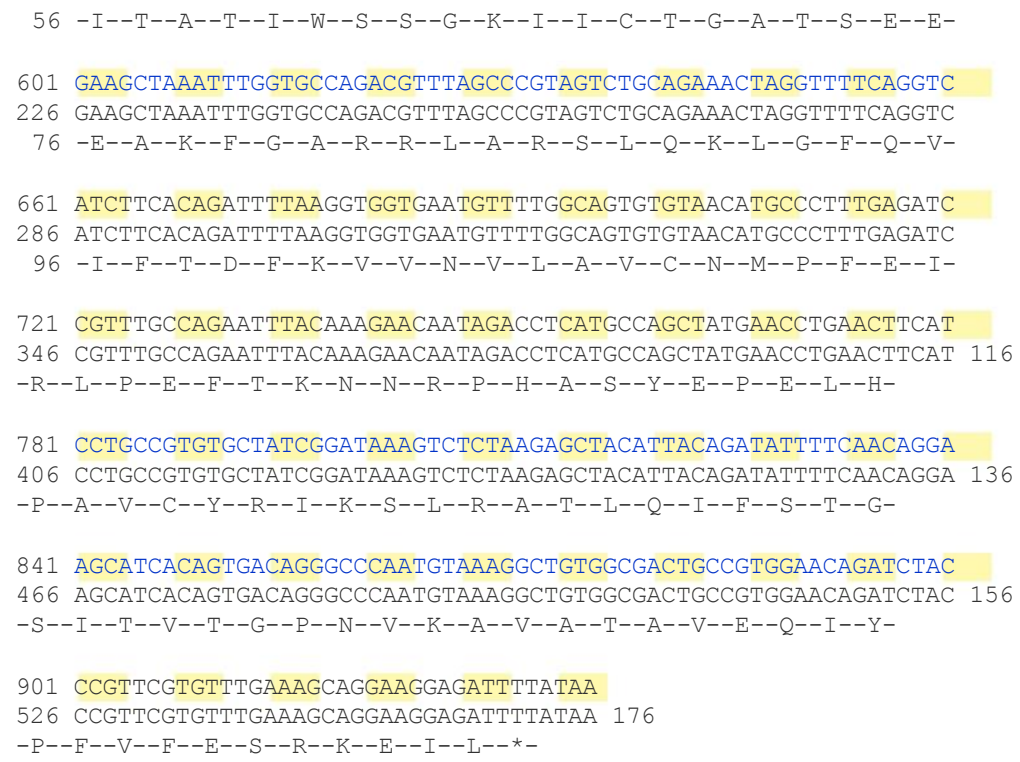

Figure 7.3: DNA (top line) and transcript (middle line) sequences of Tbpl1 gene and its corresponding peptide sequences (bottom line). The untranslated region of the transcript is highlighted yellow, exons are alternately coloured black and blue (and codons are alternately coloured pale yellow/black or blue). Taken from www.ensembl.org.

7.3.3.1 Tbpl1

7.3.3.1.1 Tbpl1 PCR

Following RNA isolation from mouse testis, the gene of interest, Tbpl1, was amplified by RT-PCR. Custom primers were designed to amplify the 558 bp gene using the genomic DNA sequences of mus-musculus ATCC 2873 obtained at the Ensembl website, gene ID # ENSMUSG00000071359.

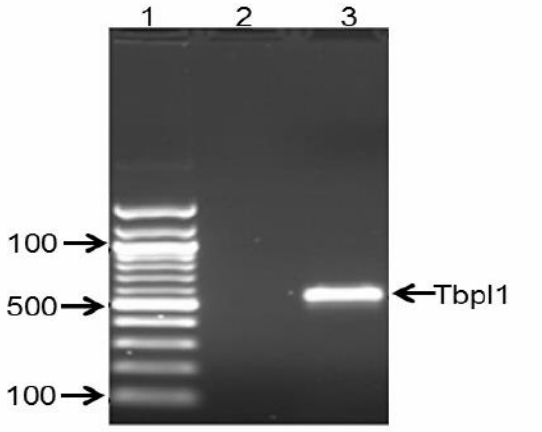

Figure 7.4: PCR amplification of Tbpl1 product (558 bp). The samples were subjected to electrophoresis through a 1.5 % w/v agarose gel in 1XTBE with 1µg/ml ethidium bromide staining. The PCR amplification conditions were 94°C (30sec), 61°C (30sec), 72 ºC (30sec) for 30 cycles. The primers were forward 5' CACCATGGATGCAGACATGAT-GTT-3' and reverse 5'-TAAAATCTCCTTCCTGCTTTCA-3´. Lane 1 shows DNA ladder. Lane 2 is a negative control containing no cDNA template. Lane 3 shows positive amplification of Tbpl1 (558bp) product.

Due to the fact that pET100/D is a eukaryotic expression vector, DNA from Tbpl1 was amplified using Pfu DNA polymerase for integration into pET100/D-TOPO (Figure 7.4) to produce a PCR product with blunt ends. Ligation of the PCR product into this TOPO vector inserted the sequences CACC via the forward primer of Tbpl1. The linearized vector contains a region complementary to this sequence, thus allowing directional binding of the PCR product to the vector that is also in frame with other genes on the vector. Primers were designed with the CACC located in the forward primer (Tbpl1 forward) without a stop codon following the sequences that allowed expression of a fusion protein containing the N-terminal polyhistidine tag and Xpress epitope, while the reverse primer (Tbpl1 reverse) contained the native stop codon. Once the PCR product was obtained, it was ligated into the vector and transformed into E. coli TOPO 10 cells for propagation.

7.3.3.1.2 PET100/D-TOPO vector

Following the production of mouse testicular cDNA, the gene of interest (Tbpl1) was amplified by PCR. The primers were based on the DNA sequence of Tbpl1. The aim was to amplify the gene from the start codon (ATG) through to the stop codon (TAA). Once the 558 bp amplicon was obtained and confirmed by agarose gel electrophoresis (Figure 7.4), the gene was cloned into PET100/D-TOPO vector for sequence analysis. ThePET100/D-TOPO vector (Invitrogen) is an easy and efficient way to clone PCR products. This resulted in blunt ended PCR products added by *Pfu* taq polymerase to the 3' end of PCR products. The recombinant plasmid was identified by a chance screening for the plated bacterial transformants as there is no selective manner of choosing positive recombinants. Fifteen

colonies were selected and analyzed for the presence of the Tbpl1 gene. The cloning efficiency was as high as 80%. Only one positive clone was used for further analyses. After plasmid isolation, the recombinant plasmid (Tbpl1-pET) was subjected to restriction enzyme digestion by EcoRV, HindIII and PCR analysis. As anticipated, restriction enzyme digestion gave two distinct bands around (4926bp) and (838bp) (Figure 7.7) corresponding to the linearized vector and the Tbpl1 insert, respectively. PCR amplification using 20 ng of the Tbpl1-pET as a template and T7 forward primer (vector) and Tbpl1 complementary R1 reverse primer confirmed these results as a single discrete band of approximately 558bp was obtained (Figure 7.5).

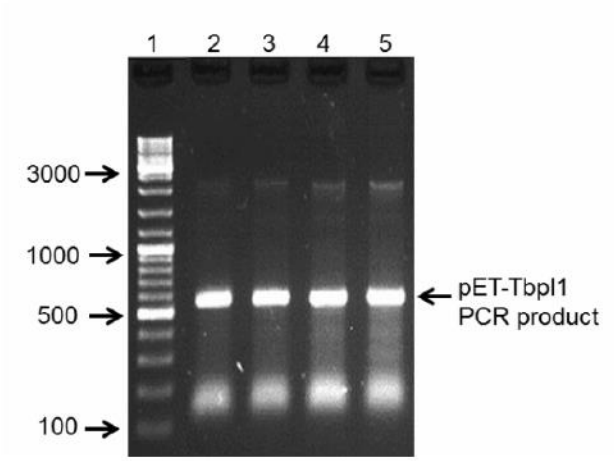

Figure 7.5: Confirmation of successful insertion of the Tbpl1 gene into pET100/D-TOPO. The samples were subjected to electrophoresis through a 1% w/v agarose gel in 1X TBE with 1µg/ml ethidium bromide staining. The PCR conditions were 98°C (1sec), 61°C (30sec), 72 °C (30sec) for 30 cycles. Lane 1 shows DNA ladder. Lane 2, 3, 4 and 5 shows PCR products generated by different primer sets and confirmed as successful the correct orientation of the insert.

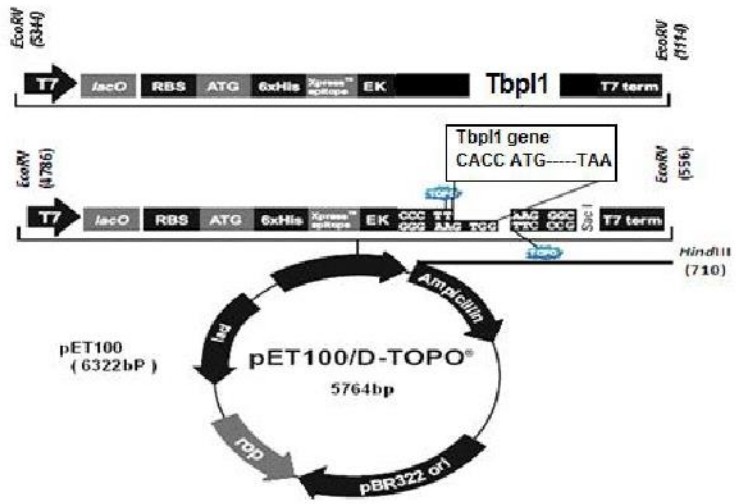

Figure 7.6: Map of pET 100/D-TOPO with Tbpl1 insert. The 5'-CACC-3' in the 5' end of the insert provides directional and in-frame cloning of the gene with the 6x His fusion tag. Ampicillin resistant positive clones were selected and the recombinant plasmid was subjected to sequence analysis.T7 promoter was IPTG induced for high expression of the gene.

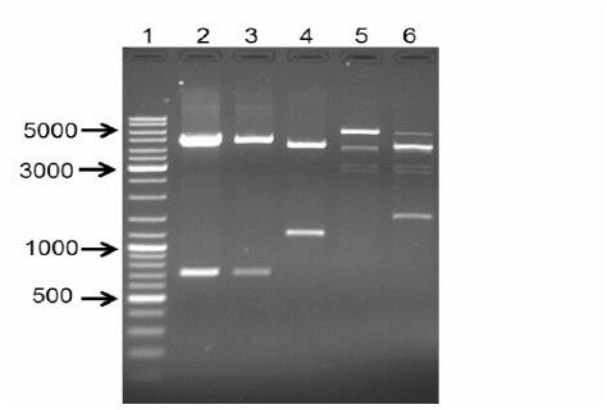

Figure 7.7: Restriction enzyme digestion of pET100 and pET100- Tbpl1 clone. The samples were subjected through a 1.5% w/v agarose gel in 1x TBE buffer with 1µg/ml ethidium bromide staining. . Lane 1 shows DNA ladder. Lane 2 shows positive control cut with HindIII. Lane 3 shows pET100-Tbpl1 cut with HindIII. Lane 4 shows pET100- Tbpl1 cut with EcoRV. Lanes 5, 6 show negative control (non-recombinant plasmid).

7.3.3.1.3 Effect of ENU and MMS treatment on the DNA plasmid of TbpI1

This experiment was performed in order to assess the effect of ENU and MMS on the untreated or treated DNA plasmid isolated from the host cells BL21 (DE3).The cells were cultured and treated with ENU and MMS (0.05 mM, 0.5 mM and 1 mM) for 1h as described earlier (sections 2.10.2). Untreated cells were chosen as a control for the experiment. After that the cells were collected and DNA plasmid of TbpI1 was extracted and analyzed by qRT-PCR to quantify DNA expression of TbpI1. There was no statistically significant difference on the level of TbpI1, after 1h of treatment with ENU and MMS (0.05 mM) compared with non-treated control cells.

When the cells were treated with ENU and MMS 0.5 mM there was a statistically significant decrease on the TbpI1level expression (P <0.05) and a further decrease in the level of TbpI1 was shown when the cells were treated with ENU and MMS 1 mM (P < 0.01). These results are shown in Figure 7.8 and 7.9 respectively. Moreover, this result showed that ENU and MMS showed down-regulation of TbpI1 expression.

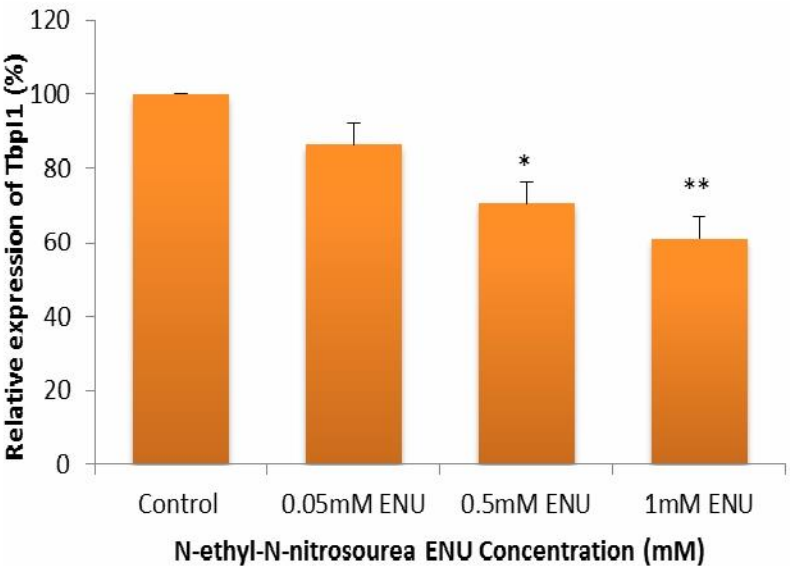

Figure 7.8: Effect of ENU on the TbpI1 expression in DNA plasmid purified from the host cells BL21 (DE3) by qPCR after 1 h treatment at 37 ºC with ENU at different concentrations: 0.05 mM, 0.5 mM and 1 mM. Non-treated cells values were defined as 100% and other values were adjusted accordingly. Data are expressed as the mean ± SEM. n=3 different biological replicates performed on three different occasions (*p<0.05, **p<0.01).

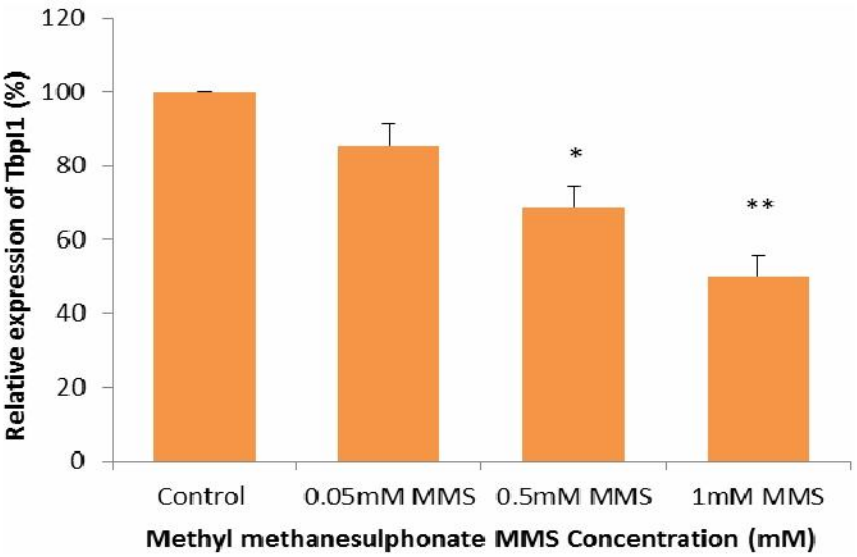

Figure 7.9: Effect of MMS on the TbpI1 expression in DNA plasmid purified from the host cells BL21 (DE3) by qPCR after 1 h treatment at 37 ºC with MMS at different concentrations: 0.05 mM, 0.5 mM and 1 mM. Non-treated cells values were defined as 100% and other values were adjusted accordingly. Data are expressed as the mean ± SEM. n=3 different biological replicates performed on three different occasions (*p<0.05, **p<0.01).

7.3.3.1.4 Western Blot analysis of Purified Recombinant Protein of Tbpl1

The Western blot of the purified TbpI1 His-tagged protein isolated under native conditions was free of degradation products and showed distinctive and thick bands at a molecular mass of approximately 24 kDa that was confirmed using an antibody directed at the histidine tag as shown in Figure 7.10. Furthermore, it showed a distinctive band at molecular masses of approximately 21 kDa that was confirmed using anti-TBPL1 antibody as shown in Figure 7.11. The purification of protein from uninduced cells

containing the pET100-TbpI1plasimd shows no expression of the TbpI1 protein showing that expression is controlled.

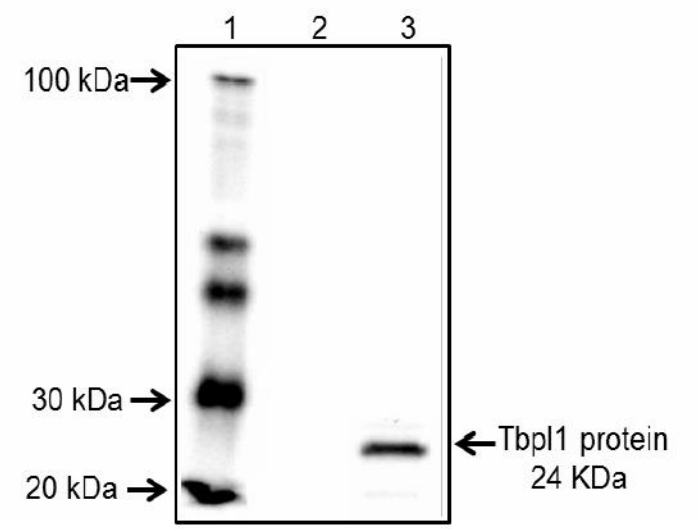

Figure 7.10: Western blotting analysis of his tagged Tbpl1 protein expressed in the pET vector system. Lane 1 shows a biotinylated protein ladder. Lane 2 shows negative control of host strain without protein expression. Lane 3 show purified recombinant protein using his select spin column under native condition from a 10 ml culture of expressed from the PET100- Tbpl1 induced with 1 mM IPTG for 4 hours at 37 ºC. Expression of the fusion protein was tested by western blot analysis using a mouse specific antibody to his-tag as a primary antibody and HRP conjugated mouse as a secondary antibody.

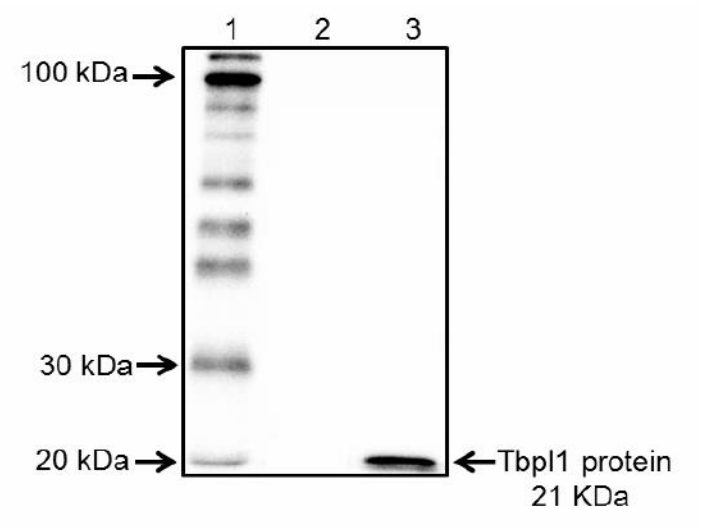

Figure 7.11: Western blotting analysis of (untagged) Tbpl1 protein expressed in the pET vector system. Lane 1 shows a biotinylated protein Ladder. Lane 2 shows negative control of host strain without protein expression. Lane 3 shows purified recombinant protein using his select spin column under native condition. From a 10 ml culture of expressed from the PET100- Tbpl1 induced with 1 mM IPTG for 4 hours at 37 C. Expression of the fusion protein was tested by Western blot analysis using a rabbit anti-TBPL1 antibody as a primary antibody and HRP conjugated rabbit as a secondary antibody.

The relative level of Tbpl1 expression in exponentially growing E.coli was determined. Presence of Tbpl1 protein was determined by quantitative western blotting. The samples were taken at 1 h following ENU and MMS treatment for both treated and untreated-control cultures, and the expression levels of Tbpl1 were compared to GAPDH. Tbpl1protein was differentially expressed in ENU and MMS-treated cells compared with the controls and were therefore considered to have been down-regulated by both compounds ENU and MMS treatment.

There was no statistically significant different in the levels of Tbpl1 protein at 0.5 mM concentration of both ENU and MMS. Moreover, further decrease was shown when the cells were treated with ENU and MMS 0.5 mM and 1 mM (*p<0.05, ***p<0.001 respectively). These results are shown in Figures 7.12 A and B and 7.13 A and B.

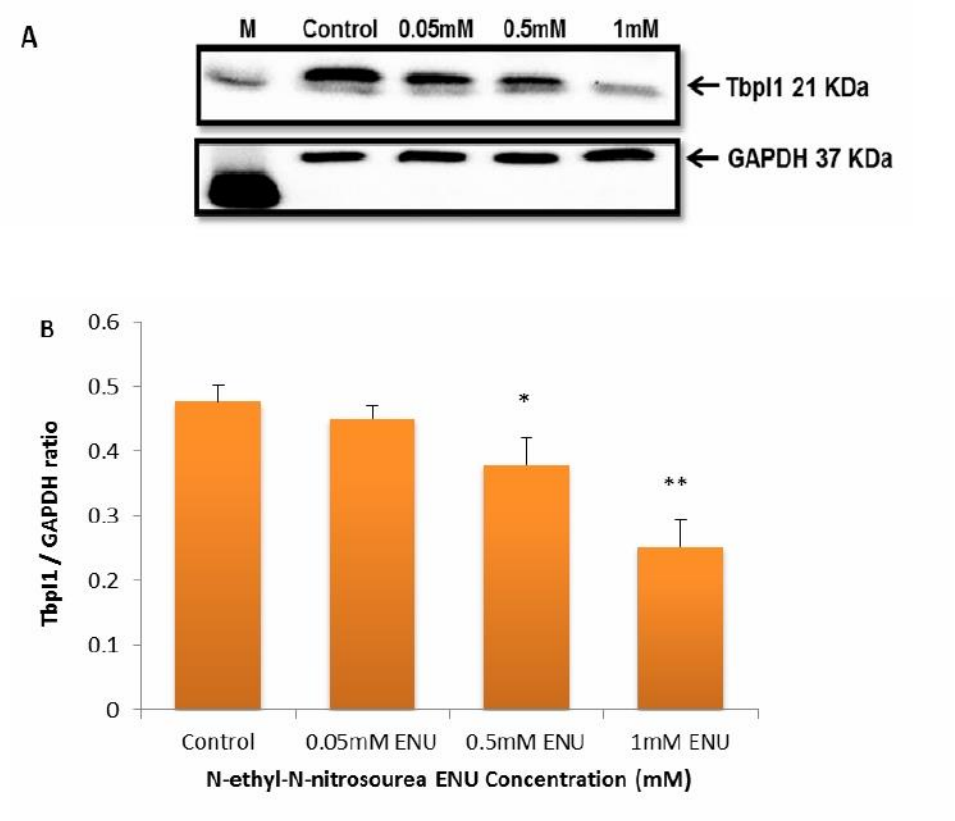

Figure 7.12: Western blot analysis of purified recombinant TbpI1 protein expression after treatment with ENU at different concentrations and 1 h treatment. Sample Western blots of TbpI1 and GAPDH proteins are shown in (A) and quantified summary data are shown in (B). The density of each band was quantified by the use of Image 1.45 software. The relative expression level of TbpI1 was measured by TbpI1 / GAPDH ratio. Data are expressed as the mean ± SEM. n=3 biological replicates performed on three different occasions (*P <0.05, **P <0.01).

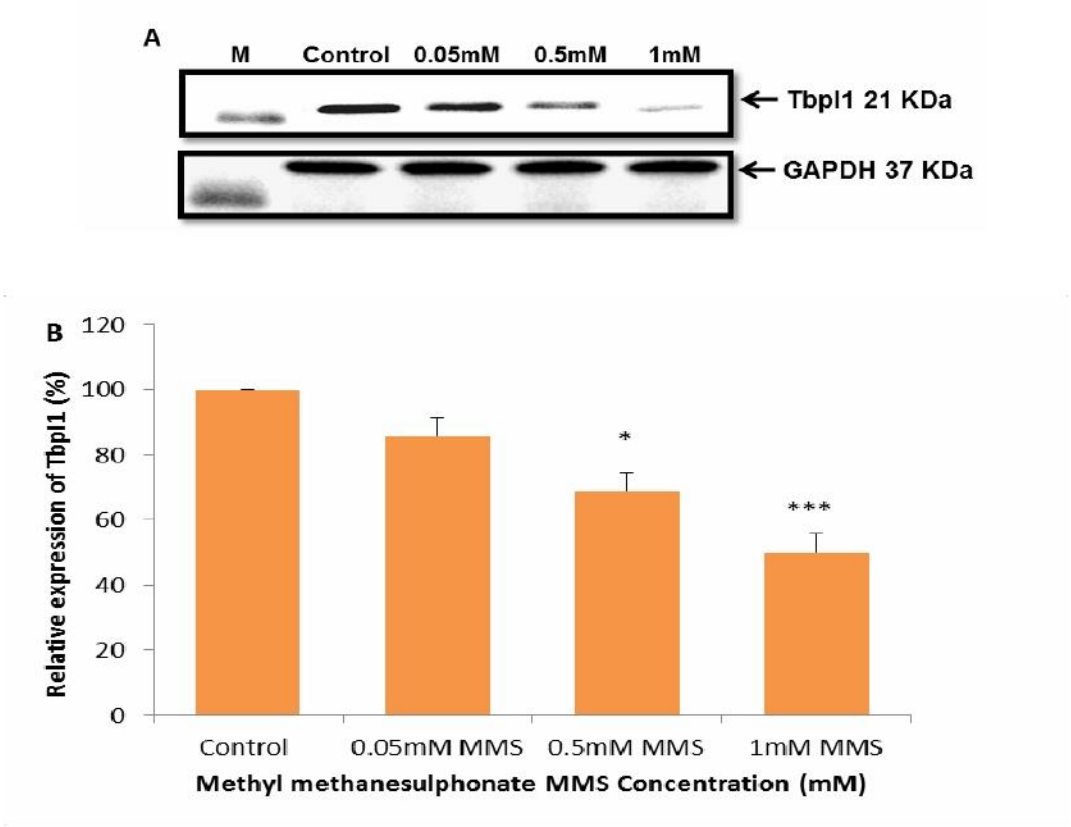

Figure 7.13: Western blot analysis of purified recombinant TbpI1 protein with TbpI1 antibody treated with MMS at different concentrations and 1 h of treatment. Sample Western blots of TbpI1 and GAPDH proteins are shown in (A) and quantified summary data are shown in (B). The density of each band was quantified by the use of Image 1.45 software. The relative expression level of TbpI1 was measured by TbpI1 / GAPDH ratio. Data are expressed as the mean ± SEM. n=3 different biological replicates performed on three different occasions (*p<0.05, ****p*<0.001).

7.3.4 Four and a half LIM domains 5 (FHL5)

The full genomic sequence of the FHL5 protein is located on chromosome 4 at location 25,199,908-25,242,876 the genomic sequence spanning over 42.97 kb. FHL5 has 6 exons with a transcription length 1,106 bps, which encodes a peptide 186 amino acids in size. The protein of FHL5 is 32,906.78 g/mol (32 kda).

```
   1 GGGGACCCAGGCAGAAGTCCAAGCACACTGAGAGTACAGAAAGCAGGTAACAATCCTGAG
  61 TTATTTTCTTCAAAGCCAACACTACTCAGAGTTCTCAAATTTCCCAAGAAAGAACTGAAG
 121 AGTGGCAACAAAGAACACTTCATCCGCTGCTCTACAAAGAACTCCAAAGGATAAAACTGA
 181 AATGACAAGTAGTCAATTTGATTGTCAATACTGCACTTCATCCCTGATTGGGAAGAAATA
     .ATGACAAGTAGTCAATTTGATTGTCAATACTGCACTTCATCCCTGATTGGGAAGAAATA
     .-M--T--S--S--Q--F--D--C--Q--Y--C--T--S--S--L--I--G--K--K--Y
 241 TGTACTCAAGGATGATAATCTATACTGCATCTCCTGCTACGATCGTATCTTTTCTAACTA
  60 TGTACTCAAGGATGATAATCTATACTGCATCTCCTGCTACGATCGTATCTTTTCTAACTA
  20 --V--L--K--D--D--N--L--Y--C--I--S--C--Y--D--R--I--F--S--N--Y
 301 TTGTGAGCAGTGTAAAGAACCAATTGAATCAGATTCTAAGGATCTTTGCTACAAAAACCG
 120 TTGTGAGCAGTGTAAAGAACCAATTGAATCAGATTCTAAGGATCTTTGCTACAAAAACCG
  40 --C--E--Q--C--K--E--P--I--E--S--D--S--K--D--L--C--Y--K--N--R
 361 TCACTGGCATGAAGGATGCTTCAGGTGCAACAAATGCCATCACTCTTTGGTGGAAAAGCC
 180 TCACTGGCATGAAGGATGCTTCAGGTGCAACAAATGCCATCACTCTTTGGTGGAAAAGCC
  60 --H--W--H--E--G--C--F--R--C--N--K--C--H--H--S--L--V--E--K--P
 421 TTTCGTTGCCAAGGATGATCGCCTGCTGTGCACAGACTGCTATTCCAACGAGTGTTCCTC
 240 TTTCGTTGCCAAGGATGATCGCCTGCTGTGCACAGACTGCTATTCCAACGAGTGTTCCTC
  80 --F--V--A--K--D--D--R--L--L--C--T--D--C--Y--S--N--E--C--S--S
 481 CAAGTGCTTCCACTGCAAGAGAACCATCATGCCAGGTTCTCGGAAAATGGAATTTAAGGG
 300 CAAGTGCTTCCACTGCAAGAGAACCATCATGCCAGGTTCTCGGAAAATGGAATTTAAGGG
 100 --K--C--F--H--C--K--R--T--I--M--P--G--S--R--K--M--E--F--K--G
 541 CAATTACTGGCATGAAACCTGCTTTGTGTGTGAGCACTGCCGACAGCCAATAGGAACCAA
 360 CAATTACTGGCATGAAACCTGCTTTGTGTGTGAGCACTGCCGACAGCCAATAGGAACCAA
 120 --N--Y--W--H--E--T--C--F--V--C--E--H--C--R--Q--P--I--G--T--K
 601 GCCTTTGATCTCCAAAGAGAGTGGCAATTATTGTGTGCCATGTTTTGAGAAGGAGTTTGC
 420 GCCTTTGATCTCCAAAGAGAGTGGCAATTATTGTGTGCCATGTTTTGAGAAGGAGTTTGC
 140 --P--L--I--S--K--E--S--G--N--Y--C--V--P--C--F--E--K--E--F--A
 661 TCATTACTGCAACTTCTGTAAGAAGGTGATAACTTCCGGTGGGATAACCTTCCGTGATCA
 480 TCATTACTGCAACTTCTGTAAGAAGGTGATAACTTCCGGTGGGATAACCTTCCGTGATCA
 160 --H--Y--C--N--F--C--K--K--V--I--T--S--G--G--I--T--F--R--D--Q
 721 GATATGGCATAAAGAGTGTTTTCTGTGCAGCGGCTGCAGGAAAGAGCTTTATGAGGAGGC
 540 GATATGGCATAAAGAGTGTTTTCTGTGCAGCGGCTGCAGGAAAGAGCTTTATGAGGAGGC
 180 --I--W--H--K--E--C--F--L--C--S--G--C--R--K--E--L--Y--E--E--A
 781 ATTTATGTCAAAGGATGATTTCCCATTCTGCCTGGATTGCTACAACCATCTTTATGCTAA
 600 ATTTATGTCAAAGGATGATTTCCCATTCTGCCTGGATTGCTACAACCATCTTTATGCTAA
 200 --F--M--S--K--D--D--F--P--F--C--L--D--C--Y--N--H--L--Y--A--K
 841 AAAGTGTGCAGCCTGCACCAAACCCATCACTGGCCTCAGAGGTGCCAAGTTCATCTGCTT
 660 AAAGTGTGCAGCCTGCACCAAACCCATCACTGGCCTCAGAGGTGCCAAGTTCATCTGCTT
 220 --K--C--A--A--C--T--K--P--I--T--G--L--R--G--A--K--F--I--C--F
 901 TCAAGACCGCCAGTGGCACAGTGAGTGCTTCAACTGCGGAAAGTGCTCGGTCTCCTTGGT
 720 TCAAGACCGCCAGTGGCACAGTGAGTGCTTCAACTGCGGAAAGTGCTCGGTCTCCTTGGT
 240 --Q--D--R--Q--W--H--S--E--C--F--N--C--G--K--C--S--V--S--L--V
 961 GGGTGAAGGATTCTTGACCCATAACATGGAAATCTTATGCCGCAAGTGTGGCTCCGGGGC
 780 GGGTGAAGGATTCTTGACCCATAACATGGAAATCTTATGCCGCAAGTGTGGCTCCGGGGC
 260 --G--E--G--F--L--T--H--N--M--E--I--L--C--R--K--C--G--S--G--A
1021 AGACACTGACGCTTAG
```

```
840 AGACACTGACGCTTAG
280 --D--T--D--A--*-
```

Figure 7.14: DNA (top line) and transcript (middle line) sequences of FHL5 gene and its corresponding peptide sequences (bottom line). The untranslated region of the transcript is highlighted yellow, exons are alternately coloured black and blue (and codons are alternately coloured pale yellow/black or blue). Taken from www.ensembl.org.

7.3.4.1 Amplification of FHL5 by PCR and Cloning into the pET100/D-TOPO®

Following isolation of mouse testis RNA and production of cDNA from it, FHL5 was amplified as described in the methods section (2.8.9). The final PCR products were analyzed by electrophoresis through a 1% w/v agarose gel, and DNA was stained with ethidium bromide for observation under UV light (Figure 7.15).

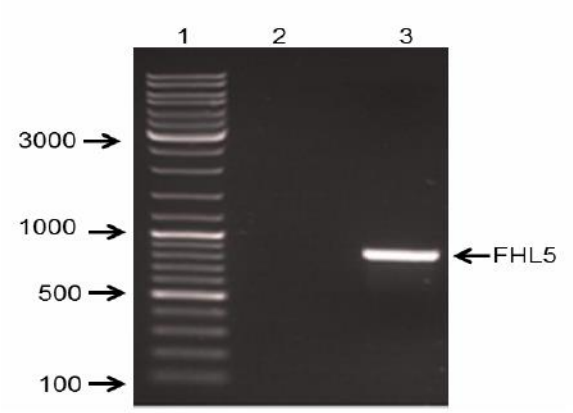

Figure 7.15: PCR amplification of FHL5 product (854bp). The samples were subjected to electrophoresis through a 1.5% w/v agarose gel in 1 X TBE with 1 µg/ml ethidium bromide staining. The PCR conditions were 94°C (30sec), 57°C (30sec), 72°C (30sec) for 30 cycles. The primers were forward 5-CACCATGACAAGTAGTCAATTTGATTGT-3 and reverse 5-CTAAGCGTCAGTGTCTGC-3. Lane 1 shows a DNA ladder. Lane 2 is a negative control containing no cDNA template. Lane 3 shows positive amplification of FHL5 (854bp) product.

To confirm the FHL5 PCR product was correct the product was restriction enzyme digested with PstI (data not shown). Full length of FHL5 PCR product was cut with PstI at correct position (277 to 577 bp) respectively of the act PCR product (854bp), which confirmed the likely complete correct sequence of FHL5 PCR product.

7.3.4.2 Confirmation of the Successful Cloning into pET100/D-TOPO®

Plasmid DNA from 15 *E. coli* clones was obtained and screened for the presence of the FHL5 gene using PCR (Figure 7.16). The plasmid DNA containing the FHL5 gene was PCR amplified using the primers sets T7 forward / Native FHL5 reverse and pET- FHL5 forward / T7 reverse yielding fragments of 854 bp and 679 bp respectively, confirming that FHL5 was inserted into the vector (Figure 7.16).

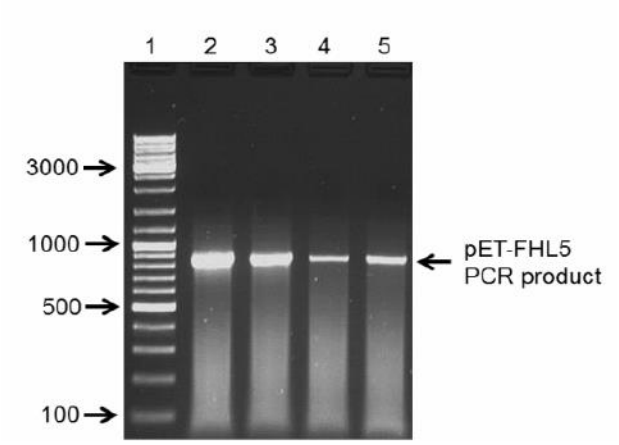

Figure 7.16: Confirmation of the Successful Cloning into pET100/D-TOPO®. The samples were subjected to electrophoresis through a 1% w/v agarose gel in 1X TBE with 1ug/ml ethidium bromide staining. Lane 1 shows DNA ladder. Lane 2, 3, 4 and 5 shows PCR products generated by primers sets, which successfully confirmed the correct orientation of the insert (854bp).

7.3.4.3 Effect of ENU and MMS treatment on FHL5

Quantitative real-time PCR assay was conducted on untreated or treated DNA plasmid isolated from the host cells BL21 (DE3) treated with 0.05 mM, 0.5 mM, 1 mM, ENU or MMS as described in sections 2.10.2. ENU and MMS showed down-regulation of FHL5 expression.

Statistical analysis showed that there was no significant effect on expression level of FHL5 gene after treatment with ENU and MMS (0.05 mM) compared with untreated control cells. There was however a significant decrease in the level of expression of FHL5 when cells treated with 0.5 mM ENU or MMS (both $*P < 0.05$). These results are shown in Figures 7.17 and 7.18. However, further decrease was shown when the cells were treated with ENU and MMS 1mM ($**p<0.01$) these results are shown in Figures 7.17 and 7.18.

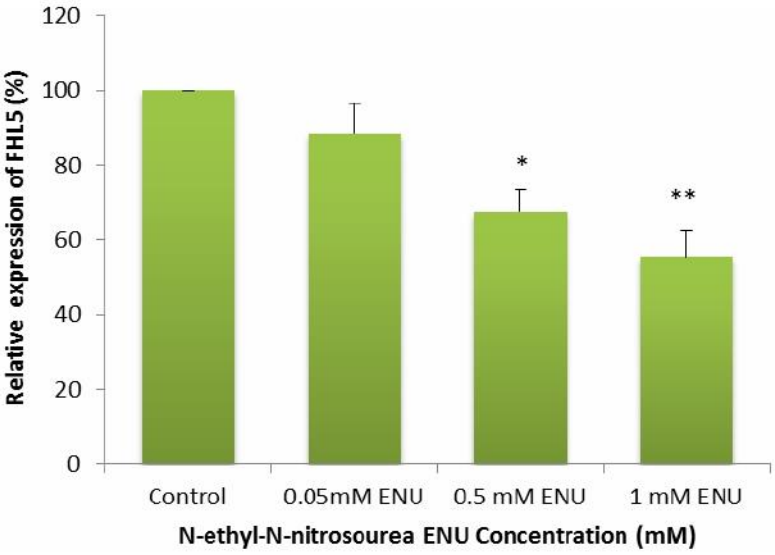

Figure 7.17: Effect of ENU on FHL5 expression in DNA plasmid purified from the host cells BL21 (DE3) and analysed by qPCR after 1 h treatment at 37 ºC with ENU at different concentrations: 0.05 mM, 0.5 mM and 1 mM. Non-treated cells values were defined as 100% and other values were adjusted accordingly. Data are expressed as the mean ± SEM. n=3 different biological replicates performed on three different occasions (*p<0.05, **p<0.01).

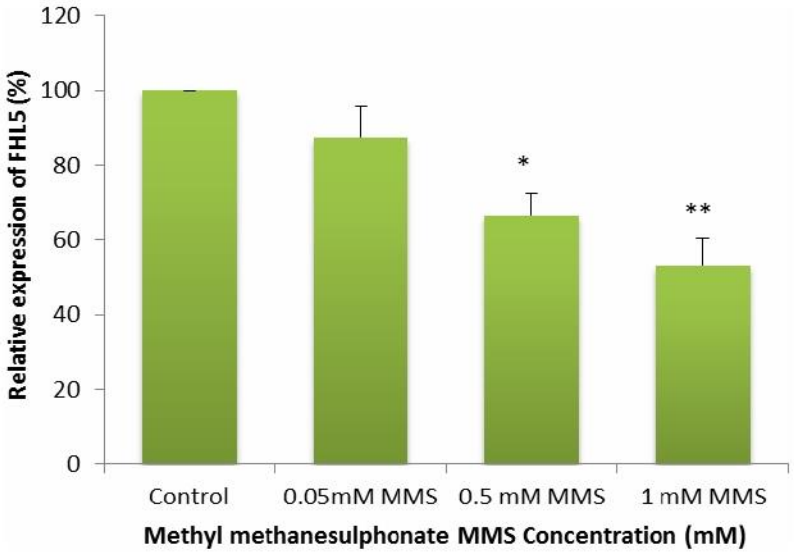

Figure 7.18: Effect of MMS on FHL5 expression in DNA plasmid purified from the host cells BL21 (DE3) analysed by qPCR after 1 h treatment at 37 ºC with MMS at different concentrations: 0.05 mM, 0.5 mM and 1 mM. Non-treated cell values were defined as 100% and other values were adjusted accordingly. Data are expressed as the mean ± SEM. n=3 different biological replicates performed on three different occasions (*p<0.05, **p<0.01).

7.3.4.4 Western blot analysis of purified recombinant protein of FHL5

Expression of FHL5-pET100D was performed as for the TbpI1-pET100 construct. IPTG was used to turn on the lacUV5 promoter in FHL5-PET 100/D transformed E. coli which resulted in overexpression of the protein encoded by the FHL5 PCR product that had been inserted into the pET vectors cloning site. Since overexpression can be a problem with toxic proteins, the BL21 Star™ (DE3) pLysS strain were used to express FHL5 since they also produce a T7 lysozyme that slowed expression by binding to T7 RNA polymerase and inactivating it. The BL21 cells transformed with

FHL5-pET100D were induced with IPTG for 4 hours. After each hour, samples were taken and stored for further analysis. The Western blot of native FHL5 protein under identical conditions showed that a high concentration of the protein was obtained. There was a major 35 kDa recombinant protein band corresponding to the 32 kDa Gtf2a1l fused with a 3 kDa His-Tag as shown in 7.19. The FHL5 protein preparation was equally free of degradation product as shown Figure 7.20. The purified protein from cells containing the pET100 FHL5 plasmid that had not been induced showed no expression of the FHL5 protein showing that its expression was controllable.

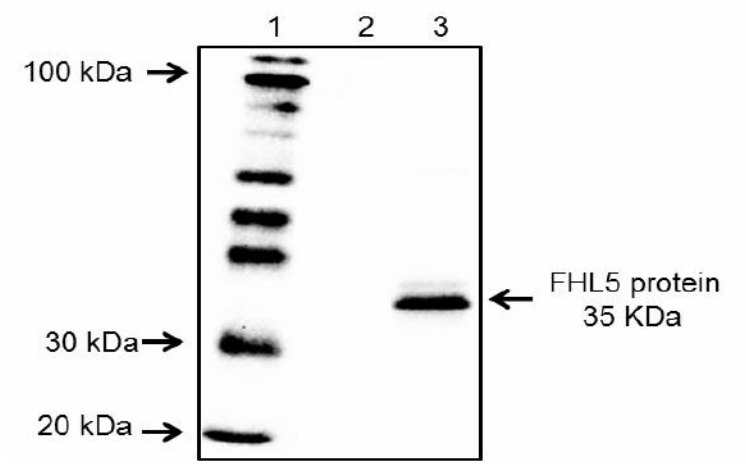

Figure 7.19: Western blotting analysis of his tagged FHL5 protein expressed in the pET vector systems. Lane 1 shows the biotinylated protein ladder. Lane 2 shows negative control of host strain without protein expression. Lane 3 Purified recombinant protein using his select spin column under native condition from a 10 ml culture of expressed from the PET100- FHL5 induced with 1 mM IPTG for 4 hours at 37 ºC. Expression of the fusion protein was tested by western blot analysis using a mouse specific antibody to his-tag as a primary antibody and HRP conjugated mouse as a secondary antibody.

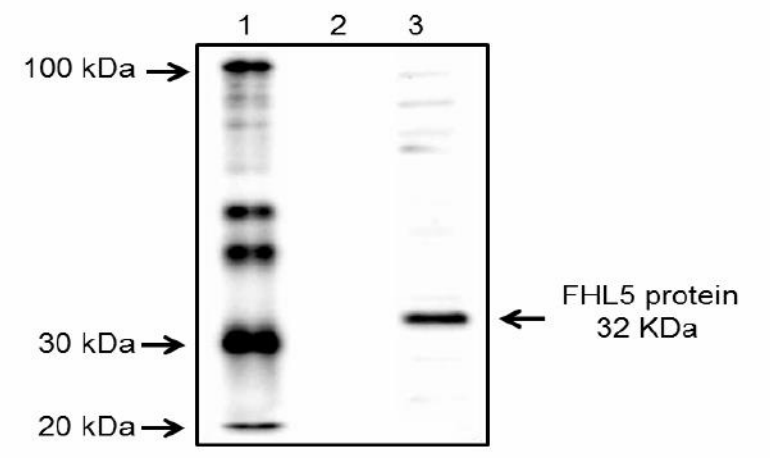

Figure 7.20: Western blotting analysis of FHL5 protein expressed in the pET vector systems. Lane 1 shows biotinylated protein Ladder. Lane 2 shows negative control of host strain without protein expression. Lane 3 shows purified recombinant protein using his select spin column under native condition. from a 10 ml culture of expressed from the PET100- FHL5 induced with 1mM IPTG for 4 hours at 37 C. Expression of the fusion protein was tested by western blot analysis using a rabbit anti- FHL5 antibody as a primary antibody and HRP conjugated rabbit as a secondary antibody.

To determine the effect of ENU and MMS treatment on FHL5 gene expression, FHL5 was produced as recombinant protein in E. coli after exposure. A Western blot analysis was performed for the samples taken at 1 h following ENU and MMS treatment for both ENU and MMS treated and untreated control cultures, and the expression levels were compared. A FHL5 protein which was differentially expressed in ENU or MMS-treated cells compared with the controls (ENU and MMS-untreated cells) was considered to be meaningfully down-regulated by ENU or MMS treatment. Statistical analysis has shown that there was not any effect of the expression level of FHL5 protein, when cells treated with at low concentration of ENU and MMS (0.05 mM). The concentrations of ENU and MMS 0.5 mM and 1 mM

significantly decreased FHL5 protein levels compared with GAPDH (*P* <0.05, and *P* <0.01, respectively).

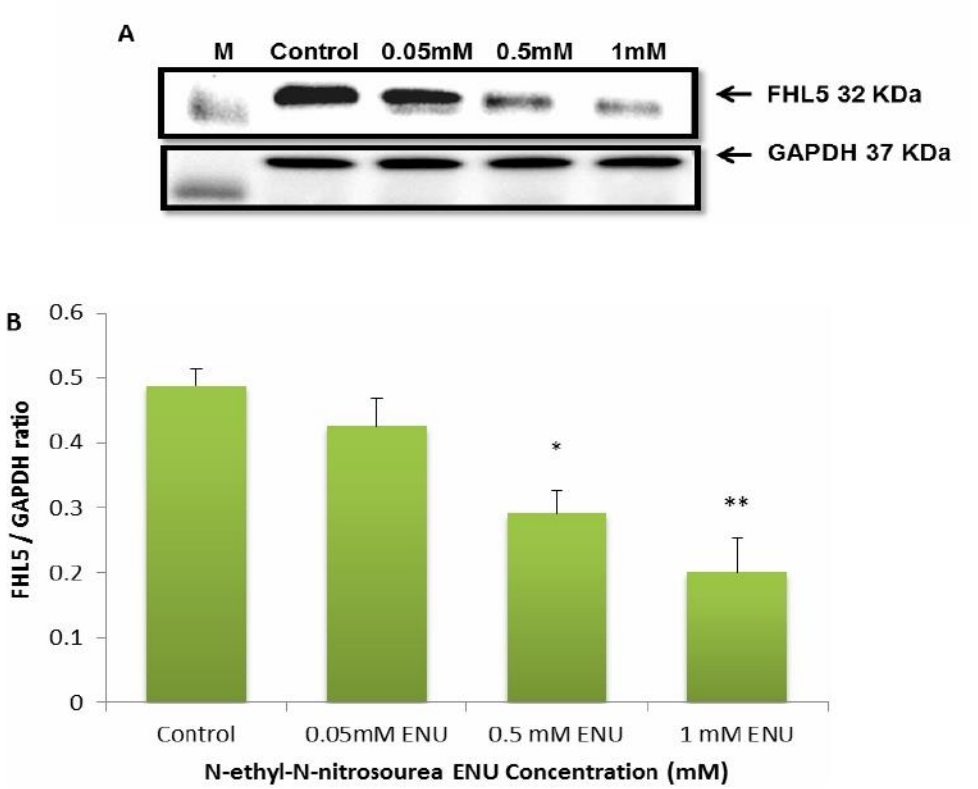

Figure 7.21: Western blot analysis of purified recombinant FHL5 protein with FHL5 antibody treated with ENU at different concentration at 1 h after treatment. Sample Western blots of FHL5 and GAPDH proteins are shown in (A) and quantified summary data are shown in (B). The density of each band was quantified by the use of Image 1.45 software. The relative expression level of FHL5 was measured by FHL5 / GAPDH ratio. Data are expressed as the mean ± SEM. n=3 different biological replicates performed on three different occasions (**p*<0.05, ***p*<0.01).

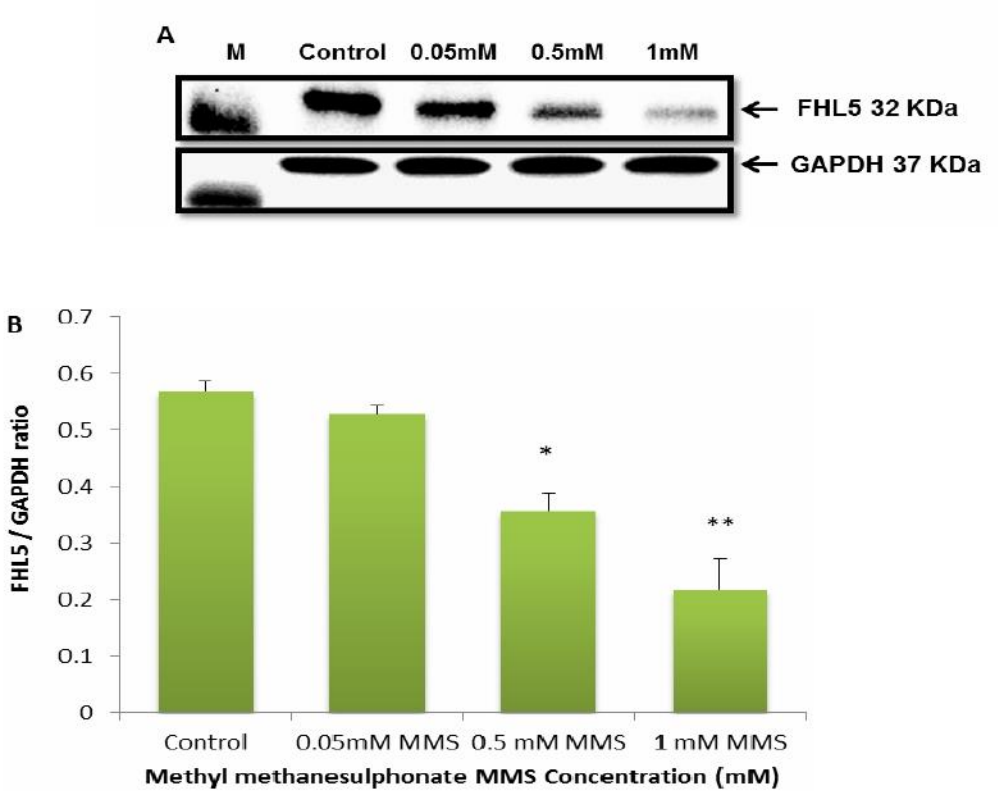

Figure 7.22: Western blot analysis of purified recombinant FHL5 protein with FHL5 antibody treated with MMS at different concentrations, 1 h after treatment. Sample Western blots of FHL5 and GAPDH proteins are shown in (A) and quantified summary data are shown in (B). The density of each band was quantified by the use of Image 1.45 software. The relative expression level of FHL5 was measured by FHL5 / GAPDH ratio. Data are expressed as the mean ± SEM. n=3 different biological replicates performed on three different occasions (*p<0.05, **p<0.01).

7.3.5 General transcription factor IIA, 1-like (Gtf2a1l)

The full genomic sequence of the Gtf2a1l is located on chromosome 17 at location 88.668.660-88.715.152 the genomic sequence spanning over 46.49 kb. Gtf2a1l has 9 exons with a transcription length 1,621 bps, which encodes a peptide 468 amino acids in size. The protein of Gtf2a1l is 51,524.58 g/mol (52Kda).

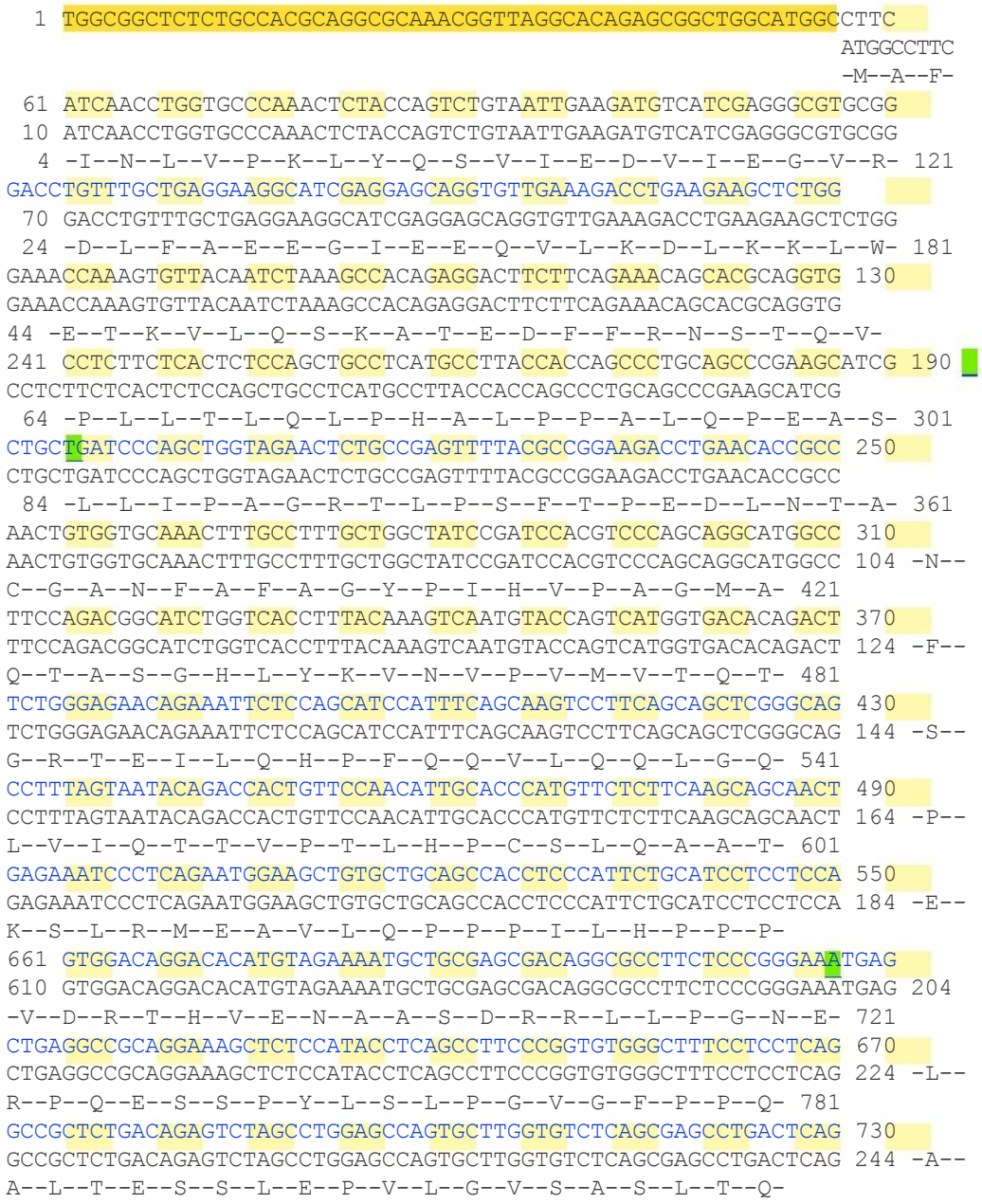

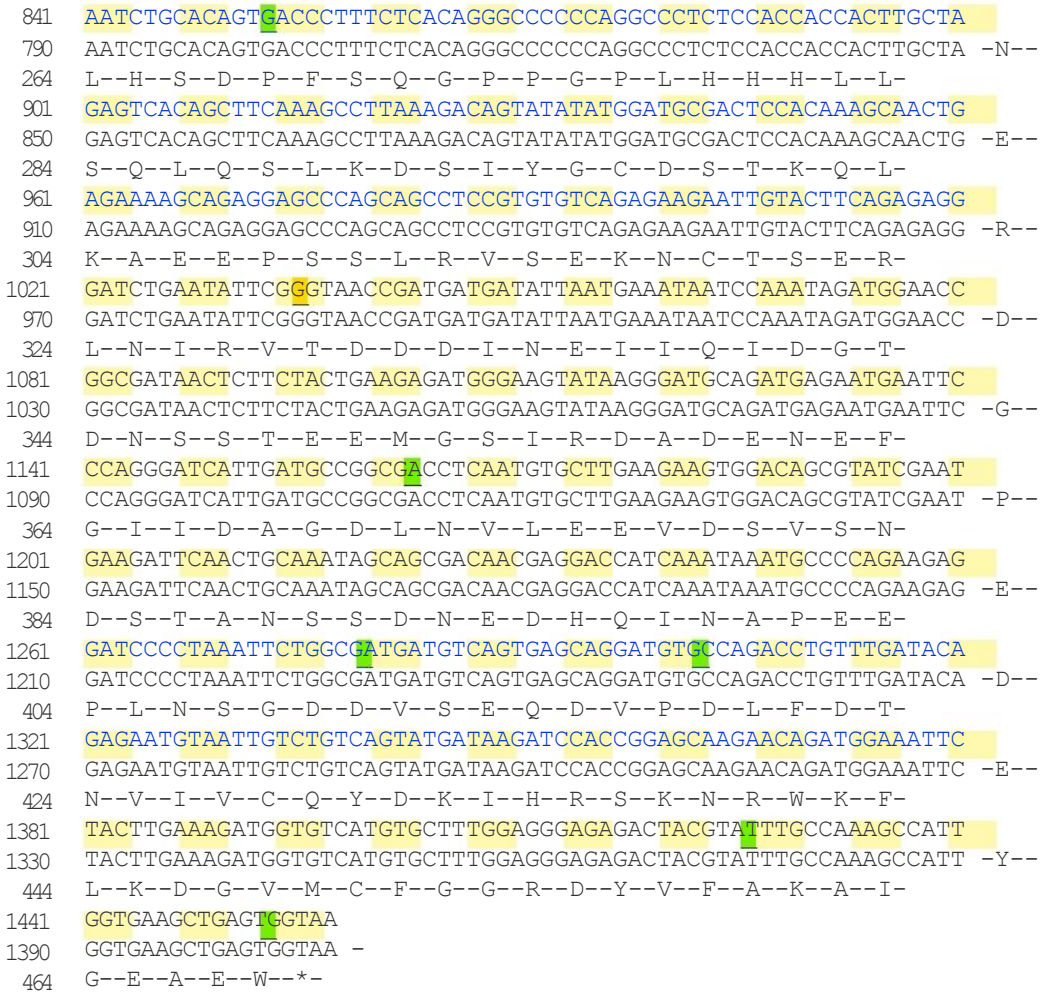

Figure 7.23: DNA (top line) and transcript (middle line) sequences of Gtf2a1l gene and its corresponding peptide sequences (bottom line). The untranslated region of the transcript is highlighted yellow, exons are alternately coloured black and blue (and codons are alternately coloured pale yellow/black or blue). Taken from www.ensembl.org.

7.3.5.1 Amplification of Gtf2a1l by PCR and Cloning into the pET100/D-TOPO®

PCR was performed on the genomic DNA for identification and cloning of the Gtf2a1l gene in open reading frame The PCR products for the pET100/D-TOPO® were amplified using the Pfu DNA polymerase (Promega), which resulted in blunt ended PCR products (Figure7.24).

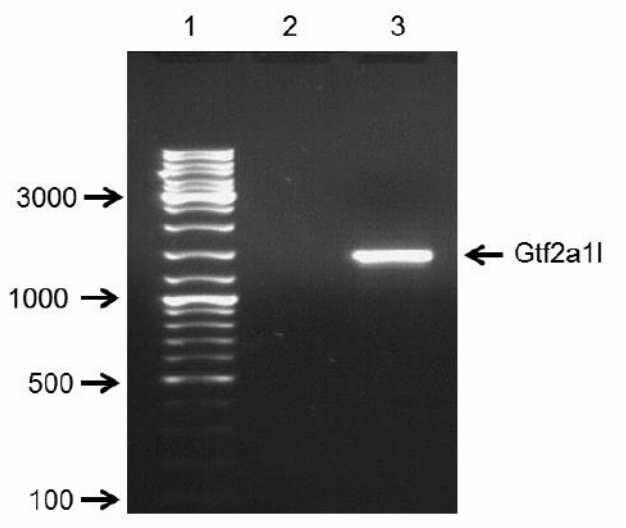

Figure 7.24: PCR amplification of Gtf2a1l product (1404 bp) the sample was subjected to electrophoresis through a 1.5 % w/v agarose gel in 1 X TBE with 1ug/ml ethidium bromide staining. The PCR reactions were 94°C (30sec), 62°C (30sec), 72°C (30sec) for 30 cycles. The primers were forward 5´CACCATGGCCTTCATCAACCTG'3 and reverse 5´ CCACTCAGCT-TCACCAATG'3. Lane 1 shows the DNA ladder. Lane 3 is a negative control containing no cDNA template. Lane 3 shows positive amplification of Gtf2a1l (1404 bp) product.

7.3.5.2 Confirmation of the Successful Cloning into pET100/D-TOPO®

Plasmid DNA from five *E. coli* clones were obtained and screened for the presence of the Gtf2a1l gene using PCR (Figure 7.25). The plasmid DNA containing the Gtf2a1l gene was PCR amplified using the primers sets T7 forward / native Gtf2a1l yielding fragments of 1404 bp, confirming that Gtf2a1l had been inserted into the vector. Correct orientation was confirmed by amplification with different primers (Figure 7.25).

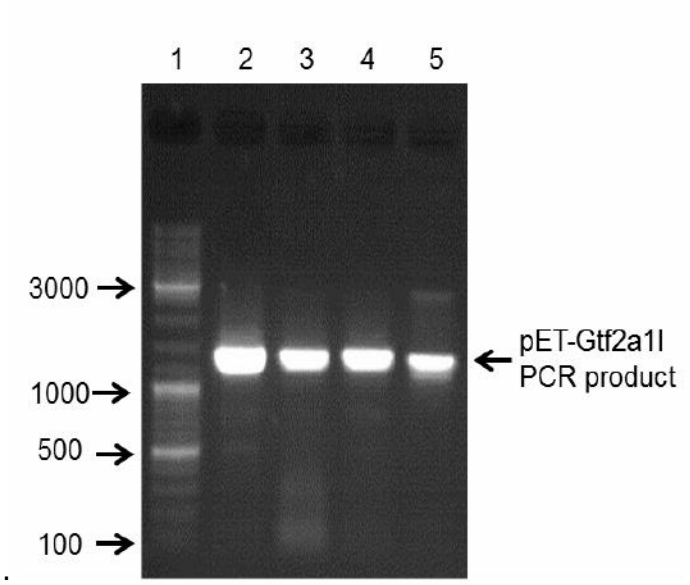

Figure 7.25: Confirmation of successful insertion of the Gtf2a1l gene into PET100/D-TOPO. The samples were subjected to electrophoresis through a 1% w/v agarose gel in 1X TBE with 1ug/ml ethidium bromide staining. Lane 1 shows DNA ladder. Lane 2, 3, 4 and 5 shows PCR products generated confirmed successfully the correct orientation of the insert (1404bp).

7.3.5.3 Effect of ENU and MMS treatment on Gtf2a1l

Real Time PCR was chosen as the technique to provide confirmation of the changes in Gtf2a1l gene expression that was seen after cells treated with different concentrations of both ENU and MMS compounds.

There was no statistically significant difference in the levels of Gtf2a1l after 1h of treatment with ENU or MMS (0.05 mM) compared with non-treated control cells. Statistical analysis showed a significant decrease in the level of expression of Gtf2a1l when cells treated with 0.5 mM ENU or MMS respectively (*p<0.05) and a further decrease was shown when the cells were treated with 1mM ENU or MMS (***p<0.001) these results are shown in Figures 7.26 (ENU) and 7.27 (MMS).

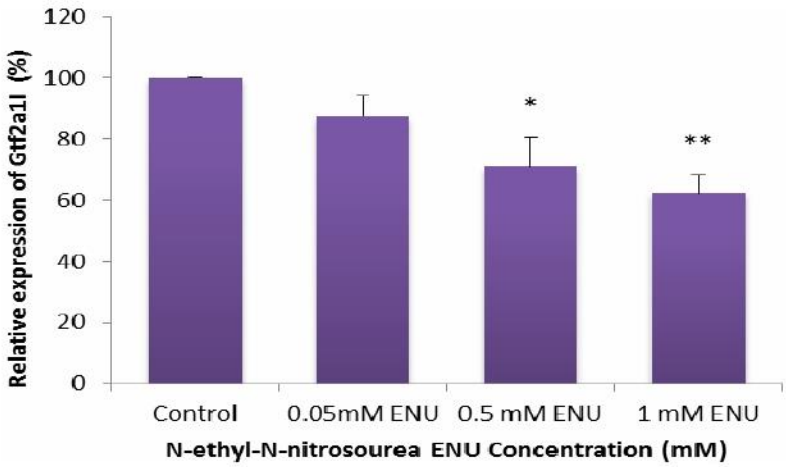

Figure 7.26: Effect of ENU on the Gtf2a1l expression in DNA plasmids purified from the host cells BL21 (DE3) by qPCR after 1 h treatment at 37 ºC with ENU at different concentrations: 0.05 mM, 0.5 mM and 1 mM. Non-treated cells values were defined as 100% and other values were adjusted accordingly. Data are expressed as the mean ± SEM. n=3 different biological replicates performed on three different occasions (*p<0.05, **p<0.01).

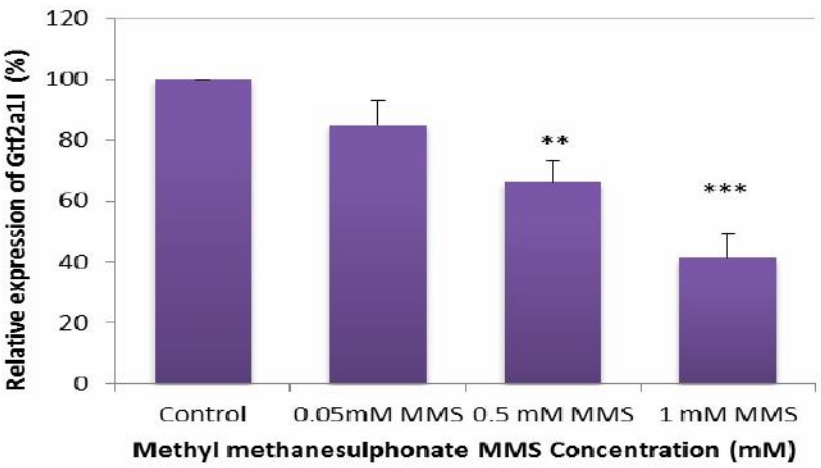

Figure 7.27: Effect of MMS on the Gtf2a1l expression in DNA plasmids purified from the host cells BL21 (DE3) by qPCR after 1 h treatment at 37 ºC with MMS at different concentrations: 0.05 mM, 0.5 mM and 1 mM. Non-treated cells values were defined as 100% and other values were adjusted accordingly. Data are expressed as the mean ± SEM. n=3 different biological replicates performed on three different occasions (**p<0.01, ***p<0.001).

7.3.5.4 Western Blot analysis of Purified Recombinant Protein of Gtf2a1l

The Western blot of the Gtf2a1l His-tagged protein isolated under native condition was free of degradation products and showed that a high concentration of the protein was obtained at a molecular mass of approximately 55 kDa that was confirmed using an antibody directed at the histidine Tag as shown in 7.28, there was a major 55 kDa recombinant protein band corresponding to the 52 kDa Gtf2a1l fused with a 3kDa His-Tag. Furthermore, it showed that distinctive band at molecular masses of approximately 52 kDa that confirmed using anti-Gtf2a1l antibody as shown in

figure 7.29.The purification of protein from uninduced cells containing the pET100- Gtf2a1l plasmid shows no expression of the TbpI1 protein, showing that expression is controllable.

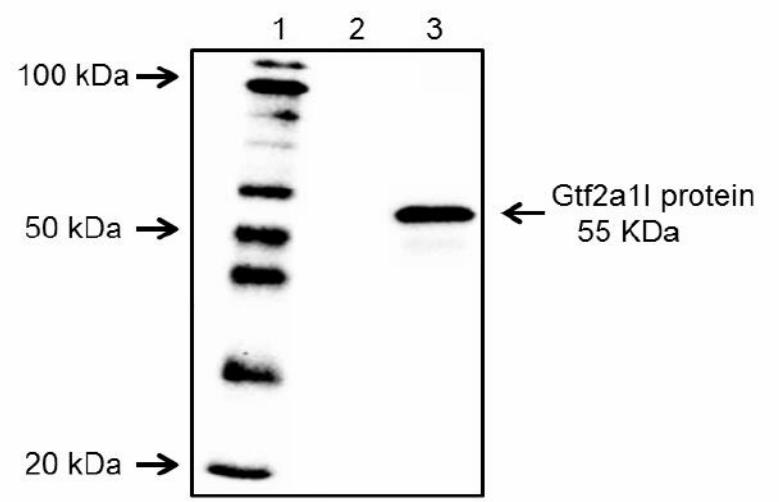

Figure 7.28: Western blotting analysis of his tagged Gtf2a1l protein expressed in the pET vector systems. Lane 1 shows biotinylated protein Ladder. Lane 2 shows negative control of host strain without protein expression. Lane 3 Purified recombinant protein using his select spin column under native conditions from a 10 ml culture of expressed from the Gtf2a1l-PET100 induced with 1mM IPTG for 4 hours at 37 ºC. Expression of the fusion protein was tested by western blot analysis using a mouse specific antibody to his-tag as a primary antibody and HRP conjugated mouse as a secondary antibody.

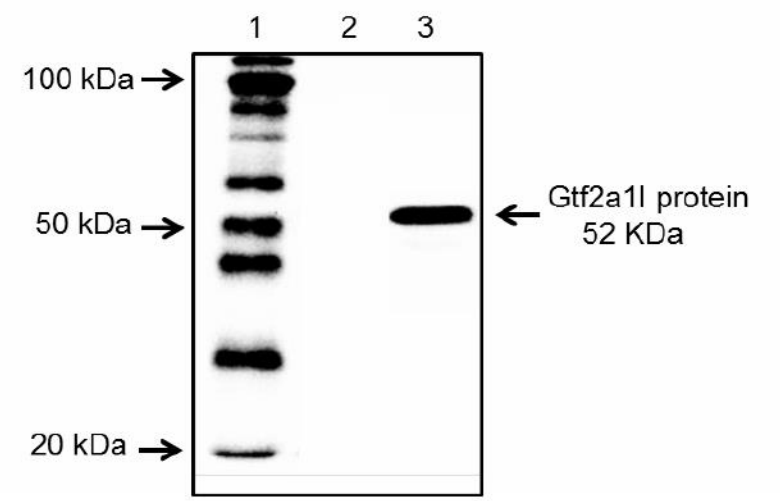

Figure 7.29: Western blotting analysis of Gtf2a1l protein expressed in the pET vector systems. Lane 1 shows biotinylated protein Ladder. Lane 2 shows negative control of host strain without protein expression. Lane 3 shows purified recombinant protein using his select spin column under native conditions from a 10 ml culture of Gtf2a1l-PET100 induced with 1 mM IPTG for 4 hours at 37 ºC. Expression of the fusion protein was tested by Western blot analysis using a mouse anti-Gtf2a1l antibody as a primary antibody and HRP-conjugated anti-mouse IgG as a secondary antibody.

To determine the effect of each ENU and MMS mutation on Gtf2a1l gene expression, Gtf2a1l was produced as recombinant proteins in E. coli. A Western blot analysis was performed for the samples taken at 1 h following ENU and MMS treatment for both ENU and MMS-treated and untreated control cultures, and the expression levels were compared. A Gtf2a1l protein that was differentially expressed in ENU and MMS-treated cells compared with the controls were considered to be meaningfully down-regulated by ENU and MMS treatment. Statistical analysis has shown that there was no significant effect on the expression level of Gtf2a1l protein when cells were

treated with a low concentration of ENU or MMS (0.05 mM). The concentrations of ENU or MMS 0.5 mM and 1 mM significantly decreased the Gtf2a1l protein levels compared with GAPDH (*p<0.05, **p<0.01and ***p<0.01, respectively) results shown in Figure 7.30 A and B and 7.31 A and B.

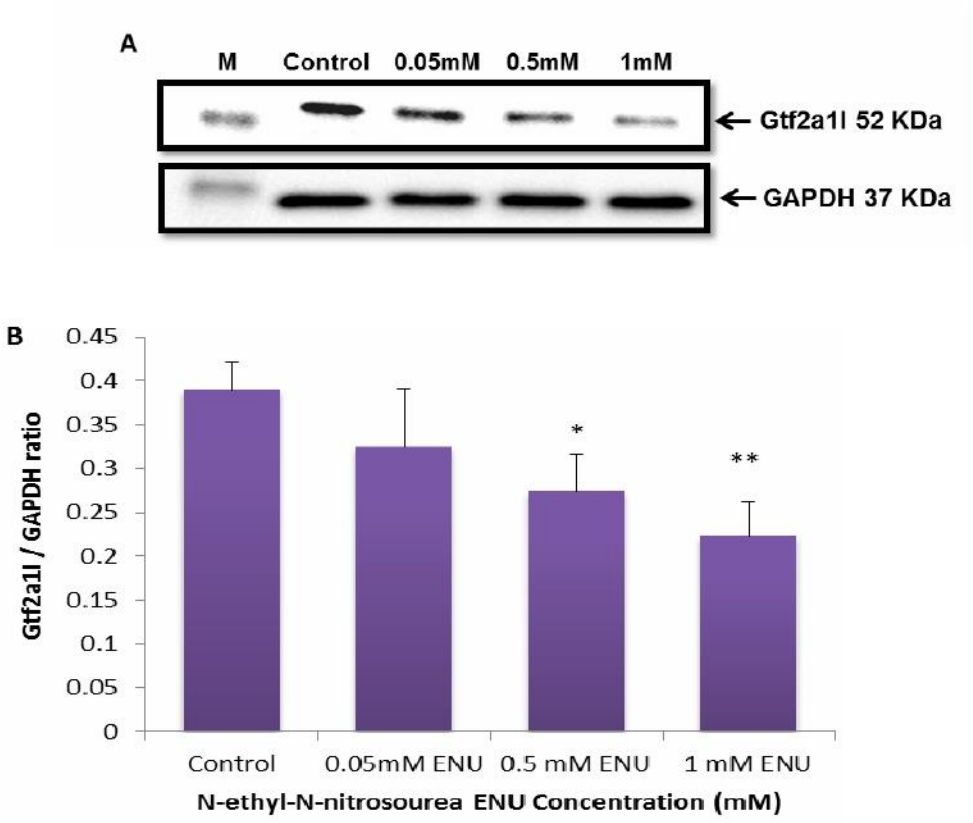

Figure 7.30: Western blot analysis of purified recombinant Gtf2a1l protein with Gtf2a1l antibody treated with ENU at different cocentrations, 1 h after treatment. Sample Western blots of Gtf2a1l and GAPDH proteins are shown in (A) and quantified summary data are shown in (B). The density of each band was quantified by the use of Image 1.45 software. The relative expression level of Gtf2a1l was measured by Gtf2a1l / GAPDH ratio. Data are expressed as the mean ± SEM. n=3 different replicates performed on three different occasions (*p<0.05, **p<0.01).

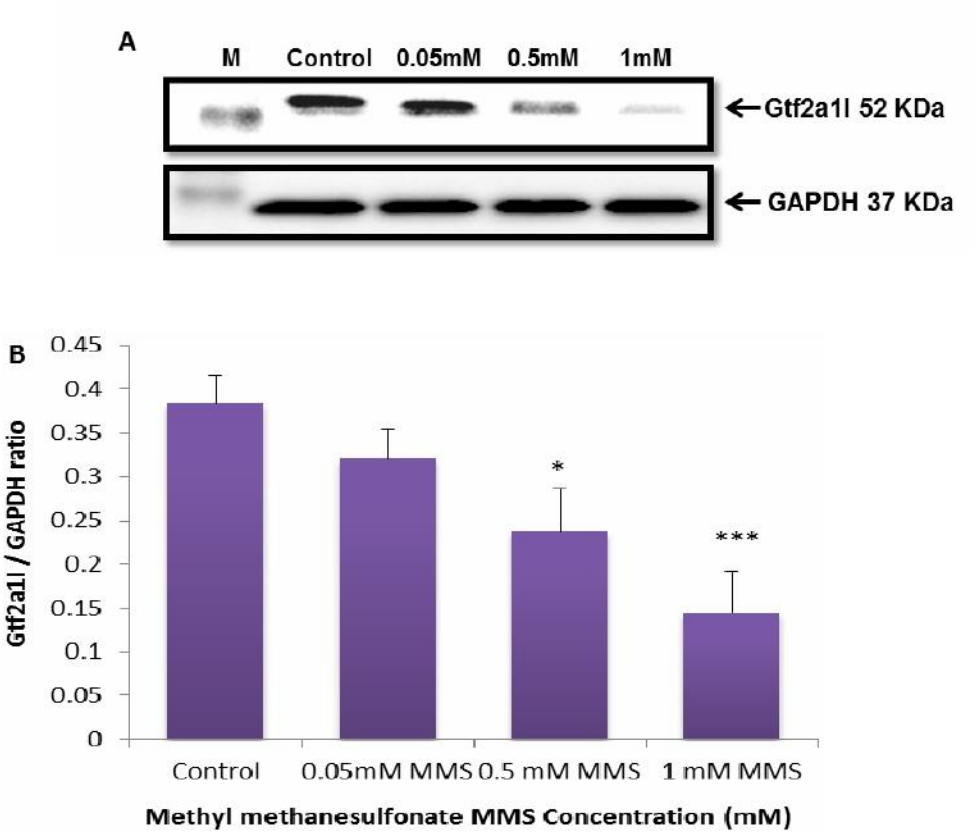

Figure 7.31: Western blot analysis of purified recombinant Gtf2a1l protein with Gtf2a1l antibody treated with MMS at different concentration at 1 h after the treatment. Sample Western blots of Gtf2a1l and GAPDH proteins are shown in (A) and quantified summary data are shown in (B). MMS treatment decreased Gtf2a1l protein level. The density of each band was quantified by the use of Image 1.45 software. The relative expression level of Gtf2a1l was measured by Gtf2a1l / GAPDH ratio. Data are expressed as the mean ± SEM. n=3 different biological replicates performed on three different occasions (*p<0.05, ***p<0.001).

7.4 Discussion

The present study is aimed at the production and use of cDNA from testicular mRNA and PCR-amplification of the spermiogenesis-specific transcription factors Tbpl1, FHL5 and Gtf2a1l respectively, since it was shown in Chapter 6 that, in spermatids particularly, they can be susceptible to genotoxins in a way that housekeeping genes are not. The TOPO system was used in the cloning of amplified Tbpl1, FHL5 and Gtf2a1l cDNAs into the expression vector pET100/D-TOPO in frame and directionally in order to ensure their expression. Primers were designed directly on the start and stop codons so that only the open reading frame could be amplified by PCR. The construct was sub cloned into *E. coli* and cultures exposed to the same genotoxins that were used in the equivalent experiments with isolated mouse testicular cells (chapter 6).

The recombinant protein appeared to be associated with the insoluble membrane fraction of the recombinant *E. coli* and consequently was difficult to recover from the insoluble pellet. Yet, Western blot analysis of the purified protein confirmed that the expressed, purified protein was the desired proteins.

To enable the recombinant construct of Tbpl1, FHL5 and Gtf2a1l proteins to be used for in vitro studies the Tbpl1, FHL5 and Gtf2a1l was first amplified by RT-PCR. The present study is aimed at the production of cDNA from testicular mRNA and PCR-amplification of the spermiogenesis-specific transcription factors Tbpl1, FHL5 and Gtf2a1l respectively and TOPO was used in the cloning of amplified Tbpl1, FHL5 and Gtf2a1l genes for further

sequence analysis. Once the sequences were established a strategy was devised in order to clone the Tbpl1, FHL5 and Gtf2a1l gene into the expression vector pET100/D-TOPO in frame and directionally in order to insure its expression. Primers were designed directly on the start and stop codon so that only the open reading frame can be amplified by PCR. Due to the error prone nature of Taq polymerase as compared to the proof reading Pfu polymerase, *the latter* was used in the Tbpl1, FHL5 and Gtf2a1l genes amplification for cloning into pET100/D-TOPO. This enzyme is characterized by a 3'-5' exonuclease activity that minimizes the possibility of inserting mutations during RT-PCR amplification. The current study demonstrated that the full open reading frames of the three transpiration factors TbpI1, FHL5 and Gtf2a1l were successfully amplified using RT-PCR as shown in Figures 7.4, 7.15 and 7.24 respectively). Moreover, the results showed that the TbpI1, FHL5 and Gtf2a1l PCR products were cloned successfully into the expression vector pET100/D-TOPO to enable the recombinant TbpI1, FHL5 and Gtf2a1l proteins to be expressed as a fusion protein with an N-terminal HIS Tag. Furthermore, the confirmation of insertion of the PCR product of TbpI1, FHL5 and Gtf2a1l gene into PET100/D-TOPO was showed confirmed successfully in the correct orientation of the insert which was generated by different primers sets as shown in Figure 7.5, 7.16 and 7.25 respectively. The cloned Tbpl1, FHL5 and Gtf2a1l genes were successfully expressed as a 21, 32 and 52 kDa protein at high levels after induction with IPTG (Figures 7.11, 7.19 and 7.29). The recombinant protein appeared to be associated with the insoluble membrane fraction of the recombinant E. coli and consequently was difficult to recover from the insoluble pellet. Yet, western

blot analysis of the purified protein confirmed that the expressed, purified protein was the desired proteins. As shown in (Figures 7.10, 7.20 and 7.28) the recombinant protein Tbpl1, FHL5 and Gtf2a1l of 21, 32 and 52 kDa on fusion with 3 KDa his tag increased their mass to 24, 35 and 55 kDa. These results showed that the expression of Tbpl1 studies by using standard techniques such as, RT-PCR demonstrated the presence of Tbpl1 in mouse testis. The fusion protein containing full-length Tbpl1 was expressed in the developing male germ cells and purified in E. coli (Martianov et al., 2001, Martianov et al., 2002). Furthermore, the expression studies utilizing standard techniques such as RT-PCR have previously confirmed that FHL5 is present in the mouse testis (Palermo et al., 2001, Lardenois et al., 2009). Moreover, many studies have showed that Gtf2a1l is expressed in developing ale germ cells (Han et al., 2001, Han et al., 2004).

Alkylating agents such as, ENU and MMS are electrophilic chemicals that can modify cellular macromolecules. Damage to both proteins and nucleic acids can be occurred after exposure to alkylating agents, due to alkylation of adenine, cytosine, and guanine bases in nucleic acids, and arginine, lysine, and cysteine residues in proteins these represents common sites of damage (Burgis and Samson, 2007). The baseline results in this study showed that recombinant DNA and recombinant protein of the three transcriptions factors Tbpl1, FHL5 and Gtf2a1l were detected in E. coli and found to be down regulated.

QPCR data has showed ENU and MMS mutagenesis induced a significant decreased of the Tbpl1 level in DNA at 0.5 mM ($p \leq 0.05$). Following treatment with 1 mM ENU and MMS DNA Tbpl1level showed further significant

decreased the Tbpl1 DNA level in expression, which was statistically significant when compared with the corresponding controls ($p \leq 0.05$, $p \leq 0.01$, Figure 7.8 and Figure 7.9). Western blot data has showed ENU and MMS mutagenesis induced a significant decreased of the expression protein level Tbpl1 at 0.5 mM ($p \leq 0.05$). Following treatment with 1 mM ENU showed further significant decreased the of the expression protein level Tbpl1, which was statistically significant when compared with the corresponding controls ($p \leq 0.01$, Figure 7.12 A and B). However, further decrease was shown when the cells were treated with MMS 1 mM ($p \leq 0.001$) these results are shown in Figure 7.13 A and B.

From qPCR data, ENU and MMS mutagenesis induced a significant decrease of the FHL5 level in DNA at 0.5 mM ($p \leq 0.05$) as shown in Figure 7.17 and 7.18. Following treatment with 1 mM ENU and MMS DNA FHL5 level showed significant decreased the FHL5 DNA level in expression, which was statistically significant when compared with the corresponding controls ($p \leq 0.05$, $p \leq 0.01$) as shown in Figure 7.17 and 7.18. Western blot data has showed ENU and MMS mutagenesis induced a significant decreased of the expression protein level FHL5 at 0.5 mM ($p \leq 0.05$, Figure 7.21 A and B, Figure 7.22 A and B). Following treatment with 1 mM ENU and MMS showed further significant decreased the of the expression protein level Fhl5, which was statistically significant when compared with the corresponding controls ($p \leq 0.01$, Figure 7.21 A and B, Figure 7.22 A and B). The level of Gtf2a1l was significantly decreased when cells were treated with ENU or MMS 0.5 mM ($p \leq 0.05$ and $p \leq 0.01$) Figures 7.26 and 7.27. Moreover, further

significant decreased was shown on the level of Gtf2a1l expression when the cells were treated with 1 mM ($p \leq 0.01$ and $p \leq 0.001$) Figures 7.26 and 7.27.

Western blot data has showed ENU and MMS mutagenesis induced a significant decreased of the expression protein level Gtf2a1l at 0.5 mM ($p \leq 0.05$) Figures 7.30 A and B and 7.31 A and B. Following treatment with 1 mM ENU showed further significant decreased the of the expression protein level Gtf2a1l, which was statistically significant when compared with the corresponding controls ($p \leq 0.01$) Figure 7.30 A and B. However, further decrease was shown when the cells were treated with MMS 1 mM ($p \leq 0.001$) Figure 7.31 A and B.

In the current study, the data clearly showed that DNA and protein expression decreased with increased ENU or MMS. This result was consistent with evidence from the literature. It has been reported that alkylating agent caused damage in nucleic acids and proteins, thus promoting mutagenesis and cell death (Burgis and Samson, 2007, Smith and Grisham, 1983). However, functional and computational mapping of the alkylating agent toxicity modulating gene produces identified protein networks specific to transcription, mRNA processing, and translation has being vital after alkylation damage (Rooney et al., 2009)

In vitro reconstruction of *E.coli* transcription initiation during this study demonstrates a general strategy for in vitro experimental reconstruction of a multi-component biological process. The strategy couples expression of multiple gene products with detection of the resulting biological activities in a reconstituted protein synthesis system and allows rapid *in vitro*

reconstruction of a functional biological complex or process from DNA templates instead of purified components.

The results suggest that both ENU and MMS decreased level expression due to DNA alteration and decreased protein expression in a dose-dependent manner in *E.coli*. Moreover, Tbpl1, FHL5 and Gtf2a1l expression on treated with ENU and MMS was highly down-regulate so this suggests that the Tbpl1, FHL5 and Gtf2a1l appear essential for the progression of germ cells development and changes in the expression levels of Tbpl1, FHL5 and Gtf2a1l in the treated samples lead us to believe that Tbpl1, FHL5 and Gtf2a1l may function in spermatogenesis.

Chapter 8. Discussion and future work

8.1 Discussion

Male germ cell is a complex and ordered differentiation process that takes place continuously in adult organisms. In mammals, spermatogenesis occurs in the seminiferous epithelium under complex endocrine control. A spermatogonial stem cell population undergoes self-renewal and gives rise to primary spermatocytes followed by a major biochemical and structural reorganization of the haploid cells to generate maturation-phase elongating spermatids (White-Cooper and Davidson, 2011, de Rooij, 2001). This process is regulated by complex regulatory program leading the expression of specific sets of genes at various developmental stages of spermatogenesis. In mouse, a first set of germ cell specific genes are expressed in pachytene spermatocytes followed by a second wave of postmeiotic transcription in round spermatids where most genes required for morphological and biochemical reprogramming are expressed (Sassone-Corsi, 2002). Male germ cells are well known to be susceptible to environmental factors, such as free radicals, anticancer alkylating agents, radiation, reproductive and somatic pathologies, and by endogenous factors, such as genetic predisposition and stress, which can result in an increase in the constitutive levels of apoptosis, DNA repair, cell cycle arrest, mutation or unrepaired genetic damage in germ cells (Tripathi et al., 2009, Lagos-Cabre and Moreno, 2012). Despite current advances in the study of male germ cells in terms of genetics and development, our understanding of the effect of toxins on specific cell types has been largely limited to what can be achieved by, often cumbersome, in vivo studies to make such distinctions. The results presented here demonstrate that a suspension of mouse germ cells obtained

from testicular tissue and fractionated into large, almost homogeneous populations of spermatogonia, spermatocytes, spermatids and spermatozoa using staput Velocity Sedimentation at unit gravity. Validation of the system involved using immunohistochemistry to deter-mine the purity of the cells populations isolated by Staput (Bellve et al., 1977), using antibodies against: TP1 to detect spermatids; SCP3 to detect spermatocytes; and GDNFR to detect spermatogonia. TP1 is an important nuclear protein in spermatids as histones are replaced by protamines during spermiogenesis. Its specificity to the haploid phase of spermatogenesis makes it a useful marker for spermatids (Meistrich et al., 1994a). Spermatocytes can be located by the presence of synaptonemal complex protein 3 (SCP 3). Synaptonemal complexes are structures formed between homologous chromosomes during meiotic pro-phase, thought to be involved in chromosome pairing and recombination (Dobson et al., 1994b, Lammers et al., 1995). Spermatogonia can be labeled by Glial cell line-derived neurotrophic factor receptor (GDNFR). Sertoli cells secrete a ligand to GDNFR called GFRα-1 (Viglietto et al., 2000). The binding of this substrate-ligand complex activates the Ret receptor tyrosine kinase (Tadokoro et al., 2002b). This mediates an intracellular response that is linked to the proliferation of an undifferentiated type A spermatogonium and is therefore considered a good marker for these types of spermatogonia (Meng et al., 2000).

Hydrogen peroxide (H_2O_2) has been found to induce apoptosis in a diversity of cells and although the sensitivity of germ line cells to H_2O_2 is not fully understood, DNA strand breakage by the production of free radicals is the trigger for the programmed cell death. The results of the present study show

that H_2O_2, even at a low concentration of H_2O_2 of 1μM, has the ability to induce apoptosis in testicular germ cells *in vitro*. Furthermore, statistically significant differences were observed between DNA strand breaks in spermatogonial cells incubated with ENU and MNU cells showed significantly increased in apoptotic cells in spermatogonia. These results showed similarities to studies by Russell et al., (2007) who also found genetic damage in spermatogonia when treated with ENU and MNU but *in vivo*, and (Verhofstad et al., 2011) who found ENU and MNU to be highly mutagenic in the rodent germline. The present work also supports an early study that showed 6-MP be the most potent chemical for inducing DNA damage in spermatocytes (Mosesso and Palitti, 1993) and one 10 years later that showed that spermatocytes was highly sensitive to 5-BrdU (Perrard et al., 2003). Likewise, the results are in agreement with those indicating that quantitative evaluation of germ cells treated with MMS showed a decrease in the number of spermatids and high frequency of chromosome aberrations induced in spermatids (Kuriyama et al., 2005, Matsuda et al., 1989). This is in line with what has been reported previously, demonstrating concordance between our approach to preparing testicular germ cells and previous methodologies (Maheshwari et al., 2009). Thus, it is highly likely that the methodology developed here has the potential to enable the rapid screening of chemicals for male reproductive genetic toxicity and reduce dependence on animal-intensive time-consuming *in vivo* studies. The results with H_2O_2 and doxorubicin also demonstrate that the spermatogonia was significantly more affected than the spermatocytes, which in turn were significantly more affected than spermatids. This correlates with the proportion of dividing cells

expected to be present in these populations. Thus, if dividing cells are more susceptible to genetic damage than non-dividing cells, this could account for the lowest amount of apoptosis occurring in the latter population. Indeed, there are a number of different types of cells within spermatogonia, spermatocytes and spermatids, each of which could have different susceptibilities to genetic damage, depending on which phase of the cell cycle they represent.

It is well recognized that doxorubicin induces apoptosis in early spermatogonia, which results in a decrease in the size of the pool of germline stem cells (Holm et al., 2009, Hou et al., 2005). These cells are extremely vulnerable to cytotoxic effects due to their rapid proliferation, whereas the non-proliferating cells survive most of the cytotoxic therapies, although they could suffer functional damage (Wang et al., 1998). The findings of the present study showed a statistically significant minor effect of the doxorubicin on germ cells. These results suggest that the initiation phase of spermatogenesis is highly sensitive to doxorubicin-induced apoptosis. The observations confirm the genotoxic capacity of doxorubicin as previously demonstrated by other authors using rat testes, suggests that the initiation phase of spermatogenesis is especially sensitive to the toxic effects of this compound (Hou et al., 2005). Moreover, a previous study has also demonstrated testicular vulnerability to the toxicity of doxorubicin at critical stages of maturation (Bechter et al., 1987) and recent research has also established its serious impact on spermatogenesis. Alkylating agent exposure resulted in a substantial decrease in gene expression, in spermatocytes and spermatids. Cytotoxic effects are exerted by the transfer

of the alkyl group(s) to many cellular constituents; however, DNA alkylation events during the nucleus may be the major changes that lead to cell death (Shiraishi et al., 2000). It also can be lead to DNA repair, mutation, persistence of unrepaired DNA damage, cell cycle arrest. Altered transcription patterns may be a new response to genotoxicity. RT-PCR was used to detect the expression of transcripts factor of TbpI1, FHL5 and Gtf2a1I selected genes in two types of germ cells, and found that the transcripts were highly expressed in spermatocytes and spermatids. The results agree with the observations of Martianov et al., 2001; and Zhang et al., 2001a, who found that TbpI1 is strongly upregulated with the appearance of spermatocytes and spermatids (Martianov et al., 2001, Zhang et al., 2001). They also support the expression of FHL5 highly specifically in spermatocytes and spermatids (Steger et al., 2004, De Cesare et al., 2003). Lastly, the results also agree with the observations by Han et al and Huang et al, (2001 and 2006). Who showed that Gtf2a1I mRNA is present in mouse spermatocytes and spermatids (Han et al., 2001, Huang et al., 2006), abnormal sperm formation (Huang et al., 2006). Thus, the use of RT-qPCR in isolated cells appears to give the same result as the equivalent in vivo studies. The present work also shows that treating spermatocytes and spermatids isolated by staput with ENU and MMS reduced the effect on mRNA level and proteins of TbpI1, FHL5 and Gtf2a1I. Therefore, it is proposed that consideration be given to investigating mRNA and protein production in routine genotoxicity studies.

Interestingly, it was found that mRNA levels and proteins were more affected by MMS and ENU in spermatids than in spermatocytes. This is probably

unlikely to be due to the mutational susceptibility of the different germ cell types because the spermatids were still more heavily affected than the spermatocytes, even when a spermatogonial toxin (ENU) was used. (Work in Chapter 5 shows that in terms of apoptosis induction and Comet assay, the order of susceptibility was reversed and spermatids were the least susceptible cell type to ENU). This might be due to high sensitivity of the postmeiotic period to mutagenic exposure which has been found associated with the reduced DNA repair capacity, recombination and the types of chromosome-associated proteins and the extent of chromosomal condensation of late spermatids and sperm as compared other spermatogenic cell types (Singer et al., 2006, Sega, 1974, Olsen et al., 2005). Functional and computational mapping of the alkylating agent toxicity modulating gene produces identified protein networks specific to transcription, mRNA processing, and translation as being vital after alkylation damage (Rooney et al., 2009).

8.2 Future work

Staput separation of specific germ cell types, coupled with short term in vitro culture shows potential for the rapid assessment of toxins in multiple germ cell types with high sensitivity. Particularly, it allows the examination of high numbers of cells for example spermatogonia, which are normally present in relatively low amounts in vivo, compared with spermatocytes and spermatids. Therefore further work should focus on developing this as a viable assay for reproductive genetic toxicology. The addition of flow cytometry to sort and purify cells and to detect apoptotic cells would dramatically enhance the efficiency of such an assay. Many of the results of this study were in agreement with other studies in that a decrease in germ cells viability was observed when cells were treated with H_2O_2, doxorubicin, N-ethyl-N-nitrosourea, N-methyl-N-nitrosourea, 6-mercaptopurine, 5-bromodeoxyuridine, Methyl methanesulfonate and Ethyl methanesulfonate. The results also suggest that these compounds increase apoptosis in male germ cells types. Male germ cells types in a dose-dependent manner. More studies are needed to fully understand the mechanism of this action and to assess the effect of genotoxicity and in the extrinsic and intrinsic pathways of apoptosis.

Caspases are central components for apoptosis. Caspases involved in apoptosis are generally divided into two groups, the initiator caspases, which include caspase-2, -8, -9, and -10, and the effector caspases, which include caspase-3, -6, and -7. It will be useful to assess the capacity of this toxicity to activate the caspases. Changes in levels of caspase expression can be measured using Western blotting and changes in activity by specific ELISAs.

These experiments will clarify which caspases important in apoptosis are modulated by toxins. Also in parallel with this, it will be useful to compare other compounds which play an important role in modulating the apoptosis pathways such as cytochrome c, BAX and BAD. Activation of the extrinsic apoptosis pathway may also be a mechanism of toxicity drugs action to induce apoptosis. This pathway is commonly activated by death receptors. Death receptors may be activated directly by the toxicity or their bioactive mediators. This could be assessed by treating the male germ cells with toxicity in the presence and absence of specific inhibitors of the death receptors. A better understanding of how toxicity modulates apoptosis may help to explain the mechanisms of action for this toxicity in the spermatogenesis and in turn help refine future assays.

The intracellular concentration of ROS appears to dictate stress survival apoptotic responses. Low levels of ROS are used during the cells as signalling intermediates for normal homeostasis. However, high levels of ROS directly damages cellular structural components and can induce apoptosis. Furthermore, it has been reported that certain toxins such as doxorubicin can produce ROS resulting in the formation of free radicals leading to induced apoptosis and prevention of the growth of cancer cells. This mechanism can be followed by co-treating the germ cells with anti-oxidants such as vitamin C or superoxide dismutase. If antioxidants could be upregulated in normal cells but not cancer cells, this could then be utilised to prevent some of the adverse effects of anti-cancer drugs.

References

ABRAHAM, S. K. & FRANZ, J. 1983. Induction of sister-chromatid exchanges by chemotherapeutic drugs in spermatogonia of mice: effects of procarbazine, adriamycin, cyclophosphamide and mitomycin C. *Mutat Res,* 108**,** 373-81.

ACHERMANN, J. C., OZISIK, G., MEEKS, J. J. & JAMESON, J. L. 2002. Genetic causes of human reproductive disease. *Journal of Clinical Endocrinology & Metabolism,* 87**,** 2447-2454.

ADLER, I. D. 2000. Spermatogenesis and mutagenicity of environmental hazards: extrapolation of genetic risk from mouse to man. *Andrologia,* 32**,** 233-237.

AGUILAR-MAHECHA, A., HALES, B. F. & ROBAIRE, B. 2002. Chronic cyclophosphamide treatment alters the expression of stress response genes in rat male germ cells. *Biol Reprod,* 66**,** 1024-32.

AITKEN, R. J., GORDON, E., HARKISS, D., TWIGG, J. P., MILNE, P., JENNINGS, Z. & IRVINE, D. S. 1998. Relative impact of oxidative stress on the functional competence and genomic integrity of human spermatozoa. *Biology of Reproduction,* 59**,** 1037-1046.

AKHTAR, W. & VEENSTRA, G. J. 2011. TBP-related factors: a paradigm of diversity in transcription initiation. *Cell Biosci,* 1**,** 23.

ALLEN, J. W., LIANG, J. C., CARRANO, A. V. & PRESTON, R. J. 1986. Review of Literature on Chemical-Induced Aneuploidy in Mammalian Male Germ-Cells. *Mutation Research,* 167**,** 123-137.

ALSHABANAH, O. A., HAFEZ, M. M., AL-HARBI, M. M., HASSAN, Z. K., AL REJAIE, S. S., ASIRI, Y. A. & SAYED-AHMED, M. M. 2010. Doxorubicin toxicity can be ameliorated during antioxidant L-carnitine supplementation. *Oxid Med Cell Longev,* 3**,** 428-33.

ANDERSON, D., DOBRZYNSKA, M. M. & BASARAN, N. 1997. Effect of various genotoxins and reproductive toxins in human lymphocytes and sperm in the comet assay. *Teratogenesis Carcinogenesis and Mutagenesis,* 17**,** 29-43.

ANDERSON, D., HODGE, M. C. E., PALMER, S. & PURCHASE, I. F. H. 1981. Comparison of Dominant Lethal and Heritable Translocation Methodologies. *Mutation Research,* 85**,** 417-429.

ANDERSON, D. & PLEWA, M. J. 1998. The International Comet Assay Workshop. *Mutagenesis,* 13**,** 67-73.

ATTIA, S. M., AL-BAKHEET, S. A. & AL-RASHEED, N. M. 2010. Proanthocyanidins produce significant attenuation of doxorubicin-induced mutagenicity via suppression of oxidative stress. *Oxid Med Cell Longev,* 3**,** 404-13.

BADKOOBEH, P., PARIVAR, K., KALANTAR, S. M., HOSSEINI, S. D. & SALABAT, A. 2013. Effect of nano-zinc oxide on doxorubicin- induced oxidative stress and sperm disorders in adult male Wistar rats. *Iran J Reprod Med,* 11**,** 355-64.

BARTKE, A. 1995. Apoptosis of Male Germ-Cells, a Generalized or a Cell-Type-Specific Phenomenon. *Endocrinology,* 136**,** 3-4.

BASTOS, H., LASSALLE, B., CHICHEPORTICHE, A., RIOU, L., TESTART, J., ALLEMAND, I. & FOUCHET, P. 2005. Flow cytometric characterization of viable meiotic and postmeiotic cells by Hoechst 33342 in mouse spermatogenesis. *Cytometry A,* 65**,** 40-9.

BAUMGARTNER, A., CEMELI, E. & ANDERSON, D. 2009. The comet assay in male reproductive toxicology. *Cell Biol Toxicol,* 25**,** 81-98.

BAUMGARTNER, A., SCHMID, T. E., CEMELI, E. & ANDERSON, D. 2004. Parallel evaluation of doxorubicin-induced genetic damage in human lymphocytes and sperm using the comet assay and spectral karyotyping. *Mutagenesis,* 19**,** 313-8.

BECHTER, R., HAEBLER, R., ETTLIN, R. A., HASEMAN, J. K. & DIXON, R. L. 1987. Differential Susceptibility of Immature Rat Testes to Doxorubicin at Critical Stages of Maturation - Biochemical and Functional Assessment. *Archives of Toxicology,* 60**,** 415-421.

BECKWITH, L. G., MOORE, J. L., TSAO-WU, G. S., HARSHBARGER, J. C. & CHENG, K. C. 2000. Ethylnitrosourea induces neoplasia in zebrafish (Danio rerio). *Lab Invest,* 80**,** 379-85.

BELLVE, A. R., CAVICCHIA, J. C., MILLETTE, C. F., O'BRIEN, D. A., BHATNAGAR, Y. M. & DYM, M. 1977. Spermatogenic cells of the prepuberal mouse. Isolation and morphological characterization. *J Cell Biol,* 74**,** 68-85.

BERK, A. J. 2000. TBP-like factors come into focus. *Cell,* 103**,** 5-8.

BRILHANTE, O., OKADA, F. K., SASSO-CERRI, E., STUMPP, T. & MIRAGLIA, S. M. 2012. Late morfofunctional alterations of the Sertoli cell caused by doxorubicin administered to prepubertal rats. *Reprod Biol Endocrinol,* 10**,** 79.

BRINKWORTH, M. H. 2000. Paternal transmission of genetic damage: findings in animals and humans. *Int J Androl,* 23**,** 123-135.

BROCKWAY, H., BALUKOFF, N., DEAN, M., ALLEVA, B. & SMOLIKOVE, S. 2014. The CSN/COP9 Signalosome Regulates Synaptonemal Complex Assembly during Meiotic Prophase I of Caenorhabditis elegans. *PLoS Genet,* 10**,** e1004757.

BRYANT, J. M., MEYER-FICCA, M. L., DANG, V. M., BERGER, S. L. & MEYER, R. G. 2013. Separation of spermatogenic cell types using STA-PUT velocity sedimentation. *J Vis Exp*.

BUNZ, F., DUTRIAUX, A., LENGAUER, C., WALDMAN, T., ZHOU, S., BROWN, J. P., SEDIVY, J. M., KINZLER, K. W. & VOGELSTEIN, B. 1998. Requirement for p53 and p21 to sustain G2 arrest after DNA damage. *Science,* 282**,** 1497-501.

BURGIS, N. E. & SAMSON, L. D. 2007. The protein degradation response of Saccharomyces cerevisiae to classical DNA-damaging agents. *Chemical Research in Toxicology,* 20**,** 1843-1853.

CHANEY, S. G. & SANCAR, A. 1996. DNA repair: enzymatic mechanisms and relevance to drug response. *J Natl Cancer Inst,* 88**,** 1346-60.

CHANG, Y. F., LEE-CHANG, J. S., PANNEERDOSS, S., MACLEAN, J. A., 2ND & RAO, M. K. 2011. Isolation of Sertoli, Leydig, and spermatogenic cells from the mouse testis. *Biotechniques,* 51**,** 341-2, 344.

CHEN, T., HARRINGTON-BROCK, K. & MOORE, M. M. 2002. Mutant frequencies and loss of heterozygosity induced by N-ethyl-N-nitrosourea in the thymidine kinase gene of L5178Y/TK+-3.7.2C mouse lymphoma cells. *Mutagenesis,* 17**,** 105-109.

CHENG, C. Y. & MRUK, D. D. 2010. A local autocrine axis in the testes that regulates spermatogenesis. *Nature Reviews Endocrinology,* 6**,** 380-395.

CHONG, J. A., MORAN, M. M., TEICHMANN, M., KACZMAREK, J. S., ROEDER, R. & CLAPHAM, D. E. 2005. TATA-binding protein (TBP)-like factor (TLF) is a functional regulator of transcription: reciprocal regulation of the neurofibromatosis type 1 and c-fos genes by TLF/TRF2 and TBP. *Mol Cell Biol,* 25**,** 2632-43.

CICCIA, A. & ELLEDGE, S. J. 2010. The DNA Damage Response: Making It Safe to Play with Knives. *Molecular Cell,* 40**,** 179-204.

CLERMONT, Y. 1972. Kinetics of Spermatogenesis in Mammals - Seminiferous Epithelium Cycle and Spermatogonial Renewal. *Physiological Reviews,* 52**,** 198-&.

CORDES, S. P. 2005. N-ethyl-N-nitrosourea mutagenesis: Boarding the mouse mutant express. *Microbiology and Molecular Biology Reviews,* 69**,** 426-+.

DACUNHA, M. F., MEISTRICH, M. L., RIED, H. L., GORDON, L. A., WATCHMAKER, G. & WYROBEK, A. J. 1983. Active Sperm Production after Cancer-Chemotherapy with Doxorubicin. *Journal of Urology,* 130**,** 927-930.

DADOUNE, J. P. 2003. Expression of mammalian spermatozoal nucleoproteins. *Microscopy Research and Technique,* 61**,** 56-75.

DANTONEL, J. C., WURTZ, J. M., POCH, O., MORAS, D. & TORA, L. 1999. The TBP-like factor: an alternative transcription factor in metazoa? *Trends Biochem Sci,* 24**,** 335-9.

DE CESARE, D., FIMIA, G. M., BRANCORSINI, S., PARVINEN, M. & SASSONE-CORSI, P. 2003. Transcriptional control in male germ cells: General factor TFIIA participates in CREM-dependent gene activation. *Molecular Endocrinology,* 17**,** 2554-2565.

DE ROOIJ, D. G. 2001. Proliferation and differentiation of spermatogonial stem cells. *Reproduction,* 121**,** 347-54. DELBES, G., HALES, B. F. & ROBAIRE, B. 2010. Toxicants and human sperm chromatin integrity. *Molecular Human Reproduction,* 16**,** 14-22.

DOBSON, M. J., PEARLMAN, R. E., KARAISKAKIS, A., SPYROPOULOS, B. & MOENS, P. B. 1994. Synaptonemal Complex Proteins - Occurrence, Epitope Mapping and Chromosome Disjunction. *Journal of Cell Science,* 107**,** 2749-2760.

EDDY, E. M. 2002b. Male germ cell gene expression. *Recent Prog Horm Res,* 57**,** 103-28.
EHLING, U. H. 1971. Comparison of radiation-and chemically-induced dominant lethal mutations in male mice. *Mutat Res,* 11**,** 35-44.
EHLING, U. H., MACHEMER, L., BUSELMAIER, W., DYCKA, J., FROHBERG, H., KRATOCHVILOVA, J., LANG, R., LORKE, D., MULLER, D., PEH, J., ROTHRBORN, G., ROLL, R., SCHULZE-SCHENCKING, M. & WIEMANN, H. 1978. Standard protocol for the dominant lethal test on male mice set up by the work group "Dominant Lethal Mutations of the ad hoc Committe Chemogenetics". *Arch Toxicol,* 39**,** 173-85.
ELIOT, H., GIANNI, L. & MYERS, C. 1984. Oxidative destruction of DNA by the adriamycin-iron complex. *Biochemistry,* 23**,** 928-36.
ELMORE, S. 2007. Apoptosis: a review of programmed cell death. *Toxicol Pathol,* 35**,** 495-516.
FAIRBAIRN, D. W., OLIVE, P. L. & O'NEILL, K. L. 1995. The comet assay: a comprehensive review. *Mutat Res,* 339**,** 37-59.
FIMIA, G. M., DE CESARE, D. & SASSONE-CORSI, P. 1999. CBP-independent activation of CREM and CREB by the LIM-only protein ACT. *Nature,* 398**,** 165-9.
FIMOGNARI, C., SESTILI, P., LENZI, M., BUCCHINI, A., CANTELLI-FORTI, G. & HRELIA, P. 2008. RNA as a new target for toxic and protective agents. *Mutat Res,* 648**,** 15-22.
FINN, N. A., FINDLEY, H. W. & KEMP, M. L. 2011. A switching mechanism in doxorubicin bioactivation can be exploited to control doxorubicin toxicity. *PLoS Comput Biol,* 7**,** e1002151.
FRANCAVILLA, S., D'ABRIZIO, P., RUCCI, N., SILVANO, G., PROPERZI, G., STRAFACE, E., CORDESCHI, G., NECOZIONE, S., GNESSI, L., ARIZZI, M. & ULISSE, S. 2000. Fas and Fas ligand expression in fetal and adult human testis with normal or deranged spermatogenesis. *J Clin Endocrinol Metab,* 85**,** 2692-700.
GAIVAO, I. & SIERRA, L. M. 2014. Drosophila comet assay: insights, uses, and future perspectives. *Front Genet,* 5**,** 304.
GAVRIELI, Y., SHERMAN, Y. & BEN-SASSON, S. A. 1992. Identification of programmed cell death in situ via specific labeling of nuclear DNA fragmentation. *J Cell Biol,* 119**,** 493-501.
GENEROSO, W. M., PRESTON, R. J. & BREWEN, J. G. 1975. 6-Mercaptopurine, an Inducer of Cytogenetic and Dominant-Lethal Effects in Premeiotic and Early Meiotic Germ-Cells of Male Mice. *Mutation Research,* 28**,** 437-447.
GENSCHOW, E., SPIELMANN, H., SCHOLZ, G., SEILER, A., BROWN, N., PIERSMA, A., BRADY, M., CLEMANN, N., HUUSKONEN, H., PAILLARD, F., BREMER, S. & BECKER, K. 2002. The ECVAM international validation study on in vitro embryotoxicity tests: Results of the definitive phase and evaluation of prediction models. *Atla-Alternatives to Laboratory Animals,* 30**,** 151-176.
GOUAZE, V., MIRAULT, M. E., CARPENTIER, S., SALVAYRE, R., LEVADE, T. & ANDRIEU-ABADIE, N. 2001. Glutathione peroxidase-1 overexpression prevents ceramide production and partially inhibits apoptosis in doxorubicin-treated human breast carcinoma cells. *Molecular Pharmacology,* 60**,** 488-496.
GUENET, J. L. 2004. Chemical mutagenesis of the mouse genome: an overview. *Genetica,* 122**,** 9-24.
GUO, R., YU, Z., GUAN, J., GE, Y., MA, J., LI, S., WANG, S., XUE, S. & HAN, D. 2004. Stage-specific and tissue-specific expression characteristics of differentially expressed genes during mouse spermatogenesis. *Mol Reprod Dev,* 67**,** 264-72.
HABAS, K., ANDERSON, D. & BRINKWORTH, M. 2014. Development of an in vitro test system for assessment of male, reproductive toxicity. *Toxicol Lett,* 225**,** 86-91.
HAINES, G. A., HENDRY, J. H., DANIEL, C. P. & MORRIS, I. D. 2002. Germ cell and dose-dependent DNA damage measured by the comet assay in murine spermatozoaa after testicular X-irradiation. *Biol Reprod,* 67**,** 854-61.
HAMER, G., ROEPERS-GAJADIEN, H. L., VAN DUYN-GOEDHART, A., GADEMAN, I. S., KAL, H. B., VAN BUUL, P. P. & DE ROOIJ, D. G. 2003. DNA double-strand breaks and gamma-H2AX signaling in the testis. *Biol Reprod,* 68**,** 628-34.

HAMPTON, M. B. & ORRENIUS, S. 1997. Dual regulation of caspase activity by hydrogen peroxide: Implications for apoptosis. *Febs Letters,* 414**,** 552-556.

HAN, S. Y., XIE, W. S., KIM, S. H., YUE, L. M. & DEJONG, J. 2004. A short core promoter drives expression of the ALF transcription factor in reproductive tissues of male and female mice. *Biology of Reproduction,* 71**,** 933-941.

HAN, S. Y., ZHOU, L., UPADHYAYA, A., LEE, S. H., PARKER, K. L. & DEJONG, J. 2001. TFIIAalpha/beta-like factor is encoded by a germ cell-specific gene whose expression is up-regulated with other general transcription factors during spermatogenesis in the mouse. *Biol Reprod,* 64**,** 507-17.

HARTMANN, A., AGURELL, E., BEEVERS, C., BRENDLER-SCHWAAB, S., BURLINSON, B., CLAY, P., COLLINS, A., SMITH, A., SPEIT, G., THYBAUD, V., TICE, R. R. & TH INTERNATIONAL COMET ASSAY, W. 2003. Recommendations for conducting the in vivo alkaline Comet assay. 4th International Comet Assay Workshop. *Mutagenesis,* 18**,** 45-51.

HECHT, N. B. 1998. Molecular mechanisms of male germ cell differentiation. *Bioessays,* 20**,** 555-561.

Hess, R., França, L.R. History of the sertoli cell discovery. In: Griswold, M., Skinner, M. eds. (2005) Sertoli Cell Biology. Academic Press, New York

HITOTSUMACHI, S., CARPENTER, D. A. & RUSSELL, W. L. 1985. Dose-repetition increases the mutagenic effectiveness of N-ethyl-N-nitrosourea in mouse spermatogonia. *Proc Natl Acad Sci U S A,* 82**,** 6619-21.

HOLM, B., MELLEMGAARD, A., SKOV, T. & SKOV, B. G. 2009. Different Impact of Excision Repair Cross-Complementation Group 1 on Survival in Male and Female Patients With Inoperable Non-Small-Cell Lung Cancer Treated With Carboplatin and Gemcitabine. *Journal of Clinical Oncology,* 27**,** 4254-4259.

HOOD, R. D. 2006. Developmental and Reproductive Toxicology: A Practical Approach, Second Edition.

HOU, M., CHRYSIS, D., NURMIO, M., PARVINEN, M., EKSBORG, S., SODER, O. & JAHNUKAINEN, K. 2005. Doxorubicin induces apoptosis in germ line stem cells in the immature rat testis and amifostine cannot protect against this cytotoxicity. *Cancer Research,* 65**,** 9999-10005.

HSU, S. M., RAINE, L. & FANGER, H. 1981. Use of Avidin-Biotin-Peroxidase Complex (Abc) in Immunoperoxidase Techniques - a Comparison between Abc and Unlabeled Antibody (Pap) Procedures. *Journal of Histochemistry & Cytochemistry,* 29**,** 577-580.

HUANG, M., WANG, H., LI, J., ZHOU, Z., DU, Y., LIN, M. & SHA, J. 2006. Involvement of ALF in human spermatogenesis and male infertility. *Int J Mol Med,* 17**,** 599-604.

HUGHES, C. M., LEWIS, S. E. M., MCKELVEYMARTIN, V. J. & THOMPSON, W. 1997. Reproducibility of human sperm DNA measurements using the alkaline single cell gel electrophoresis assay. *Mutation Research-Fundamental and Molecular Mechanisms of Mutagenesis,* 374**,** 261-268.

IMAHIE, H., ADACHI, T., NAKAGAWA, Y., NAGASAKI, T., YAMAMURA, T. & HORI, M. 1995. Effects of adriamycin, an anticancer drug showing testicular toxicity, on fertility in male rats. *J Toxicol Sci,* 20**,** 183-93.

IMAI, Y., FELDMAN, B., SCHIER, A. F. & TALBOT, W. S. 2000. Analysis of chromosomal rearrangements induced by postmeiotic mutagenesis with ethylnitrosourea in zebrafish. *Genetics,* 155**,** 261-72.

INJAC, R. & STRUKELJ, B. 2008. Recent advances in protection against doxorubicin-induced toxicity. *Technol Cancer Res Treat,* 7**,** 497-516.

IONA, S., KLINGER, F. G., SISTI, R., CICCALESE, R., NUNZIATA, A. & DE FELICI, M. 2002. A comparative study of cytotoxic effects of N-ethyl-N-nitrosourea, adriamycin, and mono-(2-ethylhexyl)phthalate on mouse primordial germ cells. *Cell Biology and Toxicology,* 18**,** 131-145.

IVELL, R., DANNER, S. & FRITSCH, M. 2004. Post-meiotic gene products as targets for male contraception. *Molecular and Cellular Endocrinology,* 216**,** 65-74.

JAHNUKAINEN, K., HOU, M., PARVINEN, M., EKSBORG, S. & SODER, O. 2000. Stage-specific inhibition of deoxyribonucleic acid synthesis and induction of apoptosis by antracyclines in cultured rat spermatogenic cells. *Biol Reprod,* 63**,** 482-7.

JAN, S. Z., HAMER, G., REPPING, S., DE ROOIJ, D. G., VAN PELT, A. M. & VORMER, T. L. 2012. Molecular control of rodent spermatogenesis. *Biochim Biophys Acta,* 1822**,** 1838-50.

JANES, K. A., CALVO, P. & ALONSO, M. J. 2001. Polysaccharide colloidal particles as delivery systems for macromolecules. *Adv Drug Deliv Rev,* 47**,** 83-97.

JUSTICE, M. J. 2000. Capitalizing on large-scale mouse mutagenesis screens. *Nature Reviews Genetics,* 1**,** 109-115.

JUSTICE, M. J., CARPENTER, D. A., FAVOR, J., NEUHAUSER-KLAUS, A., DE ANGELIS, M. H., SOEWARTO, D., MOSER, A., CORDES, S., MILLER, D., CHAPMAN, V., WEBER, J. S., RINCHIK, E. M., HUNSICKER, P. R., RUSSELL, W. L. & BODE, V. C. 2000. Effects of ENU dosage on mouse strains. *Mammalian Genome,* 11**,** 484-488.

KAGAWA, Y., NOGE, I., HIGASHIGAWA, M. & KOMADA, Y. 2008. Combined antitumor effect of cyclophosphamide and bromodeoxyuridine in BDF1 mice bearing L1210 ascites tumors. *Biological & Pharmaceutical Bulletin,* 31**,** 57-61.

KALTENBACH, L., HORNER, M. A., ROTHMAN, J. H. & MANGO, S. E. 2000. The TBP-like factor CeTLF is required to activate RNA polymerase II transcription during C. elegans embryogenesis. *Mol Cell,* 6**,** 705-13.

KANEMITSU, H., YAMAUCHI, H., KOMATSU, M., YAMAMOTO, S., OKAZAKI, S. & NAKAYAMA, H. 2009. Time-course changes in neural cell apoptosis in the rat fetal brain from dams treated with 6-mercaptopurine (6-MP). *Histology and Histopathology,* 24**,** 317-324.

KARAMOUZIS, M. V., GORGOULIS, V. G. & PAPAVASSILIOU, A. G. 2002. Transcription factors and neoplasia: Vistas in novel drug design. *Clinical Cancer Research,* 8**,** 949-961.

KATOH, M., INOMATA, T., HORIYA, N., SUZUKI, F., SHIDA, T., ISHIOKA, K. & SHIBUYA, T. 1994. Studies on Mutations in Male Germ-Cells of Transgenic Mice Following Exposure to Isopropyl Methanesulfonate, Ethylnitrosourea or X-Ray. *Mutation Research-Genetic Toxicology,* 341**,** 17-25.

KATOH, M. A., CAIN, K. T., HUGHES, L. A., FOXWORTH, L. B., BISHOP, J. B. & GENEROSO, W. M. 1990. Female-Specific Dominant Lethal Effects in Mice. *Mutation Research,* 230**,** 205-217.

KENNEDY, C. L. & O'BRYAN, M. K. 2006. N-ethyl-N-nitrosourea (ENU) mutagenesis and male fertility research. *Human Reproduction Update,* 12**,** 293-301.

KENNEDY, C. L., O'CONNOR, A. E. O., SANCHEZ-PARTIDA, L. G., HOLLAND, M. K., GOODNOW, C. C., DE KRETSER, D. M. & O'BRYAN, M. K. 2005. A repository of ENU mutant mouse lines and their potential for male fertility research. *Molecular Human Reproduction,* 11**,** 871-880.

KHALFAOUI, T., MKANNEZ, G., COLIN, D., IMEN, A., ZBIBA, W., ERRAIS, K., ANANE, R., BELTAIEF, O., ZHIOUA, R., BEN HAMIDA, J., LIZARD, G. & OUERTANI-MEDDEB, A. 2011. Immunohistochemical analysis of vascular endothelial growth factor (VEGF) and p53 expression in pterygium from Tunisian patients. *Pathol Biol (Paris),* 59**,** 137-41.

KIMMINS, S., KOTAJA, N., DAVIDSON, I. & SASSONE-CORSI, P. 2004. Testis-specific transcription mechanisms promoting male germ-cell differentiation. *Reproduction,* 128**,** 5-12.

KOJI, T. & HISHIKAWA, Y. 2003. Germ cell apoptosis and its molecular trigger in mouse testes. *Archives of Histology and Cytology,* 66**,** 1-16.

KONDO, N., TAKAHASHI, A., ONO, K. & OHNISHI, T. 2010. DNA damage induced by alkylating agents and repair pathways. *J Nucleic Acids,* 2010**,** 543531.

KOTAJA, N., DE CESARE, D., MACHO, B., MONACO, L., BRANCORSINI, S., GOOSSENS, E., TOURNAYE, H., GANSMULLER, A. & SASSONE-CORSI, P. 2004. Abnormal sperm in mice with targeted deletion of the act (activator of cAMP-responsive element modulator in testis) gene. *Proc Natl Acad Sci U S A,* 101**,** 10620-5.

KURIYAMA, K., KITAMURA, T., YOKOI, R., HAYASHI, M., KOBAYASHI, K., KURODA, J. & TSUJII, H. 2005. Evaluation of testicular toxicity and sperm morphology in rats treated with methyl methanesulphonate (MMS). *Journal of Reproduction and Development,* 51**,** 657-667.

LAHDETIE, J., KEISKI, A., SUUTARI, A. & TOPPARI, J. 1994. Etoposide (Vp-16) Is a Potent Inducer of Micronuclei in Male-Rat Meiosis - Spermatid Micronucleus Test and DNA Flow-Cytometry after Etoposide Treatment. *Environmental and Molecular Mutagenesis,* 24**,** 192-202.

LAMMERS, J. H. M., VANAALDEREN, M., PETERS, A. H. F. M., VANPELT, A. A. M., GAEMERS, I. C., DEROOIJ, D. G., DEBOER, P., OFFENBERG, H. H., DIETRICH, A. J. J. & HEYTING, C. 1995. A Change in the Phosphorylation Pattern of the 30000-33000 M(R) Synaptonemal Complex Proteins of the Rat between Early and Mid-Pachytene. *Chromosoma,* 104**,** 154-163.

LARDENOIS, A., CHALMEL, F., DEMOUGIN, P., KOTAJA, N., SASSONE-CORSI, P. & PRIMIG, M. 2009. Fhl5/Act, a CREM-binding transcriptional activator required for normal sperm maturation and morphology, is not essential for testicular gene expression. *Reprod Biol Endocrinol,* 7**,** 133.

LEDUC, F., NKOMA, G. B. & BOISSONNEAULT, G. 2008. Spermiogenesis and DNA repair: A possible etiology of human infertility and genetic disorders. *Systems Biology in Reproductive Medicine,* 54**,** 3-10.

LI, Y., WANG, X., FENG, X., LIAO, S., ZHANG, D., CUI, X., GAO, F. & HAN, C. 2014. Generation of male germ cells from mouse induced pluripotent stem cells in vitro. *Stem Cell Res,* 12**,** 517-30.

LIAO, W., MCNUTT, M. A. & ZHU, W. G. 2009. The comet assay: a sensitive method for detecting DNA damage in individual cells. *Methods,* 48**,** 46-53.

LINDAHL, T. & BARNES, D. E. 2000. Repair of endogenous DNA damage. *Cold Spring Harbor Symposia on Quantitative Biology,* 65**,** 127-133.

LIU, Z., ZHOU, S., LIAO, L., CHEN, X., MEISTRICH, M. & XU, J. 2010. Jmjd1a demethylase-regulated histone modification is essential for cAMP-response element modulator-regulated gene expression and spermatogenesis. *J Biol Chem,* 285**,** 2758-70.

LU, C. C. & MEISTRICH, M. L. 1979. Cytotoxic effects of chemotherapeutic drugs on mouse testis cells. *Cancer Res,* 39**,** 3575-82.

MACHO, B., BRANCORSINI, S., FIMIA, G. M., SETOU, M., HIROKAWA, N. & SASSONE-CORSI, P. 2002. CREM-dependent transcription in male germ cells controlled by a kinesin. *Science,* 298**,** 2388-90.

MAHESHWARI, A., MISRO, M. M., AGGARWAL, A., SHARMA, R. K. & NANDAN, D. 2009. Pathways involved in testicular germ cell apoptosis induced by H2O2 in vitro. *FEBS J,* 276**,** 870-81.

MAKRIS, S. L., KIM, J. H., ELLIS, A., FABER, W., HARROUK, W., LEWIS, J. M., PAULE, M. G., SEED, J., TASSINARI, M. & TYL, R. 2011. Current and future needs for developmental toxicity testing. *Birth Defects Res B Dev Reprod Toxicol,* 92**,** 384-94.

MALLERY, S. R., CLARK, Y. M., NESS, G. M., MINSHAWI, O. M., PEI, P. & HOHL, C. M. 1999. Thiol redox modulation of doxorubicin mediated cytotoxicity in cultured AIDS-related Kaposi's sarcoma cells. *Journal of Cellular Biochemistry,* 73**,** 259-277.

Manochantr, S., Sretarugsa, P., Wanichanon, C., Chavadej, J., Sobhon, P. 2003. Classification of spermatogenic cells in *Rana tigerina* based on ultrastructure. Sci Asia, 29:241-254.

MARCHETTI, F. & WYROBEK, A. J. 2008. DNA repair decline during mouse spermiogenesis results in the accumulation of heritable DNA damage. *DNA Repair (Amst),* 7**,** 572-81.

MARKER, P. C., SEUNG, K., BLAND, A. E., RUSSELL, L. B. & KINGSLEY, D. M. 1997. Spectrum of Bmp5 mutations from germline mutagenesis experiments in mice. *Genetics,* 145**,** 435-43.

MARTIANOV, I., BRANCORSINI, S., GANSMULLER, A., PARVINEN, M., DAVIDSON, I. & SASSONE-CORSI, P. 2002. Distinct functions of TBP and TLF/TRF2 during spermatogenesis: requirement of TLF for heterochromatic chromocenter formation in haploid round spermatids. *Development,* 129**,** 945-55.

MARTIANOV, I., FIMIA, G. M., DIERICH, A., PARVINEN, M., SASSONE-CORSI, P. & DAVIDSON, I. 2001. Late arrest of spermiogenesis and germ cell apoptosis in mice lacking the TBP-like TLF/TRF2 gene. *Mol Cell,* 7**,** 509-15.

MATSUDA, Y., TOBARI, I., MAEMORI, M. & SEKI, N. 1989. Mechanism of Chromosome Aberration Induction in the Mouse Egg Fertilized with Sperm Recovered from Postmeiotic Germ-Cells Treated with Methyl Methanesulfonate. *Mutation Research,* 214**,** 165-180.

MEISTRICH, M. L. 2013. Effects of chemotherapy and radiotherapy on spermatogenesis in humans. *Fertility and Sterility,* 100**,** 1180-1186.

MEISTRICH, M. L. & HESS, R. A. 2013. Assessment of spermatogenesis through staging of seminiferous tubules. *Methods Mol Biol,* 927**,** 299-307.

MEISTRICH, M. L. & TROSTLE, P. K. 1975. Separation of mouse testis cells by equilibrium density centrifugation in renografin gradients. *Exp Cell Res,* 92**,** 231-44.

MEISTRICH, M. L., TROSTLEWEIGE, P. K. & VANBEEK, M. E. A. B. 1994. Separation of Specific Stages of Spermatids from Vitamin-a-Synchronized Rat Testes for Assessment of Nucleoprotein Changes during Spermiogenesis. *Biology of Reproduction,* 51**,** 334-344.

MEISTRICH, M. L., VAN BEEK, M. E., LIANG, J. C., JOHNSON, S. L. & LU, J. 1990. Low levels of chromosomal mutations in germ cells derived from doxorubicin-treated stem spermatogonia in the mouse. *Cancer Res,* 50**,** 370-4.

MENDEZ PALACIOS, N., ESCOBAR, M. E., MENDOZA, M. M., CRISPIN, R. H., ANDRADE, O. G., MELANDEZ, J. H. & MARTINEZ, A. A. 2014. Prepubertal male rats with high rates of germ-cell apoptosis present exacerbated rates of germ-cell apoptosis after serotonin depletion. *Reprod Fertil Dev*.

MENG, X., LINDAHL, M., HYVONEN, M. E., PARVINEN, M., DE ROOIJ, D. G., HESS, M. W., RAATIKAINEN-AHOKAS, A., SAINIO, K., RAUVALA, H., LAKSO, M., PICHEL, J. G., WESTPHAL, H., SAARMA, M. & SARIOLA, H. 2000. Regulation of cell fate decision of undifferentiated spermatogonia by GDNF. *Science,* 287**,** 1489-93.

MILTENBERGER, R. J., WAKAMATSU, K., ITO, S., WOYCHIK, R. P., RUSSELL, L. B. & MICHAUD, E. J. 2002. Molecular and phenotypic analysis of 25 recessive, homozygous-viable alleles at the mouse agouti locus. *Genetics,* 160**,** 659-74.

MOHAMMADNEJAD, D., ABEDELAHI, A., SOLEIMANI-RAD, J., MOHAMMADI-ROSHANDEH, A., RASHTBAR, M. & AZAMI, A. 2012. Degenerative effect of Cisplatin on testicular germinal epithelium. *Adv Pharm Bull,* 2**,** 173-7.

MORRIS, S. M. 1991. The Genetic Toxicology of 5-Bromodeoxyuridine in Mammalian-Cells. *Mutation Research,* 258**,** 161-188.

MOSESSO, P. & PALITTI, F. 1993. The Genetic Toxicology of 6-Mercaptopurine. *Mutation Research,* 296**,** 279-294.

MOUSTAFA, M. H., SHARMA, R. K., THORNTON, J., MASCHA, E., ABDEL-HAFEZ, M. A., THOMAS, A. J. & AGARWAL, A. 2004. Relationship between ROS production, apoptosis and DNA denaturation in spermatozoa from patients examined for infertility. *Human Reproduction,* 19**,** 129-138.

MYERS CE, C. B. 1990. Anthracyclines. In: Chabner BA, Collins JM, editors. Cancer chemotherapy: principles and practice. Philadelphia: JB Lippincott;.

NOVEROSKE, J. K., WEBER, J. S. & JUSTICE, M. J. 2000. The mutagenic action of N-ethyl-N-nitrosourea in the mouse. *Mammalian Genome,* 11**,** 478-483.

O'BRIEN, J. M., WILLIAMS, A., GINGERICH, J., DOUGLAS, G. R., MARCHETTI, F. & YAUK, C. L. 2013. No evidence for transgenerational genomic instability in the F1 or F2 descendants of Muta(Tm)Mouse males exposed to N-ethyl-N-nitrosourea. *Mutation Research-Fundamental and Molecular Mechanisms of Mutagenesis,* 741**,** 11-17.

O'BRYAN, M. K. & DE KRETSER, D. 2006. Mouse models for genes involved in impaired spermatogenesis. *Int J Androl,* 29**,** 76-89; discussion 105-8.

O'SHAUGHNESSY, P. J., MORRIS, I. D., HUHTANIEMI, I., BAKER, P. J. & ABEL, M. H. 2009. Role of androgen and gonadotrophins in the development and function of the Sertoli cells and Leydig cells: Data from mutant and genetically modified mice. *Molecular and Cellular Endocrinology,* 306**,** 2-8.

OHBAYASHI, T., MAKINO, Y. & TAMURA, T. 1999. Identification of a mouse TBP-like protein (TLP) distantly related to the Drosophila TBP-related factor. *Nucleic Acids Research,* 27**,** 750-755.

OLSEN, A. K., LINDEMAN, B., WIGER, R., DUALE, N. & BRUNBORG, G. 2005. How do male germ cells handle DNA damage? *Toxicol Appl Pharmacol,* 207**,** 521-31.

OZER, J., MOORE, P. A. & LIEBERMAN, P. M. 2000. A testis-specific transcription factor IIA (TFIIAtau) stimulates TATA-binding protein-DNA binding and transcription activation. *J Biol Chem,* 275**,** 122-8.

PALERMO, I., LITRICO, L., EMMANUELE, G., GIUFFRIDA, V., SASSONE-CORSI, P., DE CESARE, D., FIMIA, G. M., D'AGATA, R., CALOGERO, A. E. & TRAVALI, S. 2001. Cloning and expression of activator of CREM in testis in human testicular tissue. *Biochemical and Biophysical Research Communications,* 283**,** 406-411.

PARASURAMAN, S. 2011. Toxicological screening. *J Pharmacol Pharmacother,* 2**,** 74-9.

PELTOLA, V., MANTYLA, E., HUHTANIEMI, I. & AHOTUPA, M. 1994. Lipid-Peroxidation and Antioxidant Enzyme-Activities in the Rat Testis after Cigarette-Smoke Inhalation or Administration of Polychlorinated-Biphenyls or Polychlorinated Naphthalenes. *Journal of Andrology,* 15**,** 353-361.

PERRARD, M. H., HUE, D., STAUB, C., LE VERN, Y., KERBOEUF, D. & DURAND, P. 2003. Development of the meiotic step in testes of pubertal rats: comparison between the in vivo situation and under in vitro conditions. *Molecular Reproduction and Development,* 65**,** 86-95.

POIRSON-BICHAT, F., GONCALVES, R. A. B., MICCOLI, L., DUTRILLAUX, B. & POUPON, M. F. 2000. Methionine depletion enhances the antitumoral efficacy of cytotoxic agents in drug-resistant human tumor xenografts. *Clinical Cancer Research,* 6**,** 643-653.

PRAHALATHAN, C., SELVAKUMAR, E. & VARALAKSHMI, P. 2005. Protective effect of lipoic acid on adriamycin-induced testicular toxicity. *Clin Chim Acta,* 360**,** 160-6.

PROVOST, G. S. & SHORT, J. M. 1994. Characterization of Mutations Induced by Ethylnitrosourea in Seminiferous Tubule Germ-Cells of Transgenic B6c3f(1) Mice. *Proceedings of the National Academy of Sciences of the United States of America,* 91**,** 6564-6568.

PULTE, D., GONDOS, A. & BRENNER, H. 2008. Trends in 5- and 10-year survival after diagnosis with childhood hematologic malignancies in the United States, 1990-2004. *J Natl Cancer Inst,* 100**,** 1301-9.

QUILES, J. L., HUERTAS, J. R., BATTINO, M., MATAIX, J. & RAMIREZ-TORTOSA, M. C. 2002. Antioxidant nutrients and adriamycin toxicity. *Toxicology,* 180**,** 79-95.

RAFF, M. C., BARRES, B. A., BURNE, J. F., COLES, H. S., ISHIZAKI, Y. & JACOBSON, M. D. 1993. Programmed Cell-Death and the Control of Cell-Survival - Lessons from the Nervous-System. *Science,* 262**,** 695-700.

RAVI, D. & DAS, K. C. 2004. Redox-cycling of anthracyclines by thioredoxin system: increased superoxide generation and DNA damage. *Cancer Chemother Pharmacol,* 54**,** 449-58.

REUTER, K., SCHLATT, S., EHMCKE, J. & WISTUBA, J. 2012. Fact or fiction: In vitro spermatogenesis. *Spermatogenesis,* 2**,** 245-252.

ROONEY, J. P., GEORGE, A. D., PATIL, A., BEGLEY, U., BESSETTE, E., ZAPPALA, M. R., HUANG, X., CONKLIN, D. S., CUNNINGHAM, R. P. & BEGLEY, T. J. 2009. Systems based mapping demonstrates that recovery from alkylation damage requires DNA repair, RNA processing, and translation associated networks. *Genomics,* 93**,** 42-51.

RUSSELL, L. B., HUNSICKER, P. R. & RUSSELL, W. L. 2007. Comparison of the genetic effects of equimolar doses of ENU and MNU: While the chemicals differ dramatically in their mutagenicity in stem-cell spermatogonia, both elicit very high mutation rates in differentiating spermatogonia. *Mutation Research-Fundamental and Molecular Mechanisms of Mutagenesis,* 616**,** 181-195.

RUSSELL, W. L. & HUNSICKER, P. R. 1983. Extreme Sensitivity of One Particular Germ-Cell Stage in Male-Mice to Induction of Specific-Locus Mutations by Methylnitrosourea. *Environmental Mutagenesis,* 5**,** 498-498.

RUSSO, A. & LEVIS, A. G. 1992. Detection of Aneuploidy in Male Germ-Cells of Mice by Means of a Meiotic Micronucleus Assay. *Mutation Research,* 281**,** 187-191.

SAKALLIOGLU, A. E., OZDEMIR, B. H., BASARAN, O., NACAR, A., SUREN, D. & HABERAL, M. A. 2007. Ultrastructural study of severe testicular damage following acute scrotal thermal injury. *Burns,* 33**,** 328-333.

SAVITT, J., SINGH, D., ZHANG, C., CHEN, L. C., FOLMER, J., SHOKAT, K. M. & WRIGHT, W. W. 2012. The in vivo response of stem and other undifferentiated spermatogonia to the reversible inhibition of glial cell line-derived neurotrophic factor signaling in the adult. *Stem Cells,* 30**,** 732-40.

SCHULTE, R. T., OHL, D. A., SIGMAN, M. & SMITH, G. D. 2010. Sperm DNA damage in male infertility: etiologies, assays, and outcomes. *Journal of Assisted Reproduction and Genetics,* 27**,** 3-12.

SCHWARTZMAN, R. A. & CIDLOWSKI, J. A. 1993. Apoptosis - the Biochemistry and Molecular-Biology of Programmed Cell-Death. *Endocrine Reviews,* 14**,** 133-151.

SEELEY, M. R. & FAUSTMAN, E. M. 1995. Toxicity of four alkylating agents on in vitro rat embryo differentiation and development. *Fundam Appl Toxicol,* 26**,** 136-42.

SEGA, G. A. 1974. Unscheduled DNA synthesis in the germ cells of male mice exposed in vivo to the chemical mutagen ethyl methanesulfonate. *Proc Natl Acad Sci U S A,* 71**,** 4955-9.

SHAHA, C., TRIPATHI, R. & MISHRA, D. P. 2010. Male germ cell apoptosis: regulation and biology. *Philos Trans R Soc Lond B Biol Sci,* 365**,** 1501-15.

SHAMBERGER, R. C., SHERINS, R. J. & ROSENBERG, S. A. 1981. The Effects of Postoperative Adjuvant Chemotherapy and Radiotherapy on Testicular Function in Men Undergoing Treatment for Soft-Tissue Sarcoma. *Cancer,* 47**,** 2368-2374.

SHINODA, K., MITSUMORI, K., YASUHARA, K., UNEYAMA, C., ONODERA, H., HIROSE, M. & UEHARA, M. 1999. Doxorubicin induces male germ cell apoptosis in rats. *Arch Toxicol,* 73**,** 274-81.

SIEPKA, S. M. & TAKAHASHI, J. S. 2005. Forward genetic screens to identify circadian rhythm mutants in mice. *Circadian Rhythms,* 393**,** 219-229.

SIMON, L., EKMAN, G. C., GARCIA, T., CARNES, K., ZHANG, Z., MURPHY, T., MURPHY, K. M., HESS, R. A., COOKE, P. S. & HOFMANN, M. C. 2010. ETV5 regulates sertoli cell chemokines involved in mouse stem/progenitor spermatogonia maintenance. *Stem Cells,* 28**,** 1882-92.

SINGER, B. & DOSANJH, M. K. 1990. Site-Directed Mutagenesis for Quantitation of Base Base Interactions at Defined Sites. *Mutation Research,* 233**,** 45-51.

SINGER, T. M., LAMBERT, I. B., WILLIAMS, A., DOUGLAS, G. R. & YAUK, C. L. 2006. Detection of induced male germline mutation: Correlations and comparisons between traditional germline mutation assays, transgenic rodent assays and expanded simple tandem repeat instability assays. *Mutation Research-Fundamental and Molecular Mechanisms of Mutagenesis,* 598**,** 164-193.

SJOBLOM, T., WEST, A. & LAHDETIE, J. 1998. Apoptotic response of spermatogenic cells to the germ cell mutagens etoposide, adriamycin, and diepoxybutane. *Environmental and Molecular Mutagenesis,* 31**,** 133-148.

SMITH, G. J. & GRISHAM, J. W. 1983. Cytotoxicity of monofunctional alkylating agents. Methyl methanesulfonate and methyl-N'-nitro-N-nitrosoguanidine have different mechanisms of toxicity for 10T1/2 cells. *Mutat Res,* 111**,** 405-17.

SMITH, R. E. 2003. Risk for the development of treatment-related acute myelocytic leukemia and myelodysplastic syndrome among patients with breast cancer: review of the literature and the National Surgical Adjuvant Breast and Bowel Project experience. *Clin Breast Cancer,* 4**,** 273-9.

SPIELMANN, H., POHL, I., DORING, B., LIEBSCH, M. & MOLDENHAUER, F. 1997. The embryonic stem cell test (EST), an in vitro embryotoxicity test using two permanent mouse cell lines: 3T3 fibroblasts and embryonic stem cells. *Animal Alternatives, Welfare, and Ethics,* 27**,** 663-669.

SPRIGGS, K. A., BUSHELL, M. & WILLIS, A. E. 2010. Translational Regulation of Gene Expression during Conditions of Cell Stress. *Molecular Cell,* 40**,** 228-237.

STEGER, K. 1999. Transcriptional and translational regulation of gene expression in haploid spermatids. *Anat Embryol (Berl),* 199**,** 471-87.

STEGER, K., BEHR, R., KLEINER, I., WEINBAUER, G. F. & BERGMANN, M. 2004. Expression of activator of CREM in the testis (ACT) during normal and impaired spermatogenesis: correlation with CREM expression. *Molecular Human Reproduction,* 10**,** 129-135.

SURESH, A., GUEDEZ, L., MOREB, J. & ZUCALI, J. 2003. Overexpression of manganese superoxide dismutase promotes survival in cell lines after doxorubicin treatment. *British Journal of Haematology,* 120**,** 457-463.

TADOKORO, Y., YOMOGIDA, K., OHTA, H., TOHDA, A. & NISHIMUNE, Y. 2002. Homeostatic regulation of germinal stem cell proliferation by the GDNF/FSH pathway. *Mechanisms of Development,* 113**,** 29-39.

TALBOT, P. & CHACON, R. S. 1981. A Triple-Stain Technique for Evaluating Normal Acrosome Reactions of Human-Sperm. *Journal of Experimental Zoology,* 215**,** 201-208.

TANAKA, H. & BABA, T. 2005. Gene expression in spermiogenesis. *Cell Mol Life Sci,* 62**,** 344-54.

TICE, R. R., AGURELL, E., ANDERSON, D., BURLINSON, B., HARTMANN, A., KOBAYASHI, H., MIYAMAE, Y., ROJAS, E., RYU, J. C. & SASAKI, Y. F. 2000. Single cell gel/comet assay: guidelines for in vitro and in vivo genetic toxicology testing. *Environ Mol Mutagen,* 35**,** 206-21.

TOHAMY, A. A., EL-GHOR, A. A., EL-NAHAS, S. M. & NOSHY, M. M. 2003. Beta-glucan inhibits the genotoxicity of cyclophosphamide, adriamycin and cisplatin. *Mutat Res,* 541**,** 45-53.

TOPHAM, J. C. 1980. Chemically-induced transmissible abnormalities in sperm-head shape. *Mutat Res,* 70**,** 109-14.

TOPPARI, J., LARSEN, J. C., CHRISTIANSEN, P., GIWERCMAN, A., GRANDJEAN, P., GUILLETTE, L. J., JEGOU, B., JENSEN, T. K., JOUANNET, P., KEIDING, N., LEFFERS, H., MCLACHLAN, J. A., MEYER, O., MULLER, J., RAJPERTDEMEYTS, E., SCHEIKE, T., SHARPE, R., SUMPTER, J. & SKAKKEBAEK, N. E. 1996. Male reproductive health and environmental xenoestrogens. *Environmental Health Perspectives,* 104**,** 741-803.

TREMELLEN, K. 2008. Oxidative stress and male infertility--a clinical perspective. *Hum Reprod Update,* 14**,** 243-58.

UPADHYAYA, A. B., KHAN, M., MOU, T. C., JUNKER, M., GRAY, D. M. & DEJONG, J. 2002. The germ cell-specific transcription factor ALF - Structural properties and stabilization of the TATA-binding protein (TBP)-DNA complex. *Journal of Biological Chemistry,* 277**,** 34208-34216.

VAN BOXTEL, R., GOULD, M. N., CUPPEN, E. & SMITS, B. M. 2010. ENU mutagenesis to generate genetically modified rat models. *Methods Mol Biol,* 597**,** 151-67.

VAN DELFT, J. H., BERGMANS, A. & BAAN, R. A. 1997. Germ-cell mutagenesis in lambda lacZ transgenic mice treated with ethylating and methylating agents: comparison with specific-locus test. *Mutat Res,* 388**,** 165-73.

Van der Jagt, K., Munn, S.J., Torslov, J. & de Brujin, J. 2004. Alternative approaches can reduce the use of test animals under REACH. Addendum to the Report "Assessment of addtional testing needs under REACH. Effects of (Q)SARs, risk based testing and voluntary industry initiatives". Ispra, European Commission Joint Research Centre.

VENDRAMINI, V., SASSO-CERRI, E. & MIRAGLIA, S. M. 2010. Amifostine reduces the seminiferous epithelium damage in doxorubicin-treated prepubertal rats without improving the fertility status. *Reprod Biol Endocrinol,* 8**,** 3.

VIGLIETTO, G., DOLCI, S., BRUNI, P., BALDASSARRE, G., CHIARIOTTI, L., MELILLO, R. M., SALVATORE, G., CHIAPPETTA, G., SFERRATORE, F., FUSCO, A. & SANTORO, M. 2000. Glial cell line-derived neutrotrophic factor and neurturin can act as paracrine growth factors stimulating DNA synthesis of Ret-expressing spermatogonia. *Int J Oncol,* 16**,** 689-94.

WALTER, C. A., INTANO, G. W., MCCARREY, J. R., MCMAHAN, C. A. & WALTER, R. B. 1998. Mutation frequency declines during spermatogenesis in young mice but increases in old mice. *Proceedings of the National Academy of Sciences of the United States of America,* 95**,** 10015-10019.

WHITE-COOPER, H. & DAVIDSON, I. 2011. Unique Aspects of Transcription Regulation in Male Germ Cells. *Cold Spring Harbor Perspectives in Biology,* 3.

WILLIAMS, G. T. 1991. Programmed cell death: apoptosis and oncogenesis. *Cell,* 65**,** 1097-8.

WINN, R. N., NORRIS, M. B., BRAYER, K. J., TORRES, C. & MULLER, S. L. 2000. Detection of mutations in transgenic fish carrying a bacteriophage lambda cII transgene target. *Proceedings of the National Academy of Sciences of the United States of America,* 97**,** 12655-12660.

XIE, H., VUCETIC, S., IAKOUCHEVA, L. M., OLDFIELD, C. J., DUNKER, A. K., UVERSKY, V. N. & OBRADOVIC, Z. 2007. Functional anthology of intrinsic disorder. 1. Biological processes and functions of proteins with long disordered regions. *J Proteome Res,* 6**,** 1882-98.

XU, G., SPIVAK, G., MITCHELL, D. L., MORI, T., MCCARREY, J. R., MCMAHAN, C. A., WALTER, R. B., HANAWALT, P. C. & WALTER, C. A. 2005. Nucleotide excision repair activity varies among murine spermatogenic cell types. *Biol Reprod,* 73**,** 123-30.

XU, J., SUN, X. J., JING, Y. D., WANG, M., LIU, K., JIAN, Y. L., YANG, M., CHENG, Z. K. & YANG, C. L. 2012. MRG-1 is required for genomic integrity in Caenorhabditis elegans germ cells. *Cell Research,* 22**,** 886-902.

YAGMURCA, M., BAS, O., MOLLAOGLU, H., SAHIN, O., NACAR, A., KARAMAN, O. & SONGUR, A. 2007. Protective effects of erdosteine on doxorubicin-induced hepatotoxicity in rats. *Archives of Medical Research,* 38**,** 380-385.

YEH, Y. C., LAI, H. C., TING, C. T., LEE, W. L., WANG, L. C., WANG, K. Y., LAI, H. C. & LIU, T. J. 2007. Protection by doxycycline against doxorubicin-induced oxidative stress and apoptosis in mouse testes. *Biochem Pharmacol,* 74**,** 969-80.

YEH, Y. C., LIU, T. J., WANG, L. C., LEE, H. W., TING, C. T., LEE, W. L., HUNG, C. J., WANG, K. Y., LAI, H. C. & LAI, H. C. 2009. A standardized extract of Ginkgo biloba suppresses doxorubicin-induced oxidative stress and p53-mediated mitochondrial apoptosis in rat testes. *Br J Pharmacol,* 156**,** 48-61.

YOKOCHI, T. & ROBERTSON, K. D. 2004. Doxorubicin inhibits DNMT1, resulting in conditional apoptosis. *Molecular Pharmacology,* 66**,** 1415-1420.

YU, Y. E., ZHANG, Y., UNNI, E., SHIRLEY, C. R., DENG, J. M., RUSSELL, L. D., WEIL, M. M., BEHRINGER, R. R. & MEISTRICH, M. L. 2000. Abnormal spermatogenesis and reduced fertility in transition nuclear protein 1-deficient mice. *Proceedings of the National Academy of Sciences of the United States of America,* 97**,** 4683-4688.

ZANETTI, S. R., MALDONADO, E. N. & AVELDANO, M. I. 2007. Doxorubicin affects testicular lipids with long-chain (C18-C22) and very long-chain (C24-C32) polyunsaturated fatty acids. *Cancer Res,* 67**,** 6973-80.

ZHANG, D., PENTTILA, T. L., MORRIS, P. L. & ROEDER, R. G. 2001. Cell- and stage-specific high-level expression of TBP-related factor 2 (TRF2) during mouse spermatogenesis. *Mechanisms of Development,* 106**,** 203-205.